MINISTRY OF SCIENCE AND HIGHERMINISTRY OF SCIENCE AND HIGHER EDUCATION OF RUSSIAN FEDERATION
RUSSIAN ACADEMY OF SCIENCES

DIVISION OF CHEMISTRY AND MATERIAL SCIENCES
SCIENTIFIC COUNCIL ON PHYSICAL CHEMISTRY
FEDERAL STATE BUDGETARY INSTITUTION OF SCIENCE
A.N. FRUMKIN INSTITUTE OF PHYSICAL CHEMISTRY AND ELECTROCHEMISTRY OF RAS

All-Russian conference with international participation

PHYSICOCHEMICAL PROBLEMS OF ADSORPTION, STRUCTURE, AND SURFACE CHEMISTRY OF NANOPOROUS MATERIALS

devoted to the 120th birth anniversary of Academician M.M. Dubinin

October 18 – 22, 2021

Book of Abstracts

Moscow, Russia

MINISTRY OF SCIENCE AND HIGHER EDUCATION OF RUSSIAN FEDERATION
RUSSIAN ACADEMY OF SCIENCES

DIVISION OF CHEMISTRY AND MATERIAL SCIENCES
SCIENTIFIC COUNCIL ON PHYSICAL CHEMISTRY
FEDERAL STATE BUDGETARY INSTITUTION OF SCIENCE
A.N. FRUMKIN INSTITUTE OF PHYSICAL CHEMISTRY AND ELECTROCHEMISTRY OF RAS

ZELINSKY GROUP

All-Russian conference

with international participation

devoted to the 120th birth anniversary of Academician M.M. Dubinin

PHYSICOCHEMICAL PROBLEMS OF ADSORPTION, STRUCTURE, AND SURFACE CHEMISTRY OF NANOPOROUS MATERIALS

Book of Abstracts
October 18 – 22, 2021

Moscow, Russia

2021

541.127:541.183

Approved by the Federal State Budgetary Institution of Science A.N. Frumkin Institute of Physical Chemistry and Electrochemistry, Russian Academy of Sciences

Physicochemical problems of adsorption, structure, and surface chemistry of nanoporous materials: All-Russian conference with international participation (on 120th anniversary of M.M. Dubinin's birth), October 18–22, 2021, Moscow Russia. Book of Abstracts. – M.: IPCE RAS, 2021. – p.252 ISBN 978-5-4465-3448-7

The book contains the materials of the All-Russian conference with international participation "Physicochemical problems of adsorption, structure and surface chemistry of nanomaterials" devoted to the 120th anniversary of Academician M.M. Dubinin's birth, an outstanding, prominent Russian physico-chemist, who made a significant contribution to the science of adsorption phenomena, synthesis of adsorbents, application in various industries, chemical defense of humans in extreme environments, ecology, and medicine.

The book is a collection of articles describing the latest advances in adsorption theory, synthesis problems, studies of properties and applications of novel highly active nanoporous, and selective functional materials. Methods of analysis of the porous structure of adsorbents, state of an adsorbed substance, specific features of molecular diffusion in pores and on surface, kinetics and dynamics of adsorption, numerical simulations of adsorption processes are described. Problems of adsorbent non-inertness, calculations of parameters of adsorption processes, and thermodynamic characteristics of adsorption, including high-pressure conditions, are discussed. Results concerning computer simulations of adsorption processes, theoretical approaches to describe the adsorption of individual substances and mixtures, self-organization processes, and phase transitions in an adsorbate are presented.

The book covers recent advances in synthesis and properties of new carbon and mineral adsorbents, zeolites, silica gels, composite materials based on fullerenes and nanotubes, metal-organic framework (MOF) structures, and their use in various industries, medicine, and environmental protection.

The book is aimed at a wide range of chemists, physicists, engineers, researchers, PhD students, and students engaged in the field of studies and applications of adsorption phenomena, synthesis of adsorbents and porous functional materials, and development of new adsorption-based technologies.

Scientific publication

Responsible for the publication: *Doctor of Physics and Mathematics A.A. Fomkin, Candidate of Chemistry G.A. Petukhova, Candidate of Physics and Mathematics E.V. Khozina, T.A. Kul'kova*

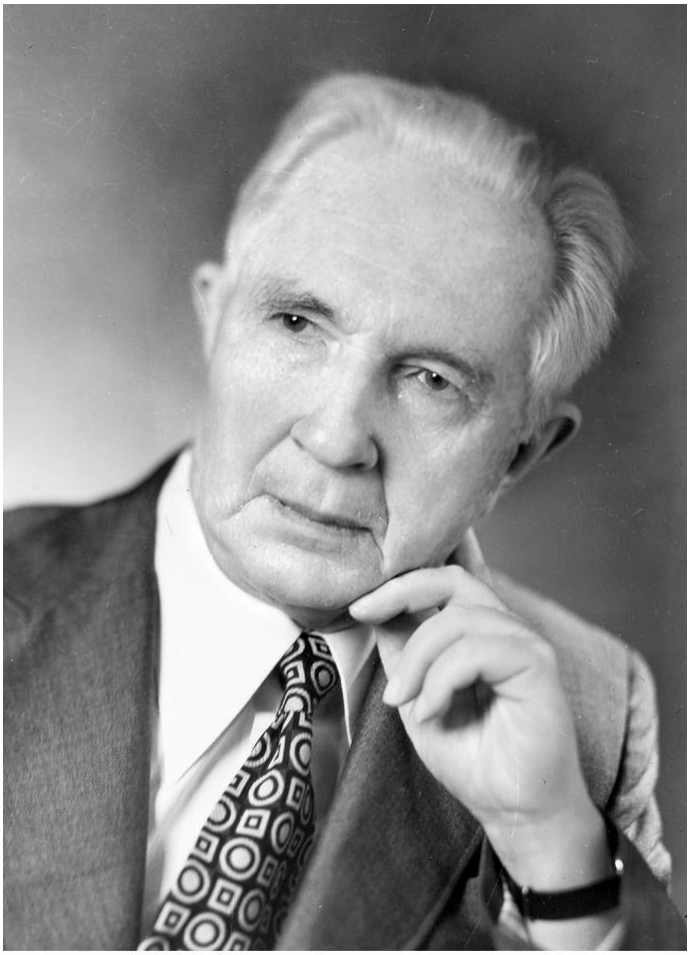

Мих Дубинин

1901–1993

ON THE 120th ANNIVERSARY OF THE BIRTH OF ACADEMICIAN M.M. DUBININ

Fomkin A.A.

Fomkinaa@mail.ru
M.M. Dubinin's Laboratory of Sorption Processes, A.N. Frumkin Institute of Physical Chemistry and Electrochemistry, Russian Academy of Sciences, 119071, Moscow, Russia

Mikhail M. Dubinin was born on January 01, 1901, in Moscow. His name is known to all researchers pursuing physical chemistry. Mikhail M. Dubinin is remembered as the founder of the largest scientific school in the field of adsorption phenomena. He has taken a rightful place in the list of members of the Academy of Sciences of Russia since 1724. It is difficult to overestimate his merits as a teacher and a science and social leader.

After graduation from the Moscow high technical school (MHTS) in 1921, M.M. Dubinin started teaching and researching activities at the Faculty of Chemistry. His first scientific achievements were related to studies of adsorption of various substances onto activated carbons from solutions. In 1932, M.M. Dubinin headed the Department of Chemical Defense at the Military Academy of Chemical Defense, founded at the basis of MHTS. At this stage, his activity was related to teaching and solving the most relevant tasks of chemical defense, including test methods and technological aspects of the production of sorbents. In 1942, M.M. Dubinin was awarded the Stalin (State) prize in recognition of his achievements in chemical defense. In 1943, he was elected a full member of the USSR Academy of Sciences. In the same year, he was awarded a rank of Major-General-Engineer.

In 1946, M.M. Dubinin created the Laboratory of Sorption Processes at the Institute of Physical Chemistry of the USSR Academy of Science. Then, it was expanded to the Department that brought together three laboratories dealing with various theoretical and practical aspects of adsorption. Academician Dubinin managed the research activity in thermodynamics, kinetics and dynamics of sorption processes, and porous solids characterization.

The famous theory of volume filling of micropores was created under Dubinin's direction. Moreover, he proposed a scientifically grounded and rational classification of adsorbents according to their structural features with respect to the adsorption mechanism. The principle he proposed to distinguish porous solids formed the basis for the IUPAC pore size classification adopted in 1972. Without question, his works belong to those investigations which gave rise to the development of modern nanotechnologies. Indeed, his achievements in the theory of adsorption phenomena remain in high demand in gas and petroleum processing, the chemistry of high purity substances, synthesis of catalysts for polymer materials, pharmaceutical and food industry, medicine, and ecological proptection.

In 1959, the Commission on zeolite attached to the Presidium of the USSR Academy of Sciences was created at the initiative of M.M. Dubinin and under his direction to coordinate work on creating the industry of zeolites and catalysts for some industries. In 1964, the Commission was transformed into the Scientific Council of the USSR Academy of Sciences on the synthesis, study, and application of adsorbents. This council coordinated all research, and practical works on adsorption and adsorbents carried out throughout the country and subsequently became a part of the modern united Scientific Council of the Russian Academy of Sciences on physical chemistry.

From 1946 to 1950, M.M. Dubinin was the President of the All-Union Chemical Society named after D.I. Mendeleev. From 1948 to 1951, M. Dubinin served as Academician-Secretary of the USSR Academy of Sciences Department of Chemistry. He was elected a member of the Presidium of the Academy from 1948 to 1963.

Along with scientific work, M.M. Dubinin directed efforts to educational and organizational work and social duty. He taught at MHTS, Moscow Institute of Transport Engineers, and Military Academy of Chemical Defense. He trained more than 100 Candidates of Sciences. More than 30 scientists defended the Doctor thesis under Dubinin's supervision and thanks to his advice. For almost 40 years, M.M. Dubinin was the Editor-in-Chief of the Russian Chemical Bulletin, editorial board member of the Russian Chemical Reviews, and depute editor of the Carbon journal.

The outstanding achievements and distinguished service of M.M. Dubinin as a scientist and social leader were highly appreciated. He was twice the winner of the Stalin (State) prize (in 1942 and 1950). Academician Dubinin was awarded numerous Soviet orders and medals, including three Orders of Lenin, two Orders of Red Banner, one first Order of the Patriotic War, one Medal for Valorous Labor. In 1969, Dubinin was awarded the title of the Hero of Socialist Labor.

Academician M.M. Dubinin was distinguished by high erudition, deep knowledge, and exceptional work ethic. While remaining true to the fundamental principles of life and scientific principles, M.M. Dubinin always maintained a sensitivity and benevolent attitude towards people.

Mikhail Mikhailovich Dubinin passed away on July 13, 1993, but the scientific school he created continues to develop. His numerous students and followers in Russia and all over the world follow in the footsteps of prominent scientist M.M. Dubinin.

CONCERTED STRUCTURE AND DYNAMICS OF MOLECULES ON CARBON NANOSTRUCTURES

K. Kaneko

kkaneko@shinshu-u.ac.jp
Research Initiatives for Supra-Materials, Shinshu University, 4-17-1 Wakasato, Nagano, 380-8553, Japan

Importance of nanostructured carbons has been increasing for construction of sustainable technologies due to their high electrical conductivity, chemically and mechanically robustness, and biocompatibility. This presentation will introduce excellent nanoconfinement functions of nanostructured carbons, indicating new innovations. Confinement of atoms, molecules, and ions in nanoscale carbon pore spaces induces novel high pressure-compression effect. This is because the graphene-like structure has the highly dense layer structure of carbon atoms, providing the strongest interaction with atoms and molecules per weight. For example, we can prepare an atomically 1D chain sulfur crystal inside single wall carbon nanotube (SWCNT) and double wall carbon nanotube[1]. The synchrotron XRD gives the sharp diffraction peak coming from the atomically 1D structure and the 1D sulfur inside carbon nanotube is metallic from Raman spectroscopy and the resistivity measurement.

When ions are confined in the extremely narrow carbon micropores, the confined ions induce the image charges in the defective carbon walls. The in-wall image charges compensate the repulsion interaction between the same ions, showing the partial breaking of Coulombic law [2]. This partial breaking effect gives a new insight of the high performance supercapacitors [3].

The carbide-derived carbon should have novel in-pore strong adsorption sites, which induce highly selective adsorption property for mixed gas of $^{18}O_2$ and $^{16}O_2$. This does not come from so-called quantum molecular sieving for light isotope molecules such as H_2 and D2. The oxygen isotope is separable with a new lattice motion associated quantum mechanical mechanism [4].

We must introduce a new concept for 2D materials like graphene. If we donate a nanoscale window (nanowindow) in the graphene, the nanowindow has a different

function from nanopore spaces. The nanopore space is fit for adsorption of supercritical gas [5] and

trace molecules [6], while the nanowindows are not efficient for adsorption, but separation. The promising air separation ability of the nanowindow was shown [7]

References

1. T. Fujimori, A. Morelos-Gómez, Z. Zhu, H. Muramatsu, R. Futamura, K. Urita, M. Terrones, T. Hayashi, M. Endo, S. Y. Hong, Y. C. Choi, D. Tománek, K. Kaneko, Nature Comm. (2013), **4**, 2162.
2. R. Futamura, T. Iiyama, Y. Takasaki, Y. Gogotsi, M.J. Biggs, M. Salanne, J. Ségalini, P. Simon, K. Kaneko, Nature Materials (2017), **16**, 1163.
3. M. Salanne B. Rotenberg, K. Naoi, K. Kaneko, P.-L. Taberna, C. P. Grey, B. Dunn, P. Simon, Nature Energy (2016), **1**, 16070.
4. S.K. Ujjain, A. Bagusetty, Y. Matsuda, H. Tanaka, P. Ahuja, C. de Tomas, M. Sakai, F. Vallejos-Burgos, R. Futamura, I. Suarez-Martinez, M. Matsukata, A. Kodama, G. Garberoglio, Y. Gogotsi, J. K. Johnson, K. Kaneko, Nature Comm. (2021) **12**, 546.
5. K. Kaneko, F. Rodriguez-Reinoso eds., Nanoporous Materials for Gas Storage, Springer (2019).
6. Y. Yoshikawa, K. Teshima, R. Futamura, H, Tanaka, T. Iiyama, K. Kaneko, *Carbon* (2020), **171**, 681.
7. F. Vallejos-Burgos, F.-X. Coudert, K. Kaneko, Nature Comm. **9** (2018), 1812.2. R. Futamura, T. Iiyama, Y. Takasaki, Y. Gogotsi, M.J. Biggs, M. Salanne, J. Ségalini, P. Simon, K. Kaneko, Nature Materials, (2017), **16** 1163.

THERMODYNAMICS OF ADSORPTION DEFORMATION OF MICROPOROUS CARBONS

A.V. Neimark

aneimark@rutgers.edu
Department of Chemical and Biochemical Engineering, Rutgers University, USA

Phenomenon of adsorption-induced deformation recently attracted a considerable attention owing to its relevance to practical problems of mechanical stability and integrity of novel nanoporous materials and their adsorption properties. Guest molecules adsorbed in nanopores cause a substantial stress in the host matrix leading to its contraction or swelling depending on the specifics of host-guest interactions. Dubinin and his disciples pioneered the studies of deformation of microporous carbons and zeolites during gas adsorption, revealing enigmatic specifics of this phenomenon. In particular, it has been demonstrated in multiple examples that adsorption-induced deformation does not necessarily imply swelling. In many cases, the strain isotherm is nonmonotonic, indicating that upon the increase of adsorption, the adsorbent contracts at low pressures and then expands. I will present a general thermodynamic approach to predicting adsorption stress and respective deformation based on the classical theoretical models of adsorption, including Dubinin-Radushkevich and Langmuir models, as well as on the molecular level methods of Monte Carlo simulation and density functional theory. As a topical practical application, I will discuss the deformation of coal and shale in the process of methane displacement by carbon dioxide during the enhanced gas recovery and CO_2 sequestration at the geological conditions of elevated pressures and temperatures.

RECENT DEVELOPMENTS IN CARBONACEOUS MATERIAL CHARACTERIZATION

S. Lucena

lucena@ufc.br
Federal University of Ceará - UFC, Brazil

The use of adsorption experiments with different probe gas molecules has helped reveal the intricate microstructure of carbonaceous materials. Modeling and simulation tasks become exceptionally challenging because carbon material lacks long-range order and the difficulty of extracting data from advanced experimental techniques. Our group has sought procedures for generating less arbitrary heterogeneous model morphologies, particularly explicit heterogeneous structures based on reactive molecular dynamics. We obtained new heterogeneous models that organically reproduce the simultaneous structural defects (edges, corrugations, and amorphization) that coexist on real carbonaceous surfaces, experimentally identified by studies carried out in recent years. This new heterogeneous model, appropriated to kernels, allows extensive studies which were previously not possible. As examples of these studies, we present the concept of multikernel, the virtual pore model based on reactive molecular dynamics, kernels comparative performance, and how homogeneous and heterogeneous surfaces impact the pore size distribution obtained by different probe molecules.

THREE TYPES OF TWO-PHASE SURFACE TENSIONS OF ADSORBATE IN MESOPOROUS SYSTEMS AND METHODS FOR CALCULATING IT

Yu.K. Tovbin*, *E.S. Zaitseva

tovbinyk@mail.ru
Kurnakov Institute of General and Inorganic Chemistry RAS,
119991 Moscow, Russia

In many adsorption porous systems at temperatures T below the critical separation temperature $Tc(H)$, the two-phase state of the adsorbate "vapor in the pore" and "liquid in the pore" is realized as two coexisting phases with the formation of a meniscus of the vapor-liquid interface. Such menisci arise both in the equilibrium distribution of the adsorbate and in the case of the so-called capillary mechanisms of fluid flows. Surface tension (ST) determines the nature of the spatial distribution of mobile phases inside the solid lattice of polydisperse matrices (adsorbents, absorbents, catalysts, membranes, composites, etc.), which have a wide degree of heterogeneity caused by the porous, grain, and mixed porous-grain structure of real materials [1-4]. In such matrices, direct observations and measurements of all characteristics are difficult. Therefore, the development of a sufficiently accurate theory is required to provide reliable modeling of the properties of mobile components, especially ST.

It is shown in [5] that all existing methods for calculating the ST even for the vapor-liquid interface in the bulk phase [6–9] are incorrect since they don't correspond to the thermodynamic definition of Gibbs [10] as an excess value of the free energy of the phase boundary by in relation to the free energies of the coexisting phases. In [11,12], a method for calculating the ST according to Gibbs definition was formulated: the calculation of the volume state of coexisting phases of vapor and liquid should satisfy the Yang – Lee condensation theory [13,14], additional conditions of chemical and mechanical equilibrium are imposed on the properties of the transition region of the equilibrium boundary of any curvature in each layer. The new method for determining the ST is correct for considering other types of boundaries in a three-aggregate system [15].

The report provides an analysis of the state of molecular theory, focused on the description of three-aggregate systems from a unified point of view, including their three bulk phases and three types of phase boundaries: vapor-liquid, solid–vapor, and solid-liquid [15]. The calculation is carried out within the framework of the lattice gas model (LGM), which takes into account the direct correlations of interacting adsorbate molecules in the quasi-chemical approximation (QCA) [16,17]. The ideas of this model were used to describe a two-level structural model of mesoporous bodies and calculate the distributions of the adsorbate in a given structure of the adsorbent [17,18]. The supramolecular level of the model is presented in the form of a granule/grain of a porous material with a given distribution function, interconnected pores of different types and sizes. At the molecular level, LGM makes it possible to describe with equal accuracy the molecular distributions of the adsorbate in coexisting phases and at the interface between them. The transition region of the liquid-vapor interface between the pore walls is a complex inhomogeneous system in which the density of the substance changes both along the pore width and along the transition region between vapor and liquid, depending on the pore width and the potential of its walls. In this case, the existence of a multilayer adsorbate film on the surface of the pore wall in both the vapor and liquid phases is taken into account. The menisci between the vapor and liquid phases inside the pores are regions of coexistence of three phases of vapor, liquid, and solid [19].

The methodology for calculating the three types of ST consists of the following stages:

1) Formulation of the structural model of the sample observed (two-level model). In [18], a two-level structural model was proposed for porous systems: the supramolecular level reflected the type of pores and their size distribution, including taking into account the inhomogeneity of the pore walls in the joints of pores of different types, as well as their connectivity through paired structural distribution functions.

2) Calculation of local isotherms for different parts of an inhomogeneous system as a function of the external pressure of the adsorptive gives a description of molecular distributions over inhomogeneous sites of the general system in the LGM, which

reflects the intrinsic volume of molecules, excluding the double filling of the site with different molecules, and the interaction between them in the QCA [16,17].

3) Calculation of the total adsorption isotherm by weighing local isotherms using the structural distribution functions of sites of different types. This step is necessary for comparison with the experimentally observed adsorption isotherm.

4) Identification of areas of adsorbate condensation inside different sections of pores and finding coexisting densities of vapor and liquid inside each section of pores. The average densities of the coexisting vapor and liquid phases of the adsorbate in each of the pore types are determined using the Maxwell construction [14–17].

5) Calculation of the densities in the transition regions between the identified coexisting phases vapor-liquid, as well as concentration profiles between the coexisting phases liquid-vapor in their transition regions with a solid inside each type of pore [19-22]. This stage requires the expansion of the dimension of the structural functions of the first stage in order to reflect the transition region of the meniscus between two mobile phases within the pore under consideration. In the junction of pores of variable diameter and for any structural heterogeneity of the pore walls, the type of the site in the fluid-solid transition region depends both on the distance from the pore wall and on the coordinate along with the pore space.

6) Calculation according to the found profiles in point 5 of the vapor–solid and liquid-solid ST [20–22].

7) Calculation according to the found profiles in point 5 of the local values of meniscus vapor-liquid ST [19,20].

The developed method for calculating the ST allows one to obtain the average value of vapor-liquid ST, which is needed for comparison with the experiment, and its local changes depending on the physical properties of the system for analyzing the mechanisms of hysteresis. The difference between theoretical information and thermodynamic information lies in its more detailed nature, reflecting the dimensional and energy characteristics of the system. According to the existing tradition, solid-fluid STs are practically not used in adsorbents, although they are essential for analyzing the behavior of thin films outside porous systems. On the other hand, without these ST values, it is impossible to discuss the values of the contact angles of

the menisci in the pores. It is also shown that the traditional use of the ST value in thermodynamic estimates based on the Laplace and Kelvin equations [6,23] leads to distorted information about the system [13,17].

The traditional problem of assessing the ST is taking into account the roughness of a solid [6,21]. The real surface has chemical and structural heterogeneity, including different levels of roughness. The complex geometry of the pore walls is always a consequence of their nonequilibrium state with respect to the adsorbate. In thermodynamics, roughness is taken into account in an efficient way through the concept of the ratio of the areas of real and observed surfaces [24]. This introduces an empirical parameter into the assessment of areas and the ST value itself.

To clarify the analysis of the mechanisms of the appearance of adsorption-desorption hysteresis, the stability of a junction in slot-like porous systems was considered [25] depending on the length of the section and the energy of the walls. All the listed possibilities of the theory are generalized to the case of taking into account the deformation of the adsorbent under the influence of the adsorbate and external forces [26].

Thus, at present, a three-aggregate version of the discrete-continuum theory for calculating the distributions of molecules at the interface and a method for calculating three types of ST in a wide temperature range has been developed. A method for localizing three-phase contact areas and a description of the properties of these areas have been developed. Proposals for the algorithmization of approximating constructions of three-phase contact regions are discussed. Criteria for the organization of calculations in the region of three-aggregate solid-liquid-vapor contact are formulated, and the size effects for the contact angle are investigated depending on the geometry of the pore cross-section and the potential of the pore walls.

The proposed approach was used to study slit-like pores with smooth and rough walls, as well as isolated and interconnected cylindrical pores and small closed pores limited in volume.

References

1. T.G. Plachenov, S.D. Kolosentsev, Porometry (Khimiya, Leningrad, 1988), p. 175.
2. L.I . Kheifets, A.V. Neimark, Multiphase processes in porous solids (Khimiya, Moscow, 1982), p. 320.

3. P.G. Cheremskoi, Methods of studying the porosity of solids (Energoatomizdat, Moscow, 1985), p. 112.
4. A.P. Karnaukhov, Adsorption. Texture of dispersed porous materials (Nauka, Novosibirsk, 1999), p. 469.
5. Yu.K. Tovbin, Russian Journal of Physical Chemistry A (2018) **92**, p. 1045.
6. A.W. Adamson, Physical chemistry of surfaces. Third edition (Wiley, New–York–London–Sydney–Toronto, 1976).
7. S. Ono, S. Kondo Molecular theory of surface tension (IL, Moscow, 1963). [Handbuch der Physik, Vol X (Springer) 1960].
8. J. Rowlinson, B. Widom, Molecular theory of capillarity (Mir, Moscow, 1986). [Oxford: ClarendonPress, 1982].
9. A.I. Rusanov, Phase equilibria and surface pnehomena (Khimiya, Leningrad, 1967).
10. J.W. Gibbs, Thermodynamics. Statistical mechanics (Nauka, Moscow, 1982).
11. Yu.K. Tovbin, Russian Journal of Physical Chemistry A (2018) **92**, p. 2424.
12. Yu.K. Tovbin, Russian Journal of Physical Chemistry A (2019) **93**, p. C. 1662.
13. Yu.K. Tovbin, Small systems and fundamentals of thermodynamics (CRC Press, Boca Raton, 2019), p. 415.
14. T.L. Hill, Statistical Mechanics. Principles and Selected Applications (McGraw–Hill Book Comp.Inc., New York, 1956).
15. Yu.K. Tovbin, Russian Journal of Physical Chemistry A (2020) **94**, p. 1515.
16. Yu.K. Tovbin, Theory of physical chemistry processes at a gas-solid surface processes (CRC Press, Boca Raton, 1991), p. 348.
17. Yu.K. Tovbin, Molecular theory of adsorption in porous solids (CRC Press, Boca Raton, 2017), p. 726.
18. Yu.K. Tovbin, Russian Chemical Bulletin (2003) No. 4. p. 827.
19. Yu.K. Tovbin, D.V. Eremich, V.N. Komarov, E.E. Gvozdeva, Khim. Fizika (2007) **26**, p. 98.
20. Yu.K. Tovbin, E.S. Zaitseva, Russian Journal of Physical Chemistry A (2020) **94**, p. 2526.
21. E.S. Zaitseva, Yu.K. Tovbin**,** Protection of Metals and Physical Chemistry of Surfaces (2021), **57**, p. 260.
22. E.S. Zaitseva, E.E. Gvozdeva, Yu.K. Tovbin**,** Protection of Metals and Physical Chemistry of Surfaces (2021) **57**, p. 647.
23. S.J. Gregg, K.S.W. Sing, Adsorption, Surface Area and Porosity (Academic Press., London, 1982).
24. R.N. Wenzel, Ind. Eng. Chem. (1936) **28**, p. 988.
25. E.S. Zaitseva, E.E. Gvozdeva, Yu.K. Tovbin, Prot. Met. Phys. Chem. Surf. (2020), **56**, p. 1107.
26. Yu.K. Tovbin, Prot. Met. Phys. Chem. Surf. (2021), **57**, p. 1.

SURFACE TENSION OF STRATIFYING ADSORBATE INSIDE CYLINDRICAL PORES

***E.S. Zaitseva*, Yu.K.Tovbin**

zaya261011@gmail.com
Kurnakov Institute of General and Inorganic Chemistry RAS, 119991, Moscow, Russia

Various methods of molecular modeling based on interparticle potential functions [1] have played an active role in studying the properties of the adsorbate–adsorbent system. These methods make it possible to obtain detailed information on numerous features of molecular distribution and their effect on the observed characteristics of adsorption processes. The greatest difficulty is presented by the work on calculating surface tension (ST) in porous systems. This is connected both with the complexity of calculating the free energy of the system in order to estimate the ST value and with the existing problems of thermodynamic analysis within the framework of classical Gibbs thermodynamics [2]. In [3], the conditions for calculating the ST value were formulated, and in [4], these conditions were realized for an isolated slit pore.

In the present work, we study the molecular distributions of the adsorbate at the interface between vapor and liquid located in cylindrical pores of infinite length, diameter D, and field potential Q in a monolayer adjacent to the pore wall. The equations of the studied solid–mobile phase system were obtained in [5].

The cylindrical pores contain (see Fig. 1) homogeneous regions of liquid (1) and vapor (2). Liquid and vapor are separated from the pore walls by transition regions solid-liquid (4) with width κ_{sl} and solid – vapor (5) with width κ_{sv}, respectively. Between the phases, there is a transition region liquid-vapor (3) with a width of κ_{lv}, and below, near the pore wall, there is a region of three phases solid – liquid-vapor (6).

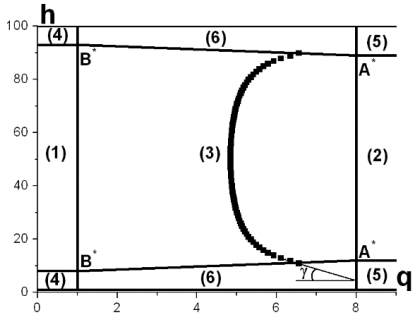

Fig. 1. Scheme of phase regions and transition regions between coexisting phases and a solid wall in cylindrical pores

Between the homogeneous regions (1) and (2) (Fig. 1) of the phases, a density gradient θ_q is realized in the liquid – vapor transition region (region (3), Fig. 1), shown in Fig. 2 for system 1 (pore of diameter D = 100 with potential Q = 5) – (curve 1), and system 2 (pore of diameter D = 30 with Q = 0.5) – curve 2, at κ_{lv} = 6 and reduced temperature τ = 0.82 normalized to the critical stratifying temperature outside the pores.

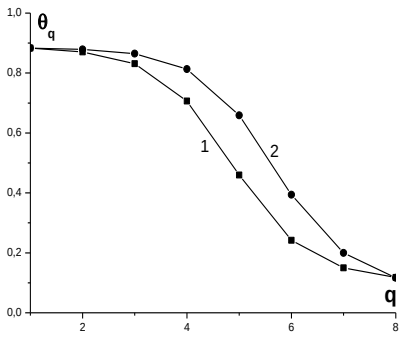

Fig. 2. Local density profiles

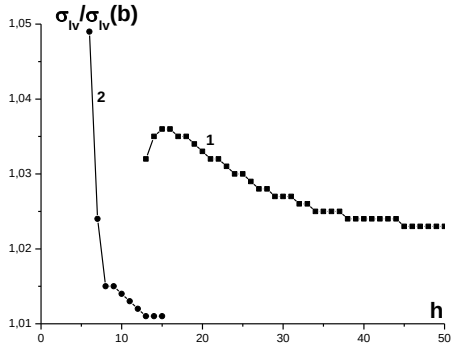

Fig. 3. Profile of local values of the liquid-vapor ST

Fig. 3 demonstrates the profiles of the local values of the liquid-vapor ST, normalized to liquid-vapor ST in an unlimited system σ_{lv}(b), for systems 1 and 2 (curves 1-2, respectively), which were obtained from the density profiles in Fig. 2 in the area (3), Fig. 1. The local value of the liquid-vapor ST is calculated by the method [6] at each point of the equimolecular surface (a line with square symbols in Fig. 1).

At the boundary with a solid, the values of ST are calculated for a solid-liquid and a solid–vapor interfaces inside regions (4) and (5) in Fig. 1, respectively.

The table below demonstrates for systems 1 and 2: the values of the widths κ_{lv}, κ_{sl}, and κ_{sv}, the values of the liquid-vapor ST at the center of the pore σ^*_{lv}, the liquid-vapor σ^{av}_{lv} value averaged over the pore width, the solid-liquid ST σ_{sl} and the solid – vapor ST σ_{sv}.

Table. The ST values of three two-phase boundaries

Systems	κ_{lv}	κ_{sl}	κ_{sv}	$\sigma^*_{lv}/\sigma_{lv}$(b)	$\sigma^{av}_{lv}/\sigma_{lv}$(b)	σ_{sl}/σ_{lv}(b)	σ_{sv}/σ_{lv}(b)
1	8	8	12	1.023	1.028	-53.81	-52.52
2	8	6	8	1.010	1.017	-1.78	-0.51

Negative values of the solid-fluid ST are due to the accepted condition for choosing the position of the phase boundary for nonequilibrium states of the walls of the adsorbent [4].

This work demonstrates the possibilities of the microscopic approach for calculating the ST, which excludes the introduction of any thermodynamic constructions and the presence of metastable states. The results obtained make it possible to arrive at the calculations of the molecular distributions within the liquid-vapor menisci and the ST values in polydisperse materials. This possibility will make it possible to study the role of the distributions of two phases in complex porous materials, which affect both the equilibrium distribution of adsorbate during capillary condensation and the flows in various models of adsorbate transport.

References

1. Yu.K. Tovbin, Molecular theory of adsorption in porous solids (CRC Press, Boca Raton, 2017), 726 p.
2. J.W. Gibbs, Thermodynamics. Statistical mechanics. Moscow, Nauka. 1982.
3. Yu.K. Tovbin, Russ. J. Phys. Chem. A (2018) **92**, 2424.
4. Yu.K. Tovbin, E.S. Zaitseva, Russ. J. Phys. Chem. A (2020) **94**, 2526.
5. Yu.K. Tovbin, Russ. J. Phys. Chem. A (1992) **66**, 741.
6. Yu.K. Tovbin, D.V. Eremich, V.N. Komarov, E.E. Gvozdeva. Khim. Fizika. (2007) **26**, 98.

DEVELOPMENT OF QUANTUM CHEMICAL METHODS FOR THEORETICAL STUDY OF COMPLEX CARBON-BASED ADSORBENTS

I. Popov, A. Tchougréeff

ilya.vl.popov@gmail.com
M.M. Dubinin's Laboratory of Sorption Processes,
A.N. Frumkin Institute of Physical Chemistry and Electrochemistry, Russian Academy of Sciences, 119071, Moscow, Russia

Carbon-based solid materials form a wide and actively studied class of adsorbents proving useful for the storage and transportation of energy gases [1] such as methane, hydrogen etc. However, with all the advances made in carbon adsorbents, many problems devoted to the characterization of their crystal structures or adsorption on the defected surfaces remain unsolved. Most of these problems require the involvement of theoretical modeling due to the inability of modern experimental techniques to measure all the desired properties in such complex systems directly. In turn, theoretical modeling substantially relies on the quality and effectiveness of quantum chemical methods used to calculate the electronic structure.

In the present contribution, authors demonstrate their recent advances in the development and programmatic realization of quantum chemical methods suitable for the theoretical modeling of adsorbents. Two new methods are presented available in the form of standalone programs: deductive molecular mechanics of carbon allotropes (ADAMAS) [2,3] and the Green's function method to describe defected crystals (GoGreenGo) [4]. The first program employs group function formalism and valence bond theory to describe the energy, structural and mechanical properties of solid carbon allotropes. It demonstrates accuracy comparable to one of the high-level PAW-DFT methods, being more efficient by order of magnitude. The second program performs efficient calculations of the electronic structure of locally perturbed crystals and, therefore, allows the modeling of single adsorption acts on the defected surfaces. The authors present a theoretical basis, workflow, and test results for both approaches.

As a practical application of the proposed methods, we introduce and analyze a structural model of the bulged graphite with C_2 bridge defects connecting graphite's mono-layers arranged in the AAA configuration (see the Figure below). Our results

obtained with ADAMAS and GoGreenGo supported by the PAW-DFT calculations show that the proposed structural model demonstrates an increase of inter-layer distance experimentally observed in the bulged graphite. Moreover, results indicate that in the case of the low concentration of the C_2 bridges, the energy of the defected structure exceeds the energy of the hexagonal graphite by 10-20 kJ/mol, which means it could be formed under experimental conditions. First estimations show that mass-fraction of adsorbed H_2 in the proposed model can reach 5-6%. A more detailed study of adsorption processes in the C_2-bridge model of the bulged graphite will be performed in the future.

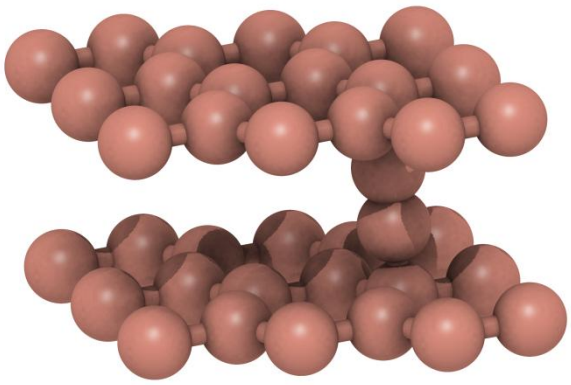

References

1. Tsivadze A. Yu., Aksyutin O.E., Ishkov A.G., Men'shchikov I.E., Fomkin A.A., Shkolin A.V., Khozina E.V., Grachev V.A. Russ. Chem. Rev. (2018) **87**, 950.

2. Popov I.V., Görne A.L., Tchougreeff A.L., Dronskowski R. Phys. Chem. Chem. Phys. (2019) **21**, 10961.

3. Popov I.V., Slavin V.V., Tchougreeff A.L., Dronskowski R. Phys. Chem. Chem. Phys. (2019) **21**, 18138.

4. Popov I.V., Kushnir T.S., Tchougreeff A.L. J. Comput. Chem. (2021) *Just accepted*.

ERROR PROPAGATION IN MULTISCALE SIMULATIONS OF PRESSURE-SWING ADSORPTION PROCESSES FOR CARBON CAPTURE

C. Cleeton, A. Farmahini, L. Sarkisov

lev.sarkisov@manchester.ac.uk
the University of Manchester, United Kingdom

A new recent concept in the screening of porous materials for carbon capture using Pressure Swing Adsorption is based on multiscale workflows, where data from molecular simulation is passed on to detailed process models to evaluate the performance of a particular candidate material [1]. For PSA processes based on either experimental data or data from simulations, a single Pareto front linking energy penalty and productivity of the process is commonly taken as the performance indicator for a given material.

In reality, experimental measurements performed on the same materials by different groups indicate a significant degree of scattering. Recently, Park et al. [2] discussed how to systematically quantify the uncertainty of experimental adsorption data and identify potential outliers amongst interlaboratory data sets. Recent studies from Farmahini et al. [3] indicate that uncertainty in the material properties, such as heat capacity, may have a significant effect on the overall performance of the material at the actual process level.

The question we pose in this study is how the uncertainty in all material-specific experimental data propagates across the multiscale workflows and manifests itself in the process level of description.

We consider the case of 13X zeolite, a well-known benchmark for carbon capture studies. Using curated experimental data from the literature, we develop a probabilistic isotherm model using hierarchical Bayesian inference. In the next step, we combine detailed process optimization and surrogate models to explore how the uncertainty of all experimental data propagates to the process level.

We observe that i) the performance of the 13X material is more accurately represented by a cloud of possible performances rather than by a single Pareto front; ii) the dimensions of this cloud are comparable to the differences in performance of various materials based on their single Pareto front. These observations cast some

doubts on the reliability of performance rankings for materials recently reported in process-based computational screening. We, therefore, encourage future studies to publish their Pareto data along with some uncertainty analyses for a more representative interpretation of performance.

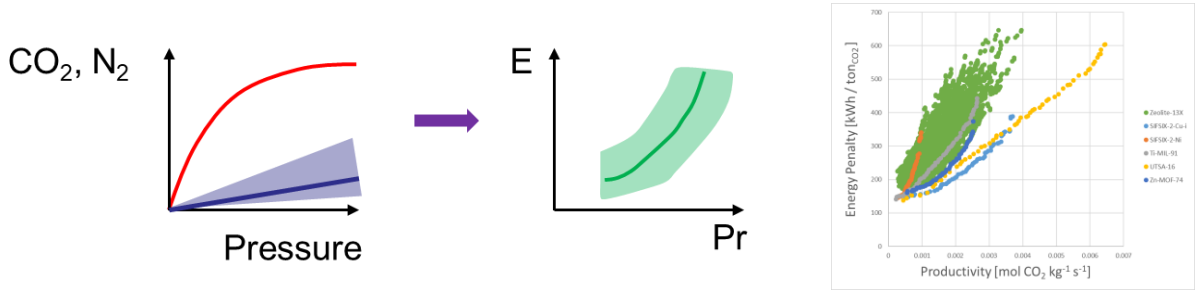

Fig. 1. Error propagation in multiscale workflows, on the left. Performance cloud for 13X zeolite (green symbols) compared to the Pareto performance fronts for several materials based on a single set of experimental data (on the right).

References:

1. A. Farmahini, et al. Chem. Rev. (2021) **121**, 10666–10741
2. J. Park, et al. Chem. Mater. (2017) **29**, 10487–10495
3. A. Farmahini, et al. Ind. Eng. Chem. Res. (2018) **57**, 15491–15511

COMPRESSIBILITY OF ADSORBED WATER FROM MOLECULAR SIMULATIONS

G.Y. Gor

gor@njit.edu; web: http://porousmaterials.net
Otto H. York Department of Chemical and Materials Engineering
New Jersey Institute of Technology, University Heights, Newark, NJ 07102, USA

Compressibility of a fluid in a porous medium determines the response of the medium to mechanical loads and elastic waves propagation in particular. If the pores of the medium are in the nanometer range, many thermodynamic properties of the fluid confined in such pores are altered. In this talk, I will show that fluid compressibility is not an exception [1]. I will show how the compressibility of a fluid in a mesopore can be calculated based on Monte Carlo molecular simulation and illustrate them with the example calculations for simple fluids: argon, nitrogen, and methane. The results of the simulations agree well with the compressibilities of these fluids measured in adsorption-ultrasonic experiments on Vycor glass samples [2]. In addition to that, molecular simulations for a range of pore sizes showed that there is a simple relation between the compressibility of the confined fluid and the size of the confining pore. Finally, I will also show preliminary results on the compressibility of water in mesopores, which behavior differs from that of the simple fluids.

References

1. Dobrzanski, C. D.; Gurevich, B.; Gor, G. Y. "Elastic Properties of Confined Fluids from Molecular Modeling to Ultrasonic Experiments on Porous Solids" Appl. Phys. Rev. 2021, 8, 021317, DOI: 10.1063/5.0024114
2. Maximov, M. A.; Gor, G. Y. "Molecular Simulations Shed Light on Potential Uses of Ultrasound in Nitrogen Adsorption Experiments" Langmuir 2018, 34(51), 15650-15657, DOI: 10.1021/acs.langmuir.8b02909

MOLECULAR DYNAMICS SIMULATION OF ADSORPTION OF A METHANE-ETHANE MIXTURE IN SLIT-LIKE MICROPORES

A.V. Shkolin, V.V. Gaidamavichyute, A.A. Fomkin, I.E. Men'shchikov

shkolin@phyche.ac.ru
Laboratory of sorption processes, A.N. Frumkin Institute of Physical Chemistry and Electrochemistry, Russian Academy of Sciences, 119071 Moscow, Russia

The problem of identifying the optimal conditions of the adsorption-based accumulation and separation of normal hydrocarbons, especially methane and ethane, is relevant. To solve it, one needs to have an idea of the structure and behaviors of adsorbed molecules in the micropores of an adsorbent. In the present work, the molecular dynamics (MD) method was used to carry out numerical experiments in a model microporous carbon adsorbent. Two graphene layers form the model pore, and the distance between the outer parts of carbon atoms on the opposite pore walls was varied from 0.8 to 1.2 nm. Recently [1], a model system composed of such micropores was analyzed in terms of Dubinin's theory of volume filling of micropores. The modeling cell was a parallelepiped with a square base with a side of 10 nm and a height limited by the planes drawn along the centers of carbon atoms of the graphene layers. Periodic conditions were set at the boundaries of the simulation cell. A different number of methane and ethane molecules was introduced into the cell in such a way that a molar ethane/methane ratio was constant and equal to 95/5.

The MD simulation was carried out for the microcanonical ensemble (*N,V,T*) at a constant temperature. The temperature of the numerical experiment was 298 K. The Tinker Molecular Modeling [2] software package was employed. The structure of adsorbed hydrocarbons was simulated using the atom-atom potential in the form of a universal OPLSAA force field [3]. For all the systems, we examined the MD trajectories with the same length of 2×10^{-9} s. Numerical integration of the equation of motion was performed with the elementary step of 10^{-15} s.

The MD simulations revealed that the distribution of the mixture components depended on the pore width (see Figs. 1 and 2).

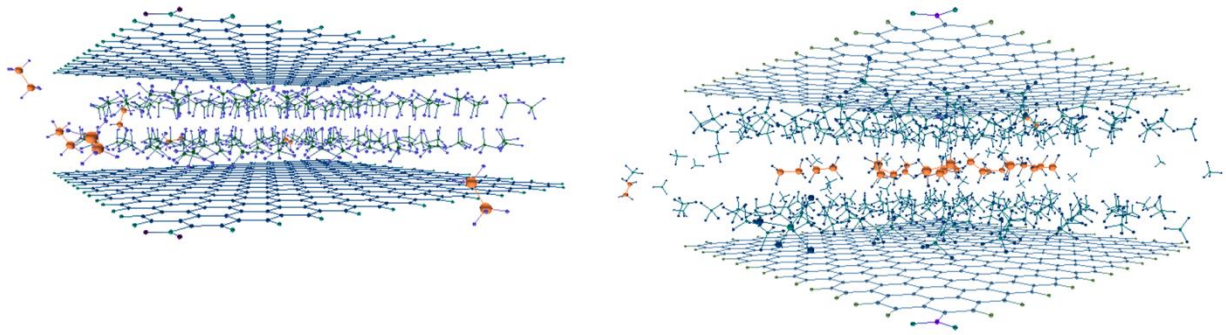

а *б*

Fig. 1. MD trajectory snapshots for the simulated system, involving two graphene layers, which compose a pore with a width of 0.8 (*a*) and 1.2 nm (*b*), and 300 molecules of the 95%CH_4 + 5%C_2H_6 mixture. Solid lines show the atom bonds in the graphene layers. Methane and ethane molecules are represented by non-scalable blue and orange graphic objects, respectively. Methane and ethane molecules outside the pore are not shown.

At the early stage (Fig. 2), the adsorption of methane and ethane increases smoothly with the number of molecules in the simulation system. The adsorbed methane and ethane molecules are predominantly located near the graphene surfaces. Ethane molecules are closer to the edges of the graphene layers due to potential barriers at the exit of the pore. With a further increase in the total number of molecules in the simulation system, methane molecules almost completely fill near-surface regions, whereas ethane molecules change their location depending on the pore width. In the pore with a width of 0.8 nm, ethane molecules are gradually displaced from the pore (see Fig. 1a) until their adsorption does not become zero (Fig. 2). In the 1.2 nm pore, ethane molecules move close to the central regions of the pore due to the changes in the balance between the enhancing ethane-ethane intermolecular attraction and methane-ethane interactions. In this case, the number of adsorbed methane molecules in the pore remains virtually unchanged. In contrast, the number of adsorbed ethane increases progressively (see Fig. 2).

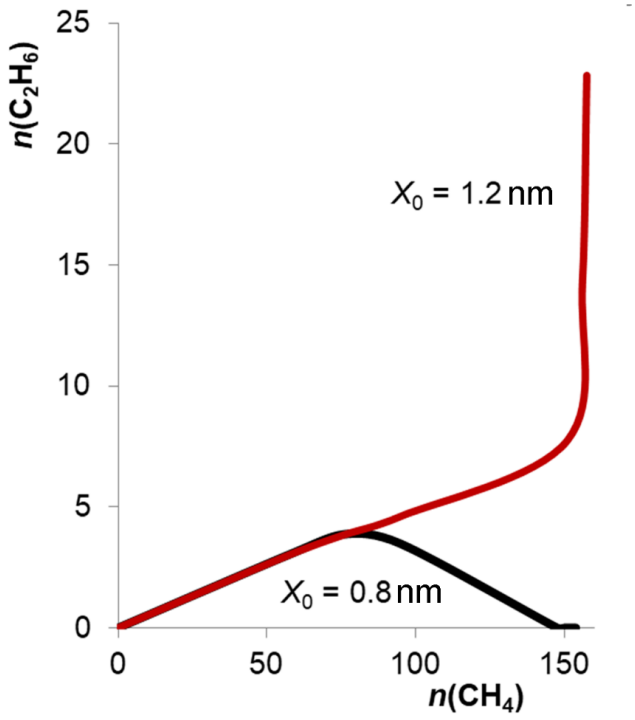

Fig. 2. The number of adsorbed ethane molecules, $n(C_2H_6)$, versus the number of adsorbed methane molecules, $n(CH_4)$, during adsorption of the $95\%CH_4 + 5\%C_2H_6$ mixture in the model pore with a width X_0 = 0.8 and 1.2 nm.

Thus, the distribution of adsorbed molecules of the methane-ethane mixture depends on the micropore width and the degree of its filling. In the region of small fillings, the adsorption of the mixture components occurs mainly near the pore walls regardless of the pore width in the studied range (Fig. 2). With the increase in the pore filling, the redistribution of the mixture components in a pore (and the corresponding value of adsorption) is determined by the pore width and the molecular structure.

Funding and acknowledgments

The work was carried out within the framework of the State Task (no. 0081-2019-0018).

References

1. I.E. Men'shchikov, A.A. Fomkin, A.V. Shkolin, V.Yu. Yakovlev, E.V. Khozina. Russ. Chem. Bull. (2018) **67**. 1814.
2. TINKER 8: Software Tools for Molecular Design,
3. J.A. Rackers, Z. Wang, C. Lu, M.L. Laury, L. Lagardère, M.J. Schnieders, J.-P. Piquemal, P. Ren, J.W. Ponder, J. Chem Theor. Comput. (2018) **14**, 5273.
4. W.L. Jorgensen, D.S. Maxwell, J. Tirado-Rives. J. Am. Chem. Soc. (1996) **118**, 11225.

MOLECULAR DYNAMICS STUDY OF SPATIAL ORIENTATION OF THE N-PENTANE MOLECULE ADSORBED IN MODEL SLIT-LIKE PORES OF CARBON ADSORBENT

V.V. Gaidamavichyute, A.V. Shkolin, A.A. Fomkin, I.E. Men'shchikov

shkolin@phyche.ac.ru
Laboratory of sorption processes, A.N. Frumkin Institute of Physical Chemistry and Electrochemistry, Russian Academy of Sciences, 119071 Moscow, Russia

The molecular dynamics (MD) method provides valuable insights in the structure of adsorbate in pores and the time variations in intermolecular interactions under given conditions [1]. The MD method was used to study the adsorption of one n-pentane molecule in the slit-like microporous carbon structure at the temperature of 293 K. The model slit-like pore was formed by graphene layers. The pore width was calculated as a distance between the outer parts of carbon atoms on the graphene layers and varied from ~6 Å to ~15 Å. The TINKER software package [2] and the OPLS-AA atom force field potential [3] were employed for the MD simulations. The numerical experiment was carried out in a simulation cubic cell with an edge length of 10 nm. Two separated graphene layers composed the model carbon adsorbent in the central part of the simulation cell. One n-pentane molecule was introduced in the simulation cell. When the molecule occurred in the pore, the probability density functions and its spatial orientations were evaluated.

The numerical experiments revealed the changes in the position of the adsorbed molecule in the adsorbent, which depended on the pore width.

When the pore width ranged from 6 to 10 Å, the n-pentane molecule was found in the central region of the pore. As the pore width increased, the n-pentane molecule changed its orientation. The wider the pore, the greater the angle of rotation of the symmetry axis of the molecule relative to the axial plane in the center of the pore.

When the pore width was 11 Å, the n-pentane molecule is predominantly oriented perpendicular to the pore walls (Fig. 1). There was also a possibility that the molecule would turn in a plane parallel to the pore walls while it was located closer to one of the pore walls (Fig. 2).

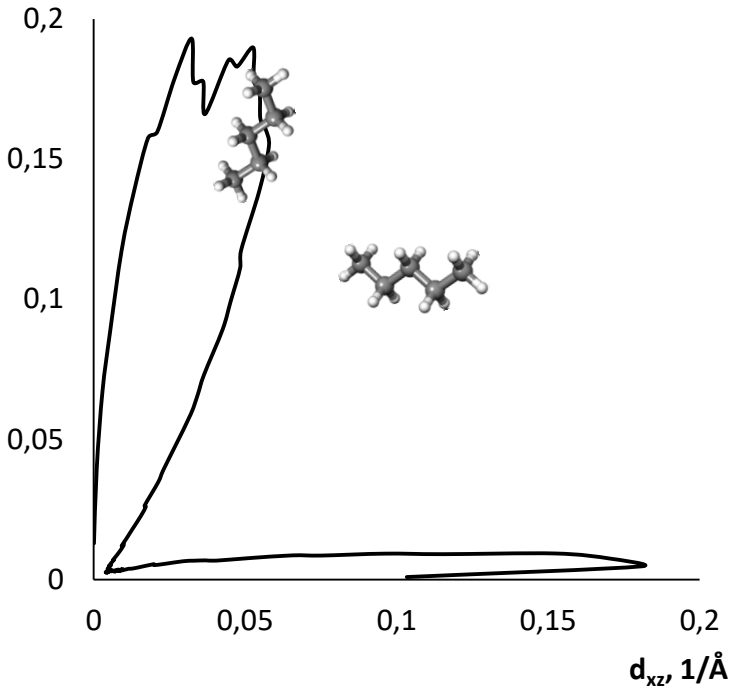

Fig. 1. The probability density of the spatial orientation of the n-pentane molecule in the *xz* plane (perpendicular to the pore walls) in the pore with the width of 11 Å plotted in polar coordinates.

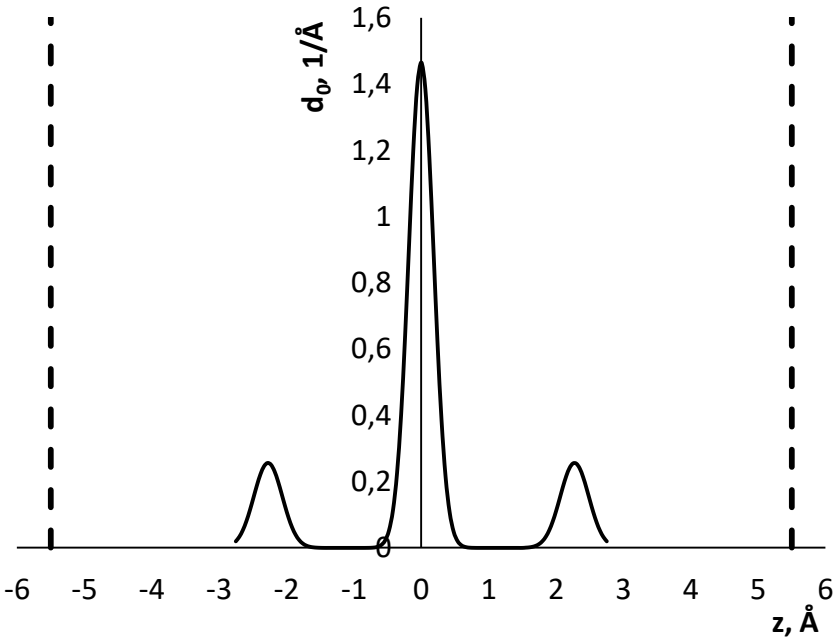

Fig. 2. The probability density of the location of the n-pentane molecule along the z-axis (perpendicular to the pore walls) of the pore. The pore width is 11 Å. The dashed lines show the pore surfaces composed of the outer parts of the carbon atoms of graphene layers.

As seen from Fig. 1, the n-pentane molecule is predominantly (with a probability 0f 73 %) located at the angle of 80.5 degrees to the graphene walls. The probability of the parallel orientation of the n-pentane molecule relative to the pore walls was 27 %.

According to the calculations for the wider pores with the width from 12 to 15 Å, the n-pentane molecule could be found with equal probability near one of the pore walls at a distance of 3.1 Å. Note that it is oriented parallel to the pore walls.

Funding and acknowledgments

The work was carried out within the framework of the State Task (no. 0081-2019-0018) "Fundamental physicochemical patterns of adsorption, adsorption-based separation, adsorption-electrochemical ion-exchange processes in nanoporous materials and fundamentals of targeted synthesis of new adsorbents".

The authors would like to thank the developers of the Tinker software package "A Modular Software Package for Molecular Design and Simulation" for the opportunity to use it in their work.

References

1. A.V. Shkolin, A.A. Fomkin. Phys. Prot. Met. Phys. Chem. Surf. (2013) **49**, 373.
2. J.A. Rackers, Z. Wang, C. Lu, M.L. Laury, L. Lagardère, M.J. Schnieders, J.-P. Piquemal, P. Ren, J.W. Ponder, J. Chem Theor. Comput. (2018) **14**, 5273.
3. W.L. Jorgensen, D.S. Maxwell, J. Tirado-Rives. J. Am. Chem. Soc. (1996) **118**, 11225.

THE CALCULATION OF THE THERMODYNAMIC CHARACTERISTICS OF ISOMERS ADSORPTION ON THE GRAPHITE BY THE MONTE CARLO METHOD

S.Yu. Kudryashov, V.A. Gladarenko

e-mail: kstasu@mail.ru
Samara State Technical University, Samara, 443100, Russia

The work considers the adsorption of vapors of volatile organic compounds on the basal plane of graphite crystal in the region of extremely low surface coverage (Henry's law region for adsorption equilibria). The aim is to establish the possibility of calculating the thermodynamic characteristics of adsorption (TCA) of various compounds, including isomers. Such calculations make it possible to identify the components of mixtures separated by gas-adsorption chromatography (on columns with graphitized thermal blacks) and establish the order of the release of isomers from the chromatographic column [1]. If the composition of the mixture to be separated is known (even if only partially), then predicting the TCA values of its intended components can be used to establish the possibility (or impossibility) of separating from each other substances similar in properties (primarily isomers) under the given conditions, as well as for the selection of optimal conditions separation of the mixture as a whole.

Henry's constants, heat values, and entropy changes during adsorption were calculated by the Gibbs Ensemble Monte Carlo method (GEMC) [2, 3]. The potential energy of the adsorbed molecule was computed using the well-known Crowell approximation [4] (see also [5]) by summing the semiempirical atom-atom potentials (AAP) in the form of Lennard-Jones potentials. For nonrigid molecules with one or two degrees of freedom of internal rotation, the corresponding hindered internal rotation potentials were assigned, approximately assuming that adsorption does not affect the value of the internal rotation barriers. The structural parameters of the adsorbate molecules were taken from the literature.

The main objects are isomeric xylenes (o-, m- and p-) and anthracene and phenanthrene. Methane (H, $C(sp^3)$) and benzene (C(ar)) molecules are the references in determining the AAP constants. The AAP parameters of the graphite carbon atom

(C(gr)) were taken from the literature [6, 7], the parameters of mixed potentials were calculated according to the most straightforward combination rules. The assumptions' correctness was tested using the example of toluene (a molecule with one degree of freedom of internal rotation). The rotation of two methyl groups in the case of xylene molecules was considered independent. The possibility of transferring the AAP parameters to atoms that make up polycyclic aromatic hydrocarbon (PAH) molecules was tested using naphthalene as an example. PAH molecules can be considered quasi-rigid molecules (there are no intramolecular types of motion), which significantly simplifies the TCA calculation.

The results obtained by modeling adsorption were compared with experimental and calculated data taken from the literature [5, 8, 9]. In all cases, the calculation by the Monte Carlo method is in perfect agreement with the experiment. Thus, for o- and p-xylenes, the calculated TCA values are identical, i.e., there is no selectivity for the adsorption of their molecules on graphitized carbon blacks, which entirely agrees with the experimental data (see, for example, [10]). In the case of phenanthrene and anthracene, practically identical values of the heat of adsorption are observed; therefore, the difference in the experimental Henry constants of these isomers is due to the difference in the change entropy during adsorption [5].

Thus, the results obtained in this work confirm the possibility of using the Monte Carlo method for predicting TCA for isomers of organic compounds.

References

1. A.K. Buryak. Application of molecular statistical methods for calculating the thermodynamic characteristics of adsorption in the chromatography-mass spectrometric identification of organic compounds. Russ. Chem. Rev. (2002), **71**, 695.
2. D.P. Landau, K. Binder. A guide to Monte Carlo simulations in statistical physics. New York: Cambridge University Press, 2005. 449 p.
3. A.Z. Panagiotopoulos. Direct Determination of Fluid Phase Equilibria by Simulation in the Gibbs Ensemble: A Review. Mol. Simul. (1992), **9**, 1.
4. A.D. Crowell. Approximate Method of Evaluating Lattice Sums of r^{-n} for Graphite. J. Chem. Phys. (1954), **22**, 1397.

5. N.N. Avgul, A.V. Kiselev, D.P. Poshkus. Adsorption of gases and vapors on homogeneous surfaces. Moscow: Khimia, 1975. 384 p.
6. A.D. Crowell. Potential Energy Functions for Graphite. J. Chem. Phys. (1958), **29**, 446.
7. A.D. Crowell, R.B. Steele. Interaction Potentials of Simple Nonpolar Molecules with Graphite. J. Chem. Phys. (1961), **34**, 1347.
8. E.V. Kalaschnikova, A.V. Kiselev, K.D. Shcherbakova. Gas chromatographic investigation of adsorption equilibria on graphitized thermal carbon black. II. Henry constants and heats of adsorption of C_6-C_{14} aromatic hydrocarbons at zero coverage. Chromatographia (1974), **7**, 22.
9. C. Vidal-Madjar, E. Bekassy-Molnar. Molecular statistical theory of adsorption for hydrocarbons on graphite. Effect of polarizability anisotropy in adsorption potential. J. Phys. Chem. (1984), **88**, 232.
10. T. Halász, C. Horváth. Thin-Layer Graphited Carbon Black as the Stationary Phase for Capillary Columns in Gas Chromatography. Nature (1963), **197**, 71.

MACHINE LEARNING EXERCISE FOR THE ADSORPTION-DESORPTION HYSTERESIS LOOP RECOGNITION

M.S. Mel'gunov

max@catalysis.ru
FRC Boreskov Institute of Catalysis, SB RAS, 630090, Novosibirsk, Russia

Gas porosimetry has become widespread nowadays as never due to the worldwide availability of numerous instruments for adsorption-desorption isotherms measurements from different manufacturers. More and more researchers with insufficient background in adsorption science apply this method in various fields. There are two ways to meet this wave: the scientific popularization of the essential features and complications of this method through webinars, teaching programs, etc., and, the second, employment of prior analysis of raw experimental data into modern software prompting inexperienced researchers the most reliable ways for the proper analysis. Both ways are important. In this contribution, we discuss the possibility of automatic recognition of the adsorption-desorption hysteresis loop type by means of the machine learning based on numerous data accumulated in the Boreskov Institute of Catalysis for dozens of years.

The proper attribution of the hysteresis loop type is important for the successive choice of the method for the pore size distribution, prompting which branch reflects more reliable information on porous structure, presence or absence of evaporation induced cavitation, pore-blocking effects, and their deconvolution. There are six known canonical types of the hysteresis loops. But our practice shows that intermediate shapes are also important. E.g., frequently, we observed the loops very similar to the case of incomplete pore filling, as it is observed when the hysteresis loop scanning technique is applied (Figure 1). In this case, the traditionally recommended desorption branch cannot be used for the pore size distribution evaluation since only the unknown part of pores is involved in desorption. This and some other illustrative examples are discussed in the presentation, showing the significance of the problem.

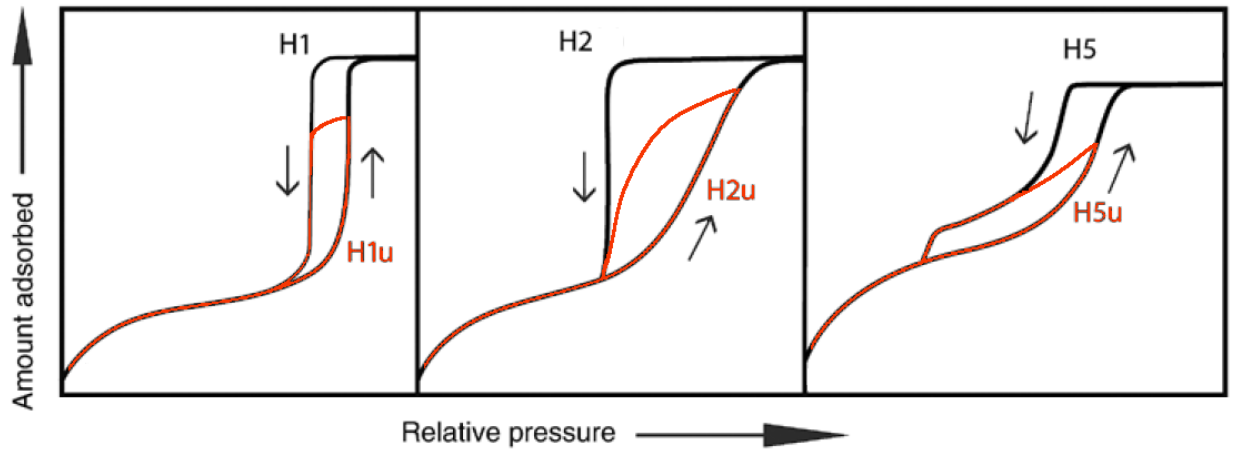

Fig 1. Possible shapes of plateau-absent loops (red) compared to their canonical ancestor loops (black).

According to our cumulative knowledge inspection of only one mathematical parameter, such as the slope, inflection, widening, narrowing towards both axis of adsorption-desorption curves, is not sufficient for the robust attribution of the loop. The particular values of all these parameters show a fairly widespread, and only the machine learning approach allows establishing the reliable correlations that allow the proper attribution of the loop type with the reliable probability. These aspects are discussed in the presentation.

Acknowledgments

This work was supported by the Ministry of Science and Higher Education of the Russian Federation within the governmental order for Boreskov Institute of Catalysis (project AAAA-A21-121011390054-1).

HIGH-RESOLUTION ADSORPTION ISOTHERMS WITH PRECISE TEMPERATURE CONTROL AS A TOOL FOR INSIGHT TO THE ADSORPTION THERMODYNAMICS AND MODELS

A.B. Ayupov [1], ***S. Ehrling*** [2]

artem@catalysis.ru
[1]*Boreskov Instituite of Catalysis, 630090, Novosibirsk, Russia*
[2]*3P INSTRUMENTS GmbH & Co. KG, Branch office Leipzig, 04129 Leipzig, Germany*

All adsorption measurements need temperature control and monitoring. In industrial applications, it is necessary to know how the adsorbent pellets heat up during adsorption and cool down during desorption. Often, information about the adsorption temperature and its accuracy are mandatory in order to calculate the enthalpy of adsorption or to evaluate the adsorption activation energy in kinetic measurements. In the course of adsorption isotherm measurements, the temperature stability and the correct information about its value are required for a precise calculation of adsorption uptake and to be able to estimate the characteristics of the porous structure accurately. Despite this categorical demand, the measurements of several adsorption isotherms at different temperatures with some given steps, especially at cryogenic temperatures, are much less frequent in common research practice. Here we present the opportunities of our new temperature controlling device series **cryoTune**.

The **cryoTune** series consists of three models of devices, which differ in their working temperature range (see Table 1). The accuracy of temperature control provides the standard deviation ±0.004 K.

Table 1. The **cryoTun**e series models

Model	Working temperature, K	Examples of gases at boiling points
cryoTune 87	82 – 135	Ar at 87 K, O_2 at 90 K, CH_4 at 112 K, Kr at 120 K
cryoTune 120	115 – 230	Kr at 120 K, Xe at 165 K, CO_2 at 195 K
cryoTune 195	180 – 323	CO_2 at 195 K and 273 K, C_2H_6 at 185 K, C_3H_8 at 231 K, n-C_4H_{10} at 273 K

The use of the **cryoTune** technology for adsorption studies of different materials (see an example in Fig.1) shows that such precise temperature control could become a routine method in adsorption studies.

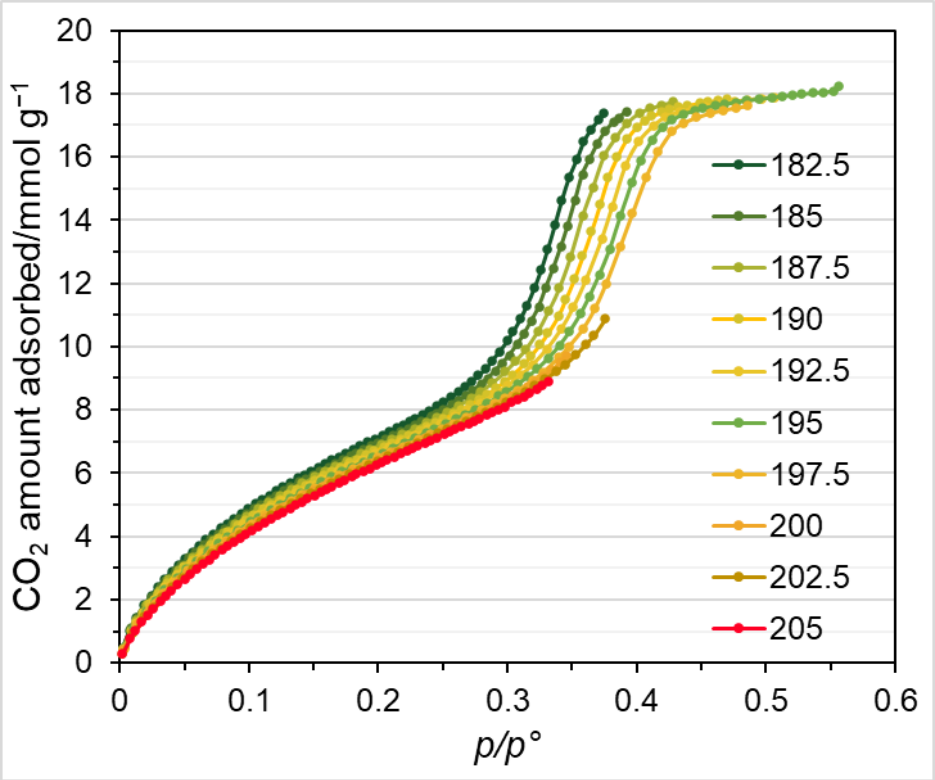

Fig.1. CO_2 adsorption on silica MCM-41 at different temperatures, controlled by cryoTune.

Acknowledgments

This work was supported by the Ministry of Science and Higher Education of the Russian Federation within the governmental order for Boreskov Institute of Catalysis (project AAAA-A21-121011390054-1).

A METHODOLOGY TO OBTAIN MICROPORE VOLUME IN NANOPOROUS SOLIDS BASED ON THE DUBININ METHODS

J. Villarroel-Rocha*, *J. J. Arroyo-Gómez, D. Barrera, *K. Sapag

jhonny@unsl.edu.ar, sapag@unsl.edu.ar
Laboratorio de Sólidos Porosos (LabSoP), INFAP-CONICET,
Universidad Nacional de San Luis, San Luis, Argentina

Introduction

According to the IUPAC [1], gas adsorption is a well-known technique to characterize porous solids and fine powders; this characterization requires the use of various subcritical fluids (e.g., N_2 at 77 K, Ar at 87 K, and CO_2 at 273 K). After measuring the adsorption isotherm and applying several procedures and models, we can obtain the textural properties in a given sample, i.e., specific surface area, pore volumes, and pore size distribution. Among these properties, the micropore volume ($V_{\mu P}$) directly affects the porous material performance, and it can be assessed by Dubinin methods, in particular Dubinin-Radushkevich method (DR), plot methods (α_S-plot and *t*-plot), and microscopic methods based on molecular simulations such as Monte Carlo and Density Functional Theory (DFT). It is well known that microscopic methods provide the best description, at the molecular level, of the adsorption behavior in pore structures. However, access to these methods is still limited, and, to describe a given porous system, an adequate Kernel is required. On the other hand, the plot methods are a suitable option for the calculation of $V_{\mu P}$ but are susceptible to the selected relative pressures interval. Finally, based on the micropore filling theory and Polanyi potentials, the DR method is commonly used due to its simplicity and reliable results when the studied sample has a Type I isotherm. Nonetheless, it has been demonstrated that when the sample presents mesoporosity, the DR method overestimates the micropore volume [2-4]. To improve the calculation of $V_{\mu P}$, in this work, we propose a more general methodology based on the Dubinin methods and the *t* concept, naming it the DR_t method [5], which was evaluated for different nanoporous materials.

Experimental and materials

Two ordered mesoporous materials (CMK-8 carbon and Al-modified SBA-15 silica), and a micro-mesoporous material (Aluminum Pillared Clay, Al-PILC) were studied. N_2 adsorption-desorption isotherms a 77 K of the samples were performed in an ASAP 2000.

DR_t method

Dubinin and Kadlec (DK) proposed a method to assess the micropore volume and the external surface area using the adsorption data of N_2 at 77 K or benzene at 293 K [6]. Besides, they assumed that the adsorbed volume (V_{ads}) on a porous solid in the micro-mesopore range is the sum of adsorbed volumes in the micro and mesopores, given by the following expression:

$$V_{ads}=V_{micro}+V_{meso} \quad (1)$$

Considering that the surface area of the mesopores is S_{meso} and that t is the thickness of the adsorbed layer on the mesopores, equation (1) transforms in:

$$V_{ads}=V_{micro}+S_{meso}\cdot t \quad (2)$$

Therefore, if, instead of thinking that *the total adsorbed volume over a porous solid is the sum of the micro and mesopore volume*; we think that *the* ***isotherm*** *of a given micro-mesoporous material is the linear combination of the individual isotherms of the microporous and mesoporous contribution*, then it could be possible to separate these two contributions, and thus evaluate the micropore volume from the individual micropore isotherm. Meaning that the microporous part of a porous solid, from the adsorbed volume in function of p/p^0, can be mathematically expressed as:

$$V_{\mu P}^{*}(p/p^0) = V_{ads}(p/p^0)-S_{meso}\cdot t(p/p^0) \quad (3)$$

where $V_{\mu P}^{*}(p/p^0)$ is the isotherm corresponding to the microporous region of the sample and $t(p/p^0)$ is the thickness of the adsorbed layer as a function of p/p^0. The individual isotherm of the microporous part of the studied solid must be Type I in IUPAC classification, which is graphically achieved by varying the S_{meso} value. From this microporous isotherm, we can calculate a more precise $V_{\mu P}$ value using the Dubinin-Radushkevich (DR) method.

Results

Fig. 1a shows the different individual isotherms with several S_{meso} values for the N_2 adsorption isotherm at 77 K of an SBA-15 sample (which presents an isotherm

Type IV). As shown in this figure, there will be a unique value of S_{meso}, whose new isotherm corresponds to a net Type I isotherm (at low relative pressures).

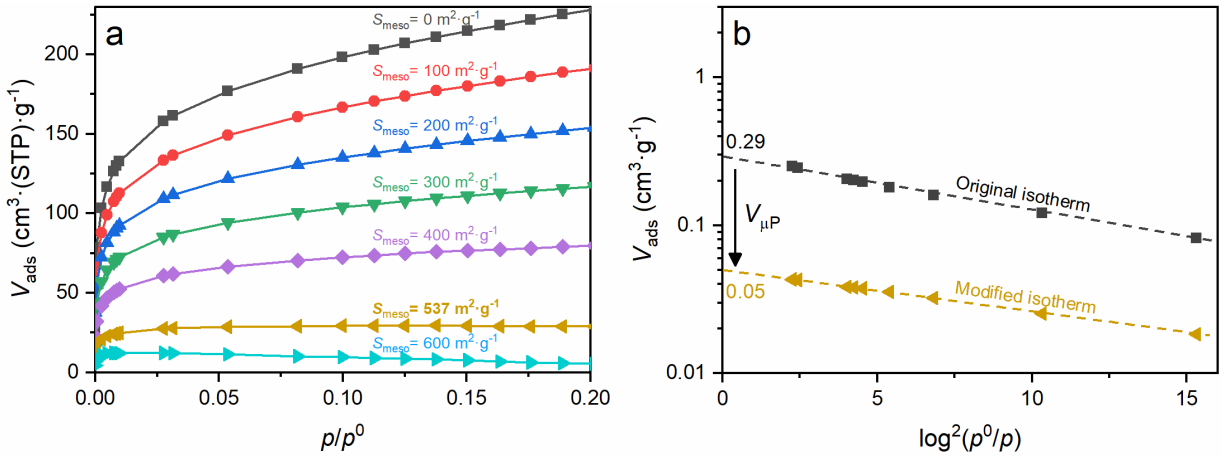

Fig.1. N_2 adsorption at 77 K on SBA-15: a) Methodology of S_{meso} calculation, and b) $V_{\mu P}$ determination.

From the data of the new adsorption isotherm and the DR equation, $V_{\mu P}$ can be obtained, as shown in Fig. 1b. The $V_{\mu P}^{*}(p/p^0)$ isotherm is that corresponding to S_{meso} =537 m^2·g^{-1} in Fig. 1. The values of t for carbon and silica/aluminosilicate materials were estimated from the reference isotherms of Cabot BP-280 and LiChrospher Si-1000, respectively.

Fig. 2 displays the micropore volumes of the samples under study obtained by different methodologies. It is possible to observe that the $V_{\mu P}$ values obtained whit α_S-plot and DR_t methods agree, whereas that obtained with DR is overestimated.

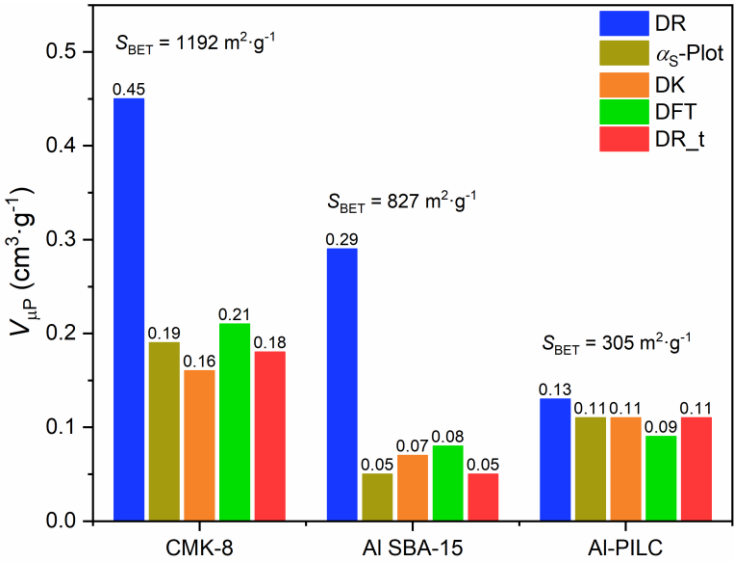

Fig.2. $V_{\mu P}$ values obtained by different methods.

Conclusion

The exposed methodology presents the advantage of applying to any micro-mesoporous material, regardless of the mesoporosity degree, to determine S_{meso} and $V_{\mu P}$. To properly use the methodology, it is only necessary to know the $t(p/p^0)$ function obtained from a standard reference isotherm representing the studied sample.

Acknowledgments

The authors wish to thank UNSL and CONICET for the financial support of this work.

References

1. M. Thommes, K. Kaneko, A.V. Neimark, J.P Olivier, F. Rodriguez-Reinoso, J. Rouquerol, K.S.W. Sing, Pure Appl. Chem. (2015) **87**, 1051.
2. E. Falabella Sousa-Aguilar, A. Liebsch, B.C. Chaves, A.F. Costa, Micropor. Mesopor. Mat. (1998) **25**, 185.
3. S. Brouwer, J.C. Groen, L.A.A Peffer, Stud. Surf. Sci. Catal. (2007) **160**, 145.
4. J. Villarroel-Rocha, D. Barrera, A.A. García-Blanco, M.E. Roca-Jalil, K. Sapag, Adsorpt. Sci. Technol. (2013) **31**, 165.
5. J. Villarroel-Rocha. Adsorption of different gases and vapors in the textural and structural characterization of nanoporous materials. Doctoral Thesis. San Luis University, Argentine (2015).
6. M.M. Dubinin, O. Kadlec, Carbon (1975) **13**, 263.

MATHEMATICAL MODELING AND EXPERIMENTAL VERIFICATION OF CV CURVES FOR SUPERCAPACITORS BASED ON ACTIVATED CARBON ELECTRODES

D.A. Bograchev, Yu.M. Volfkovich

yuvolf40@mail.ru
A.N. Frumkin Institute of Physical chemistry & Electrochemistry of RAS,
119071 Moscow, Russian Federation

As is known, cyclic volt-ampere (CV) curves are one of the most informative characteristics of electrode processes. To obtain CV curves, we measured currents at various potential or voltage sweep rates (w) from 1 mV / s to 1000 mV / s, and then a current versus potential curve is plotted. In this case, it is important to achieve equilibrium so that the rate of potential or voltage sweep does not exceed the rate of electrode processes. Then equilibrium CV curves can be obtained, which can be simply used to analyze the processes occurring in electrochemical cells.

For electric double-layer supercapacitors (EDLSC), the equilibrium CV curves have a shape close to rectangular with an insignificant dependence of the differential capacitance on the electrode potential. When the equilibrium value w is exceeded, the shape of the CV curves deviates from rectangular and takes the form of elongated "fish" inclined at an angle to the potential or voltage axis. Until now, no mathematical model has been developed for the CV curves for EDLSC.

For a porous electrode, De Levie applied an equivalent electrical circuit in the form of an endless transmission line consisting of series elements in the form of parallel-connected resistances and capacitance of an electric double layer (EDL) [1]. We were the first to obtain both a numerical and an analytical solution for calculating the CV curves for EDLSC. Let us write a model that describes the EDL charging and considers the electric potential of the electrolyte and the electric potential in the solid phase.

$$aC_{dl}\frac{\partial(\Phi_e-\Phi_{s,C})}{\partial t}-\frac{\partial}{\partial x}(\kappa_{eff}\frac{\partial\Phi_e}{\partial x})=0\,, \qquad (1)$$

$$aC_{dl}\frac{\partial(\Phi_{s,C}-\Phi_e)}{\partial t}-\frac{\partial}{\partial x}(\sigma_{eff}\frac{\partial\Phi_{s,C}}{\partial x})=0 \qquad (2)$$

The conductivity of the solid phase of the porous electrode - σ_{eff} , the conductivity of the electrolyte - κ_{eff} , which in the general case can be a function of concentration, and also take into account the surface conductivity of activated carbon (AC) electrodes, - a is the specific surface area, the specific capacity on the true surface. The problem was solved with appropriate boundaries and initial conditions. As a result, the following analytical solution was obtained for the dependence of the current on the potential with a linear sweep of the latter in time:

$$i = -\kappa_{eff} \left.\frac{\partial \Phi_e}{\partial x}\right|_{x=L_{elec}} = W\frac{aC}{2}L_{elec} - W\frac{aC}{4}\sum_{n=0}^{\infty} C_n \lambda_n \sin(\lambda_n)\exp(-\frac{\kappa_{eff}}{aCL_{elec}^{\ 2}}\lambda_n^{\ 2}t) \qquad (2)$$

To verify the obtained mathematical model of CV curves, we used the results of work [2], in which such curves were measured for symmetric EDLSC based on AC electrodes. Figure 1 shows a comparison of the experimental CV curves with those calculated using the DSC model.

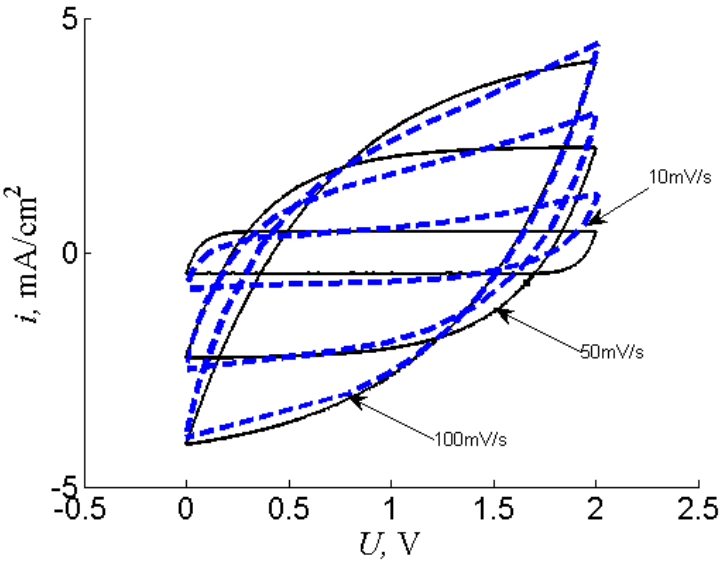

Fig. 1. The result of comparing the experimental CV curves with those calculated using the mathematical model for EDLSC. Solid curves are calculated, experimental curves are dashed.

As shown in Fig. 1, there is a satisfactory agreement between the experimental and calculated CV curves for w = 50 and 100 mV / s, which indicates the adequacy of the model. However, for w = 10 mV / s, this agreement takes place only in the voltage range from 0 to ~ 1.5 V. The EDL is charged - discharged in this voltage range.

However, in the region of ~ 1.5 V to 2 V, there is some deviation from these processes due to the onset of the Faraday reaction, probably a redox reaction of surface groups. At high sweep speeds, the redox reaction does not have time to occur. The potential distributions were calculated using the developed model. In fig. 2. shows a 3D profile of the electric potential over the thickness of the electrode for different points in time at a voltage sweep rate of 500 mV / s.

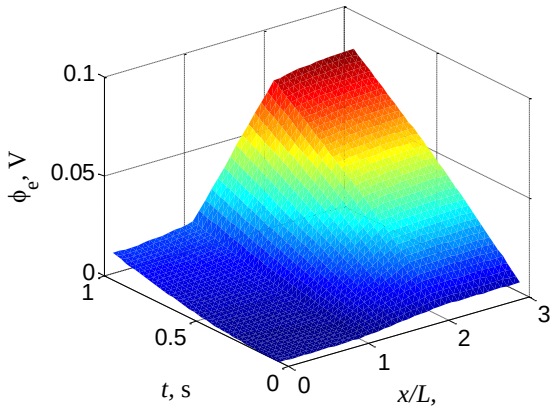

Fig.2. 3D profile of the electric potential over the thickness of the electrode for different times up to 1 s.

As can be seen, potential jumps take place on the x / L axis when passing from the electrodes to the separator.

Acknowledgment

The study was carried out with the financial support of the Ministry of Science and Higher Education of the Russian Federation.

References

1. R De Levie. On porous electrodes in electrolyte solutions—IV - Electrochimica Acta. (1964) **9**, 1231.
2. N. Yadav, K. Mishra, S.A. Hashmi Nitish. Optimization of porous polymer electrolyte for quasi-solid-state electrical double layer supercapacitor. Electrochimica Acta. (2017) **235**, 570.

DISCRETE MODELS IN LINEAR ELUTION DYNAMICS OF ADSORPTION

A.V. Larin

larin@phyche.ac.ru
A.N. Frumkin Institute of Physical Chemistry and Electrochemistry Russian Academy of Sciences, Moscow, 119071, Leninsky pr., 31

Currently, there are two types of discrete material balance equations proposed in the theory of plates and the model of the equilibrium adsorption layer. The purpose of this work is to analyze these equations and solutions based on them in the developmental version of the dynamics of adsorption.

The idea that made it possible to create a discrete material balance equation was formulated in the article [1]. It led to the creation of the theory of plates, where the axiomatically correct proposition was introduced that in the process of adsorption dynamics (at a fixed moment – author's note), it is always possible to single out the length of the adsorbent layer, the concentration at the outlet of which will be in equilibrium with the average value of adsorption on this layer.

Indeed, the axiomatic concept presented in [1] about the existence of an equilibrium adsorption layer in a dynamic system at a fixed time instant is beyond doubt. Whether the magnitude of this layer will change over time is a pressing question. Yes, it can if some component of the equilibrium adsorption layer depends on the degree of filling of the adsorption space. This cannot occur in the linear dynamics of adsorption due to small fillings. All components of the equilibrium adsorption layer, among which we single out the coefficients of vortex diffusion, external and internal mass transfer, etc., with a linear adsorption isotherm practically, do not depend on the degree of filling.

The material balance equation for the linear isotherm of adsorption has the form

$$da_n/dt + dc_n/dt = (1 + H)\, dc_n/dt = (u/L_e)[c_{n-1} - c_n], \qquad (1)$$

where a_n is the average value of adsorption on the considered adsorbent layer, accept that, c_n is in equilibrium with a_n, t is the time, H is a Henry constant, u is the mobile phase speed, L_e is the equilibrium adsorption layer, c_n is a concentration at the inlet/outlet of the equilibrium adsorption layer.

For some time, using Eq. (1) a solution was obtained for linear elution of adsorption dynamics as:

$$c_n/c_{max} = \exp(-bt) \cdot (bt)^{n-1}/(n-1)! \quad (2)$$

where c_n is the elution curve on the adsorbent layer equal to n, $n = L/L_e$ is the relative length of the adsorbent layer, L is the absolute length of the adsorbent layer, c_{max} is the maximum concentration of the elution curve at the length of the adsorbent bed n = 1, and $b = u/L_e(1 + H)$.

The resulting equation was not actually used: the authors of [1] introduced (2) into correct analytical reasoning and, through the Stirling approximation, obtained the Gaussian curve, which is known to this day. In addition, the exponent and factorial in (2) were equal to n, and not equal to n–1, and the solution itself was interpreted and interpreted as different mathematical distributions. We have shown that equation (2) is the integrand of the Euler gamma function. Let us add that in the equilibrium adsorption layer model, numerical solutions of Eq. (2) have been used since the 80s, and analytical ones since the 90s of the last century.

The equilibrium adsorption layer model is mainly used to obtain numerical solutions for arbitrary adsorption isotherms [2]. An analytical solution is possible for a linear adsorption isotherm. Then the material balance equation under the assumption that $dc/dt \ll da/dt$ will be

$$da_n/dt = (u/L_e)[c_{n-1} - c_n], \text{ or } Hdc_n/dt = (u/L_e)[c_{n-1} - c_n]. \quad (3)$$

With a linear adsorption isotherm for the concentration leaving the first layer of equilibrium adsorption, the following solution was obtained in [3]

$$c_1 = c_{max}\exp(-b_1 t). \quad (4)$$

where $b_1 = u/L_e \cdot H$.

Note that it is this equation that was used to prove the existence of an equilibrium adsorption layer. Experimental results on the elution dynamics of adsorption of different sizes of ethyl chloride samples on activated carbon at high temperatures are given in [4].

Using equation (3) with the translation of H into its right part and (4), we obtain

$$dc_2/dt = b_1[c_{max}\exp(-b_1 t) - c_2]. \quad (5)$$

Equation (5) is solved by the constant variation method, and at the end, we have equation (2), but with another constant: $b_1 = u/L_e H$.

Thus, it has been shown that the analytical solutions in the development dynamics of adsorption obtained in the framework of plate theory and the model of the equilibrium adsorption layer are basically the same but slightly differ in the representation of the Henry constant. When working with Henry's small constants, this circumstance must be taken into account.

The analytical solutions of the direct problem of the elution dynamics of adsorption, considered above, make it possible to obtain results not only for integer values but also for arbitrary values of the relative length of the adsorbent layer. This becomes possible only when (2) is represented with an exponent and a factorial in the form of n - 1.

Numerical solutions in the framework of the equilibrium adsorption layer model are possible only for natural values of the relative length of the adsorbent layer, but at the same time, the initial conditions or the shape of the input signal can be changed within wide limits.

Funding and acknowledgments

The work was carried out within the framework of the State task (IPCE RAS).

References

1. A.J.P. Martin, R.L.M. Synge, Biochem. J. (1941) **35**,1358.
2. A.V. Larin, Bull. Acad. Sci. USSR, Div. Chem. Sci., (1983) **32,** 211.
3. A.V. Larin, Bull. Acad. Sci. USSR, Div. Chem. Sci., (1984) **33,** 1112
4. A.V. Larin, J. Chromatogr. (1986) **364**, 87.

MINIMIZATION OF INTERVALS OF INTEGRATION IN THE METHOD OF MOMENTS USING NORMALIZED CONCENTRATIONS

A.G. Dmitrienkova*, *A.V. Larin

larin@phyche.ac.ru
A.N. Frumkin Institute of Physical Chemistry and Electrochemistry Russian Academy of Sciences, 119071, Moscow, Russia

The method of moments is used to determine the adsorption constants of solid materials in linear chromatography. Errors occur due to the overestimation of the integration interval when calculating the moments of the elution curves. The calculation accuracy increases with controlled minimization of the integration interval of the experimental curve.

In a recent work [1], the study of minimizing the integration intervals led to obtaining functional dependences of the normalized integration intervals on the relative length of the adsorbent layer, which were linearized in the range 4≤n≤200. In this case, the normalization of the interval of integration was carried out in time. An attempt to tie the obtained linear function to the value n = 3 failed for both the left and right parts of the elution curve: the error in calculating the integration interval was rather large. The aim of this work was to minimize the integration interval when calculating the center of gravity of the elution curve in the region of small n using normalized concentrations.

Calculations of the moments and their errors were carried out for the equation of the theory of plates:

$$c_n/c_{max} = \exp(-bt) \cdot (bt)^{n-1}/(n-1)!\,, \qquad (1)$$

where c_n – elution curve on an adsorbent layer equal to n, $n = L/L_e$ – relative length of the adsorbent layer, L – absolute length of the adsorbent layer, L_e – effective kinetic constant, t – time, c_{max} – maximum concentration of the elution curve at the length of the adsorbent bed n = 1, constant $b = u/(1+H) \cdot L_e$, u – linear velocity of eluent, H – Henry's constant. The constant $b = 0.303$ с$^{-1}$.

For the left side of the elution curve, the results are shown in Fig. 1.

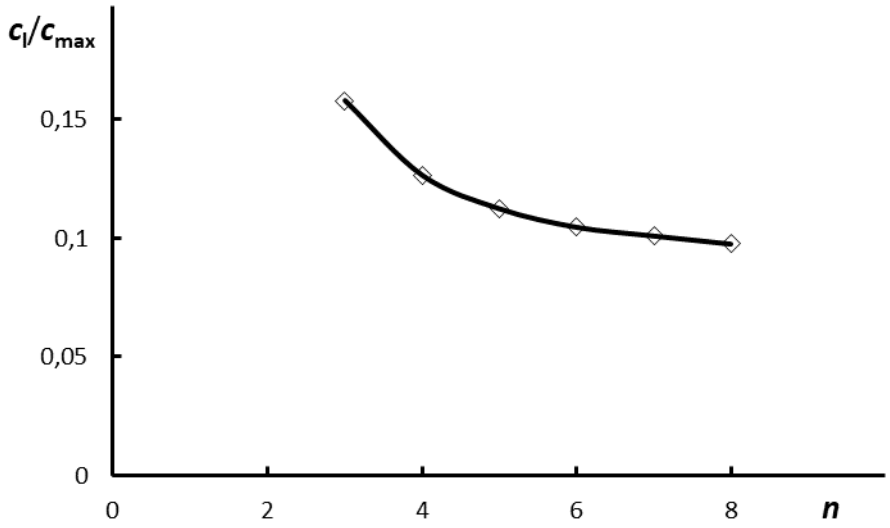

Fig. 1. Dependence of the concentration-normalized integration interval on the relative length of the adsorbent layer with an error in calculating the center of gravity equal to 0.5% for the left side of the elution curve.

For the left side of the elution curve in the range n from 3 to 8, the dependence in the form of a hyperbola, shown in Fig. 1, was linearized as $c_{max}/c_l = 18.825(1/n) + 12.613$ at $R^2 = 0.9993$.

For the right side of the elution curve, the dependence of the concentration-normalized integration interval on the relative length of the adsorbent layer is represented by a linear dependence in the range n from 3 to 8 $c_r/c_{max} = 0.002n - 0.0005$ at $R^2 = 0.9981$.

Thus, the dependences of the concentration-normalized integration interval on the relative length of the adsorbent layer obtained for the left and right parts of the elution curve significantly differ from those dependencies when using the time normalization and increase the error determination interval to $n = 3$.

In the future, it is planned to carry out the same simulation in a wider range of variations in the relative length of the adsorbent layer.

Funding and acknowledgments

The work was carried out within the framework of the State task (IPCE RAS).

References

1. Dmitrienkova A.G., and Larin, A.V., Prot. Met. Phys. Chem. Surf., 2019, **55**, 1025

ADSORPTION-STIMULATED DEFORMATION OF A PRECISION MICROPOROUS ADSORBENT UPON ADSORPTION OF GASES AND VAPORS

***A.V. Shkolin**, A.A. Fomkin, I.E. Men'shchikov*

shkolin@phyche.ac.ru
M.M. Dubinin Laboratory of Sorption Processes
A.N. Frumkin Institute of Physical Chemistry and Electrochemistry RAS,
119071 Moscow, Russia

During adsorption, a microporous solid is involved in the adsorption interactions, which leads to its deformation and variations of the elastoplastic properties [1]. The deformation effect depends on the adsorption value and many other factors, including the porosity, surface chemistry, rigidness of the adsorbent, physicochemical properties of adsorbed molecules, and thermodynamic parameters of the adsorption system.

In the present work, we studied the microporous carbon adsorbent, AUK, prepared by thermochemical leaching of silicon from crystalline SiC in the chlorine flow. A narrow pore size distribution characterizes the porous structure of AUK; its structure and energy characteristics are as follows: micropore volume W_0 = 0.41 cm^3/g, standard characteristic energy of adsorption E_0 = 29.3 kJ/mol, effective micropore diameter X_0 = 0.82 nm. As follows from the data on the strain of AUK during adsorption of different substances (Figs. 1a,b), the adsorbent may experience compression and expansion deformation depending on the properties of adsorbed molecules and pore filling. The distinctive region of the AUK deformation corresponds to the adsorption equilibrium at low and medium values of pore fillings.

The compression of AUK was observed during the adsorption of gases as N_2, O_2, CO_2, CH_4, Ne, Kr, and Xe (Fig. 1a). Probably, this compression is caused by interactions of adsorbed molecules with the opposite micropore walls due to the proximity of the pore sizes and molecular diameters of these gases. The gas molecules have small critical diameters, for example, 0.32 nm (Ne), 0.38 nm (CH_4), 0.31 (CO_2), and therefore their adsorption, occurring near the pore walls, leads to an imbalance of forces in the solid. The observed deformation effects can be attributed to this imbalance. Indeed, the numerical simulation performed for methane adsorption onto a model porous carbon

structure with similar structure and energy characteristics by molecular dynamics revealed the location of adsorbed molecules near the pore walls.

As follows from Fig. 1b, the adsorption of oblong molecules as n-pentane, n-heptane, n-octane with transverse dimensions comparable to the micropore sizes of AUK does not lead to noticeable deformation effects in the region of low and middle pore fillings. It should be noted that the critical diameter of linear hydrocarbons evaluated from their passage through the windows of synthetic zeolites attains the value of 0.49 nm [7], which is comparable with the effective micropore size X_0 of AUK. It was found that oblong hydrocarbon molecules occupied the central regions of

the micropores of AUK during adsorption. We suggest that in the case of comparable pore sizes and molecular dimensions of adsorbed molecules, the intensity of the adsorption-induced deformation effects is determined by the ratio of adsorbent-adsorbate and adsorbate-adsorbate interactions.

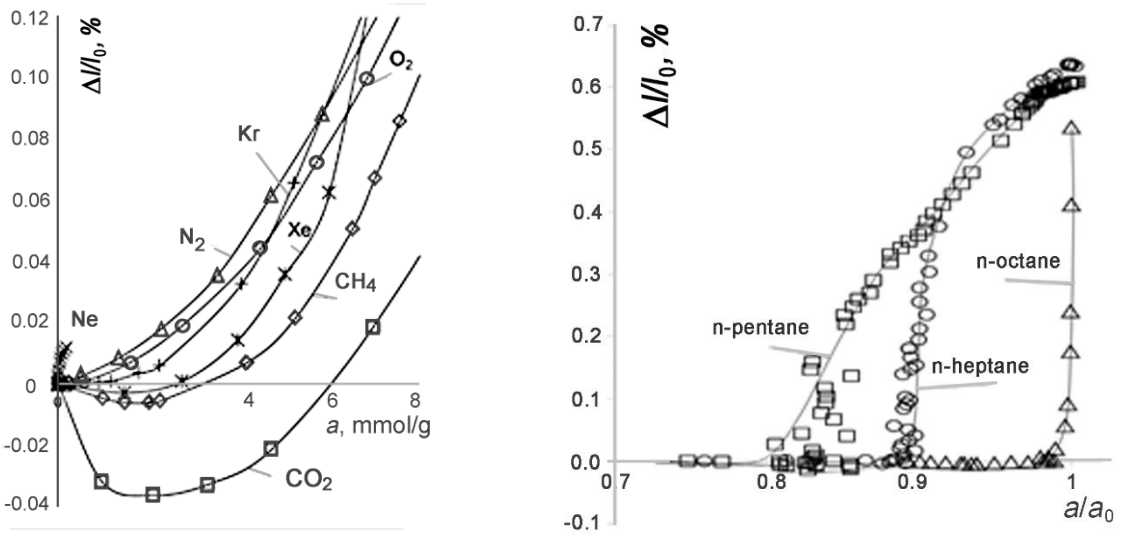

а *б*

Fig. 1. Dependences of the adsorption-stimulated strain of microporous carbon adsorbent AUK on the amount of adsorbed gases N_2, O_2, CO_2, CH_4, Ne, Kr, and Xe (*a*) and vapors of n-pentane, n-heptane, n-octane (*b*) at the temperature of 273 K. The plots were built from data reported in [2–6].

Thus, the predominant adsorbate-adsorbate interactions and the formation of adsorption molecular associates in the central region of micropores preserve the initial

balance of forces in the solid adsorbent. Consequently, no noticeable deformation effects are observed during the adsorption of normal hydrocarbons in AUK (Fig. 1b).

The sharp adsorption-induced expansion of the adsorbent observed at high pore fillings, exceeding 70–80 % (Figs 1a and b), is caused by an increase in the repulsion forces due to a decrease in the average distances between adsorbed molecules and the pore walls.

Funding and acknowledgments

The work was carried out within the framework of the State Task (no. 0081-2019-0018).

References

1. Fomkin, A.A., Shkolin, A.V., Pulin, A.L., Men'shchikov, I.E., Khozina E.V. Adsorption-Induced Deformation of Adsorbents. Colloid J. (2018) **80**, 578.
2. Shkolin, A.V., Potapov, S.V. & Fomkin, A.A. Deformation of AUK microporous carbon adsorbent induced by xenon adsorption. Colloid J. (2015) **77**, 812.
3. Potapov, S.V.; Shkolin, A.V.; Fomkin, A.A. Deformation of AUK microporous carbon adsorbent induced by krypton adsorption. Colloid J. (2014) **76**, 351.
4. Shkolin, A.V., Fomkin, A.A. & Sinitsyn, V.A. Adsorption-induced deformation of AUK microporous carbon adsorbent in adsorption of n-pentane. Prot. Met. Phys. Chem. Surf. (2011) **47**, 555.
5. Shkolin, A.V., Fomkin, A.A. Adsorption deformation of AUK microporous carbon adsorbent at adsorption of n-heptane. Prot. Met. Phys. Chem. Surf. (2013) **49**, 373.
6. Shkolin, A.V.; Fomkin, A.A.; Men'shchikov, I.E.; Pulin. AL; Yakovlev, VY Deformation of AUK Adsorbent and Adsorbate Structure upon n-Octane adsorption. Colloid J. (2019) **81**, 613.
7. Kel’tsev N.V. Osnovy adsorbtsionnoy tekhniki (Fundamentals of adsorption techniques), Moscow, Khimiya, 1976. 512 p. (*in Russian*)

ADSORPTION DEFORMATION OF HETEROGENEOUS CATALYSTS FOR HYDROGENATION REACTIONS DURING CYCLIC TREATMENT BY A HYDRATED COMPOUND

A.V. Afineevskii, T.Yu. Osadchaya, D.A. Prozorov

afineevskiy@mail.ru
ISUCT, 153000 Ivanovo, Russia

In the chemical industry, it is especially important to obtain and use nickel-based skeletal catalysts in the reduction reactions of the main classes of industrially important organic compounds: caprolactam, aniline, alcohols, and fats.

Skeletal nickel contains residual aluminum, which is highly reactive, is possible to dissolve, and it gives side processes in liquid-phase hydrogenation reactions.

Earlier it was found that the kinetic curves of the rate of hydrogen absorption in the course of cyclic hydrogenation of 4-nitrotoluene over a skeletal nickel catalyst [1] are characterized by a "hump" with a single introduction of the hydrogenated substance and its disappearance upon repeated injections. This fact is explained only by the occurrence of side physicochemical processes that take place only in the first two cases, and for the third injection of the reagent are absent. This requirement is ideally satisfied by the adsorption deformation caused by catalytic processes [2]. Catalytic adsorption deformation can lead to a decrease in the particle size only up to certain limits, which are obviously achieved at the second inlet [3]. Thus, during the first and second inputs, a side physicochemical process occurs, and it is catalytic adsorption deformation, which leads to the splitting of the catalyst particles, which leads to the formation of a new surface on the chips. Obviously, this newly formed surface will be similar in composition and properties to the initial alloy from which the skeletal nickel catalyst we used was obtained. This newly formed surface should contain nickel and aluminum, while the hydrogenation reaction of 4-nitrotoluene can proceed on such a surface [1] and oxidize aluminum, which should lead to a temporary increase in the catalyst activity, which will decrease with the oxidation of the newly formed surface.

In this work, the adsorption deformation of the support is considered, in particular, the removal of residual aluminum from the skeletal nickel catalyst. It is

known from the literature [1] that the removal of residual aluminum from skeletal nickel consists in treating the nickel catalyst in a 6-8M aqueous alkali solution at 50-75 °C with the cyclic introduction of hydrogen peroxide in an argon atmosphere followed by a reduction in a hydrogen atmosphere. However, this method has some disadvantages: labor intensity (more technological operations are required), the need for an inert gas, the use of concentrated solutions of hydrogen peroxide.

In this work, cyclic treatment with a hydrogenated compound was carried out in an aqueous solution of sodium hydroxide 25% in a hydrogen atmosphere at a temperature of 55–65 °C. Skeletal nickel catalyst (7–15 g) was placed in a hydrogenation reactor (300 ml) in sodium hydroxide solution (100 ml), then a hydrogenated compound (sodium maleate, or propen-2-ol-1, or hydrogen peroxide) was an inlet in quantity sufficient for the sorption of hydrogen from the catalyst surface from each gram of catalyst, i.e., V_{H2} / m_{kt} was 20–60 $cm^3 \cdot g^{-1}$. The choice of substances to be hydrogenated (sodium maleate, propene-2-ol-1, hydrogen peroxide) is due to their availability. The products of their hydrogenation are easily removable when the catalyst is cleaning from sodium hydroxide; when using them, a minimum number of catalyst processing cycles is required.

It was found that the number of repetitions of such cycles: for sodium maleate is 2, for propen-2-ol-1 is 4, for hydrogen peroxide is 3.

The results obtained had an economic effect due to a decrease in the number of preparation operations, which makes the process cheaper. The process is carried out without the use of inert gas, a more accurate setting of modes, and an expansion of the range of substances that can be used.

Acknowledgments

This work was supported by the Russian Science Foundation (grant no. 21-73-10210).

References

1. Barbov, A.V., Gostikin, V.P., Koifman, O.I., Theory and practice of liquid-phase hydrogenation processes of substituted nitrobenzenes (KRASAND, Moscow, 2016), p. 518.
2. A.V. Shkolin, A.A. Fomkin, I.E. Men'shchikov, A.L. Pulin, V.Yu. Yakovlev, Colloid Journal, Pleiades Publishing, Ltd (Road Town, United Kingdom) (2019) 81, P.613.
3. Parfit G., Rochester K. Adsorption from solutions on the surfaces of solids (MIR, Moscow, 1986), p. 601.

SORPTION AND INTERPLANE TRANSFORMATION – TWO STAGES OF GRAPHITE OXIDE SWELLING IN POLAR SOLVENTS

***N.V. Avramenko*, A.M. Parfenova, A.T. Rebrikova, L.O. Usoltseva, I.V. Mikheev, D.S. Volkov, V.M. Senyavin, M.V. Korobov**

natvas2709@gmail.com
Lomonosov Moscow State University, Chemistry Department, 119991 Moscow, Russia

The practical interest of graphiteoxide (GO) powder swelling in polar solvents is associated with possible separation/filtration of liquids and storage of gases by means of thin, tunable and mechanically strong GO layered structures, respectively membranes and pillared frameworks. Swelling is a combination of two processes, namely: sorption of liquids into the interplane space of GO and of simultaneous increase of interplane distance. Sorption typically decreased with the increase of temperature, leading to the decrease of interplane distances. The structures formed by the interaction of GO with polar liquids (swollen structures, SwSt) are defined by temperature and external pressure and are different for different types of polar liquids and GO. The difference in properties of Brodie GO (B-GO) and Hummers GO SwSt may be caused by the difference in the number and type of oxygen-containing groups on graphene planes. Sorption measurements at $T=298 \pm 1$ K were performed by the isopiestic method (Table). Equilibration of GO with organic liquid vapors occurred within the desiccators and persisted until the mass of GO saturated with organic liquids became constant (5-10, 30 days for 1-octanol). Each saturated sample was checked by DSC-30 Mettler for the absence of the free organic liquid excess. DSC was also employed to detect phase transformations in the SwSt the scanning rates 2-5 K/min. Isothermal desorption of organic liquids from the B-GO saturated swollen B-GO was studied using thermogravimetric (TG) analysis (TG-50 Mettler thermobalance). X-ray diffraction (XRD) measurements were performed with a PANalytical X'Pert diffractometer with Cu Kα radiation. Several experiments were also performed using synchrotron radiation $\lambda=0{,}46794$ Å at ID22 beamline, ESRF, France.

In this study, we provide consistent use of the thermodynamic approach to follow changes in the SwSt of B-GO along with the series of normal alcohols (1-ROH)

from methanol to 1-nonanol using primarily sorption/desorption and also XRD data B-GO was specially chosen as it was reported to form more regular structures compared to other forms of GO. It was demonstrated that normal alcohols in the methanol – 1-nonanol set Intercalate into B-GO, forming several SwSt, which may be considered as binary phases in the two-component systems B-GO – (1-ROH) and as the simple solid solvates of B-GO.

Table. Specific Sorption of Normal Alcohols into B-GO

System	Sorption, T=298 K, $g \cdot g^{-1}$ B-GO [a]	Sorption, $g \cdot g^{-1}$ B-GO [b] (T, K)	d (001) T=298 K
B-GO – methanol	0.31 [c]		8.97
B-GO – propanol	0.37		8.9
B-GO – 1-butanol	0.64	0.63 (335)	16.5
B-GO – 1-pentanol	0.67	0.73 (343)	18.0
B-GO – 1-hexanol	0.84	0.78 (353)	18.5
B-GO – 1-heptanol	0.75	0.85 (368)	19.0
B-GO – 1-octanol	0.88		23.3
B-GO – 1-nonanol	1.16 [c]		25.5

[a] Isopiestic data ± 0.02; for 1-heptanol and 1-octanol ± 0.05.

[b] TG data ± 0.1. [c] DSC data ± 0.15

We prepared sketches of typical binary phase diagrams to account for the observed transformation of SwSt both with temperature and the change of composition. Discussing the internal arrangement of the SwSt, the concept of the liquid layer in the interplane space of B-GO was carefully examined. The averaged sorption capacity and the size of such a layer were estimated. These parameters were correlated with the geometry and chemical formula of B-GO.

Funding

This work was supported by the RFBR grant 19-08-00498.

METHOD FOR STUDYING OF SORPTION-STIMULATED STRESSES IN ADSORBENT

V.N. Simonov [1,2], A.A. Fomkin [1], A.V. Shkolin [1]

simonov.valer@yandex.ru
[1] A.N. Frumkin Institute of Physical Chemistry and Electrochemistry, Russian Academy of Sciences, 119071 Moscow, Russia
[2]National Research Nuclear University "MEPHI", 115409 Moscow Russia

Carrying out studies of sorption-stimulated deformations of the adsorbent allows choosing the most optimal operating parameters of adsorption technological units, thereby reducing energy consumption and increasing their service life [1,2]. However, the overwhelming majority of such studies are carried out on adsorbents with unlimited freedom of deformation, i.e., "free" from mechanical stress. In real technological installations, the adsorbent granules are in a stress-strain state, being limited by the transverse and vertical dimensions of the installation and loaded with layers of adsorbent located on top. This circumstance complicates using research results on "free" adsorbents to describe the processes occurring in real technological conditions.

In this work, we propose a method for studying the sorption-stimulated stress in an adsorbent under conditions of limiting its deformation. The method is based on the use of a strain gauge sensor (SGS), which measures the voltage in an adsorbent granule (AG), clamped together with the SGS between two rigid walls (RW) Fig. 1. A quartz strain-sensitive resonator with a resonance frequency of 10 MHz and a conversion coefficient K_C = 270 Hz / MPa was used as SGS, included in the circuit for measuring the frequency of the SGS (CMF). To limit deformation, AG and SGS were clamped in a micrometer. In this case, the heel and micro screw of the micrometer play the role of rigid walls.

The described design achieves several results. Firstly, high mechanical rigidity of the walls is ensured due to the high rigidity of the micrometer clamp. Secondly, it becomes possible to smoothly adjust the degree of clamping of AG and SGS, thanks to the use of a micrometer screw and clamping of the micrometer spindle, and thirdly, it is possible to control the degree of clamping by the readings of the strain gauge sensor.

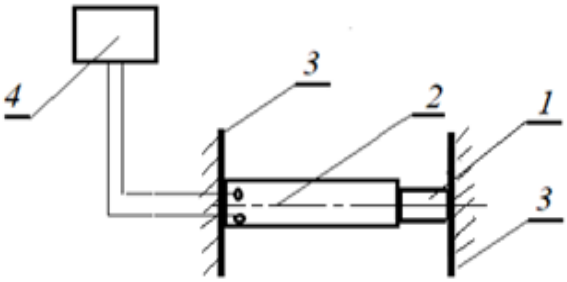

Fig. 1. Method diagram.1 – AG, 2 – SGS, 3 – RW, 4 - CMF

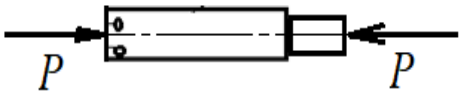

Fig. 2. Scheme of action of forces P on AG and SGS

Figure 2 shows a diagram of the action of the forces P on AG and SGS. It follows from this diagram that the stresses T_{AG} in AG and T_{SGS} in SGS are related by a ratio:

$$T_{AG} = T_{SGS}\,(S_{SGS}/S_{AG}) = \Delta f_{SGS}\,(S_{SGS}/S_{AG})/\,K_C, \qquad (1)$$

where S_{AG} and S_{SGS} are the cross-sectional areas of AG and SGS, respectively, Δf_{SGS} is the change of SGS frequency caused by sorption deformation.

By measuring the change in the frequency of SGS and knowing the cross-sectional areas of AG and SGS, it is possible to calculate the voltage in the adsorbent granule.

In the experiment, a volume of acetone vapors of various concentrations was fed into a sealed vessel with SGS and AG of brand AR-1(diameter and height ~3 mm). The adsorption of vapors tended to increase the granule size; however, as a result of restrictions on the side of the RW walls, mechanical compressive stresses appeared in the adsorbent and sensor. The stresses in the adsorbent were calculated from the value of Δf_{SGS} and using equation (1).

As an illustration of the capabilities of the method, Fig. 3 shows transient processes of changes in mechanical stresses with time when acetone vapor is supplied to the volume from HA and SGS.

The fluctuations in the frequency of the SGS are 0.03–0.05 Hz. Therefore, the described method allows one to notice changes in the stress in the adsorbent at the level of 100–200 Pa, which at the modulus of elasticity of 5–6 GPa [2] corresponds to a relative deformation of $\sim (1.6–2) \cdot 10^{-8}$.

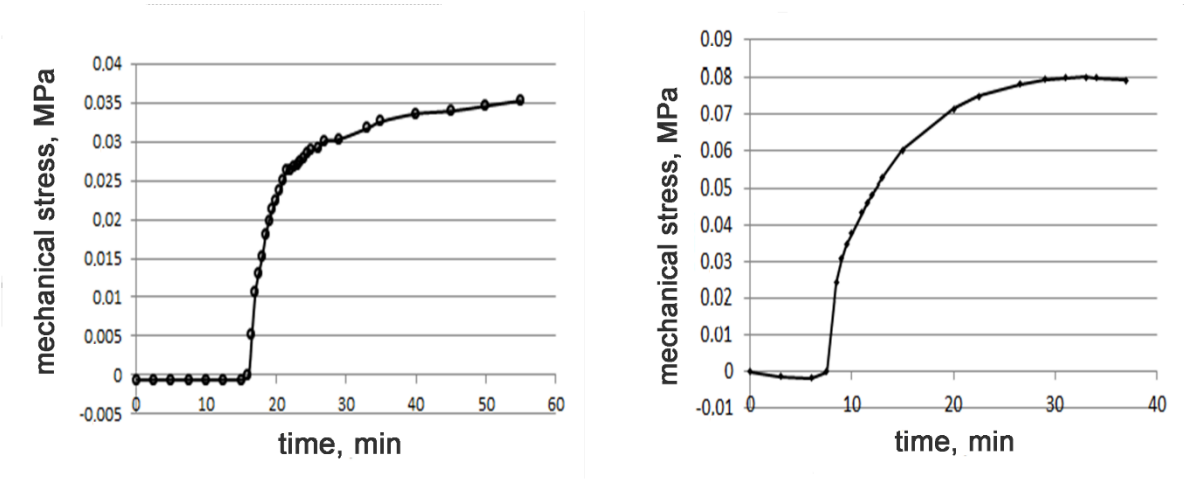

a *b*

Fig. 3. Transient processes of changes in mechanical stresses in AG grade AR-1 during adsorption of acetone vapors with a concentration of 20.3% (*a*) and 86% (*b*)

The described method combined with the well-known method of controlling the adsorption characteristics of a "free" adsorbent [1] opens up new possibilities in studying those adsorption phenomena in which mechanical stresses in the adsorbent play a significant role, for example, in studies of changes in the properties of sorbents during storage and under operating conditions [2].

Funding and acknowledgments

The work was carried out within the framework of State Assignment No. 0081-2019-0018 "Fundamental physicochemical laws of adsorption, adsorption separation, adsorption-electrochemical ion-exchange processes in nanoporous materials and the basis of targeted synthesis of new adsorbents."

References

1. I.E. Men’shchikov, A.V. Shkolin, E.V. Khozina, A.A. Fomkin Peculiarities of Thermodynamic Behaviors of Xenon Adsorption on the Activated Carbon Prepared from Silicon Carbide. Nanomaterials (2021) **11**, I.4. 971.
2. I.V. Lepin, R.M. Sibileva, V.I. Sokolenko, E.I. Vinokurov, M.A. Grigorenko. Comparative characteristics of mechanical and adsorption properties of activated charcoals applied for adsorbers of npp air discharge systems. ISSN 1562-6016. PAST. 2020. No 2 (126), p. 114–118.

SPECIFICS OF OBTAINING CARBON ADSORBENTS FROM FOSSIL COALS

V.I. Dudarev*, *E.G. Filatova*, *D.I.Dudarev

vdudarev@mail.ru
Irkutsk National Research Technical University, Irkutsk, Russia

The raw material base of fossil coals intended for the production of carbon sorbents is characterized by extensiveness, large volumes, and comparatively uneven distribution throughout the country. The total geological reserves of coal in Russia in the eastern regions achieve 5281 billion tons, or about 92% [1]. A feature of coals is their metamorphism or coalification in time, which is essentially a gradual transformation of the original carbon-containing materials into coals with an ever-increasing amount of carbon. Depending on the type of sediments and sediment conditions, the composition and properties of coals that have undergone transformation processes under aerobic or anaerobic conditions have been determined. In Russia, it is customary to divide fossil coals according to the degree of coalification and technological features (GOST 21489-76 and 25543-88) into three main groups: brown, stone coals, and anthracites [2].

Brown coals are classified as the lowest degree of coalification and they are mainly humus and rarely humus-sapropel. The structure of the coals is homogeneous and hatched, less often striped. The natural humidity of coals is from 35 to 60%, mainly about 55%. The ash content of coals varies from 5% to 45% or more. Freshly mined coals are dense, shiny, and matte. With long-term storage, they crumble into trifles. Stone coals marked D and DG combines long-flame coals with an output of volatile substances above 35–45% and powdered or slightly sintered coke residue. Coals of grade D are characterized by humidity W^r 8-16%. When semi-coking, they give a high (up to 16%) yield of primary resin with a high content of phenols, which allows them to be used for semi-coking to obtain in addition to smokeless fuel, semi-coke, and some chemical products.

Gas coals (G) include coals of the I and II stages of metamorphism. They are characterized by a high yield of volatile substances (33–59%), high sulfurity (up to

7.2%), and increased sinterability, which indicates their restorability. Fatty coals (F) are the most melting sintering coals with a 27–37% release of volatile matter and a plastic layer of 6–40 mm and above. According to the ability to coking, fatty shrinkage coals are distinguished, relatively less metamorphosed, fatty, and more metamorphosed. Grade K covers sintered coals with an output of volatile substances from 17 to 27% and a thickness of the plastic layer from 10 to 25 mm. Coals with an optimal combination of these natural properties can produce conditioned coke independently. The OS brand includes coals that have a 14–27% release of volatile matter. Despite the proximity of these indicators to the K grade, the coals differ from them by the higher metamorphism, and they are most scarce after typical coke coals of grade K. The SS brand combines weakly sintered coals of a wide range of metamorphism, giving a powdery, sticky or weakly sintered non-volatile residue. Skinny coals of grade T are formed at the V and VI stages of metamorphism. These include coals with an output m of volatile substances less than 17% in the absence of a plastic layer, with powdery or slightly sintering coke residue. Anthracite includes coals of the highest stages of metamorphism VII-X with an output of volatile substances less than 8-9%. Typical anthracites are grayish-black and differ from coals by metallic luster, dense build, reduced cracking and high strength. The organic part of anthracite contains mostly carbon (94–97%), an insignificant amount of hydrogen (1–2%), and one percent of oxygen and nitrogen. Differences in coals in the carbon and hydrogen content, volatile matter release, the heat of combustion at high stages of metamorphism are smoothed out. Differences in physical properties manifest quite sharply [3]. With a wide range of technical composition and physical properties of the feedstock, it is quite difficult to obtain the same materials with a given set of characteristic parameters required for carbon sorbents. However, there are some approaches to solve this problem, and one of them is the nanostructuring process.

Typical technological schemes for obtaining sorbents include several mandatory stages: grinding, molding, high-temperature carbonation, and combined-cycle activation [4]. An important feature of the processing of coal into carbon adsorbents is that only certain technological schemes with specified processing regimes are applicable to each type of fossil coals and each type of carbon-containing raw material.

For example, when obtaining adsorbents from highly metamorphosed coals, such as anthracites, it is desirable to use inactive oxidants (CO_2) and higher activation processing temperatures (900-950 $^{\circ}$C). Comparison of fossil coals by average petrographic composition showed that there is a pattern reflecting an increase in the sorption properties of synthesized carbon adsorbents with an increase in the content of the inertinite group of microcomponents in them. According to this parameter, the coals of the Kuznetsk and Tunguska basins are most suitable for obtaining adsorbents. Comparison of adsorbents by technological properties shows that it is possible to obtain carbon adsorbents of a certain purpose and a given quality from fossil coals [5].

Funding

The work was carried out under the Coordination Research Plan of the Scientific Council of the Russian Academy of Sciences on Physical Chemistry Code 21 -03-460-09.

References

1. Zheleznova N.G., Kuznetsov Yu.Ya., Matveev A.K. et al. Coal reserves of the countries of the world.- M.: Nedra, 1983.-167p
2. Tarkovskaya I.A. One hundred professions of coal.- Kiev: Naukova Dumka, 1990. -200p
3. Geology of coal deposits and combustible shale deposits of the USSR. Volume 12. General data on coal basins and deposits of the USSR.- M.: Nedra, 1978.
4. Lipović V.G., Kalabin G.A., Kalechits I.V. et al. Chemistry and coal processing.- M.: Chemistry, 1988.- 336p
5. Keltsev N.V. Fundamentals of adsorption technology.- M.: Chemistry, 1984. -592p

CARBON ADSORBENTS FROM MAN-MADE ORGANIC WASTE

***V.V. Samonin*, E.A. Spiridonova, E.D. Khrylova, M.L. Podvyaznikov**

samonin@lti-gti.ru
Saint Petersburg State Technological Institute (Technical University),
190013 Saint Petersburg, Russia

Currently, one of the global problems of mankind is the problem of waste generated both during the production and consumption of industrial products. Waste is categorized into production waste and consumption waste. The largest volume and variety of waste are accounted for by industry [1].

The main types of waste fall into the category of organic materials and include (i) polymer materials such as plastic, car tires, and other waste from the chemical and processing industries; (ii) wood and its derivatives such as lignin and chipboard; (iii) agricultural waste mainly of plant origin including corn cake, fruit seeds, straw, etc.; (iv) waste from the oil refining industry, as well as chitin and chitosan, which are waste products from seafood processing, etc.

Polymer waste is the most promising raw material for the production of carbon adsorbents. Its advantage is a high carbon content and an ordered structure, which allows the production of carbon adsorbents with a regular porous structure and a significant volume of micropores. The volume of micropores in polymer adsorbents can exceed 0.60 cm^3/g, which is a high value, and the strength of the sorbents remains significant, exceeding 95 %.

Other promising materials from industrial waste are the products of oil refining waste. Their advantage is the regular structure and reproducible characteristics of raw materials. For producing high-quality carbon adsorbents, dense materials such as tar, bitumen, oil slurries, pitches, and cokes are the most suitable. Typically, based on these raw materials, it is possible to obtain strong carbon adsorbents (abrasion resistance of more than 90 %) with a micropore volume of more than 0.50 cm^3/g.

Wood raw material and the products of its processing are also of great interest. One of such products is lignin obtained from wood by treating it with a weak sulfuric acid solution. Lignin is promising for producing carbon adsorbents with a pore volume of more than 0.30 cm^3/g and a high sorption capacity from aqueous media.

Chitin, an amino derivative of cellulose found in the shells of sea crustaceans, algae, and fungi, plays an important role in sorption technology. Generally, this material is used as an ion-exchanger to absorb a wide range of impurities of various chemical nature, including heavy metals, radionuclides, and organic compounds, the absorption of which occurs through complex formation. However, this material can also be used to produce carbon adsorbents characterized by the specific nature of the active surface. Alongside chitin, chitosan – the material obtained by treating chitin with alkalis with cleavage of the acetyl group CH_3CO and replacing it with a hydrogen atom to form the primary amino group NH_2 - is also of interest.

Moreover, agricultural plant waste, which can be tentatively divided into high- and low-density materials, is a promising raw material for the production of carbon adsorbents. High-density waste includes fruit pits and nutshells. If certain parameters of the activation process are used, in that case, highly active carbon adsorbents can be obtained from the pits and shells of fruits and, to a degree, rival the properties of active coals from coconut shells. Owing to their high strength, sometimes exceeding 95 %, the volume of micropores in these adsorbents can significantly exceed 0.60 cm^3/g.

Therefore, the development of these technologies [2–4] will allow solving both the problem of obtaining highly active carbon adsorbents and the problem of recycling multi-ton industrial waste.

Funding and acknowledgments

The research was carried out at the expense of a grant from the Russian Science Foundation (project No. 21-79-30029).

References

1. T.F. Tsgoev, R. A. Tebloev, D. B. Byazrova. Waste of production and consumption (North Caucasus Mining and Metallurgical Institute (State Technological University, Vladikavkaz, 2020), 423 p.
2. V.V. Samonin, M.L. Podvyaznikov, E.A. Spiridonova, Sorption technologies for the protection of humans, technology, and the environment, Nauka, St. Petersburg, 2021, 536 p.
3. Yu.V. Pokonova, Solid Fuel Chemistry (2013) No. 2, p. 52
4. K.A. Khviyuzova, N. I. Bogdanovich, N. L. Voropaeva, V.V. Karpachev, Chemistry of vegetable raw materials (2020) No. 1, 337 p.

PHYSICOCHEMICAL BASES OF THE SYNTHESIS OF MODIFIED CARBON SORBENTS FOR MEDICAL PURPOSES

L.G. P'yanova, A.V. Lavrenov, N.N. Leontieva, A.V. Sedanova

Center of new chemical technologies IC SB RAS, Boreskov Institute of catalysis, Siberian Branch of the Russian Academy of Sciences, Omsk, Russia, 644040

Porous carbon-carbon materials for different purposes were developed based on nanodispersed carbon at the Center of new chemical technologies IC SB RAS (previously, Institute of Hydrocarbons Processing, Siberian Branch, Russian Academy of Sciences) [1].

The new direction of the synthesis of porous carbon materials made it possible to develop the following sorbents that meet the requirements of medicine: VNIITU-1 sterile carbon hemosorbent in physiological solution, VNIITU-2 carbon enterosorbent, molded sorbent VNIITU-1, molded VNIITU-1PVP.

Currently, attention is focused on the development of modified carbon sorbents for medical purposes. A set of methods for the chemical functionalization of the surfaces of carbon sorbents with the strong immobilization of functional groups was developed for imparting selective sorption properties to them in order to perform the adsorption of toxic protein substances, which are accumulated in the body in specific diseases [1-3].

The following lines of the synthesis of modified carbon sorbents for medicine have been currently developed at the institute (Fig. 1).

The modifiers used in the synthesis of sorbents for medicine meet the requirements of sorption therapy.

The structures of the used monomers contain functional groups capable of entering a polycondensation/polymerization reaction with the formation of oligomers or polymer chains, which are responsible for the low mobility of a modifier in the pores of the support (as applied to hemosorbents) or facilitate the free migration of the modifier into an aqueous solution (as applied to enterosorbents and application sorbents).

Depending on the problem to be solved and the line of synthesis used, the modifier is supported onto a carbon sorbent either unevenly and locally in the form of islets (for example, in the synthesis of selective hemosorbents) or over the entire surface with the filling of pores (in the development of application sorbents).

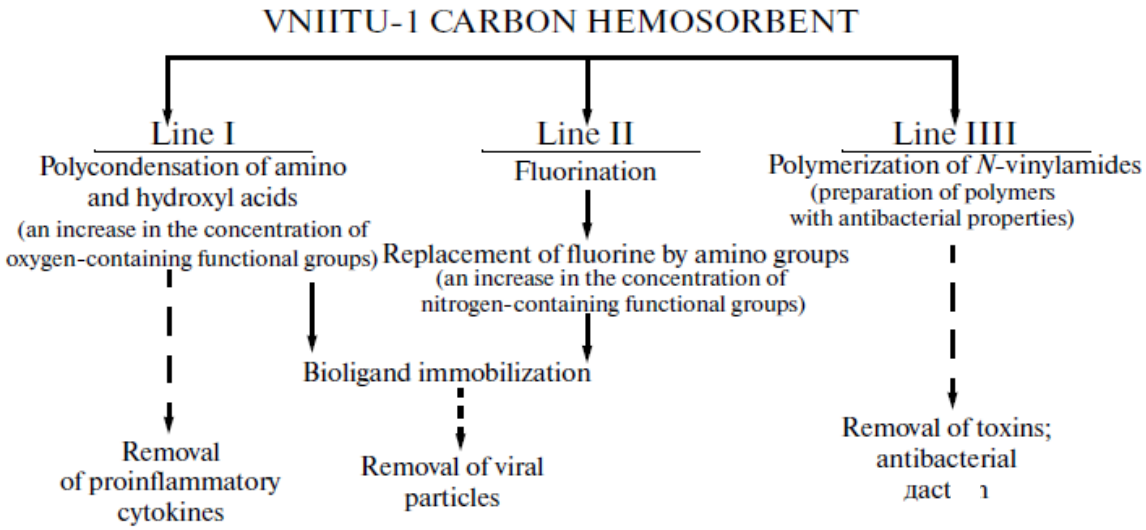

Fig.1. Lines of the synthesis of modified carbon sorbents for medical applications

A complex of physicochemical methods was used for the characterization of the modified carbon materials performed at the Institute of Center of new chemical technologies, Siberian Branch, Russian Academy of Sciences, and the Boreskov Institute of Catalysis, Siberian Branch, Russian Academy of Sciences (Novosibirsk).

The results of long-term studies on the development of modified carbon sorbents for medicine and veterinary medicine made it possible to prepare a wide range of effective carbon materials of a new generation to be used in medicine and veterinary medicine.

Funding and acknowledgments

This work was supported by the Federal Agency for Scientific Organizations of Russia in accordance with the Program for Basic Research of the Boreskov Institute of catalysis, Siberian Branch of the Russian Academy of Sciences. Development Works no. AAAA-A21-121011890076-8.

References

1. V.F. Surovikin, L.G. P'yanova and L.S. Luzyanina. Ross. Khim. Zh. (2007) **51**, 159.
2. V.A. Likholobov, L.G. P'yanova, O.N.Baklanova, V.A. Drozdov, L.S. Luzyanina, A.V. Veselovskaya, O.A. Chirkova. Zh. Prikl. Khim. (2010) **83**, 407.
3. L.G. P'yanova // Khim. Interesakh Ustoich. Razvit. (2011) **19**, 113.

NEW TECHNOLOGIES FOR OBTAINING OF ACTIVATED CARBONS AND THEIR USE FOR THE POTABILIZATION OF NATURAL WATERS

O. Petuhov [1], T. Lupascu [1], R. Nastas [1], I. Ginsari [1], I. Scutaru [2]

lupascut@gmail.com
[1]Institute of Chemistry, MD-2028, 3, Academiei str., Chisinau, Republic of Moldova
[2]Technical University of Moldova, MD-2004, 168, Chisinau, Republic of Moldova

Activated carbon has many applications in various fields of the national economy, in medicine, environmental protection, etc. Carbon adsorbents and catalysts obtained from activated carbon play a unique role in the technological processes of drinking natural water and the food industry, including improving the quality of branded wines. The quality of activated carbons is being upgraded constantly by improving synthesis technologies. The paper presents the experimental results related to the specific features of obtaining activated carbons by the microwave activation method and by the fluidized layer activation method.

The traditional methods of obtaining activated carbon are based on the thermochemical activation of carbon precursors (charcoal, wood, walnut shells, fruit kernels, synthetic polymeric waste) with the formation of a three-dimensional network of pores of nanometric dimensions. Since the activation process proceeds at high temperatures – up to 1100 ^{o}C and lasts for several hours, the cost of production remains high, especially in those countries where there are no cheap sources of energy. The solution to this problem must come through the study and implementation of technologies with low energy consumption and the obtaining of activated carbons with increased parameters.

A less common heating technology, which in recent decades has attracted the attention of researchers in various fields, is microwave treatment. The implementation of this heating process at the industrial level has brought noticeable results, which substantially reduced energy consumption and the technological production cycle. Microwaves have some features not available in traditional heating processes: selective heating, self-limiting reactions, volumetric heating, directed distribution of the electromagnetic field, rapid heating, and no direct contact with the heating source.

Another prospective method of obtaining activated carbon is fluidized bed activation. Compared to conventional methods, fluidized bed activation has the following advantages: activation time is significantly reduced from 2-4 hours to 20-40 minutes; adsorption parameters of adsorbents are 2-3 times better; activation occurs throughout the volume obtaining a homogeneous activated carbon due to the entrainment by the activating agent of the entire mass of carbonate and its maintenance in a suspended state throughout the activation.

This research aims to study and optimize the processes of synthesis and regeneration of activated carbon by microwave treatment and fluidized layer activation, highlighting the factors that determine the parameters of activated carbon, evaluating the adsorption characteristics of adsorbents obtained and identifying their fields of application.

It has been shown that, unlike the classical heating method, the activating agent has an additional role in the case of microwave heating which consists in inducing and changing the dielectric properties of the mixture, depending on the concentration of the activating agent. Microwave treatment of biomass impregnated with potassium hydroxide makes it possible to obtain activated carbon with increased specific surfaces (1600–1800 m^2/g) and a predominantly microporous structure. The use of phosphoric acid allows one to produce activated carbons with a mixed porous structure while preserving the morphology of the raw material.

In more than 50% of cases, Groundwater in the Republic of Moldova contains large amounts of inorganic pollutants such as hydrogen sulfide, ammonia, ammonium ions, sulfides, fluorides, and nitrites, bivalent iron and manganese, etc. To oxidize these pollutants in the reduced state, it is necessary to modify the surface of activated carbons, and this process enabled one to obtain carbon adsorbents with catalytic properties and ion exchangers. The oxidizing process with concentrated nitric acid was used to change the surface chemistry of the activated carbons. The quantity and quality of functional groups formed on the surface of activated carbons in the oxidation process were determined using the Boehm titration method, pH-metric titrations, and FTIR spectroscopy.

The mechanism of immobilization of heavy metal ions on oxidized activated carbons has been established. The results of pH-metric titration analysis showed that heavy metal ions are immobilized by the ion exchange mechanism and the mechanism

of formation of coordinative bonds between oxygen donor electron atoms in carboxylic, ketone, phenolic and heavy metal electron acceptor atoms. Activated carbons impregnated with iron, nickel, and copper ions were tested to determine their applicability for the oxidation of sulfur ions in groundwater. The research results showed that oxidized carbon adsorbents impregnated with copper ions favor the oxidation processes of sulfide ions to sulfite ions and sulfate ions, avoiding the stage of colloidal sulfur formation. This phenomenon is beneficial for using this catalyst for a long time because its surface is not covered with colloidal sulfur, and the catalyst does not lose its catalytic properties.

Carbon catalysts (activated carbon impregnated with copper and manganese oxides) were tested in the process of adsorption/oxidation of nitrite ions in water. The obtained results allowed us to highlight the fact that carbon adsorbents, which contain copper and manganese oxides, favor the process of removing nitrite ions from the water.

The wine industry is another area for which activated carbon is of particular interest. The recently emerging field of application of carbon adsorbents is the removal of off-odors and off-flavors. Another direction of their use is to solve the problems of a wine color, such as excessive browning or pinkness of wines. It has been known that this deterioration of the organoleptic and sensorial characteristics accompanying this browning is due to the oxidation of polyphenolic compounds which are found in wine. Due to the adsorption properties, activated carbon is a clarifying agent that tends to adsorb low polarity compounds, causing them to react easily with the benzene groups in the wine. In recent years, this adsorbent has come into common use in the enological industry in the stages prior to bottling.

Due to the increased interest in this field, the effects of activated carbons prepared from vegetal raw material by activation in a fluidized layer were studied in terms of their industrial oenological use in oxidized white wines with defects of color and microbiological composition. The obtained activated carbon proved to be comparatively effective in removing the phenolic substances with increased oxidability, and it showed superior properties in removing brown oxidation products.

Funding and acknowledgments

The study was supported by the National Project DISTOX, no. 20.80009.7007.21 within the State Program (2020-2013) of the Republic of Moldova.

PREPARATION AND STUDY OF ACTIVE COALS WITH HIGH VOLUME MICROPOROSITY

[1]V.M. Mukhin, [2]N.V. Korolev

victormukhin@yandex.ru; ma.shin@topprom.su
[1]AO "Elektrostal NPO "Neorganika", Elektrostal, Moscow Region, Russia
[2]OOO "Active coals", Novokuznetsk, Russia

Due to the physicochemical properties, carbon adsorbents (active carbons) are unique and ideal sorption materials that allow solving a wide range of issues of ensuring the ecological safety of humans, the environment, and infrastructure [1].

Currently, the production of AU in the world is characterized by a steady growth of 5 % per year and is almost 1.5 million tons/year. Coal is the most crucial resource raw material for the production of AU. Unlike other raw materials, such as peat, wood, lignin, crop waste, coal has an initial high bulk density, which determines the production of the final product – activated carbon - with a high bulk density.

In 1976, Academician M.M. Dubinin proved that in order to ensure a high adsorption capacity of activated carbon operating in a closed volume (filters, adsorbers, etc.), the highly developed volume of micropores per unit volume (cm^3/cm^3) is important, and not per unit weight (cm^3/g). It follows from this that in order to ensure a high adsorption capacity and, consequently, a high service life (filter, adsorber, etc.), it is necessary to produce an AU material with a high bulk density [2].

The Kuznetsk basin has the widest range of coal raw materials with a high initial bulk density for the production of AU.

We have developed technologies for producing AU with a high bulk density based on anthracite from the Gorlovskoye deposit by direct steam-gas activation. A coal-pitch composition of coal grade Z and coal semi-coke was also used as a raw material for producing AU by employing the steam-gas activation process.

The table shows the quality indicators of new domestic ACS of the DAS brand and the CPC brand in comparison with the best brands of domestic (AG-3) and imported (GCN 830).

As can be seen from Table 1, the adsorption properties for the development of the volume of micropores and the test substance iodine in AU with a high bulk density

are significantly higher than that of the domestic analog and are at the level of the foreign analog.

Table 1.

Indicator	Brand of AU			
	AG-3 based on the coal-resin composition	GCN 830 based on coconut	DAS based on anthracite	UPC based on a coal-pitch composition
Bulk density, g/dm^3	450	550	800	790
Volume of micropores, - cm^3/g - cm^3/cm^3	 0.20 0.09	 0.34 0.19	 0.22 0.18	 0.21 0.17
Adsorption activity by iodine, - mg/g - mg/cm^3	 650 292	 800 440	 600 480	 570 450
Abrasion resistance, %	75	92	85	78

The tests of new Russian AU for the drinking water purification showed that the service life of the adsorption columns increased by 3 times compared to AG-3.

References

1. Mukhin V. M. Production and application of carbon adsorbents / V. M. Mukhin, V. N. Klushin. Berlin: LARLAMBERT Academia Publishing, 2018. 352 p.
2. Dubinin M. M. Scientific bases of ways of development of production of active coals / M. M. Dubinin. M.: IFH RAS, 1976. 45 p.

SYNTHESIS OF BIPOROUS CARBON ADSORBENT FOR LONG-TERM LNG STORAGE SYSTEMS

***I.E. Menshchikov*, A.A. Fomkin, A.V. Shkolin, A.A. Shiryaev, S.S. Chugaev**

i.menshchikov@phyche.ac.ru
M.M. Dubinin Laboratory of Sorption Processes
A.N. Frumkin Institute of Physical Chemistry and Electrochemistry RAS,
119071 Moscow, Russia

During storage of LNG, its gradual evaporation occurs as a result of heat inflows into the cryogenic tank (~ 111 K) from the environment. In the absence of consumption, LNG vapors are discharged into the environment or burned in a flare to reduce the excess pressure inside the cryogenic vessel, leading to significant losses of this energy resource. The adsorption-based methods for capture and accumulation allow unjustified losses to be avoided. The selection of adsorbents determines the effectiveness of these methods.

One of the promising directions is the production of highly active adsorbents based on organic carbon-containing raw materials - wastes from the agricultural complex, food, and woodworking industries. Thus, according to [1], Russia has a promising raw material base for walnut shells (WS) with a volume of at least 5 thousand tons per year, which can become the basis for producing high-quality carbon adsorbents. Adsorption systems for capturing and storing vapors in autonomous LNG gasification systems, which have become widespread in recent years [2-4], can be considered one of the applications of the WS-derived carbon adsorbent.

The primary task of the study was to establish the mechanism of formation of a porous structure in carbon adsorbents upon their synthesis from WS via physical activation in a CO_2 flow and determine optimal synthesis modes. Various methods were used to examine the textural characteristics and adsorption capacities of the resulted adsorbents. In this case, one-stage activation of WS was chosen as the primary synthesis mode. It should be noted that the selection of CO_2 as an activator was caused by intensive searching for its processing or practical use. In addition, unlike chemical or steam-gas activation, this method allows an optimal micro-mesoporous structure (PS) to be formed. Moreover, it requires fewer technological resources.

Walnut shells from the Southern regions of Russia were used as a precursor. Heat treatment of WS was carried out on a thermogravimetric analyzer in a flow of carbon dioxide in one stage, without preliminary preparation and treatment of the char at temperatures from 240 to 950°C. To determine the structural and energy characteristics of the obtained samples, we measured the adsorption of nitrogen vapors at 77 K. We used X-ray powder diffraction in the range of scattering angles 2θ from 10 to 120° to study changes in the phase composition under dynamic conditions. In addition, the structural characteristics of the adsorbents were examined using the small-angle X-ray scattering method.

In order to establish the mechanism of PS development and determine the optimal synthesis modes, two series of adsorbents were prepared. The synthesis of samples of the "C" series was limited to the preparation of char and consisted of the pyrolysis of WS in a CO_2 environment at 240, 320, 400, 750, and 950 ° C. Then, the analysis of PS of the "C" series samples enabled us to select the most effective temperature regime of carbonization (T_C) of the feedstock for preparing the samples of the "A" series.

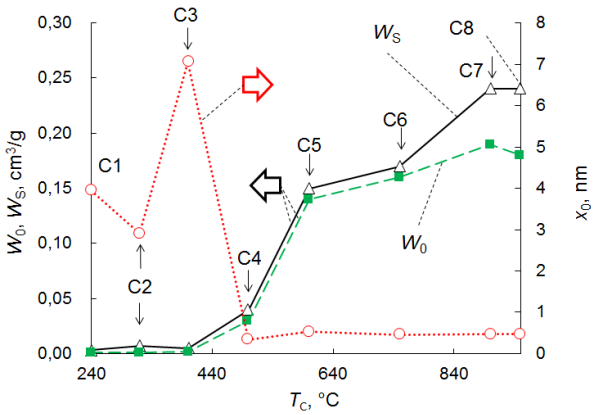

A

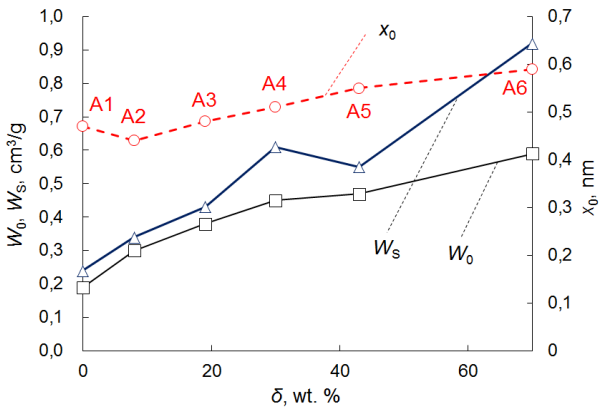

B

Fig. 1. Dependences of the specific volume of micropores, W_0, the total pore volume, W_S, and the average effective half-width of micropores, x_0, of the samples on the carbonization temperature of the precursor (samples of the "C" series) (A) and on the degree of burn-off of the char (samples of the "A" series) (B).

The temperature of about 900 °C was found to be optimal for developing a microporous system in a CO_2 atmosphere (Fig. 1A). Activation at this temperature makes it possible to achieve burn-off rates δ up to 70% of the mass (Fig. 1B) and form an optimal porous structure, particularly for the adsorption accumulation of LNG vapors. The resulting adsorbent had sufficient micropore and mesopore volumes: W_0 = 0.59 cm^3/g, W_{ME} = 0.33 cm^3/g, respectively. The BET specific surface area of 1490 m^2/g and a half-width of micropores of 0.59 nm provided the high adsorption activity towards methane. Mesopores also contribute to the adsorption capacity due to the capillary condensation of methane molecules at subcritical temperatures. Theoretical estimation showed that at temperatures of 120, 160, and 178 K and pressures up to 6 bar, the equilibrium values of methane adsorption onto the adsorbent reached no less than 15, 13.5, and 12 mmol/g, respectively. Thus, the specific capacity of the storage system was at least 200 m^3STP/m^3 under various conditions.

Thus, the concept of one-stage synthesis of microporous activated carbons from walnut shells by physical gas activation in a CO_2 atmosphere has been developed. Furthermore, the optimal synthesis procedure made it possible to produce effective adsorbents for the methane accumulation adsorption-based systems operating at low temperatures.

References

1. Agroinvestor [Electronic resource] // URL: https://www.agroinvestor.ru/markets/news/30896-dolya-rossii-v-mirovom-sbore-orekhov-ne-prevyshaet-1/.
2. Men'shchikov, I.E., Fomkin, A.A., Tsivadze, A.Y. et al. Adsorption accumulation of natural gas based on microporous carbon adsorbents of different origin. Adsorption (2017) **23**, 327.
3. Men'shchikov, I.E., Fomkin, A.A., Romanov, Y.A. et al. Carbon Nanoporous Adsorbents Prepared from Walnut Shell for Liquefied Natural Gas Vapor Recovery in Cryogenic Storage Systems. Prot. Met. Phys. Chem. Surf. (2020) **56**, 1122.
4. Chugaev, S.S., Fomkin, A.A., Men'shchikov, I.E. et al. Adsorption Accumulation of Liquefied Natural Gas Vapors. Prot. Met. Phys. Chem. Surf. (2020) **56**, 897.

STUDY OF THE POSSIBILITY OF USING PLANT RAW MATERIALS FOR PRODUCING SPHERICALLY SHAPED ACTIVATED CARBONS

E.A. Farberova [1], E.A. Pershin [1], N.V. Limonov [2], E.A. Tingaeva [1]

egorpershin96@gmail.com
[1]Perm National Research Polytechnic University, 614990 Perm, Russia
[2]Sorbent JSC, 614042 Perm, Russia

The development of industrial production is ensured by implementing an economic strategy based on modern technologies for the deep processing of raw materials and solid waste to obtain widely demanded products. The essential types of commercial products are carbonic adsorbents – activated carbons, which are effective when used in industry and ecology [1–3].

Among solid adsorbents, it is most promising to use adsorbents of organic origin for environmental purposes. As a raw material for producing this type of adsorbents, carbon-containing materials based on the solid waste of plant origin are used. Therefore, two environmental problems can be solved simultaneously: utilization of solid waste and the creation of relatively cheap high-quality activated carbons [1, 4].

In laboratory conditions, samples of spherical granular activated carbons were obtained from carbon-containing materials of plant origin: shells of fruit pits, peanuts, walnuts, buckwheat husks, and hogweed. Phenol-formaldehyde resin (PFR) of the novolac type was used as a binder to obtain spherical granular active carbons. PFR of the novolac type is easily solidified in a sulfuric acid solution and forms spherical granules with satisfactory strength [5]. We also obtained samples of granular active carbons based on PFR with the addition of various chemical activators: potassium and ammonium carbonates, potassium hydroxide in dry and dissolved forms.

Waste of plant origin was preliminarily subjected to heat treatment without air access at temperatures corresponding to the maximum yield of volatile substances. The thermally modified carbon materials were ground and sieved through a sieve no. 025. The dust of carbon materials was mixed with PFR and introduced dropwise into a 30% sulfuric acid solution through a syringe. The resulting granules were kept in an acid solution for 24–30 hours, and then they were separated from the acid and washed to

pH = 5–6 with distilled water. Then the granules were dried in air, and then in a furnace in an atmosphere of their own gases with a gradual increase in temperature from 100 ° to 300 ° C for 3 hours.

To form a porous structure, spherical granules were subjected to carbonization in an atmosphere of carbon dioxide at a temperature of (500 ± 50) °C for 1 hour and activation in an atmosphere of carbon dioxide at a temperature of (800 ± 50) °C for 1 hour. The yield of the pre-product at the stage of carbonization when using carbon-containing raw materials of plant origin was 43.9–65.6%. The output of active carbon at the activation stage for all samples was in the range of 64.5–79.9%. The table shows the characteristics of the porous structure of some of the obtained activated carbons.

Table 1. Characteristics of the porous structure of activated carbons

Sample	PFR – walnut	PFR – fruit pit	PFR – buckwheat husks	PFR – peanut
Porosity, %	0.8033	0.7487	0.7269	0.7100
Pore space, cm^3/g	1.9775	1.4964	1.3326	1.2339
Maximum scope of adsorption space, cm^3/g	0.533	0.6723	0.7177	0.4670
Micropore volume, cm^3/g	0.3677	0.4297	0.3499	0.3184
Mesopore volume, cm^3/g	0.2078	0.2649	0.4239	0.1715
Macropore volume, cm^3/g	1.444	0.8241	0.6149	0.7669

As Table 1 shows, the obtained samples of spherical active carbons have a developed system of micro- and mesopores. Changing carbon-containing raw materials - the basis for obtaining spherically shaped granular active carbons - allows you to adjust the parameters of the porous structure of active carbons.

References

1. V.M. Mukhin, A.V. Tarasov, V.N. Klushin Active coals of Russia / M.: Metallurgy. - 2000. - 352 p.
2. M.A. Perederiy Sorption materials based on fossil coal. Chemistry of solid fuel. (2000) no.1, 35.
3. I.P. Krapchin Promising carbon processing technologies developed by the Institute of Combustible Fossils and their economic assessment // Chemistry of Solid Fuel. (2005) no.1, 54.
4. S.I. Surinov, V.S. Malyshenko Obtaining medical adsorbents from fossil coal // Chemistry of solid fuel. (1996) no. 4, 39.
5. E.A. Farberova, E.A. Tingaeva, A.S. Maksimov Synthesis of activated carbons with a homogeneous porous structure. Journal of Applied Chemistry. (2015) **88**, 546.

CARBON XEROGEL FOR CONCENTRATION OF METHANE VAPORS IN THE LNG STORAGE SYSTEMS

A.V. Shkolin, A.A. Fomkin, I.E. Men'shchikov

shkolin@phyche.ac.ru
M.M. Dubinin Laboratory of Sorption Processes
A.N. Frumkin Institute of Physical Chemistry and Electrochemistry RAS,
119071 Moscow, Russia

Recently, the ongoing transformation of the global energy system aimed at its decarbonization involves the transition from traditional fuels based on oil separation products to more environmentally friendly gas fuels, among which methane is the most widespread since it has the highest level of technological readiness for widespread implementation. However, the most common methods of storing and transporting methane in liquified (LNG) and compressed (CNG) forms have certain disadvantages. The LNG storage is fraught with gas losses due to evaporation, which limits the operating time. The most promising alternative is the LNG storage combined with the adsorption accumulation of the evaporating gas. The capture of evaporating methane and its subsequent use can significantly increase the operational time of the storage system.

It was found that nanoporous xerogels can serve as an effective adsorbent for low-temperature methane storage [1]. In this context, the present work is focused on assessing the prospects for the use of specially synthesized carbon xerogel as a methane accumulator for an adsorption-based system for LNG vapor recovery.

Table 1 lists the structure and energy characteristics of the studied carbon xerogel evaluated from the standard isotherm of nitrogen vapor adsorption at 77 K. The analysis of the porous structure revealed the 4-fold excess of mesopore volume over that of micropores.

Table 1. Structure and energy characteristics of micro-/mesoporous carbon xerogel.

Microporous				*BET*	*Mesoporous*			
W_0, cm^3/g	E_0, kJ/mol	D_0, nm	d^{MI}_{MAX}, nm	S_{BET}, m^2/g	W_S, cm^3/g	W_{ME}, cm^3/g	S_{ME}, cm^2/g	d^{ME}_{MAX}, nm
0.25	24.4	0,98	0,82	600	1,10	0,85	170	47

The parameters of the porous structure of the xerogel adsorbent indicate its ability to adsorb methane at sub- and supercritical temperatures. At subcritical temperatures, methane molecules first fill micropores, and when pressure approaches the saturation vapor value, the adsorption process occurs in mesopores via capillary condensation. At supercritical temperatures, methane is predominantly adsorbed via the mechanism of volume filling of micropores. Figures 1 and 2 show the data on methane adsorption onto xerogel at and super- and subcritical temperatures, respectively.

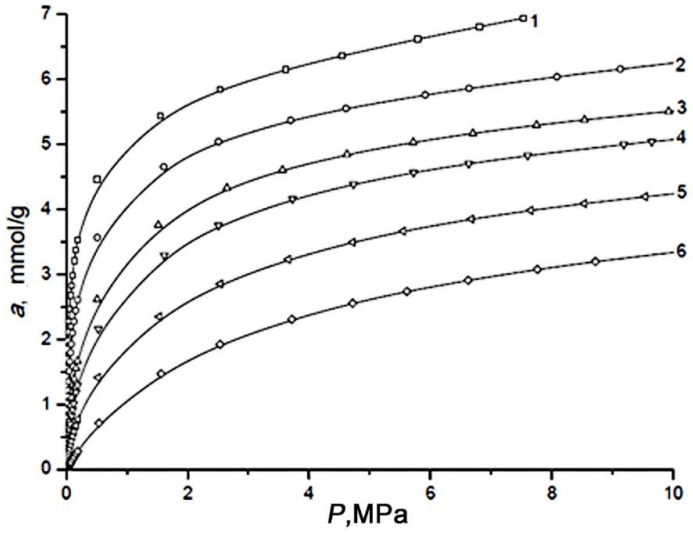

Fig. 1. Methane adsorption onto the micro-/mesoporous carbon xerogel at supercritical temperatures, K: 213(1), 243 (2), 273 (3), 293 (4), 333 (5), and 393 (6).

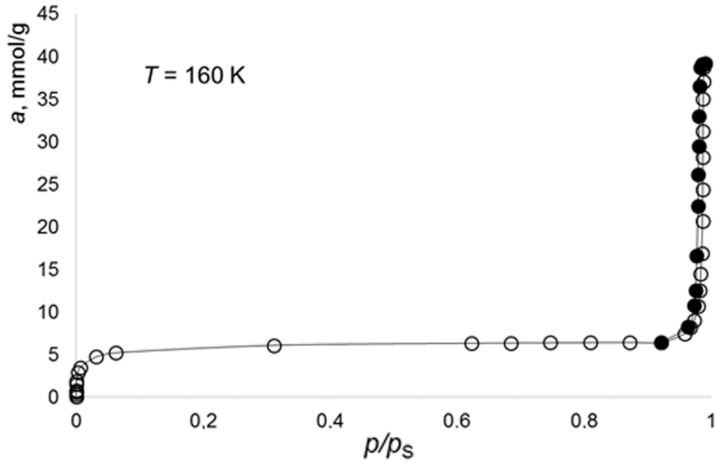

Fig. 2. Methane adsorption onto the micro-/mesoporous carbon xerogel at the temperature of 160 K.

Therefore, the use of carbon xerogel with the combined meso-/microporous structure can ensure a significant increase (3–7 times) in the LNG storage life under the conditions of rated consumption.

Funding and acknowledgements

The study was carried out within the framework of the State Task no. 0081-2019-0018.

References

1. C. Cuadrado-Collados, J. Farrando-Pérez, M. Martínez-Escandell, L.A. Ramírez-Montoya etc. Well-defined meso/macroporous materials as a host structure for methane hydrate formation: Organic versus carbon xerogels. Chem. Eng. J. (2020) **402**, 126276.

EFFECT OF ALKALINE ACTIVATION CONDITIONS ON POROUS STRUCTURE OF PETROLEUM ASPHALT-BASED CARBON

O.V. Gorbunova, O.N. Baklanova, T.I. Gulyaeva, A.V. Lavrenov

Oxana_Gorbunova@inbox.ru
Center of New Chemical Technologies BIC, Boreskov Institute of Catalysis, 644040, Omsk, Russian Federation

Activated carbon materials (ACs) have an advanced porous structure and are therefore widely used as effective adsorbents for the separation of gas mixtures. As a rule, activated carbons have high thermal and chemical stability, thermal and electrical conductivity, and high mechanical strength. In recent years, inexpensive petroleum asphalt was used as the precursor for preparing new ACs featuring high and ultrahigh surface areas [1, 2].

Asphalt is a byproduct of oil refining. It is produced from the heavy residues which remain after the separation of light-oil products. Today, asphalt as a low-cost product is produced in extremely large volumes and does not find a qualified application [3]. Since the asphaltenes included in the asphalt form nano-sized conjugated aromatic structures and asphaltene aggregates, the activation of the asphalt leads to the micro- and mesoporous carbon materials with large surface areas and excellent adsorption properties. Usually, the alkalis are used to activate asphalt [4,5].

There are many other studies where the researchers apply the alkaline activation of carbon precursors. However, there are no systematic studies focusing on how the technological parameters of the alkaline activation process affect the porous structure of the activated carbons produced from the petroleum asphalts. In this study, we demonstrate a cross-impact of the KOH/asphalt ratio and thermal pretreatment parameters on the porous structure of the asphalt-based activated carbon materials.

In this study, we report the effect of thermal pretreatment on the surface area, CO_2/N_2 adsorption capacity, and selectivity of potassium hydroxide ACs derived from petroleum asphalt. Two series of ACs were prepared by a one-stage method using KOH as an activating agent and a two-stage method including pretreatment of asphalt at 450 °C. It is found that both the KOH:asphalt ratio and asphalt pretreatment conditions affect the characteristics of the AC porous structure. The thermal

pretreatment of asphalt before activation with KOH is demonstrated to be a necessary stage for the effective control of the AC porous structure by variation in the KOH:asphalt ratio from 2 to 4. Pretreatment of asphalt at 450 °C and subsequent activation with KOH at 800 °C gives a porous carbon with a high surface area (2588 m^2/g) and total pore volume (1.3 cm^3/g). The highest CO_2 adsorption capacity (3.8 mmol/g at 25 °C and 1 bar) was achieved in the activated carbon without pretreatment asphalt. The IAST-predicted adsorption selectivity for a gas mixture containing 15% CO_2 and 85% N_2 on AC-4 at 25 °C and 1 bar is 48, which is higher than that of most activated carbons. Therefore, these excellent adsorption properties would make ACs promising adsorbents for the adsorption-based separation of the CO_2/N_2 mixture.

Funding and acknowledgments

This work was supported by the Ministry of Science and Higher Education of the Russian Federation within the governmental order for Boreskov Institute of Catalysis (project AAAA-AA21-121011890076-8).

References

8. H. Javed, D.X. Luong, C.-G. Lee, D. Zhang, J.M. Tour, P.J.J. Alvarez, Carbon (2018) **140**, 441.
9. W. Liang, Y. Zhang, X. Wang, Y. Wu, X. Zhou, J. Xiao, Y. Li, H. Wang, Z. Li, Chem. Eng. Sci. (2017) **162,** 192.
10. J. Liu, Y. Liu, P. Li, L. Wang, H. Zhang, H. Liu, J. Liu, Y. Wang, W. Tian, X. Wang, Z. Li, M. Wu, Carbon (2018) **126,** 1.
11. A.S. Jalilov, G. Ruan, C.-C. Hwang, D.E. Schipper, J.J. Tour, Y. Li, H. Fei, E.L.G. Samuel, J.M. Tour, ACS Appl. Mater. Interfaces (2015) **7**, 1376.
12. A.S. Jalilov, Y.Li, J. Tian, J.M. Tour, Adv. Energy Mater. (2016) **7**, 1600693.

PREPARATION OF HIGH-DENSITY CARBON ADSORBENTS BASED ON PLANT RAW MATERIALS

O.V. Solovtsova*, *I.E. Men'shchikov, A.V. Shkolin, A.A. Fomkin, E.V. Khozina

o.solovtsova@phyche.ac.ru
M.M. Dubinin Laboratory of Sorption Processes
A.N. Frumkin Institute of Physical Chemistry and Electrochemistry RAS,
119071 Moscow, Russia

The strategy of green energy transition and carbon footprint reduction [1] involves the creation of efficient adsorption-based storage of natural gas, and this fact determines the urgency of developing an optimal microporous adsorbent. In addition to high methane adsorption capacity, such an adsorbent must have appropriate strength properties and a sufficient source of accessible raw materials to ensure its large-scale production. In this regard, the present work focuses on the synthesis of a microporous carbon adsorbent from cheap and relatively common plant raw materials and the subsequent fabrication of an adsorbent monolith block with a developed porous structure.

The sample of activated carbon (AU) was prepared from a wood char coal by chemical KOH activation for 60 min and at 900 °C. The KOH activator:char ratio was 3:1. After the activation, the carbon sample was washed with water until the pH value of the washing effluent reached 8; then, the wet samples were dried. The bulk density of the resulting carbon adsorbent in the initial powdered form was 140 kg/m^3, and the humidity was 10 %.

Calculations of the parameters of the porous structure of the as-prepared AU sample from the low-temperature nitrogen vapor adsorption by the equations of the Dubinin theory of volume filling of micropores and standard BET method revealed the well-developed porous structure characterized by the high values of micropore volume (W_0) and specific BET surface (S_{BET}), and efficient micropore width ($2x_0$) Thus, the prepared AU material can be employed as an adsorbent for energetically essential gases, in particular, methane. Table 1 also lists the characteristics of the commercial activated carbon prepared from coconut shells, AP-1, and shaped monolith blocks prepared from the AU powder: AU-S and AU-C-S.

Table 1. Textural characteristics of a new microporous carbon adsorbent (AU), commercial activated carbon AR-1 and shaped AU samples AU-S, AU-C-S.

Structural and energy parameter	AU	AR-1	AU-F	AUC-F
Specific volume of micropores, W_0, cm^3/g	0.88	0.56	0.49	0.45
Characteristic adsorption energy of benzene, E_0, kJ/mol	20.3	20.7	20.4	21.2
Effective radius of micropores, x_0, nm	0.59	0.58	0.59	0.57
Characteristic energy of nitrogen adsorption, E, kJ/mol	6.7	6.8	6.7	7.0
Specific surface area according to BET, S_{BET}, m^2/g	2500	1470	1460	1250
Total micropores volume, W_s, cm^3/g	1.29	0.67	0.76	0.62
Packing density, d, kg/m^3	140	370	425	530

Considering the possible use of the synthesized activated carbon, we tested several functionalization methods to increase the packing density and improve the volumetric methane adsorption capacity. Following the first method, we compacted the AU powder by using a hydraulic press at room temperature. Another method with a heated press mold (hot shaping) was also employed for shaping the as-prepared AU material (AU-S) and its mixture with the activated carbon with higher density, AR-1, (AU-C-S). The SKS latex was used as a binder in all cases, and the compaction pressure was 50 MPa.

In the hot shaping, the powder sample was held under pressure for 2 hours, and this time was enough for all the processes caused by heating the press mold to be completed. In the beginning, there were the displacements and relative sliding of the particles: 90% of the maximum density was achieved at this stage. Then, the processes of boundary sliding of the particles and their volumetric deformation occurred, followed by the volumetric (elastic) deformation. The hot-shaping temperature was chosen depending on the sintered material and the binder. Table 2 lists the data on the density of the resulting shaped carbon materials prepared by two methods.

Table 2. The density of the shaped carbon blocks, AU-S and AU-C-S, prepared by compaction at room temperature and hot shaping of the as-prepared AU powder and mixed with AR-1. The SKS latex was used as a binder; the compaction pressure was 50 MPa.

Shaped samples	Density, g/cm^3	
	Shaping at room temperature	Hot shaping
AU-S	390	425
AU-C-S		530

As follows from the comparison of Tables 1 and 2, the compaction of the initial AU powder and its composite mixture with AR-1 led to noticeable degradation of the porous structure, which was evidenced by the lower values of S_{BET} and W_0 for AU-F and AUC-F compared to AU. The degradation of the porous structure can also be attributed to the pore blockage by the latex used as the binder. However, the data in Tables 1 and 2 show that the shaping of the powdered AU increased the packing density and, consequently, must improve the adsorption capacity. It should be noted that the hot shaping gives an increase in the density of the obtained samples by 8–10% compared to the samples shaping according to the standard method (see Table 2).

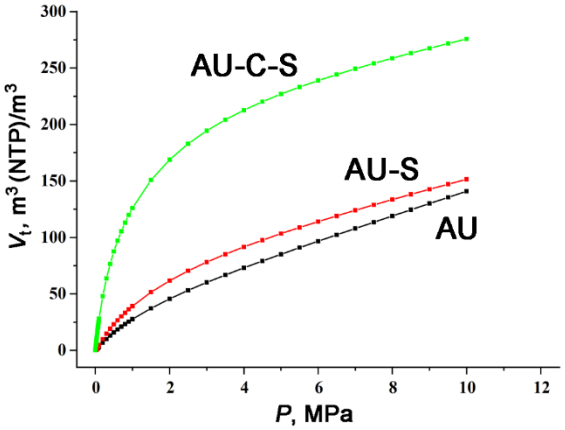

Fig. 1. Dependences of the total specific volumetric capacity for methane calculated for a methane storage system loaded with the initial powdered AU adsorbent and the blocks of the shaped adsorbents, AU-S and AU-C-S, on methane pressure at 303 K.

The significant increase in the density of the carbon adsorbents, namely AUC-F, provides a possibility to achieve the maximum total volumetric adsorption capacity of 275 m^3 (NTP)/m^3 at 303K (see Fig. 1).

Funding and acknowledgments

The research was carried out within the State Assignment of the Russian Federation (Project No. 0081-2019-0018) and the plan of the RAS Scientific Council (Theme No. 21-03-460–01).

References

1. Tsivadze A.Yu, Aksyutin O.E., Ishkov A.G., Menshchikov I.E., Fomkin A.A., Shkolin A.V., Khozina E.V., Grachev V.A. Porous carbon-based adsorption systems for natural gas (methane) storage. Russ. Chem. Rev. (2018) **87**, 950.
2. Brunauer S., Emmett P.H., Teller E. Adsorption of Gases in Multimolecular Layers J. Am. Chem. Soc. (1938) **60**, 309.

INFLUENCE OF ACTIVATED CARBON CHARACTERISTICS ON THE PROPERTIES OF THE CUPRAMITE ABSORBER

***A.N. Tsukanova*[1], *E.A. Farberova*[2], *E.A. Pershin*[2], *N.V. Limonov*[1], *N.B. Khodyashev*[2]**

angi.tsukanova@gmail.com
[1] *Sorbent JSC, 614042 Perm, Russia*
[2] *Perm National Research Polytechnic University, 614990 Perm, Russia*

Nowadays, an urgent task of the chemical industry, agriculture, and treatment facilities of water utilities is to effectively clean the air from such pollutants as ammonia and hydrogen sulfide [1, 2]. The chemisorption method of air purification using a chemical absorber of ammonia and hydrogen sulfide of the Cupramite brand, obtained from granular activated carbons, has found wide application in solving this problem [3].

In the production of granular activated carbons, coal dust of the SSOMSSH brand with a semi-coke charge and a binder with a wood-chemical resin are used as raw materials. In modern conditions of the latter's deficit, it became necessary to search for new alternative types of binders, as well as to study the possibility of using coal tar from various manufacturers. The properties of granular activated carbons and chemical absorbers based on them significantly depend on the composition of the raw materials.

The aim of this work is to study the effect of raw materials on the characteristics of the porous structure of granular activated carbons samples and the sorption properties of the chemical absorbent Cupramite, obtained on their basis. For research, samples of granular activated carbons with a particle size of 1.0-1.5 mm, made using 100% coal tar as a binder, were obtained. Various amounts of semi-coke were introduced into the composition of coal dust (from 0 to 50% by weight).

The Cupramite absorber samples were made from the obtained laboratory samples of activated carbons. The production was carried out by impregnating the coal base with a hot (70–80 °C) aqueous solution of copper (II) sulfate with a concentration of 350 g/dm^3, followed by aging and heat treatment.

The characteristics of the porous structure for activated carbon samples and chemical absorbers on its basis were determined, and their influence on the sorption properties of absorbers was analyzed (Table 1). The characteristics of the porous structure were calculated on the basis of isotherms of low-temperature adsorption of nitrogen, obtained on a NOVA 1200e high-speed analyzer for determining the specific surface area of materials.

Table 1. Characteristics of activated carbon and chemical absorbent samples

Name of indicator	Value of indicator for a sample of activated carbon (AC) and a chemical absorber (CA) based on it					
	Sample 1		Sample 2		Sample 3	
	AC-1	CA-1	AC-2	CA-2	AC-3	CA-3
The component proportion in the composition of coal dust: – coal – semi-coke	100 0	-	75 25	-	50 50	-
Ash content, %	7.1	-	7,3	-	8,9	-
Abrasion resistance, %	92	-	91	-	92	-
Total pore volume by water, cm^3/g	0.83	-	0,86	-	0,89	-
Dynamic activity for benzene, min	67	-	61	-	66	-
Active additive content, %	-	13.4	-	12.6	-	12.3
Dynamic capacity for ammonia, mol/dm^3	-	0.990	-	0.925	-	0,878
Hydrogen sulfide dynamic capacity, mol/dm^3	-	1,215	-	1,238	-	1,035
BET specific surface area, m^2/g	993	656	882	562	846	585
Total pore volume, cm^3/g	0.83	0.77	0.86	0.83	0.89	0.78
Micropore volume, cm^3/g	0.465	0,299	0.422	0.271	0.413	0.283

Mesopore volume, cm^3/g	0.050	0,037	0.071	0.059	0.113	0.092
Macropore volume, cm^3/g	0.300	0.414	0.368	0.508	0.382	0.418

As follows from Table 1, the obtained samples of granular activated carbons are distinguished by high mechanical strength, rather low ash content, and a high value of dynamic activity for benzene. An increase in the semi-coke proportion in the composition of coal dust leads to the production of activated carbon samples with a higher total pore volume.

An increase in the semi-coke proportion reduces the specific surface area (BET) of activated carbons by 15–20%, the volume of micropores by 10-15%. The volume of mesopores and macropores, on the contrary, increases significantly: the volume of mesopores – more than 2.5 times, the volume of macropores – by 20–30%.

The absorbent samples are characterized by approximately the same amount of decrease in the value of adsorption space volume - by 29–34%. In this case, the total pore volume of most absorbers decreased by 7–12%, which may indicate the distribution of the active additive in the adsorption space volume –over micro- and mesopores.

As a result of the study, it was found that the largest volume of the sorption space in the samples of activated carbon and the absorber is made up of micropores with a half-width of 0.525–0.625 nm. The application of copper sulfate to the surface of activated carbon reduces the pore volume with a half-width of 0.525–0.625 nm by 35–50% of the initial pore volume of the base.

References

1. I.P. Krivolapov, M.S. Koldin, S. Shcherbakov Research of air purification efficiency in livestock breeding complex from ammonia and hydrogen sulfide // TPP APK. - 2016. - No. 3 (11). - 9-18 pp.
2. N.I. Smolin, B.V. Zherebtsov Existing methods and technical means of air purification from hydrogen sulfide // Modern equipment and technologies. - 2013. - No. 9 (25). – 7 p.
3. E.A. Spiridonova, V.V. Samonin, M.L., Podvyaznikov, V. Morozova Obtaining and research of fullerene-modified chemical absorber of ammonia based on activated carbon // Journal of Applied Chemistry. - 2020. - T. 93, No. 5. - 683-690 pp.

SORBENT FOR THE ABSORPTION OF IODINE RADIONUCLIDES

V.M. Mukhin[1], M.A. Gutnikova[1], S.I. Gutnikov[2]

victormukhin@yandex.ru, gutnokov@gmail.com
[1]AO "Elektrostal NPO "Neorganika", Elektrostal, MR, Russia
[2] Chemical Faculty of Lomonosov Moscow State University, Moscow, Russia

Nuclear power plants (NPP) are an important alternative to hydrocarbon energy. On the other hand, it is necessary to take serious measures to clean the waste gases of nuclear power plants from radioactive iodine and radioactive inert gases krypton (Kr) and xenon (Xe), since radiation pollution of territories causes the most severe damage to the biosphere among other global technogenic factors affecting its safety (oil spills on land and at sea, soil pollution with chemicals and pesticides, soil oppression by acid rain and atmospheric destruction [1,2].

JSC "ENPO" Neorganika "together with the State Research Center of the Russian Federation" FEI named after A. I. Leypunsky " has developed a new type of sorbent based on compacted vegetable raw materials (nut shells and fruit seeds) for the absorption of gaseous radionuclides of the VSK-5IK brand (TU 2568-374-04838763-2010), which has passed all the necessary approvals in the Rosatom system. According to its sorption properties and strength characteristics, VSK-5IK significantly surpassed the previously produced industrial sorbent SKT-3IK. Table 1 shows the adsorption and strength properties of these sorbents.

Table 1. Adsorption and strength properties of sorbents

Sorbent type	Purification efficiency (sorption activity), %		Protective action time (VZD) for benzene vapors, min	Abrasion resistance (GOST 16188-70), %
	for radionuclide I^{131}	for radionuclide CH_3I		
VSK-5IK	99.992	99.91	95	91
SKT-3IK	99.9	99.0	62	69

The VSK-5IK sorbent was successfully supplied to some of the ROSATOM facilities for equipping the AUI-1500 and UFK-3500U adsorbers.

References

1. Mukhin V. M. Production and application of carbon adsorbents / Mukhin V. M., Klushin V. N.-Berlin: LARLAMBERT Academia Publishing, 2018. - 352 p.
2. Mukhin V. M. New sorbents for effective absorption of radionuclides in the CDF systems of nuclear power plants / V. M. Mukhin, S. N. Solovyov, M. A. Gutnikova. - N. Novgorod: Atomic Project Publishing House, 2010. - p. 77.

COMPARATIVE EVALUATION OF ANTIDOTE EFFECTIVENESS OF ACTIVE COALS

[1]V.M. Mukhin, [2]Yu.Ya. Spiridonov

victormukhin@yandex.ru; spiridonov@vniif.ru
[1]AO "Elektrostal NPO "Neorganika", Elektrostal, Moscow Region, Russia
[2] FGBNU Research Institute of Phytopathology of the Russian Academy of Sciences, Golitsyno, Moscow Region, Russia

Detoxification of soils from pesticide residues is an important factor in the greening of the agro-industrial complex. Recently, these works have become especially relevant in connection with the adoption of Federal Law No. 280-FZ of 03.08.2018 "On Organic Products and on Amendments to Certain Legislative Acts of the Russian Federation".

Vegetation experiments on soil detoxification were carried out in accordance with the traditional method, according to which the sod-podzolic soil was treated with the herbicide Singer SP at a dose of 0.4 g/ha using a laboratory sprayer. A day later, AU samples were introduced at a dose of 100 kg/ha. After a day, the prepared soil was distributed into waxed disposable paper cups with a capacity of 600 g of soil, and the test plants of rapeseed of the Ratnik variety were sown 3 pcs. for each vessel. The repetition of the experiment is 5 times for each dose of the studied AU samples.

The cultivation of test plants was carried out under controlled conditions of the artificial climate laboratory (LIK) in the Fetch chambers (Germany). After 25 days, the aboveground mass of test plants was cut and weighed. The level of antidote effectiveness of the experimental samples of active coals was judged by the mass of the aboveground organs of the test plants in comparison with the control variant without herbicide and active coal.

The decrease in the mass of test plants in the experimental variants relative to the control was calculated by the formula:

$$B = 100 - \left(\frac{A}{K} \cdot 100\right), \%,$$

where *B* is the decrease in the mass of test plants in the experimental variant relative to the untreated control;

A is the average value of the mass of test plants on the experimental version;

K is the average value of the mass of test plants in the control variant.

The data obtained are shown in Table 1

Table 1 – Test results for a comparative assessment of the antidote effectiveness of various brands of AU (LIK FGBNU VNIIF, Department of Herbology, 2021)

n / a	Variant	Dose of AU, kg/ha	Dose of herbicide Singer, SP, g / ha	Aboveground mass of test plants, g						Weight reduction of test plants, % to control
				by repetitions					average	
				1	2	3	4	5		
1	Agrosorb-SO	**100**	-	4.8	5.2	3.8	3.6	3.6	4.2	2.8
2			**0.4**	4.3	5.5	11.1	10.8	4.7	7.3	-23.7
3	Agrosorb-N	**100**	-	6.3	6.7	5.9	5.4	6.2	6.1	-3.4
4			**0.4**	7.1	6.8	5.8	10.7	6.3	7.3	-23.7
5	UPK-1B (Δ = 450 g/dm^3)	**100**	-	4.3	3.8	4.1	4.6	4.7	4.3	27.1
6			**0.4**	7.6	4.2	4.3	4,1	5.4	5.1	13.6
7	BCK-830 act.2	**100**	-	6.7	6.4	7.5	7.2	8.0	7.2	-22.0
8			**0.4**	9.2	6.1	5.4	6.9	5.4	6,6	-11.9
	Control (Singer)		**0.4**	5.3	4.2	3.1	3.6		4.1	30.5
	Control without AU and herbicide		-	5.5	5.0	5.7	7,2		5.9	0

Note: negative values – stimulation of plant growth.

As follows from the data given in Table 1, the introduction of active coals into the soil contaminated with the herbicide makes it possible to neutralize its depressing effect on the test culture of rapeseed, while the best results were obtained by the active coals of Agrosorb-SO and VSK-830.

ACTIVATED CARBONS AS NANOPOROUS ELECTRON-ION-EXCHANGERS

Yu.M. Volfkovich*, *A.A. Mikhalin, A.Yu. Rychagov, V.E. Sosenkin, D.A. Bograchev

yuvolf40@mail.ru
A.N.Frumkin Institute of Physical Chemistry and Electrochemistry, Russian Academy of Sciences, Moscow, 119071 Russia,

It is known that activated carbons (AC) have the following unique properties: high specific surface area (SSA) ~ 500 - 2500 m^2 / g, high adsorption capacity, electronic conductivity, and the presence of surface groups (SG). High SSA and electronic conductivity have led to the widespread use of AC in supercapacitors (SC) and for capacitive deionization of water (CDI). The aim of this work was to study the porous structure, hydrophilic-hydrophobic, capacitive properties of AC, as well as their surface conductivity. The following materials were used in the present work: AC cloth (ACC) "VISKUMAK", NPO "Inorganic", Elektrostal (RF); ACC CH900 by Kuraray Co. (Japan); SAIT electrodes (Korea) based on AC SAIT + 5% polytetrafluoroethylene (PTFE); electrodes from SKB RIKON (Voronezh, RF) based on AC Norit + 4% PTFE; and carbon black KJEC.

To study the porous structure and hydrophilic-hydrophobic properties of AC, we used the method of standard contact porosimetry (MSCP) [1]. This method allows not only to study the porous structure of any materials in the widest possible range of pore radii ~ from 1 to $3x10^5$ nm but also to study their hydrophilic-hydrophobic properties. When using octane, the porosimetric curves are measured for all pores, and when using water, only hydrophilic pores. As an example, Fig. 1 shows integral (a) and differential (b) curves of pore distribution over effective radii r *, measured in octane and water, for ACC "VISKUMAK", where $r^* = r / \cos\theta$, r is the true pore radius, and θ is the contact angle of wetting by water. Since octane almost ideally wets all materials, then for it $\theta \sim 0$ and $r^* \sim r$, and for water $\theta > 0$ and $r^* > r$.

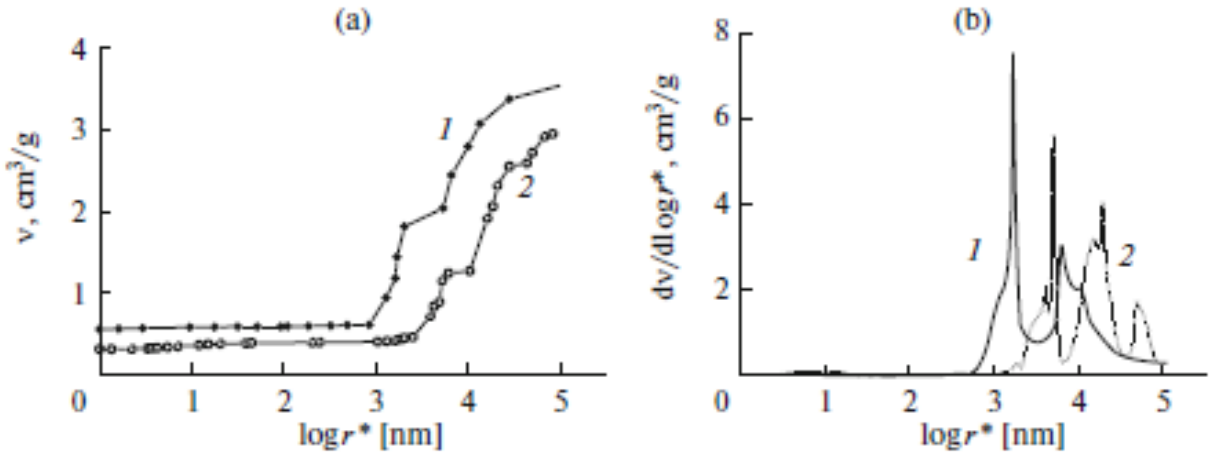

Fig. 1. Integral (a) and differential (b) curves of pore distribution over effective radii for ACC VISKUMAK.

Fig. 1 shows that AC electrodes have a very wide range of pore radii from fractions of nm to 100 μm, i.e., more than 5 orders of magnitude. The main data of MSCP are given in the table. As can be seen, the porous structure of all AC electrodes includes both hydrophilic and hydrophobic porosity.

Table 1. Characteristics of porous structure and hydrophilic-hydrophobic properties of AC electrodes

Electrode	Specific surface area, $m^2 g^{-1}$		Ratio of hydrophilic to total specific surface area	Porosity, $cm^3 cm^{-3}$		
	Пол-ная	Гидрофиль-ная		Total	Hydrophilic	Hydrophobic
CH900	1520	850	0.56	0.850	0.786	0.064
VISKUMAK	600	416	0.70	0.729	0.623	0.106
SAIT	940	520	0.55	0.715	0.490	0.225
RIKON	1580	940	0.59	0.740	0.530	0.210
KJEC	2500	2600	-	0.89	0.84	0.05

We were the first to establish the presence of surface conductivity (SC) in activated carbons. The specific electrical conductivity of the solution in the pores κ is the sum of the specific electrical conductivity of the free solution (κv) and SC. SC is the longitudinal (tangential) conductivity of an electric double layer (EDL). SC is equal to the sum of the conductivity due to the conductivity of counterions of surface groups in the carbon electrode (κsg) and the surface conductivity of the EDL (κsch). The value

of κsg depends on the concentration of SG (Csg) in carbon, i.e., their exchange capacity Q, and κsch depends on the potential E. Thus, we obtain:

$$\kappa(C, E) = \kappa v(C) + \kappa s = \kappa v(C) + \kappa sch\ (E) + \kappa sg(Q) \quad (1)$$

Fig. 2 shows the dependences of the electrical conductivity of the carbon electrode CH 900 and SAIT on the volume concentration of KCl.

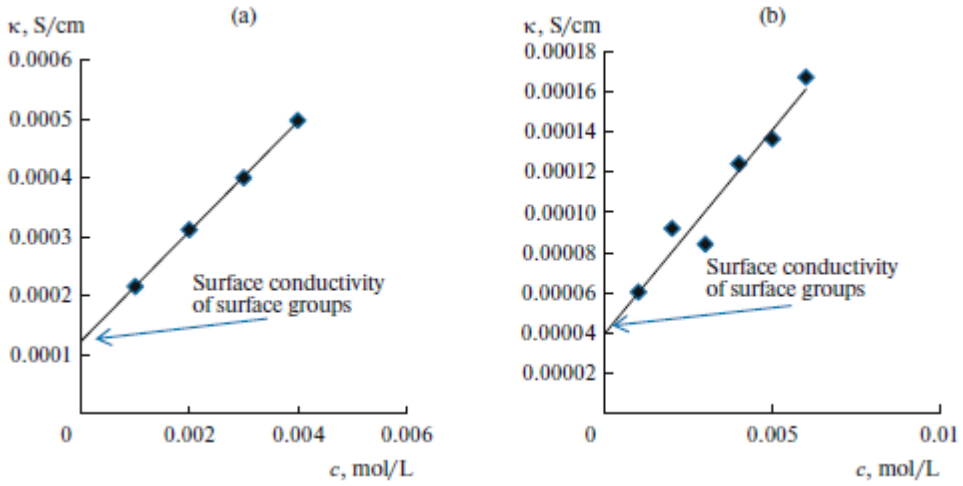

Fig. 2. Dependences of the electrical conductivity of (a) CH 900 and (b) SAIT carbon electrodes on the volume concentration of KCl. Illustration of extrapolation obtaining of the κsg value.

As one can see, by extrapolating these dependences to zero concentration of the solution, the values of surface conductivity are obtained. It was shown that the SC is proportional to the exchanged capacity of the AC. Due to the presence of SC in AC, it turned out to be possible to obtain pure water in the CDI method [2].

Funding and acknowledgments

The work was carried out with the financial support of the Ministry of Science and Higher Education of the Russian Federation.

References

1. Volfkovich, Yu.M., Filippov, A.N., and Bagotsky, V.S.,Structural properties of porous materials and powders used in different fields of science and technology, Springer Publ., London, 2014.
2. Volfkovich, Yu.M., Rychagov. A.Yu., Mikhalin, A.A.,Kardash, M.M., Kononenko, N.A., Ainetdinov, D.V., Shkirskaya, S.A., and Sosenkin, V.E. *Desalination*, 426(2018) **426**, 1.

COMPOSITE AEROGELS BASED ON REDUCED GRAPHENE OXIDE FOR ADSORPTION STORAGE AND TRANSPORTATION OF METHANE

***A.E. Memetova*[1], *E.A. Neskoromnaya*[1,2], *A.D. Zelenin*[1], *N.R. Memetov*[1], *A.V. Babkin*[1,2], *R.A. Stolyarov*[1], *N.A.Chapaksov*[1], *A.A. Gusev*[3], *A.G. Tkachev*[1]**

Anastasia.90k@mail.ru

[1]*Federal State Budgetary Educational Institution of Higher Education "Tambov State Technical University", Tambov, Russia*

[1,2]*JSC «Federal State Research and Design Institute of Rare Metal Industry Giredmet», Moscow, Russia*

[3]*Engineering Center of the Federal State Budgetary Educational Institution of the Higher Education "Plekhanov Russian University of Economics", Moscow, Russia.*

To date, environmental and energy problems associated with the consequences of burning fossil fuels are of considerable scientific and practical interest. Many research teams focus their activities on the development of renewable and clean energy sources. The use of hydrogen (H_2), methane (CH_4), and other energy sources has recently become an increasingly important topic of research [1]. However, compared to H_2, the consumption of natural gas, consisting mainly of CH_4, is very profitable and in demand, and in the near future, it may become one of the main types of fuel [2].

Methane is already used as fuel for passenger cars and is also transported in the form of compressed natural gas (CNG) or liquefied natural gas (LNG). However, the disadvantages of the CNG and LNG methods, namely, high pressures of CNG (more than 20 MPa) and ultra-low temperatures of CNG (112 K) [3] cause significant inconveniences associated with additional capital and operating costs that are necessary to ensure safety when using such systems. Adsorbed natural gas (ANG) provides an explosion-proof and cost-effective approach to its use and transportation, which is achieved due to stable and reliable working conditions, which are determined primarily by the physicochemical characteristics of the adsorbent used.

Aerogels are a new class of nanostructured carbon materials that are currently attracting increasing interest as potential adsorbents for the storage and transportation of natural gases, particularly CH_4.

The aim of this work is to study methods for the synthesis of graphene aerogels (GA) and nanostructured composite material – graphene aerogel/iron (GA/Fe) to study

adsorption processes and experimentally determine the effect of surface modification of graphene aerogel on the absorption efficiency of CH_4.

In this study, the effect of modification of the graphene aerogel surface on the adsorption of CH_4 in the temperature range of 298–313 K and pressures up to 10 MPa was studied. The synthesized graphene aerogels have been characterized by various physicochemical methods, such as adsorption-desorption of N_2 at 77 K, X-ray diffraction analysis, IR spectroscopy with Fourier transform, Raman spectroscopy, scanning electron microscopy (SEM), and transmission electron microscopy (TEM). The structural characteristics of the studied materials are presented in Table 1.

Table 1. Structural parameters of graphene aerogels

	GA	**GA/Fe**
Specific surface area for nitrogen S_{BET}, m^2/g.	657	801
Specific surface area of S_{DFT}, m^2/g.	608	693
Pore volume, V_{DFT}, cm^3/g	0.766	1,016
Specific volume of micropores, cm^3/g	0.142	0.102
Specific volume of mesopores, cm^3/g	0.624	0.914
Density, d, g/cm^3	0.029	0.022

Analysis of high-pressure isotherms showed that adsorbents (HA) and (HA/Fe) demonstrate exceptionally high gravimetric absorption of methane with an achievable capacity of 2.5 g/g and 3.6 g/g, respectively, in the pressure range of 0.5-10 MPa and 298 K, which is more than 7 times higher than the requirements formed by the US Department of Energy (DOE) for the gravimetric capacity of a porous material for methane accumulation [4]. However, despite the high gravimetric absorption, the volume absorption was 104 m^3 (STP)/m^3 and 102 m^3 (STP)/m^3 for (GA) and (GA/Fe), respectively.

The presented results allow us to conclude that the synthesized graphene aerogels can be considered potentially effective materials for the storage and transportation of CH_4. It should be noted that it is necessary to optimize their physicochemical and functional properties to ensure a high volume storage capacity by reducing their gravimetric absorption capacity.

Funding

The work was carried out within the framework of the scholarship of the President of the Russian Federation (SP-1260.2021.1).

References

1. S. Cavenati, C.A.Grande, A.E. Rodrigues Separation of CH4/CO2/N2 mixtures by layered pressure swing adsorption for upgrade of natural gas. Chem. Eng. Sci. (2006) **61**, 3893. doi: 10.1016/j.ces.2006.01.023
2. U.S.E.I.A (EIA) International Energy Outlook, 2016 U.S. Dept. of Energy, Washington (2016), pp. 1–290
3. E.C. Mirian, M.-E. Manuel, G.-R. Enrique, K. Katsumi, S.-A. Joaquín, F. Rodriguez-Reinoso. High-pressure methane storage in porous materials: are carbon materials in the pole position? Chem. Mat., (2015) **27**, 959
4. MOVE_ProgramOverview [Электронный ресурс]. // URL: https://arpae.energy.gov/sites/default/files/documents/files/MOVE_ProgramOverview.pdf

INFLUENCE OF TEMPERATURE ON THE COMPOSITION OF PYROLYSIS GASES OF WASTEWATER SEDIMENTS OF THE LUBERETSKIE TREATMENT FACILITIES

E.M. Rubin [1], A.V. Nistratov [1], A.V. Shkolin [2]

alvinist@muctr.ru
[1] D. Mendeleev University of Chemical Technology of Russia
125047 Moscow, Russia
[2]A.N. Frumkin Institute of Physical Chemistry and Electrochemistry, RAS,
119071 Moscow, Russia

Pyrolysis is a process of thermal processing of organic raw materials by heating in an oxygen-free environment. As a result of this process, three fractions are obtained: solid - char or semi-coke, liquid - tar or primary tar, as well as non-condensable pyrolysis gas (NPG). The most valuable are often liquid and gaseous products of the pyrolysis process since they are energy products [1]. Almost any organic raw material such as wood, coal, peat, and others can be pyrolytically processed. Recently, more and more information about the prospects for the processing of wastewater sludge (WWS) by the pyrolysis method is encountered [2]. A potential advantage of pyrolytic WWS processing is the production of high-energy products.

The main purpose of this work was to determine the effect of the pyrolysis temperature on the composition of the pyrolysis gas. Experiments were carried out on the pyrolysis of WWS of the Lyuberetskie treatment facilities at different temperatures, the heating rate and holding time were 10 deg/min and 10 minutes, respectively, and the range of the studied temperatures was taken from 400 to 650 °C with a step of 50 °C. This mode is considered standard for the pyrolysis process in the Fischer retort according to Russian standard GOST 3168. During the experiment, the gas evolved in an amount of 4 to 13 wt.% of WWS was collected in three flasks over the temperature ranges of 25–400 °C, 400–500 °C, and 500–650 °C (max.)

When analyzing the gas composition, the data were averaged and recalculated for pure pyrolysis gas, excluding the purge gas and air entering the reactor due to incomplete tightness of the laboratory setup (Table 1).

Table 1. Composition of WWS pyrolysis gas for different temperature ranges (vol.%)

Gas formula	Pyrolysis temperature, °C		
	25–400	400–500	500–650
H_2	9	15.9	36.3
CO_2	1.7	-	-
H_2S	14.3	9.8	2.7
N_2	0.6	-	-
CH_4	16.9	23.3	32
CO	48.9	38.5	16.3
C_2H_4	2.7	3	3.2
C_2H_6	2.2	3.6	5
C_3H_6	1.6	2.4	2.5
C_3H_8	1.4	2.3	1.7
C_4H_8	0.1	0.4	0.4
C_4H_{10}	0.3	0.4	0.3
i-C_4H_{10}	0.2	0.3	0.2

It is possible to calculate gas elemental composition (g / l), as well as the lower heat of combustion having data on the elemental composition of the gas.

Table 2. Content of elements in WWS pyrolysis gas

Pyrolysis temperature, °C	Element content, %				
	C	H	N	S	O
25–400	0.438	0.068	0.006	0.189	0.344
400–500	0.601	0.119	-	0.168	0.330
500–650	1.505	0.446	-	0.133	0.407
Total	2.544	0.633	0.006	0.490	1.081

According to the data obtained, one can judge high calorific value of the gas obtained in high temperature ranges, this is explained by an increase in the proportion of

methane, hydrogen and heavier volatile hydrocarbons and a decrease of hydrogen sulfide and carbon monoxide content.

Table 3. Calculated heats of combustion of the gas mixture $Q_{н}^{см} = \frac{1}{100} * Q_{н} * \varphi_{г}$

Pyrolysis temperature,°C	Heat of combustion of the NPG, $Q^{см}_{н}$, кДж/м^3
25–400	320
400–500	433
500–650	520

Hydrogen sulfide and carbon monoxide are undesirable products, since they are toxic; to reduce their emission, it is necessary to maintain a high pyrolysis temperature or add a certain amount of lime to the pyrolyzed raw material [2].

The presence of hydrogen sulphide will complicate the use of gas as an energy resource to some extent, since the former will be converted into sulfur oxide during combustion. If the pyrolysis process is carried out at low temperatures and the gas, accordingly, does not have a high calorific value, then it can be used on site - to maintain the temperature of the pyrolysis furnace or to heat industrial rooms.

Thus, the pyrolysis of WWS in order to obtain the maximum yield of non-condensable pyrolysis gas is a promising way of their utilization; according to the literature, pyrolysis resin can also be used as an energy source. The solid pyrolysis products of these sediments have a high ash content and low carbon content, and potentially a wide range of metals to be extracted from them, but this issue requires a more detailed study.

References

1. Zainullin R.R., Galyautdinov A.A. The use of pyrolysis technology in the disposal of sewage sludge // Innovative Science (2016), no. 6, p. 80-82.
2. Processing and neutralization of sediments and sludge / V.G. Sister, V.N. Klushin, A.I. Rodionov. – Moscow: Drofa, 20

ESTIMATION OF ADSORPTION PROPERTIES OF THE PRODUCT OF PYROLYTIC PROCESSING OF WASTES OF PRODUCTION OF COMPOSITE SANITARY WARES

M.Yu. Piskunova [1], A.V. Nistratov [1], D.V. Fedoseev [2], I.E. Menshchikov [3]

alvinist@muctr.ru
[1]D. Mendeleev University of Chemical Technology of Russia
125047, Moscow, Russia
[2] LLC "PROTON", Shchelkovo, Russia
[3]Institute of Physical Chemistry and Electrochemistry named after A.N. Frumkin RAS,
119071, Moscow, Russia

Polymer composite materials, represented by fiberglass, are increasingly used at present. With the growth of production and consumption of these materials, the question of the formation of difficult-to-recycle wastes and methods of their disposal also arises [1]. In particular, the enterprise-producer of sanitary wares in Shchelkovo forms the “laminate” which is a composite waste based on fiberglass (fiberglass and polyester resin) with the addition of microcalcite and TiO_2, and is not currently recycled.

One of the approaches to the disposal of mineral-organic waste is pyrolysis with incomplete thermal decomposition of the matrix (resin). In connection with the needs of this enterprise, this work is aimed at obtaining and assessing the quality of the sorption material by pyrolysis of the specified laminate.

In the course of the research, the conditions for carbonization of the polymer component of the composite were selected, and the regularities of its decomposition were determined [2]. For an express assessment of the adsorption properties, the carbonizate was placed in desiccators with vapors of water, benzene, and carbon tetrachloride until saturation (20 ° C). The results of determining the volume of the sorbing pores were 0.016; 0.55; 0.18 cm^3 / g, respectively, for water, benzene, carbon tetrachloride, while the total pore volume was 0.32 cm^3 / g, which makes it possible to classify the resulting adsorbent as predominantly microporous.

Since the manufacturing enterprise is interested in the adsorption of styrene vapors contained in its emissions, further experiments were carried out on the absorption of styrene vapors by the carbonizate from the saturated vapor-air flow (28.5

g / m^3) and from the flow with the lowest possible detectable concentration (3.7 g / m^3) at 20 ° C. In this case, the capacity of the adsorbent was determined by its weight increase, measured by a spring balance and a cathetometer.

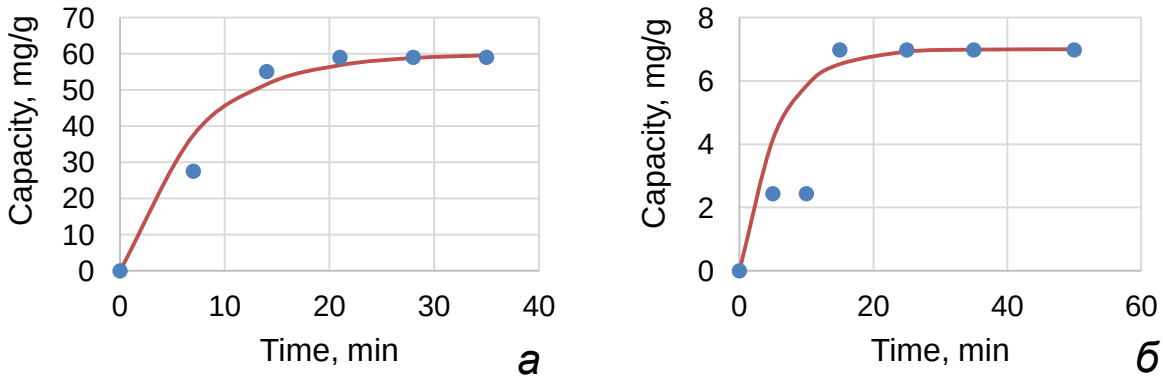

Fig. 1. Adsorption of styrene vapors with a concentration of 28.5 g / m^3 (***a***) and 3.7 g / m^3 (***b***) by carbonizate. Points - experimental data, lines - approximation by the equation $a = a_{max} (1 - \exp(-k^{ads}t))$: a_{max} - maximum capacity, k^{ads} - adsorption rate constant, t - time.

Under static conditions of adsorption of C_8H_8 vapors (in desiccators), the saturation of the carbonizate (392 mg g) was observed over 4 days. The saturation time of the sample in both flows with the developed external mass transfer is about 20 min. The capacity of the carbonizate for styrene when absorbing vapors from a vapor-air mixture (Fig. 1a) sharply decreases in comparison with static adsorption. This can be explained by the fact that the limiting stage - internal diffusion - proceeds very slowly. The capacity of the carbonizate during the purification of a diluted flow of 7 mg styrene / g (Fig. 1b) makes its use ineffective in comparison with the saturated one.

Since microcalcite is an inert component of the carbonizate, its removal from the carbonizate by leaching with hydrochloric acid would improve its performance. For the experiment, several fractions of carbonizate were treated with 20% hydrochloric acid in a six-time mass excess. During water washing, all laminate aggregates disintegrated into powder and glass fibers. However, the quality indicators of the washed adsorbents improved markedly (Table 1).

Table 1. The yield and pore volumes of washed carbonized products

Fraction, mm	Initial mass, g	Final mass, g	Yield of washed product, %	Pore volume, cm^3/g				Capacity for C_8H_8, mg/g
				H_2O	C_6H_6	CCl_4	C_8H_8	
2–5	4.0105	1.701	42.4	0.07	0.99	0.6	0.39	355
1–2	2.6378	0.888	33.7	0.08	0.93	0.596	0.52	473

0,5–1	5.4159	1.751	32.3	0.08	0.88	0.58	0.41	373
< 0,5	6.2850	1.39	22.2	-	1.26	-	0.4	364

The capacity for styrene vapor after washing is several times higher than that of the sample containing microcalcite. Also, the values of the static capacity are comparable with the analogous values of the industrial microporous active carbon AR-A, which is used for the recovery of vapors of organic solvents.

It can be noted that, in addition to an increase in the capacity for styrene vapors, the pore volume for benzene vapors increased sharply, i.e. micro- and mesopores. At the same time, the high hydrophobicity of the materials remained, assessed by the ratio of pore volumes, sorbing C_8H_8 and H_2O.

The observed regularities should be explained by the composition of the carbonizate, namely by incomplete carbonization of the laminate matrix, which retains the ability to dissolve or swell under the action of organic solvents instead of physical adsorption. The above results confirm the hypothesis of a change in the structure of the carbonized laminate upon contact with adsorptives (benzene, carbon tetrachloride, styrene), which requires further study.

References

1. Doriomedov M.S. Russian and world market of polymer composites (review) // Electronic scientific journal "Proceedings of VIAM" (2020), No. 6-7 [Electronic resource]. - Access mode: http://viam-works.ru/ru/articles?art_id=1562.
2. Nistratov A.V., Piskunova M.Yu., Fedoseev D.V. Regularities of pyrolytic processing of waste products from composite sanitary ware. Advances in chemistry and chemical technology: book of articles. (2021), V. XXXV, 123–126.

FEATURES OF FREON 114B2 SORPTION ONTO ACTIVATED CARBONS WITH DIFFERENT POROUS STRUCTURE

G.A. Petukhova, L.A. Dubinina

petukhova_galina@mail.ru
A.N. Frumkin Institute of Physical Chemistry and Electrochemistry,
Russian Academy of Sciences,
119071 Moscow, Russia

Recently, the problems of new threats to the Earth's ozone layer have attracted more and more attention from scientists. Thus, the literature provides a constantly updated list of both dangerous and safe for the atmosphere freons. Unfortunately, the latter do not destroy ozone but significantly accelerate global warming. Therefore, finding effective sorbents for protection against this type of compound is of utmost importance.

The present work focuses on the experimental study of freon vapors adsorption onto activated carbons (AC) with different porous structures, an assessment of the effect of the diameter of adsorbed freon molecules on the parameters of the microporous structure of AC, the determination of optimal parameters of the porous structure for effective absorption of freon.

Activated carbons (AC) with a wide range of changes in the porous structure, obtained from a variety of raw materials, were considered as an object of study. Freon 114B2 - 1,1,2,2, tetrafluorodibromoethane was selected as the freon under study. Table 1 lists the main characteristics of activated carbons, the methods of their production, and raw materials.

Table. Characteristics of activated carbons

Type of carbon	Raw material	Activation method
PAU	Polyvinylidene chloride	Steam-gas
SKT	Peat and potassium sulfide	Potassium sulfide
AG	Coal semi-coke mixed with low-sintering coal; forest chemical resin mixed with coal tar	Steam-gas
MAS	The same	Steam-gas
FST	Furfural	Steam-gas
FAS-E	Furfural	Steam-gas

When analyzing the adsorbability of Freon 114B2 and the microporous structure, we used the Dubinin theory of volume filling of micropores (TVFM), namely, the Dubinin-Radushkevich equation and the Dubinin-Stoeckli equation. We also employed the γ-method for analyzing the mesopore surface compared to the Kiselev-Kestler method applied to the desorption branch of the isotherm of benzene vapor sorption as a variant of the theory of capillary evaporation. Benzene was used as an adsorbate for evaluating the porous structure since the critical diameter of the Freon 114B2 molecule (0.65 nm) is comparable to that of the benzene molecule (0.58 nm). The mesopore analysis method (γ-method) was extended to the adsorption of Freon 114B2 vapors: the adsorption on graphitized soot with the specific area of 110 m2/g was studied to determine the adsorption of vapors per unit surface, and an equation was derived to describe the adsorption on the carbon surface.

Depending on the porous structure, the studied adsorbents can be divided into three groups. The first group consists of microporous AC with a narrow micropore size distribution (so-called carbons with a uniform microporous structure) and includes the PAU and SKT samples. Their distinctive feature is the presence of micropores with an almost complete absence of mesopores (PAC) or the presence of wide micropores with the weakly developed mesoporosity (SKT). The second group includes the AC samples with the wide micropore size distribution: AG, and MAS. They are characterized by the presence of micropores, supermicropores, and mesopores whose volume and surface are more significantly developed compared to that of the ACs from the first group. The third group includes the FST and FAS-E carbons with the wide micropore size distribution and the significantly developed mesoporosity.

Considering the adsorption on the mesopore surface, we calculated the real parameters of the AC micropores, which is especially important for analyzing the AC structure of the third group, i.e., with the significantly developed mesoporosity.

Figure 1 shows the adsorption isotherms measured for Freon 114B2 vapors onto some of the studied AC samples at 293 K. All the adsorption isotherms of Freon 114B2 vapors onto ACs are of the I type according to IUPAC with the H4 type loop that indicates the existence of microporosity and are characteristic of the slit-like pores composed by the plane-parallel particles.

Analysis revealed a good agreement between the real parameters of the AC micropores determined with consideration to adsorption of benzene and Freon 114B2 vapors in mesopores and the estimates of mesopore surface. The most coincidence was found for the AC samples of the first group.

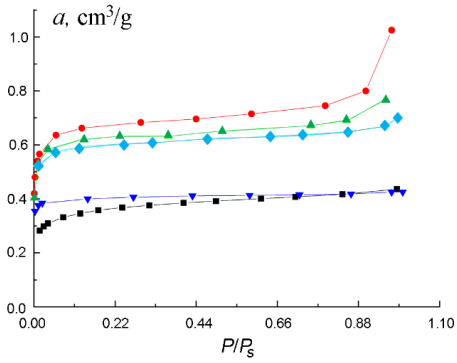

Fig. 1. Isotherms of Freon 114B2 vapors adsorption onto ACs: ● -FAS-E, ▲ - FAS, ◊ - SKT, ■ - AG, ▼ - PAU, measured at 293 K.

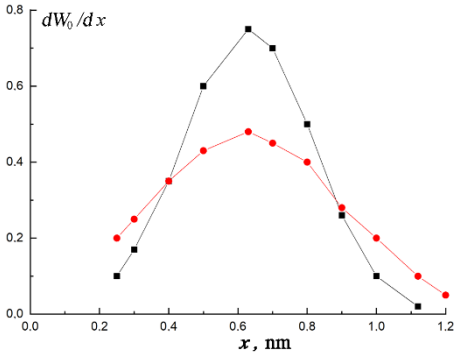

Fig. 2. Micropore size distribution curves for MAS ((■ –adsorption of C_6H_6, ♦ - adsorption of Freon 114 B2, at 293 K, Dubinin-Stoeckli equation)

Minor differences in the parameters of the Dubinin-Stoeckli equation estimated from the adsorption of Freon 114B2 and benzene vapors were found for groups 2 and 3 of AC, as a rule, for the δ - dispersion parameter, which characterizes the width of the micropore size distribution. The observed differences are associated with a change in the filling boundaries of the adsorbent pores depending on the critical diameter of the adsorbed molecules. Figure 2 shows the pore size distribution curves for the MAS samples.

The applicability of the TVFM apparatus for evaluating the adsorbability of freon onto carbon adsorbents was shown, and the optimal parameters of the porous structure of the efficient activated carbons were determined for the adsorption of freon vapors.

Funding and acknowledgments

The work was carried out within the framework of the State Task No. 0081-2019-0018 "Fundamental physicochemical laws of adsorption, adsorption separation, adsorption-electrochemical ion exchange processes in nanoporous materials and the fundamentals for the targeted synthesis of new adsorbents."

ADSORPTION OF ALKANES ONTO CARBON ADSORBENTS AT SUB- AND SUPERCRITICAL TEMPERATURES

K.O. Murdmaa, A.A. Pribylov

pribylov_34@mail.ru
A.N. Frumkin Institute of Physical Chemistry and Electrochemistry, Russian Academy of Sciences, 119071 Moscow, Russia

Recently, much attention has been paid to the problems associated with the adsorption-based methods of transporting natural gas and extracting valuable hydrocarbon impurities from it. Therefore, the study of the adsorption of these hydrocarbons onto carbon adsorbents is currently important.

The volume-gravimetric adsorption setup [1] was used to measure the isotherms of excess adsorption $\Gamma(P,T)$ of methane (T_{cr} =190.77 K) at pressures from 0.1 to 40 MPa, ethane (T_{cr} = 305.50 K) at pressures from 0.001 to 4.5 MPa, and propane (T_{cr} = 369.99 K) at pressures from 0.001 to 0.9 MPa onto the microporous carbon adsorbents MPU-007 and FAS-300. The adsorption experiments were carried out at the temperatures of 303, 313, 323, and 333 K.

The MPU-007 adsorbent with a bimodal porous structure was prepared by chemical activation of the mixture of corn dextrin, ethylene glycol, and formaldehyde resin impregnated by potassium hydroxide [2]. The FAS-300 adsorbent was prepared from furfural, and it is characterized by a well-developed porous structure [3].

The adsorption isotherms $\Gamma(P,T)$ were used to calculate the adsorption volumes W of 1.44 and 0.95 cm^3/g for MPU-007 and FAS-300, respectively. The isotherms of total content $a(P,T)$ were also derived from $\Gamma(P,T)$ and were found to be well described by the Bakaev equation [4] for all three adsorptives at the temperatures mentioned above. The isosteres of adsorption plotted from $a(P,T)$ are approximated by straight lines over the entire temperature range of the changes in the parameters of adsorption equilibria for all studied adsorption systems.

The differential isosteric heats of adsorption $q_{st}(a.T)$ were calculated from the slope of the isosteres as follows [5]:

$$q_{st}(a,T) = -RZ\left[\frac{\partial lnP}{\partial(1/T)}\right]_a - \left(\frac{(\partial P)}{\partial a}\right)_T \cdot W, \qquad (1)$$

Here R is the universal gas constant, Z is the compressibility of adsorptive, W is the micropore volume of adsorbent. Figure 1 shows the dependences $q_{st}(a,T)$ at 303 K.

As seen from the figure, the behaviors of the heat of adsorption are similar for all three adsorptives: starting from the initial heat of adsorption $q(0,T)$ determined by the adsorbent-adsorbate interactions, a slight increase in the heat is observed, which is indicative of the adsorbate-adsorbate interactions, then the heat of adsorption gradually drops to a particular value at a_{max} (P,T), which depends on the adsorbent's structure.

The initial heats of adsorption $q(0.T)$ were evaluated through the Henry constant, K_H, using the formula [6]:

$$q(0,T) = -RZ\left[\frac{\partial K_H(T)}{\partial(1/T)}\right]_a - \left(\frac{1}{K_H(T)}\right)\cdot W \qquad (2)$$

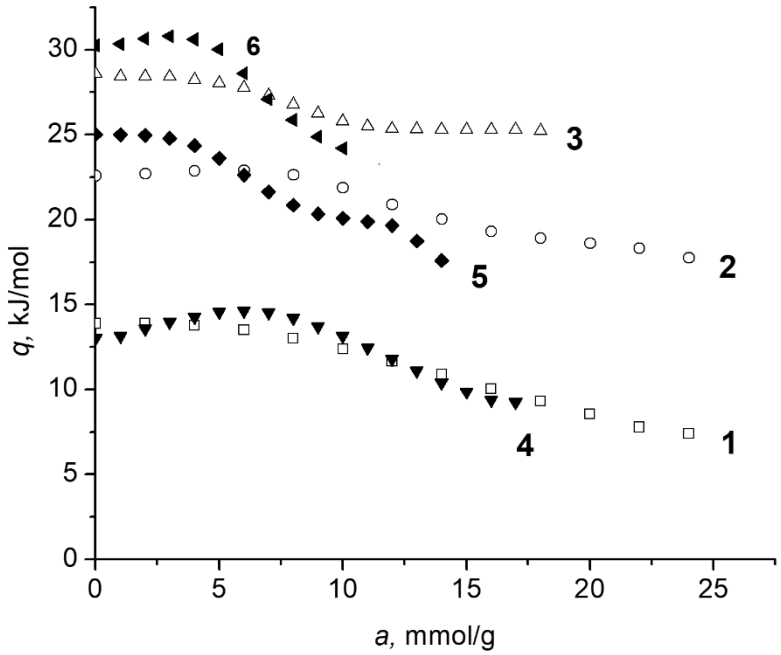

Fig. 1. Dependence $q_{st}(a,T)$ at 303 K for methane (1,4), ethane (2,5) and propane (3,6) adsorption onto MPU-007 (curves 1,2,3) and FAS-300 (curves 4,5,6).

The initial heat $q(0,T)$ of methane adsorption is almost the same for both samples and amounts to ~ 13 kJ/mol. A somewhat different picture was

observed for the adsorption of ethane and propane onto the carbon adsorbents. The values of $q(0,T)$ for ethane adsorption on both adsorbents exceeded significantly that for methane. The values of $q(0.T)$ for propane adsorption were higher than those for ethane adsorption. These trends are associated with the increasing number of atoms in the molecules when passing from methane to propane. Each atom contributes to the energy of the adsorbate-adsorbent interactions. As seen from Fig. 1, the values of $q(0.T)$ both for ethane and propane on MPU-007 exceeded those for the adsorption onto FAS-300, which can be attributed to the differences between the structure of these adsorbents.

The values of isosteric heat of methane adsorption $q_{st}(a,T)$ are almost the same for both adsorbents, and the maximal difference $\Delta q_{st}(a,T)$ was 0.5 kJ/mol. The heats $q_{st}(a,T)$ for ethane and propane change less with the adsorption onto MPU-007 than onto FAS-3, and for both ethane and propane, the maximal difference $\Delta q_{st}(a.T)$ was ~ 2.25 kJ/mol. This difference should be taken into account when designing the methods of extraction of small amounts of ethane and propane from natural gas streams.

Funding and acknowledgments

The work was carried out within the framework of the scholarship of the President of the Russian Federation (SP-1260.2021.1).

References

1. Pribylov A.A., Kalashnikov S.M., Serpinsky V.V. Bull. Acad. Sci. USSR Div. Chem. Sci. (1990), 1233.
2. Fomkin A.A., Pribylov A.A., Tkachev A.G., Memetov N.R. et al. Prot. Met. Phys. Chem. Surf. (2020) **56,** 3.
3. Men'shchikov I.E., Fomkin A.A., Shkolin A.V. Prot. Met. Phys. Chem. Surf. (2021) **57**, 469.
4. Bakaev, V.A. Dokl. Acad. Nauk SSSR [Dokl.Chem. (Engl. Transl.)] (1966) **167**, 369.
5. Pribylov A.A., Murdmaa K.A., Solovtsova O.V., Knyazeva M.K. Russ. Chem. Bull. (2018) 1807.
6. Pribylov A.A., Murdmaa K.A. Prot. Met. Phys. Chem. Surf. (2020) **56,** 115.

METHANE ADSORPTION IN CARBON ADSORBENT S-1

A.A. Pribylov, K.O. Murdmaa

pribylov_34@mail.ru
A.N. Frumkin Institute of Physical Chemistry and Electrochemistry,
Russian Academy of Sciences, 119071 Moscow, Russia

A precision volumetric-gravimetric setup [1] was employed to measure excess methane adsorption on the S1 carbon adsorbent over the pressure range from 0.1 to 40 MPa, and at the temperatures of 303, 313, 323, and 323 K. The carbon adsorbent was synthesized from wood in the laboratory of sorption process IPCE RAS. Figure 1 shows the isotherms of total content $a(P,T)$, which were calculated from the isotherms of excess methane adsorption $\Gamma(P,T)$ and well approximated by the Bakaev equation [2].

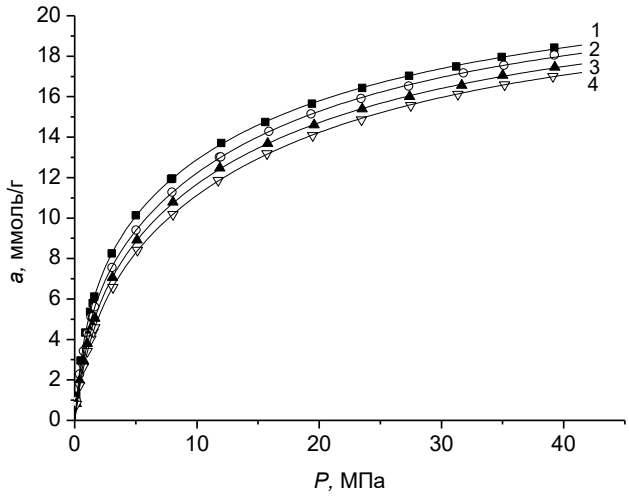

Fig. 1. Isotherms of total content for methane adsorption onto S-1 at *T*, K: 1 – 303, 2 – 131, 3 – 323, 4 – 333.

These isotherms were used to plot the isosteres of methane adsorption, which were well approximated by straight lines over the entire range of the parameters of adsorption equilibrium.

The isosteric heats of adsorption were evaluated from the slopes of the isosteres of methane adsorption by using the formula (see for ex. [3]):

$$q_{st}(a,T) = -RZ\left[\frac{\partial lnP}{\partial(1/T)}\right]_a - \left(\frac{(\partial P)}{\partial a}\right)_T \cdot W \qquad (1).$$

Figure 2 demonstrates the heats of methane adsorption as a function of the amount of adsorbed methane. These values of the heats of adsorption were used to calculate the average isosteric heats of methane adsorption $<q_{st}(a,T)>$.

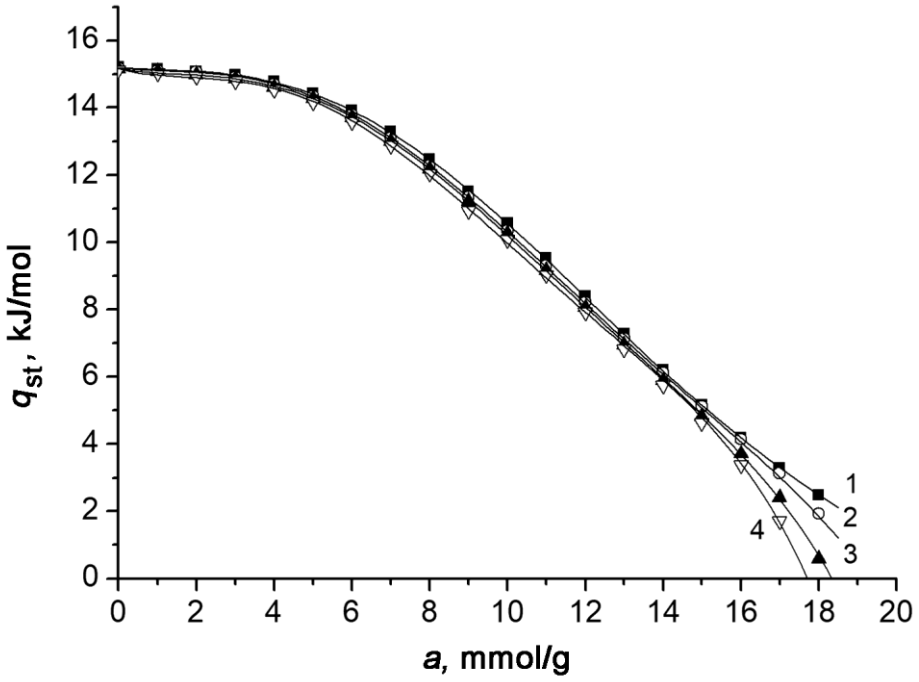

Fig. 2. Isosteric heats of methane adsorption onto S-1 as a function of the amount of adsorbed methane at *T*, K: 1 – 303, 2 – 313, 3 – 323, 4 – 333.

Recently [4], a relationship between the average heats of adsorption and the characteristic energy of adsorption *E* was calculated from the equation of the Dubinin theory of volume filling of micropores (TVFM) [5]. The limit value of methane adsorption at a given temperature a_0 and the thermal coefficient of limiting adsorption α were evaluated for all four temperatures. The average value α = 0.0018 K^{-1}. TVFM considers the "microporous adsorbent–adsorbate" adsorption systems; it can be applied for calculating the isotherms of adsorption measured at a temperature below the critical temperatures for an adsorbent. We measured the isotherms of carbon dioxide, argon, and nitrogen at temperatures both below and above the critical value [6]. It was shown that the average heats of adsorption $q(E)$ calculated via the characteristic energy of adsorption *E* from the equation:

$$q(E) = R(T \cdot T_c)^{0.5} + \left(\sqrt{\pi}/2\right) \cdot E[1 + \alpha(T \cdot T_c)^{0.5}] \qquad (2)$$

agreed well with the average isosteric heats of adsorption both for vapors and gases.

In order to calculate the characteristic energy of adsorption and average heats of adsorption of gases in the supercritical region, we introduced two new parameters, characterizing the adsorptive: critical temperature of adsorptive T_c and analog of saturated steam pressure "P_s" evaluated from the condition of equality of the densities of the adsorbate and adsorptives [7].

Table 1 summarizes the results of all calculations, which show that the average heats of methane adsorption evaluated from the characteristic energy of adsorption q(E) well agree to the average isosteric heats of adsorption $\langle q_{st}(a,T)\rangle$ for the studied adsorption system.

Table

T, K	«P_s», MPa	a_0, mmol/g	E, kJ/mol	$q(E)$, kJ/mol	$\langle q_{st}(a,T)\rangle$, kJ/mol
303	176.55	21.914	8.221	10.52	10.50
313	172.65	21.381	8.024	10.33	10.38
323	166.93	20.926	7.862	10.17	10.17
333	161.11	20.440	7.701	10.02	9.97

As follows from the above data, the value of integral heat of adsorption required for practice can be determined via the characteristic energy of adsorption E using one isotherm of adsorption by multiplying the value of the average heat of adsorption by the desired range of adsorption change without measuring adsorption isotherms at several temperatures, or from calorimetric measurements.

Funding and acknowledgments

The work was carried out within the framework of the State Task 0081- 219 – 0018.

References

1. Pribylov A.A., Kalashnikov S.M., Serpinsky V.V. Russ. Chem. Bull. (1990) **39**, 1105.
2. Bakaev, V.A. Dokl. Acad. Nauk SSSR [Dokl.Chem. (Engl. Transl.)] Vol. 167, pp. 369–372, 1966.
3. Pribylov A.A., Murdmaa K.O., Solovtsova O.V., Knyazeva M.K. Russ. Chem. Bull. (2018) **67**, 1807.
4. Pribylov A.A., Larionov O.G., Shekhovtsova L.G., Kalinnikova I. A., Belyakova L.D. Russ. Chem. Bull. (2009) **58**, 722.
5. Dubinin, M.M., *Adsorbtsiya i poristost'* (Adsorption and Porosity), Moscow: VAKhZ, 1972.127 p.
6. Pribylov A.A., Kalinnikova I. A., Murdmaa K.O., Pribylov, A.A.; Kalinnikova, I.A.; Murdmaa, K.O. Russ. Chem. Bull. (2016) **65**, 972.
7. Pribylov A.A., Murdmaa K.O. Russ. Chem. Bull. (2019) **68**, 2002.

EXPERIMENTAL STUDY OF THE THERMAL MANAGEMENT PROCESS AT CIRCULATING CHARGING OF THE NATURAL GAS ADSORPTION ACCUMULATOR

***S.S. Chugaev*[1,2], *E.M. Strizhenov*[1,2], *A.V. Shkolin*[1,2], *I.E. Men'shchikov*[1,2]**

chugaev@bmstu.ru
[1]*Bauman Moscow State Technical University, 105005, Moscow, Russia*
[2]*Frumkin Institute of Physical Chemistry and Electrochemistry RAS, 119071 Moscow, Russia*

The efficiency of adsorbed natural gas (ANG) systems strongly depends on significant thermal effects occurring during the charge and discharge processes, which requires the development of new approaches to charging processes and thermal management of the ANG tank [1]. As a rule, to reduce the influence of thermal effects, special thermal management systems are used with a circulation circuit of the heat carrier or directly charged gas, heated or cooled in an external heat exchanger.

The present work is dedicated to the experimental study of a full-scale circulating charging system with controlled thermal management for the charge of a ANG tank prototype. The accumulator is filled with a monolithic carbon material made of industrial active carbon AU-1, which has a good adsorption capacity for methane [2]. The technology of manufacturing shaped cylindrical monoliths from this carbon is described in [3]. Monolithic adsorbent samples (14 pcs) were installed in an adsorber with an internal volume of 51 liters. The average diameter and thickness of the monoliths were 196 and 101 mm, respectively. To reduce hydraulic losses and increase the heat exchange area, 37 channels with an average diameter of 4.5 mm are provided in each of the monoliths.

Natural gas with the following composition was used in the experiments, vol.: 96.1% methane, 2.2% ethane, 0.8% propane, 0.6% nitrogen, and other impurities less than 1%. Theoretical calculations and experimental data analysis were carried out for pure (100%) methane.

The processes of charging and discharging natural gas from an adsorption accumulator were studied using an experimental setup developed and manufactured, its scheme and description are described in the recent work [4]. In this experimental setup, the heat of adsorption released during the charging process is removed by a

circulating flow of natural gas, which passes through channels in the adsorbent monoliths. The charging process is carried out in two stages: 1 – "isothermal" charging with heat removal into the environment; 2 –"low-temperature" charging with heat removal employing a cooling unit. To control the temperature distribution inside the tank, temperature sensors, located at the inlet of the adsorber (1 piece), along its axis (4 pieces) and radially (4 pieces), were installed.

A series of 8 experiments was carried out in the range of charging pressures from 0.5 to 3.5 MPa and gas volumetric flow rates from 8 to 18 m^3/h. Figure 1 shows the time dependences of the effective charging capacity (without taking into account the initial amount of gas) for 4 modes of charging at different pressures.

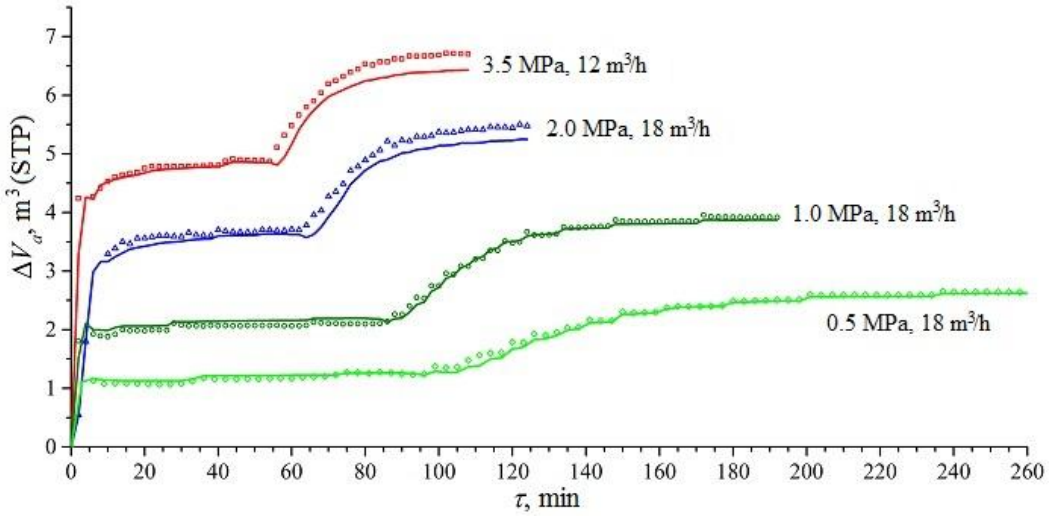

Fig. 1. Time dependence of the effective charging capacity at different modes for isothermal (stage 1) and low-temperature charging (stage 2). Lines are theoretical values; dots are experimental values.

It should be noted that the experimental and theoretical values of the effective charging capacity are in good accordance. The largest amount of charged gas corresponds to the maximum charging pressure of 3.5 MPa and is about 6.71–7.15 m^3 (STP – standard temperature 20 ° C and pressure 101 325 Pa) or 132–140 m^3 (gas)/m^3 (tank) in specific values reduced to the volume of the adsorber. If the initial gas volume (theoretically about 20 m^3/m^3) is added to this value, then the total specific volume of gas for storage will be about 152–160 m^3/m^3. Higher capacity is possible since the adsorbent only occupies about 80% of the adsorber space.

The results of the study showed the correlation between the charging mode and the charging efficiency indicators: the fastest charging was achieved at a pressure of 3.5 MPa and a gas flow rate of 12 m^3/h, and the most efficient use of the "cold" gas flow – at a pressure of 2.0 MPa and a gas flow rate of 8 m^3/h.

Acknowledgments

The research was supported by a grant from the Russian Science Foundation (project No. 20-19-00421).

References

1. I.E. Men'shchikov, A.V. Shkolin, E.M. Strizhenov, E.V. Khozina, S.S. Chugaev, A.A. Shiryaev, A.A. Fomkin, A.A. Zherdev, Thermodynamic Behaviors of Adsorbed Methane Storage Systems Based on Nanoporous Carbon Adsorbents Prepared from Coconut Shells, Nanomaterials (2020), **10**, 1.
2. E.M. Strizhenov, A.A. Zherdev, R.V. Petrochenko, D.A. Zhidkov, R.A. Kuznetsov, S.S. Chugaev, A.A. Podchufarov, D.V. Kurnasov, A Study of Methane Storage Characteristics of Compacted Adsorbent AU-1, Chemical and Petroleum Engineering (2017), **52**, 838.
3. S.S. Chugaev, E.M. Strizhenov, A.A. Zherdev, R.A. Kuznetsov, A.A. Podchufarov, D.A. Zhidkov, Fire- and Explosion-Safe Low-Temperature Filling of an Adsorption Natural Gas Storage System, Chemical and Petroleum Engineering (2017), **52**, 846.
4. E.M. Strizhenov, S.S. Chugaev, A.A. Zherdev, Mathematical Model of the Process of Circuit Charging of an Adsorption Methane Storage System, Chemical and Petroleum Engineering (2019), **54**, 760.

EFFECTIVE TOLUENE AND BENZENE ADSORPTION ON COCONUT ACTIVATED CARBON MODIFIED WITH CARBON NANOTUBES: KINETICS, ISOTHERMS, THERMODYNAMICS

A.E. Memetova*, *I.V. Burakova, A.E. Burakov, N.R. Memetov, A.G. Tkachev

iris_tamb68@mail.ru
Tambov State Technical University, Tambov, Russia

The aim of this work is to study the effect of the surface modification of coconut activated carbon (AC) on the efficiency of the toluene and benzene adsorption onto it.

The efficiency of the surface-modified activated carbon in respect to the toluene and benzene adsorption was analyzed in comparison with that of the original activated carbon and carbon nanotubes (CNTs). The authors have developed the AC modifying technology by impregnation with a catalyst solution followed by the synthesis of CNTs. As a result of the modification, the AC surface and the accessible pore area are covered by a uniform CNTs layer. Samples may contain metal-oxide catalyst particles.

The nanomodified AC structural properties were investigated using nitrogen sorption-desorption isotherms at 77 K, scanning and transmission electron microscopy, Raman spectroscopy, and FTIR.

The nanomodified AC adsorption capacity to the toluene and benzene was 123.53 and 84.92 mg g^{-1}, respectively, with a contact time is about 60 min. The kinetic data were described using pseudo-first and pseudo-second-order models, intraparticle diffusion, and the isothermal studies results were described using the Langmuir, Freundlich, Temkin, and Dubinin-Radushkevich equations. It was found that chemical interactions limit the toluene and benzene adsorption according to the pseudo-first-order model and intraparticle diffusion. In addition, the physical-adsorption nature is confirmed by the values of free energy (E = 6.92 and 8.41 kJ moL^{-1} for benzene and toluene, respectively). According to a thermodynamic study, the Gibbs energy values for nanomodified activated carbon were -16.32 kJ moL^{-1} for benzene and -33.33 kJ moL^{-1} for toluene, which corresponds to the range of the values for the physical sorption.

Thus, as a result of the comprehensive studies, it can be assumed that nanomodified AC can be considered as a promising adsorbent for removing organic pollutants from aqueous media.

ADSORPTION DEFORMATION OF FAS-3 CARBON ADSORBENT DURING ADSORPTION OF HYDROCARBONS

***D.S. Zaytsev*[1], *A.V. Tvardovsky*[1], *A.A. Fomkin*[2], *A.V. Shkolin*[2]**

tvardovskiy@tstu.tver.ru, zaytsev.d.s@mail.ru
[1]*Tver State Technical University", 170026, Tver, Russian Federation,*
[2]*Frumkin Institute of Physical chemistry and Electrochemistry,*
Russian Academy of Sciences (IPCE RAS), 119071, Moscow, Russian Federation

The study of the deformation of solids upon adsorption has great importance both for the development of adsorption thermodynamics and practical purposes. Considering the relatively large amount of experimental data on adsorption deformation under equilibrium conditions, examining this process under nonequilibrium conditions seems interesting and relevant. The aim of this work was to establish the regularities of the sorbostriction of the microporous carbon adsorbent FAS-3 during the adsorption of technically important substances of different classes and for different purposes under nonequilibrium conditions.

We used a setup for studying the adsorption deformation of solid adsorbents manufactured at IPCE RAS. A flow-through dilatometer was used for measurements, it made it possible to measure the adsorption-induced deformation of the adsorbent when a portion of the test substance or mixture is passed through it in a carrier gas flow [1]. The adsorbent FAS-3 synthesized from hyper-crosslinked furfural was used. Structural and energetic characteristics of porous FAS-3 carbon structures were determined by the standard method of Dubinin benzene adsorption isotherm at 293 K vapor (see Tabl. 1).

Table 1. Structural and energy characteristics of the porous structure of the microporous carbon adsorbent FAS-3.

Specific volume of micropores; W_0, cm^3/g	0.51
Typical characteristic energy of adsorption; E_0, kJ/mol	23.9
Effective width of micropores, X_0, nm	1.0
BET specific surface; $S_{specific}$, m^2/g	1088
Mesopore surface; $S_{ме}$, m^2/g;	32.2
Mesopore diameter; d_{max}, nm	12.8
Total pore volume; W_S, cm3/g	0.73

Figures 1, 2, 3, and 4, respectively, show the dependences of the relative linear deformation of the FAS-3 adsorbent (Δl/l) during the adsorption of carbon tetrachloride, benzene, hexane, and octane from the nitrogen carrier gas stream on time t for various amounts of the introduced adsorbent under nonequilibrium conditions.

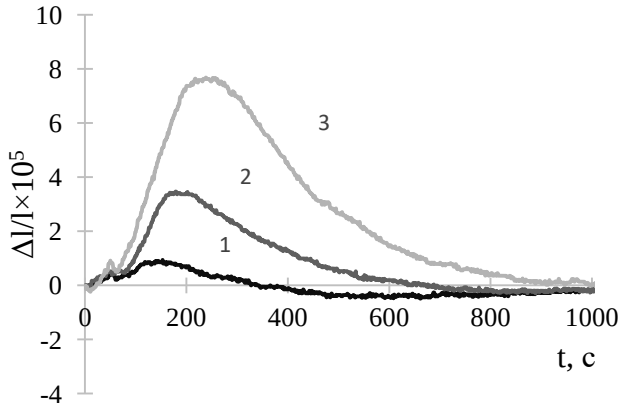

Fig. 1. Dependences of the relative linear deformation Δl/l of the microporous carbon adsorbent FAS-3 during the adsorption of carbon tetrachloride from the flow on time t for various amounts of the added adsorptive: 1 - 0.125 ml, 2 - 0.25 ml, 3 - 0.75 ml. Experiment temperature T = 493 K. Carrier gas - nitrogen. Carrier gas flow rate 2 ml/s.

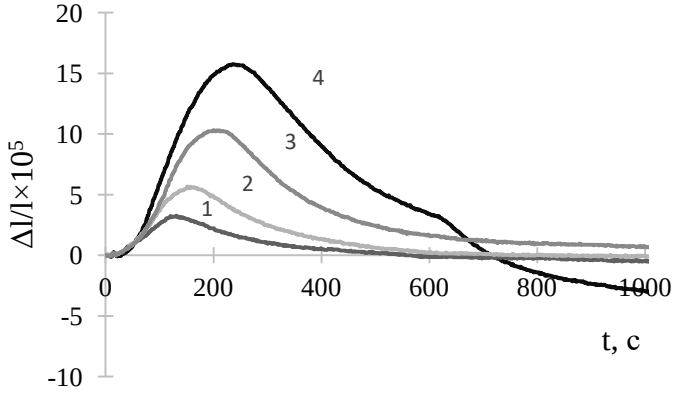

Fig. 2. Dependences of the relative linear deformation Δl/l of the microporous carbon adsorbent FAS-3 during the benzene adsorption from the flow on time t for various amounts of the added adsorptive: 1 - 0.075 ml, 2 - 0.125 ml, 3 - 0.25 ml, 4 - 0.5 ml. Experiment temperature T = 493 K. Carrier gas - nitrogen. Carrier gas flow rate 2 ml/s.

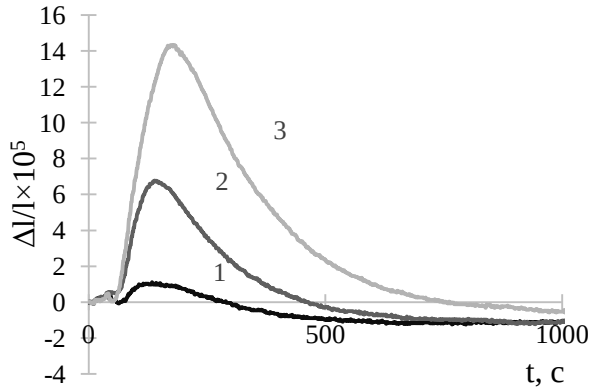

Fig. 3. Dependences of the relative linear deformation Δl/l of the microporous carbon adsorbent FAS-3 during the adsorption of n-hexane from the flow on time t for various amounts of the added adsorptive: 1 - 0.125 ml, 2 - 0.25 ml, 3 - 0.75 ml. Experiment temperature T = 493 K. Carrier gas - nitrogen. Carrier gas flow rate 2 ml/s.

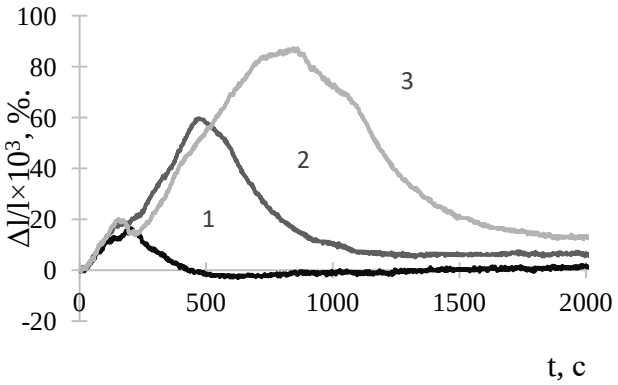

Fig. 4. Dependences of the relative linear deformation Δl/l of the microporous carbon adsorbent FAS-3 during the adsorption of n-octane from the flow on time t for various amounts of the added adsorptive: 1 - 0.075 ml, 2 - 0.125 ml, 3 - 0.5 ml. Experiment temperature T = 493 K. Carrier gas - nitrogen. Carrier gas flow rate 2 ml/s

Figures 1–4 show sorbostriction curves – changes in the relative linear adsorption deformation of the FAS-3 carbon adsorbent over time during the adsorption of carbon tetrachloride, benzene, hexane, and octane vapors from the nitrogen carrier gas flow at various volumes introduced into the carrier gas.

As can be seen in Figs. 1–4, in the very initial region for all three curves, there is a small peak in the dependence of Δl/l on t. This is due to the fact that the microporous adsorbent has some inhomogeneity of the porous space. The smallest pores have the highest energy of adsorption interaction with molecules of organic adsorptive, these

pores are filled in the first place. Further, we see a rapid increase in the adsorption deformation of the adsorbent for all curves due to the filling of the entire porous space of FAS-3 with adsorptive molecules, which is accompanied by an increase in the internal pressure in the adsorption system due to an increase in the repulsive forces between the molecules of the adsorbed substance. The main porous space of the adsorbent is filled, in which the pores have a width of about 1.0 nm. After passing the peak, the curves show a drop in the values of $\Delta l/l$ as a function of t, since there is a gradual washout of adsorptive molecules from the porous space of the adsorbent.

Figures 1–4 show that the amplitude of sorbostriction correlates with the amount of the introduced substance. In this case, the time to reach the maximum deformation also changes – in the general case, it increases with an increase in the amount of the introduced substance.

CONCLUSIONS

The work presents an analysis of the adsorption deformation of the FAS-3 adsorbent during the adsorption of carbon tetrachloride, benzene, hexane, and octane vapors under nonequilibrium conditions.

References

1. Zaytsev D.S., Tvardovsky A.V., Shkolin A.V., Fomkin A.A. Sorbostriction of the FAS-3 microporous carbon adsorbent during the adsorption of organic vapors from the nitrogen carrier gas stream. Proceedings of higher educational institutions. Series: Chemistry and Chemical Technology. (2017) **60**, 54.

EFFECT OF FLUORINATION ON INTERACTION OF METAL-DECORATED FULLERENES WITH ANTI-COVID DRUGS

E.B. Kalika [1,2], K.P. Katin [2,3], S. Kaya [4], Maslov M.M.[2,3]

kpkatin@yandex.ru
[1]Moscow Institute of Physics and Technology, 117303, Moscow, Russian Federation
[2] Laboratory of Computational Design of Nanostructures, Nanodevices, and Nanotechnologies, Research Institute for the Development of Scientific and Educational Potential of Youth, 119620 Moscow, Russia
[3] Department of Condensed Matter Physics, National Research Nuclear University MEPhI, 115409 Moscow, Russia
[4] Faculty of Science, Department of Chemistry, Cumhuriyet University, 58140 Sivas, Turkey

Targeted drug delivery (TDD) is an efficient way of treating COVID-19, as it ensures the drug release in a specific place of the organism without causing any damage to other cells and unwanted side effects. Fluorinated nanoparticles such as fullerenes are often used as drug carriers due to their high drug-loading capacity and intense near-infrared performance [1]. Fluorination of carbon nanoparticles provides a number of advantages when creating TDD systems, such as the ability to detect a nanoparticle in the organism using NMR[2], increased near-infrared adsorption, and strong electronegativity, which contributes to the non-covalent interaction of the fullerene with the drugs. Recently, TDD systems for cancer treatment based on fluorinated carbon nanomaterials have been successfully synthesized and tested [3]. Therefore, fluorinated carbon fullerenes seem to be a promising basis for TDD systems.

In the presented study, we investigated the interaction of the pristine and metal-decorated fullerenes with the most common anti-COVID drugs, such as chloroquine, favipiravir, remdesivir, and umifenovir. We considered the ions Cr, Fe, and Ni, because these metals were recognized as the most efficient adsorbents for the anti-COVID drugs [4]. Density functional theory was applied to investigate the effect of fluorination on the interaction of fullerenes with metal atoms and drugs molecules. Optimal structures of loaded fluorinated pristine and metal-doped fullerenes were considered. We studied both low- and high-fluorinated fullerenes $C_{60}F_2$ and $C_{60}F_{48}$, respectively. We found that fluorine provides stronger binging between the carrier

cage and the drug molecule in most cases. Therefore, fluorinated fullerenes can be preferably used as the drug carrier systems.

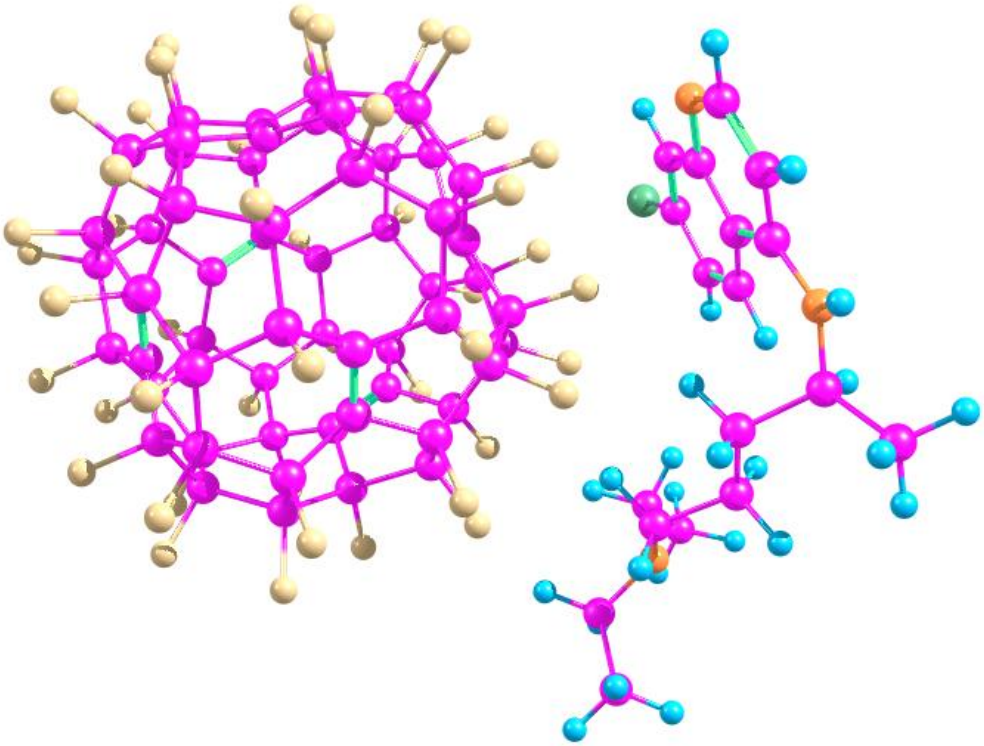

Fig. 1. Van-der-Waals interaction of the fluorinated $C_{60}F_{48}$ fullerene with the chloroquine drug molecule. Purple, blue, orange, and green balls represent carbon, hydrogen, nitrogen, and chlorine atoms, respectively.

Funding

The work was supported by the Russian Science Foundation, project No. 20-73-00245.

References

1. L. Sun, P. Gong, X. Liu, M. Pang, M. Tian, J. Chen, J. Du, Z. Liu, Fluorinated carbon fiber as a novel nanocarrier for cancer chemo-photothermal therapy, J. Mater. Chem. B (2017), **5**, 6128-6137.
2. R. Romero-Aburto, T.N. Narayanan, Y. Nagaoka, T. Hasumura, T.M. Mitcham, T. Fukuda, P.J. Cox, R.R. Bouchard, T. Maekawa, D.S. Kumar, S.V. Torti, S.A. Mani, P.M. Ajayan, Adv. Mater. (2013) **25**, 5632-5637.
3. P. Gong, L. Zhang, X.Yuan, X. Liu, X. Diao, Q. Zhao, Z. Tian, J. Sun, Z. Liu, J. You, Dyes and Pigments (2019) **162**, 573-582.
4. A.S. Rad, M. Ardjmand, M.R. Esfahani, B. Khodashenas, Spectrochim. Acta A (2021) **247**, 119082.

AN EXPERIMENTAL STUDY OF SORPTION-DESORPTION OF RADIUM 226 ON CARBON NANOMATERIALS

***A.P. Karmanov*[1], *A. P. Voznyakovsky*[2], *L. S. Kocheva*[3], *N. G. Rachkova*[1], *N.I. Bogdanovich*[4]**

apk0948@yandex.ru; n.bogdanovich@narfu.ru
[1] *Institute of Biology, Komi Scientific Center, Ural Branch of the Russian Academy of Sciences, Syktyvkar, 167982 Russia*
[2] *Unitary Enterprise "S.V. Lebedev Institute of Synthetic Rubber", St. Peterburg, 198035 Russia*
[3] *Institute of Geology, Komi Scientific Center, Ural Branch of the Russian Academy of Sciences, Syktyvkar, 167982 Russia*
[4] *Lomonosov Northern (Arctic) Federal University, Arkhangelsk, 163002 Russia*

The technology of solid-flame incineration or self-propagating high-temperature synthesis is considered a promising method for producing carbon nanomaterials (CNM) with high added value. This method is based on the thermolysis of organic compounds within the framework of the laws of dynamic self-organization, which eventually turn into stable 2D carbon nanostructures. The structure and properties of carbon nanomaterials of this type have not yet been thoroughly investigated. In particular, it has not been established how the choice of raw materials affects the structural structure and sorption properties of synthesized nanocarbon materials.

Nuclear energy is known as one of the most promising industries. However, the further development of the nuclear industry may lead to pollution of the environment, including water environments, with dangerous radioactive elements. In this regard, the search for new adsorption materials for the effective purification of natural waters from radioactive contamination is an urgent scientific, practical, and social task.

This work is devoted to the assessment of the possibility of using CNM as adsorbents of one of the most dangerous long-lived radionuclides radium 226 (Ra^{226}). Plant biopolymers (cellulose and lignins) were used as raw materials for the production of CNM. Figure 1 shows the indicators of sorption-desorption of Ra^{226} for some CNM samples synthesized from technical sulfate lignin (CLS), cellulose (CC), and natural lignin CLB

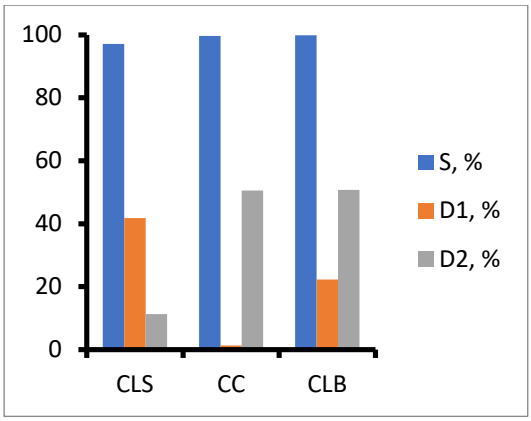

Fig. 1. Indicators of adsorption of S and desorption of D in aqueous solutions of CH3COONH4 (D1) and HCL (D2) for CNM samples for Ra^{226}

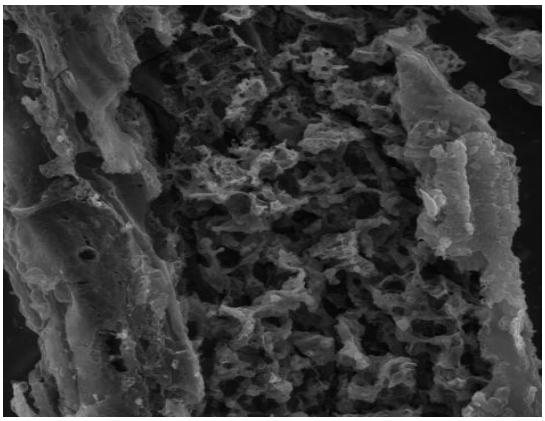

Fig. 2. SEM image of the CNM sample synthesized from CLS

The experimental results indicate that carbonized lignin-CLB has the highest sorption capacity of S with respect to Ra^{226}. For this sample, the adsorption value S reaches a value of 99.9%. CLS and CC preparations are characterized by a slightly lower sorption capacity, for which the S value is 97.1 and 99.6%, respectively, and about half of the radionuclide is adsorbed very strongly (irreversibly).

The methods of IR-EPR-X-ray analysis, as well as the method of low-temperature nitrogen adsorption (77 K), were used to characterize the adsorbents and interpret the results. It is established that the samples of CNM consist of curvilinear-planar (flaky) graphene-type particles (Fig. 2). This conclusion is based on the results of the study by electron microscopy, Raman spectroscopy, and X-ray diffractometry.

Funding and acknowledgments

The study was supported by the Russian Foundation for Basic Research [the research project number 18-29-24129 mk.

ON SELECTIVITY OF XENON ADSORPTION FROM LEAN AIR MIXTURES

***A.L. Pulin*[1], *S.D. Artamonova*[1], *A.A. Fomkin*[1], *A.A. Berezanin*[2], *A.V. Shkolin*[1], *I.E. Men'shchikov*[1]**

alpul@mail.ru
[1]*Frumkin Institute of Physical chemistry and Electrochemistry, Russian Academy of Sciences (IPCE RAS), 119071 Moscow, Russian Federation*
[2]*AO Rosenergoatom, Moscow Russia*

Ventilation gas emissions of nuclear power plants (NPP) can contain small amounts of xenon and krypton radionuclides, which are the nuclear fission products of uranium. The adsorption systems of specialized gas purification (SGP) with molecular sieve adsorbents are used to capture and store during the time of the fall of radiation activity down to a safe level. The use of carbon adsorbents for xenon capture is based on the significant differences between the energies of adsorption of the main components of the ventilation gases: nitrogen (~8.3 kJ/mol), oxygen (~ 8 kJ/mol), and radioactive Xe (23.5 kJ/mol) and Kr (~ 15.5 kJ/mol).

In the present work, the theory of volume filling of micropores (TVFM) [1] was used to simulate the xenon adsorption onto a series of carbon adsorbents with slit-like micropores. The graphite crystal was considered as a model carbon structure, whose slit-like pores of different width is a result of subsequent burnoff of the hexagonal carbon layers upon the activation process [2]. The most advanced technological porous structure, whose pores are separated by two-layered carbon walls, was chosen as an object of study. The structures with micropores formed in crystal through the burnoff of one from five (AC1:5), two from six carbon layers (AC2:6), and so on up to seven from 11 layers (AC 7:11), were analyzed. The number of the burned-out layers was restricted by the limiting size of micropores according to Dubinin's classification, i.e., the pores, in which the adsorption process is carried out by the mechanism of volume filling (TVFM): no more than 3.0–3.2 nm [2]. The structure and energy characteristics (SEC) of these model adsorbents were calculated using the TVFM equations (see Table 1). Along with the SEC values, Table lists the density of the model adsorbents with micropores.

Table. The textural characteristics of model adsorbents with slit-like micropores separated by two-layered carbon walls.

Model structure	AC 1:5	AC 2:6	AC 3:7	AC 4:8	AC 5:9	AC 6:10	AC 7:11
Effective width of micropores X_0, Å	5.3	8.6	12.0	15.3	18.7	22.0	25.4
Specific volume of micropores W_0, $cm^3 \cdot g^{-1}$	0.35	0.57	0.79	1.01	1.23	1.45	1.67
Characateristic energy of benzene adsorption, E_0, $kJ \cdot mol^{-1}$	45.5	27.8	20.0	15.7	12.8	10.9	9.5
Characateristic energy of xenon adsorption, $E_{Xe,}$ $kJ \cdot mol^{-1}$	20.47	12.51	9.00	7.06	5.76	4.90	4.27
Density of the adsorbent with micropores $\rho_{ad,}$ g cm^{-3}	1.515	1.137	0.909	0.758	0.649	0.568	0.505

Using the SEC values for the model adsorbents, the xenon adsorption was calculated in order to assess the optimal porous structure with the maximal adsorption capacity in the required pressure range. Fig. 1 shows the results of the calculations.

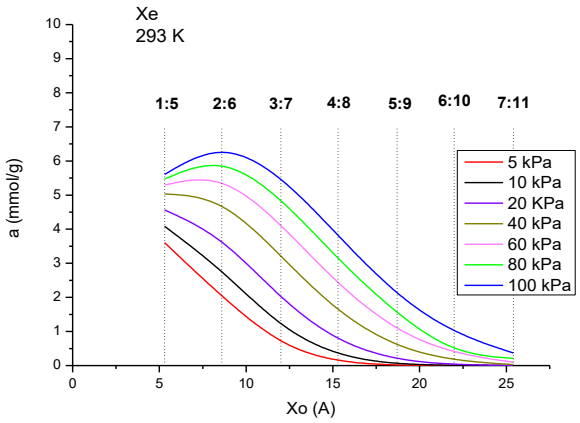

Fig. 1. Xe adsorption onto the model carbon adsorbents at 293 K versus the micropore width.

As follows from Fig. 1, the amount of adsorbed Xe increases with pressure, but a decrease in a pore width has a greater effect on the adsorption behaviors due to an increase in the energy of adsorption. However, as follows from Table, the decrease in the pore width is accompanied by the decrease in the micropore volume, which ultimately leads to a deterioration in adsorption performance of the adsorbent. Under isobaric conditions (for example, when p=60, 80, 100 kPa), the adsorption activity as a

function of micropore width passes through a maximum at X_0 = 0.8–1.0 nm (see Fig. 1). To check the reliability of our calculations, we compare these data with the SEC values of the commercial carbon adsorbent SKT-3C, which is utilized in the SGP systems of NPP. The data on the porous structure of SKT-3C evaluated from the isotherms of nitrogen vapor adsorption at 77 K are shown in Fig. 2.

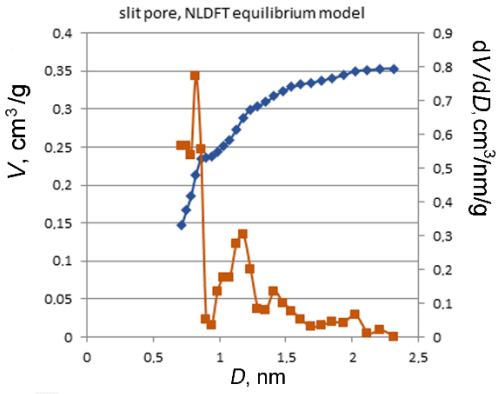

Fig. 2. The cumulative (rhomb) volume and pore size distributions (square) in SKT-3C calculated by the NLDFT method for the slit-like pore model.

The cumulative pore volume curve shows a distinctive region of change in the curvature associated with the specific features of the porous structure of SK-6, namely the presence of two characteristic pore sizes corresponding to two peaks on the pore size distribution curve at D =0.9 and 1.2 nm. As follows from the comparison, the parameters of SKT-6 are close to that of the most optimal model carbon structure AC2:6, which can be used as a criterion for selecting an adsorbent for capturing xenon from the flow of ventilation gases at NPPs.

Funding and acknowledgments

The research was carried out within the framework of the State Assignment of the Russian Federation (Project No. 0081-2019-0018).

References

1. M.M. Dubinin, Physical Adsorption of Gases and Vapors in Micropores. Progr. Surf. Membr. Sci. (1975) **9**, 1.
2. M.M. Dubinin, Fundamentals of the theory of adsorption in micropores of carbon adsorbents: Characteristics of their adsorption properties and microporous structures. Carbon. (1989) **27**, 457.
3. P.I. Ravikovitch, A. Vishnyakov, R. Russo, A.V. Neimark, Unified approach to pore size characterization of microporous carbonaceous materials from N_2, Ar, and CO_2 adsorption isotherms. Langmuir (2000) **16**, 2311.

ADSORPTION PROPERTIES OF CARBON-MINERAL MATERIALS BASED ON NATURAL MONTMORILLONITE CLAY AND TIRE CRUMB

M.B. Alekhina*, *M.M. Fidchenko, A.D. Varnavskaya

mbalekhina@yandex.ru
D.I. Mendeleev University of Chemical Technology of Russia,
125047 Moscow, Russia

Activated carbon is one of the most effective and frequently used adsorbents for water purification from organic pollutants. Along with activated carbons, carbonized materials obtained from cheaper raw materials and industrial waste are used [1,2].

Natural clays can be used as a porous matrix for such adsorbents. The advantages of clays, in comparison with other materials, are the availability of a sufficient amount of raw materials and an affordable price. Various carbonaceous materials can be used as modifiers.

In the present work, natural montmorillonite clay was used as a raw material, and tire crumb (a product of car tires processing) was used as a carbon source. A sample of montmorillonite clay was ground, dispersed, and a 0.25–1 mm fraction was selected. A mixture of clay and tire crumbs was granulated; the resulting granules were subjected to pyrolysis in an oxygen-free environment at 350–800^{0}C.

Nitrogen adsorption isotherms were recorded at 77 K for all samples of carbon-mineral material (CMM) and used for calculating the textural characteristics. The X-ray phase and elemental analyzes were performed.

The results showed that an increase in the pyrolysis temperature led to a decrease in the values of the specific surface area and pore volumes of the samples, which was attributed to the filling of the montmorillonite matrix with carbon. These results were confirmed by X-ray phase analysis. The diffraction patterns clearly show an increase in the number of peaks corresponding to carbon and graphite-like deposits on the surface of the CMM samples pyrolyzed at temperatures > 600 °C. As shown by elemental analysis, the carbon content on the montmorillonite surface varied from 17 to 48 wt. % depending on the pyrolysis temperature; this fact can have a different effect on the adsorption properties of the material.

Water vapor adsorption isotherms at 20 °C were obtained for all CMM samples. It was shown that with an increase in the pyrolysis temperature, the amount of adsorbed water by the samples decreased, which indicates an increase in the hydrophobicity of the CMM samples as a result of the coating of the montmorillonite surface with a carbon layer. The maximum adsorption value obtained on pyrolyzed CMMs (160 mg / g for the sample after pyrolysis at 600^0C) was 1.5 times less than the value of water vapor adsorption obtained on the sample of initial montmorillonite (260 mg / g). The presence of convex areas on the isotherms of water vapor adsorption onto the samples indicates that at low values of relative pressures, adsorption occurs mainly on the primary adsorption centers, which are metal cations and protons of hydroxyl groups of montmorillonite.

The adsorption of nonionic surfactants from solutions on the obtained adsorbents was studied using Neonol AF 9–10 as an example. The nonionic surfactant Neonol AF 9-10 is an oxyethylated nonylphenol, has the empirical formula $C_9H_{19}C_6H_4O(C_2H_4O)_{10}H$ and the structural formula shown in Fig. 1.

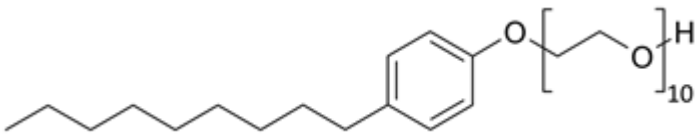

Fig. 1. Structural formula of Neonol AF 9-10.

Figure 2 shows the isotherm of excessive adsorption of Neonol AF 9–10 from aqueous solutions at 20 °C on a CMM sample pyrolyzed at 650 °C. This is one of the most hydrophobic samples we have obtained and studied. The carbon content in the CMM-650 sample was 43.8 wt. %. Here, for comparison, the isotherm of adsorption of Neonol AF 9–10 at 20^0C on active carbon F-300 is shown [3].

As can be seen from Fig. 2, the CMM-650 sample is somewhat inferior in capacity to F-300 activated carbon, but it can be used for adsorptive wastewater treatment from Neonol AF 9–10 and other surfactants.

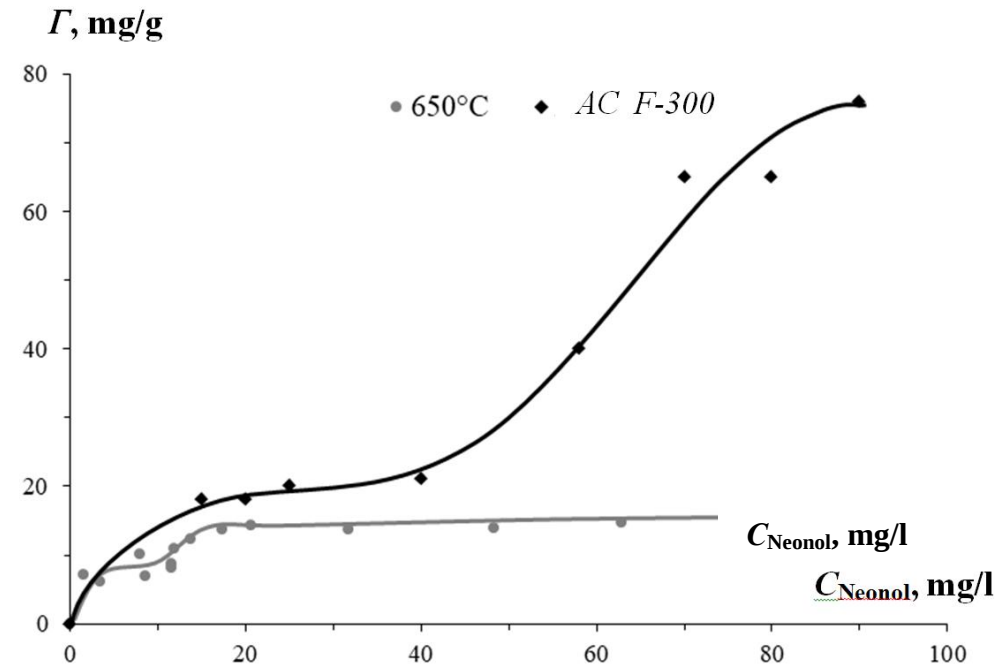

Fig. 1. Isotherms of excessive adsorption of Neonol AF 9–10 from aqueous solutions at 20^0C on a carbon-mineral adsorbent obtained at a pyrolysis temperature of 650^0C and activated carbon F-300 [3].

The work was carried out in accordance with the Plan of the Scientific Council of the Russian Academy of Sciences on Physical Chemistry, theme 2.15.4.M 2.15.7.ATP "Investigation of the physicochemical properties of natural clay materials, as well as the products of their modification and the possibility of their practical application".

References

1. X. Yang, F. Li, M. Xia, F. Luo, Y. Jiang, “Investigation on the micro-structure and adsorption capacity of cellulosic biomass carbon based montmorillonite composite”, Amsterdam: Elsevier, vol. 256. pp. 18-24, 2018.
2. Shykhaliev K.S. «Sorbent based on worn-out car tires for cleaning of water surface from oil and oil products». Bulletin of SRC IISS: topical issues of modern science. 2018. № 10. pp. 92-137. (in Russian).
3. Uchanov P.V., Kamenchuk I.N., Zholdabekova N., Mukhin V.M. «Study of equilibrium adsorption and absorption kinetics of neonol AF 9-10 by activated carbons from aqueous solutions». Chemical Industry Today, 2014, No 9, pp. 50-56. (in Russian).

COMPOSITE SORPTION-ACTIVE MATERIAL BASED ON FULLERENE SOOT AND BENTONITE CLAY

S.P. Khokhlachev, E.A. Spiridonova

Sergei.hohla4eff@yandex.ru
Saint Petersburg Institute of Technology (Technical University),
190013, Saint Petersburg, Russia

Fullerene soot is an adsorption-active material whose sorption properties were studied in [1]. It was shown that fullerene soot has a developed volume of both mesopores and micropores and that the specific surface area calculated by the BET method is 250–330 m^2/g. In addition, it was noted in [2] that fullerene soot exceeds the adsorption of heavy metal ions by 4–5 times compared to activated carbons. This suggests that this material can be effectively used as a sorbent. However, fullerene soot has a very high dispersion, which means its use for cleaning gas and liquid media is difficult in static conditions and impossible under dynamic conditions. The solution to this problem is the use of a binder in order to obtain a composite sorption-active material (CSAM) while preserving high sorption activity. In the recent work [2], CSAM was obtained from fullerene soot and a polymer organic binder. The research results showed that the obtained materials outperform activated carbons in terms of a number of parameters.

In the present work, we proposed to use the construction waste bentonite clay as a binder to lower the cost of the resulting CSAM. Since the main part of bentonite clay is montmorillonite, which has ion-exchange properties [3], it can be assumed that the sorption properties of such a CSAM will increase. According to [4], bentonite can be used as a binder for obtaining a sorbent.

The method of obtaining CSAM consists of the following stages: preparing an aqueous suspension of clay; gradually introducing the filler into the suspension; obtaining a homogeneous paste of a certain viscosity; forming cylindrical granules on a screw granulator; drying with a gradual rise in temperature to remove excess moisture. The obtained granules were subjected to high-temperature treatment, including steam-gas activation by water vapor. The CSAM composition was 23% bentonite clay and 77% fullerene soot.

As compared to the technology described in [2], this method allows not to use surfactants for wetting hydrophobic fullerene soot since the proposed sequence of stages allows to obtain a homogeneous paste during the mixing process.

The following parameters of the porous structure of the obtained materials were determined: the total pore volume for water (V_Σ, cm^3/g), the maximum volume of the sorption space for benzene (Ws, cm^3/g), the maximum volume of the adsorption space for benzene (W_0, cm^3/g), and the specific surface area for argon calculated by BET (Sud, m^2/g).

Increasing the processing temperature (from 450 to 850 °C) causes the changes in Ws from 0.55 to 0.70 cm^3/g and V_Σ from 0.65 to 0.78 with an almost unchanged value of W_0 (0.05–0.06). The specific surface of the CSAM was found in the range of 200–150 m^2/g. As illustrated, an increase in temperature, even when accompanied by an oxidizer of water vapor, does not lead to the development of a microporous structure but contributes to an increase in the strength of materials, reaching sufficiently high values of 70–80%, as well as water resistance allowing the use of CSAM for cleaning liquid media.

In conclusion, using straightforward technological methods, it is possible to obtain mesoporous CSAM based on fullerene soot and bentonite clay, with high values of the maximum volume of sorption space, applicable also under dynamic conditions

Funding and acknowledgments

The research was supported by the Russian Science Foundation (project No. 21-79-30029).

References

1. V.V. Samonin, E. M. Slutsker. Journal of Physical Chemistry (2003) **77**, 1287.
2. V.V. Samonin, M. L. Podvyaznikov, V. Yu. Nikonova, E. A. Spiridonova, A. Yu. Shevkina, Sorbing materials, products, devices and processes of controlled adsorption, Nauka, St. Petersburg, 2009, 271 p.
3. Yu.I. Tarasevich, Natural sorbents in water purification processes, Naukova dumka, Kiev, 1981, 208 p.
4. P.V. Sokolovsky, Development of the composition and determination of colloidal-chemical characteristics of a composite sorbent based on pyrolysis products of peeling waste of industrial and grain crops and montmorillonite containing clays, Belgorod State National Research Institute, Belgorod, 2016, 21 p.

FORMATION OF A MESOPOROUS STRUCTURE IN AN ALUMOSILICATE MATRIX OF NATURAL KAOLINITE AFTER THERMOCHEMICAL TREATMENT

A.V. Bondarenko[1], M.L. Ruello[2], V.V.Bondarenko[1,2], Petukhova G.A.[3], Dubinina L.A.[3]

antonina.bondarenko@gmail.com
[1] Lipetsk State Technical University, 398600 Lipetsk, Russia
[2] Marche Polytechnic University (Università Politecnica delle Marche), 60131, Ancona, Italy
[3] Frumkin Institute of Physical Chemistry and Electrochemistry of the Russian Academy of Sciences, 119991, Moscow, Russia

Nowadays, a large number of scientific works are devoted to studying the adsorption properties of clay minerals in native and modified forms, given the development of new methods of supramolecular structure studying, which created interest in clays as natural nanoscale materials.

In the Central region of the Russian Federation, the most accessible aluminosilicate is kaolinite, yet its adsorption activity is relatively low due to the "rigid" 1:1 aluminosilicate structure (TO). Earlier, the article [1] described the study of properties and synthesis conditions of the TiO_2/kaolinite composite able for passive degradation of household organic pollutants. The results demonstrate a significant improvement of the adsorption and structural characteristics of the synthesized material compared to kaolinite and titanium dioxide as separated substances.

The purpose of the present research is to model the processing of kaolinite according to the scheme, similar to [1] (without the formation of titanium dioxide on the surface, however) and to study the supramolecular structure of the resulting material, especially the formation of mesoporous. Thus, the potential of kaolinite as an adsorbent and a matrix for titanium dioxide deposition can be determined.

The studies were carried out for two samples of kaolinite – one is preparative material (Industria Chemica Carlo Laviosa), while the other was obtained from Ryazan kaolinite clays by sedimentation method. The treatment included two stages: dissolution in sulfuric acid (7.8% by weight) and heat-treatment at a temperature of 600–700 °C. The research scheme included: (1) determination of the chemical

composition, (2) microscopic examination of the surface, (3) measurements of isotherms of water and benzene vapors adsorption.

The main results demonstrated the decrease of the molar ratio of structure-forming oxides Al_2O_3/SiO_2 from 0.95 to 0.9–0.83, suggesting the leaching of the octahedral layer and the subsequent formation of the adsorption space. A significant amount of sulfur was also detected. Therefore, in order to reduce the amount of aluminum sulfate, the heat treatment temperature was increased to 750 ^oC.

The microscopic examination did not show the effect of treatment on the surface morphology of kaolinite particles. The most significant changes were revealed during the experimental construction of water vapor and benzene vapor adsorption isotherms: the monolayer capacity increased from 0.25 to 2.9 mmol/l, the maximum sorption capacity P/Ps=1 - from 60 to 300 mg/g.

After increasing the heat treatment temperature, the value of the adsorption capacity decreased to 200 mg/g, which was, according to the author, due to the destruction of aluminum sulfate, able to retain water.

The benzene isotherms did not show such high values of the parameter increase, but they allowed us to determine an increase in the specific surface area of mesopores up to 200 m^2/g.

Currently, the research goal is to increase selectivity to certain classes of organic compounds.

References

1. V.V. Bondarenko, M.L. Ruello, A.V. Bondarenko, G. A. Petukhova, L.A. Dubinina, Phys. Chem. Surf. Prot. Mat. (2019) **55**, 127.

INFLUENCE OF A METHOD OF DIATOMITE TREATMENT DURING THE OBTAINING OF SORBENTS FOR WATER PURIFICATION ON THEIR PHYSICAL AND CHEMICAL PROPERTIES

J.A. Ubaskina [1], M.B. Alekhina [2]

baseou@yandex.ru
[1]FSUE «Institute for Chemical Reagents and High Purity Chemical Substances of NRC «Kurchatov Institute», 107076, Moscow, Russia
[2]D. Mendeleev University of Chemical Technology of Russia, 125480, Moscow, Russia

Diatomite-based sorbents are used as filter media in water treatment. The high dispersion and porosity of diatomite promote the adsorption of water pollutants on its surface. The main requirements for the methods of rock processing when obtaining sorbents are manufacturability, efficiency, and environmental friendliness. It is also necessary to take into account the characteristics of the raw materials. For example, the ability of diatomite to absorb water is 149.77±0.34 wt. %, and therefore it is impossible to grind it without first drying it. In [1], the advantage of crushing and grinding processes with simultaneous drying of diatomite was shown in obtaining an adsorbent based on it. At the same time, granular filtering materials for water treatment must comply with GOST R 51641-2000, according to which they must have chemical resistance and mechanical strength. Diatomite contains up to 70 wt. % amorphous silica and up to 37 wt. % of silica soluble in alkali solution. Therefore, despite its good sorption properties with respect to pollutants, the filter material made of raw diatomite does not have chemical resistance and mechanical strength.

During heat treatment of diatomite at 1000 °C, dehydration and sintering of the rock occur, the filter material becomes more durable. Therefore, to obtain a filter media from diatomite, the raw material after the clay ripper is fed into a drum dryer, then it is placed into a drum furnace with a heat carrier temperature of 1000 ºC, air-cooled in a layered cooler, crushed and classified on fine sizers. For water treatment, a fraction of diatomite with a size of 0.8–2.0 mm is used. Traditional industrial schemes for obtaining filter media from diatomite provide the recovery of furnace heat for use in the dryer. For this purpose, fuel gases pass in countercurrent through the furnace and enter the dryer where the raw diatomite is dried. In addition, a heat generator is put

to dry the crushed diatomite so as the initial moisture content of the raw diatomite is very high (24.6-59.6%). An air aspiration system is also provided. In this case, biosilica is obtained, which is a commercial fraction of fired diatomite with a size less than 45 micron. The general disadvantages of using crushed calcified rocks are a high content of a fraction of less than 5 micron, and a low adsorption capacity in relation to fine stubborn impurities, such as soluble organic compounds.

Table 1. Comparison of physicochemical properties of granular sorbent from diatomite and crushed diatomite calcined at 1000 ºC

Parameter	Norm (by GOST R 51641-2000)	Crushed diatomite calcined at 1000 °C	Diatomite granular sorbent
1. Chemical resistance in model solutions			
1.1 Increase in oxidizability, mg O_2/dm^3			
D.W.	No more than 10	0	0
0.017 % sol. HCl		0	0
0.02 % sol. NaOH		4.5±0,5	2.5±0.5
0.05 % sol. NaCl		2.5±0,5	2.5±0.5
$Ca(ClO)_2$ sol.*		2.5±0,5	0
1.2 Increase in mass concentration of silicic acid in terms of silicon, mg/dm^3			
D.W.	No more than 10	7.10±0,10	4.43±0.77
0.017 % sol. HCl		6.00±0.10	9.96±1.75
0.02 % sol. NaOH		9.00±3.20	3.08±1.08
0.05 % sol. NaCl		5.12±0.08	5.78±1.48
$Ca(ClO)_2$ sol.*		7.02±0,02	5.72±1.22
1.3 Increase in dry residue, mg/dm^3			
D.W.	No more than 20	30.0±18,0	0
0.017 % sol. HCl		31.0±14,0	2.0±0,5
0.02 % sol. NaOH		0	1.0±0,5
0.05 % sol. NaCl		0	0
$Ca(ClO)_2$ sol.*		40.0±10,0	0
1.4 Increase in the total mass concentration of aluminum and iron in terms of oxides (III), mg/dm^3			
D.W.	No more than 2,0	2.07±0.28	1.31±0.80
0.017 % sol. HCl		1.90±0.58	1.88±0.04
0.02 % sol. NaOH		1.62±0.02	1.07±0.52
0.05 % sol. NaCl		0.92±0.39	1.47±1.24
$Ca(ClO)_2$ sol.*		0.93±0.92	1.89±0.39
2. Mechanical strength,%			
2.1 Grindability	No more than 4	0.03±0,01	0.01±0,01
2.2 Abrasion	No more than 0,5	0.03±0,02	0.08±0,01

* Mass concentration of active chlorine is 30 mg/dm^3

For example, the measured value of the excess adsorption of methylene blue (MB) on crushed diatomite calcined at 1000 °C is only 1.13±0.08 mg MB/g of adsorbent, on crushed opoka calcined at 1000 °C is 1.05±0.15 mg MB/g of adsorbent. In order to reduce energy consumption, to improve the quality of sorbents used for water treatment, we have developed a method for obtaining a granular sorbent from diatomite [3]. The granular sorbent was obtained in an intensive type mixer, and then it is heat treated at 550 ºC with the saving of the adsorption properties of raw diatomite. The value of the excess adsorption of methylene blue on the sample of the granular sorbent was 7.65±0.75 mg/g. We also tested a sample of a granular sorbent made of raw diatomite and a sample of crushed diatomite calcined at 1000 ºC according to the methods given in GOST R 51641-2000. The test results are shown in Table 1.

As a result of the tests, it was found that the obtained granular sorbent is not inferior in chemical resistance and mechanical strength to crushed diatomite calcined at 1000 °C and surpasses it in the value of the excess adsorption of methylene blue. At the same time, the production of the granular sorbent is more energy-efficient and more technologically advanced. We conclude that the granulation of diatomite with further thermal processing at 550 °C is more advantageous for treating diatomite than calcining at 1000 °C diatomite and its subsequent milling.

References

1 J. A. Ubaskina, Bulletin of Belgorod State Technological University Named After. V. G. Shukhov (2017), 123.

2 J. A. Ubaskina, M.B. Alekhina, Butlerov Communications (2020), **64**, 74

BACTERICIDAL ZEOLITE ADSORBENTS: SYNERGISTIC EFFECTS

V.G. Tsitsishvili [1], ***M.I. Panayotova*** [2], ***N.M. Dolaberidze*** [1], ***N.A. Mirdzveli*** [1], ***M.O. Nijaradze*** [1], ***Z.S. Amiridze*** [1]

v.tsitsishvili@gmail.com
[1]*Petre Melikishvili Institute of Physical and Organic Chemistry at Ivane Javakhishvili Tbilisi State University, 1086, 31 A.Politkovskaia str., Tbilisi, Georgia (Saqartvelo)*
[2]*Department of Chemistry, University of Mining and Geology "St. Ivan Rilski", "Student Town" 1700, 1 B.Kamenov str., Sofia, Bulgaria*

The coronavirus pandemic has led to a sharp increase in both the consumption of disinfectants and interest in new antibacterial and antiviral substances. Among advanced materials, zeolites $M_x[Al_xSi_yO_{2(x+y)}]\cdot mH_2O$, in which ions of alkali or alkaline-earth metals M are partially replaced by ions of a bioactive metal (Ag^+, Cu^{2+}, Zn^{2+}, etc.) are recognized as promising [1]. Studies that started at the beginning of the 21st century, continuing to this day and reflected in numerous publications, have shown that natural and synthetic zeolites enriched with bioactive metals exhibit antimicrobial activity against a wide range of microorganisms. It was found that the silver-containing zeolites are the most active, although the disadvantages of the use of silver ions were noted – silver is an expensive metal, and Ag^+ is not stable in aqueous solutions, tends to be reduced to $Ag^{0,}$ and reacts with sulfate and other anions forming insoluble salts.

Ag-, Cu-, and Zn-containing phillipsites [2] showed nearly the same bacteriostatic activity against *E. coli* – the diameter of inhibition zones of its growth was 18.6, 15.7, and 16.3 mm, respectively. A similar result was obtained for enriched analcimes – the diameter of the zones of inhibition of the growth of *E. coli* was 12.5, 10.1, and 9.5 mm for silver-, copper- and zinc-containing analcimes, respectively [3]. However, for the silver-containing synthetic zeolite A tested under the same conditions [3], the diameter of the zone of inhibition of the growth of E. coli (22.3 mm) significantly exceeded the values for copper- and zinc-containing forms, 8.4 and 3.2 mm, respectively.

Bacteriostatic properties of Ag-, Cu-, and Zn-containing heulandites (HEU) were determined using the cultures of Gram negative bacterium *Escherichia coli* (strain ATTC 8739), Gram positive bacteria *Staphylococcus aureus* (ATTC 6538) and

Bacillus subtilis (ATTC 6633), fungal pathogenic yeast *Candida albicans* (ATTC 10231) and a fungus *Aspergilus niger* (ATTC 16404 – *A. brasiliensis*), results are given in the Table 1.

Table 1. Diameter (mm) of inhibition zones of the growth of microorganisms by native (HEU) and modified heulandites from Tedzami deposit, Rkoni plot, Eastern Georgia

Microorganism	Zeolite			
	HEU	Ag-HEU	Cu-HEU	Zn-HEU
Escherichia coli	0	21	15	0
Staphylococcus aureus	0	19	19	0
Bacillus subtilis	0	30	21 – 36*	19
Candida albicans	0	20.5	15	15*
Aspergillus niger	0	25	14*	17

* zone of secondary growth

The highest activity, as expected, is shown by the silver-containing form; copper-containing heulandite is inferior in activity; zinc-containing zeolite is active against *Bacillus subtilis* and *Aspergilus niger*, weak against *Candida albicans* and inactive against *E. coli* and staphylococcus. .

However, the picture of bacteriostatic activity, especially with the participation of the zinc-containing form, changes dramatically in the case of using mechanical mixtures of metal-containing heulandites, and this is shown in Figures 1-3.

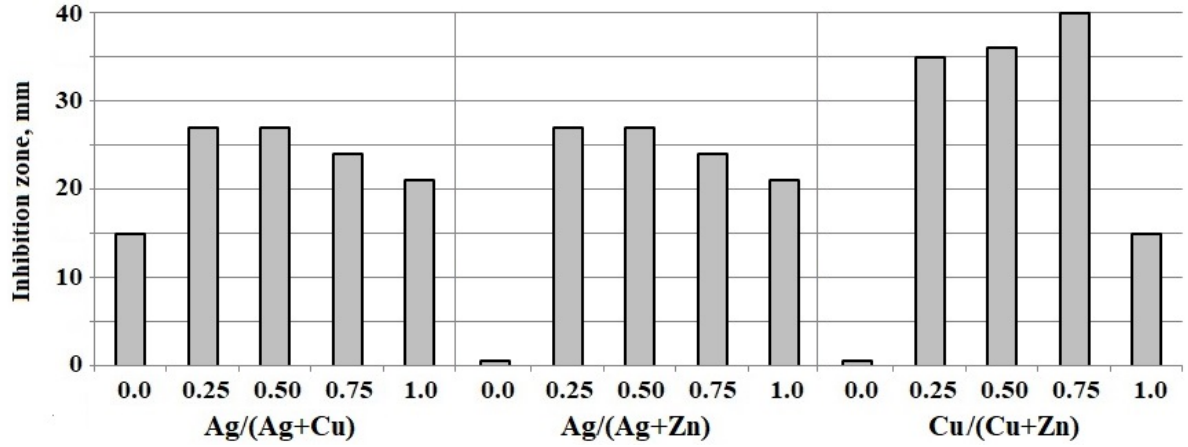

Fig.1. Inhibition zones of *E. coli* growth by Ag-, Cu-, Zn-HEUs and their mixtures.

Despite the fact that the zinc form Zn-HEU is inactive to *E. coli*, even a small addition of the silver or copper form dramatically increases the activity; the highest bacteriostatic activity is observed for the ¼Zn-HEU + ¾Cu-HEU mixture (Fig.1). The synergistic effect is also manifested in relation to Gram positive bacteria (Fig. 2), the mixtures ¼Ag-HEU+¾Cu-HEU, ½Ag-HEU+½Zn-HEU and ¼Cu-HEU+¾Zn-HEU

have the greatest activity against staphylococcus, and mixtures of copper and zinc forms are most effective against hay bacillus.

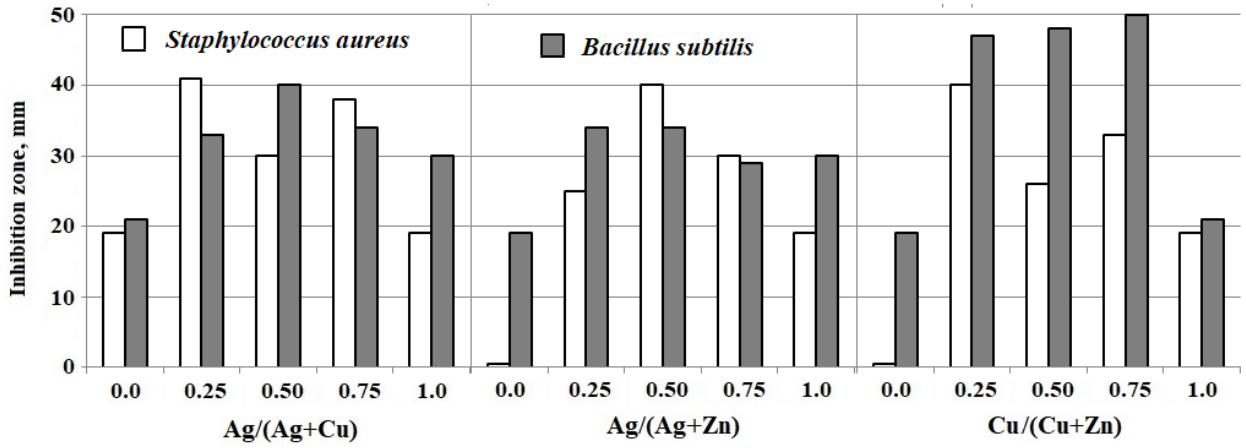

Fig.2. Inhibition of Gram positive bacteria by Ag-, Cu-, Zn-HEUs and their mixtures.

In inhibiting the growth of fungi (Fig.3), mixtures with the Ag-HEU show low activity, the most effective are mixtures of Cu-HEU and Zn-HEU, which is very important from a practical point of view.

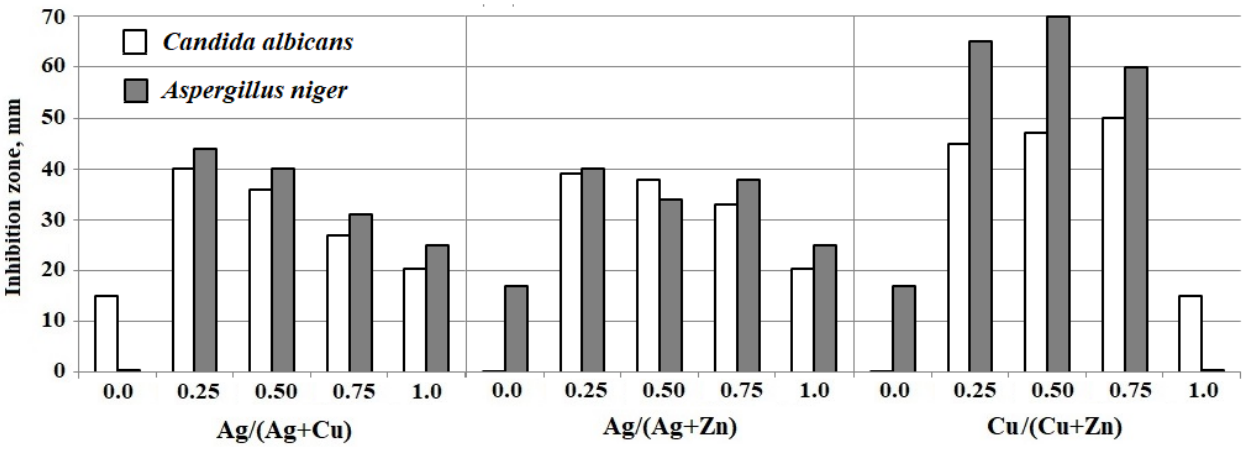

Fig.3. Inhibition of fungi growth by Ag-, Cu-, Zn-HEUs and their mixtures.

Acknowledgments

This work was supported by the Georgia National Innovation Ecosystem (GENIE) Project, grant CARYS-19-442.

References

1. A.M. Díez-Pascual. *Nanomaterials* (2018) ***8***, 359.
2. V.G. Tsitsishvili, N.M. Dolaberidze, M.O. Nijaradze, N.A. Mirdzveli, and Z.S. Amiridze. Chem. Phys. Techn. Surf. (2019) **10**(4), 327.
3. V. Tsitsishvili, N. Dolaberidze, N. Mirdzveli, M. Nijaradze, and Z. Amiridze. Bull. Georg. Natl. Acad. Sci. (2020) **14**(4), 25.

EFFECT OF MONO- AND DIVALENT EXTRA-FRAMEWORK CATIONS ON THE STRUCTURE AND ACCESSIBILITY OF POROSITY OF CHABAZITE ZEOLITES

***H.V. Doan*[1] *K.M. Leung*[2] *A. Sartbaeva*[3] *and V.P. Ting*[4]**

huan.doan@bristol.ac.uk
[1]*School of Chemistry, University of Bristol, Bristol BS8 1TS, UK.*
[2]*Department of Chemistry, The University of Hong Kong, Pokfulam, Hong Kong SAR, China.*
[3]*Department of Chemistry, University of Bath, Bath BA2 7AY, UK.*
[4]*Department of Mechanical Engineering, University of Bristol, Bristol BS8 1TR, UK*

Chabazite (CHA), one of the most common zeolite framework types, has a remarkable capacity to accommodate a wide range of different cations within the unique CHA framework. This has led to CHA being applied extensively in ion exchange, and studied for highly selective gas sorption, most notably through a trapdoor mechanism. Here, we report the systematic study of a series of six chabazite zeolites (*i.e.* K-CHA, Cs-CHA, Ca-CHA, Ba-CHA, Sr-CHA and Zn-CHA) obtained by subjecting the parent chabazite (KNaCHA) to exchange operations with cations of different valences and atomic radii. These samples were examined using numerous techniques and it was found that the difference in valence and size between extra-framework cations exert a significant effect on the abundance of these cations positioned in the framework, resulting in differing nitrogen sorption ability measured in the synthesised chabazite zeolites. These findings will help to understand how the zeolite counter-cation affects the ability of the CHA material to selectively sequester and separate gases through the use of the trapdoor mechanism.

References

1. J. W. Physick, D. J. Wales, S. H. R. Owens, J. Shang, P. A. Webley, T. J. Mays and V. P. Ting, *Chem. Eng. J.*, 2016, **288**, 161.

2. F. N. Ridha and P. A. Webley, *Sep. Purif. Technol.*, 2009, **67**, 336.

3. J. Shang, G. Li, R. Singh, P. Xiao, J. Z. Liu and P. A. Webley, *J. Phys. Chem. C*, 2013, **117**, 12841.

PURIFICATION OF WASTEWATER OF GALVANIC PRODUCTION BY MODIFIED ZEOLITES

O.I. Pomazkina

olga_pomazkina@mail.ru
[1] *Irkutsk National Research Technical University, ul. Lermontova 83, 664074 Irkutsk, Russia*

One of the main sources of pollution of natural waters with ions of heavy metals is wastewater from electroplating industries.

The environmental hazard of wastewater pollution by heavy metal ions can be prevented by implementing the following tasks: increasing the degree of wastewater treatment; using recovered metal ions; creation of a circulating water supply system.

The use of physicochemical methods combined with chemical precipitation makes it possible to extract valuable components from wastewater and reduce production losses quantitatively. In many cases, such treatment of industrial wastewater provides deep neutralization and makes it possible to reuse it in enterprises.

Adsorption-based cleaning methods are more promising than the above techniques because they almost completely extract pollutants from solutions with low concentrations. When choosing sorbents, the determining factors are their price, availability, cleaning efficiency, etc. Zeolites satisfy all of the above parameters. It is known that zeolites highly efficiently extract heavy metal ions from aqueous solutions and wastewater [1-3].

In order to achieve the maximum permissible discharge concentration, the wastewater treatment of galvanic production was carried out with zeolites modified with HCl [4,5]. The aim of this work was to study the adsorption of zinc(II) and chromium(III) ions from aqueous solutions by zeolites modified by HCl, as well as the possibility of using the zeolites for the treatment of wastewaters of the electroplating industry

The adsorption was studied on the model solutions, which were prepared using reagent grade $ZnSO_4 \cdot 7H_2O$, and $Cr_2(SO_4)_3 \cdot 6H_2O$. The model solutions were prepared by dissolving the corresponding weighed amounts of the specified chemicals in distilled water. Here, the concentration of the heavy metal ions in the solutions

corresponded to the real concentration of the pollutants at the outlet from an electroplating workshop. The concentrations of zinc(II) and chromium(III) ions in the solutions were determined by standard procedures.

The adsorption of zinc(II) and chromium(III) ions by zeolites modified by HCl was studied. The adsorption equilibrium corresponding to the constancy of the composition of the concentrations of metal ions in the adsorbate–zeolite system was 90 min. The isotherms of adsorption of zinc(II) ions in a temperature range of 298–318 K at pH 5.6–5.8 (Fig. 1) were obtained. The effect of temperature on the adsorption of chromium(III) ions was studied. Figure 2 shows the obtained isotherms in a range of 298–318 K at pH 7.6–7.9.

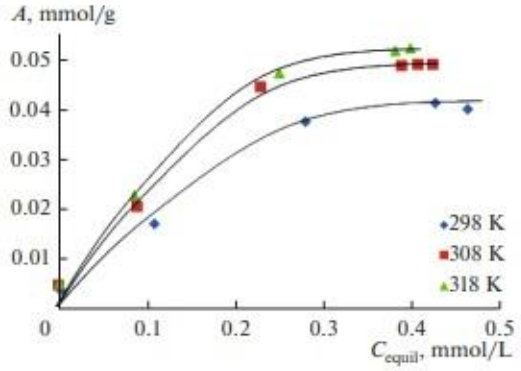

Fig. 1. Isotherms of adsorption of zinc(II) ions.

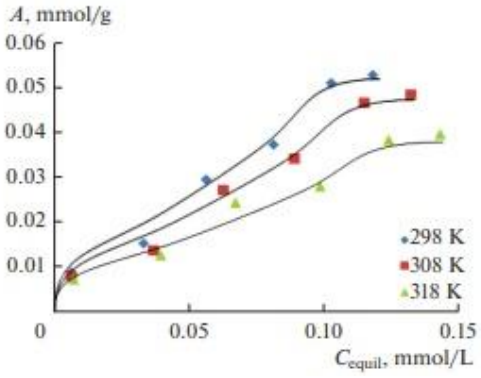

Fig. 2. Isotherms of adsorption of chromium(III) ions

The zeolites modified by HCl were used in the sorption treatment of the wastewaters of the electroplating industry. Table 1 summarizes the obtained results.

Table 1. Results of sorption treatment of wastewaters

HMI	Initial concentration, mg/L	Concentration after treatment, mg/L	Efficiency of treatment, %
Zinc(II)	1.51	0.02	98.7
Chromium(III)	1.35	0.03	97.8
pH	8.5-9.5	7.3–7.6	-

The use of modified zeolites to purify industrial wastewaters of the electroplating industry made it possible to decrease the concentration of zinc(II) ions to 0.02 mg/L and chromium(III) – to 0.03 mg/L. Here, the efficiency of the treatment is over 97%.

References

1. Pomazkina O.I., Filatova E.G., Pozhidaev Y.N. Adsorption of copper(II) ions by calcium heulandite. Prot. Met. Phys. Chem. Surf. (2015) **51**, 518. DOI: 10.1134/S2070205115040267
2. Filatova E.G., Pozhidaev Y.N., Pomazkina O.I. Investigation of adsorption of heavy metal ions by natural aluminosilicate Prot. Met. Phys. Chem. Surf. (2016) **52**, 438. DOI: 10.1134/S2070205116030102
3. Pomazkina O.I., Filatova E.G., Pozhidaev Yu.N. Adsorption of nickel(II) cations by natural zeolites. Prot. Met. Phys. Chem. Surf. (2014) **50**, 312. DOI: 10.1134/S2070205114030113
4. Filatova E.G., Pomazkina O.I., Pozhidaev Y.N. Development of the zeolite-sorption process for electroplating wastewater treatment. Journal of Water Chemistry and Technology. 2014. V. 36. N 6. pp. 303-308. DOI: 10.3103/S1063455X14060083
5. Filatova E.G., Pomazkina O.I., Pozhidaev Y.N. Adsorption of nickel(II) and copper(II) ions by modified aluminosilicates // Protection of Metals and Physical Chemistry of Surfaces. 2017. V. 53. N 6. pp. 999-1004. DOI: 10.1134/S2070205117060259

ADSORPTION OF HEAVY METAL IONS BY ZEOLITE MODIFIED BY ORGANOSILICON COMPOUND

A.D. Chugunov*, *E.G. Filatova* , *Yu.N. Pozhidaev

chugunovsasha1996@yandex.ru
Irkutsk National Research Technical University, 664074 Irkutsk, Russia

One of the most important environmental problems is the pollution of wastewater and surface water by industrial, agricultural, and household waste containing heavy metals. Numerous violations of sanitary standards for drinking and agricultural water resources are registered both in developed and developing countries [1–3].

Currently, the sorption water treatment techniques are widely used, the adsorbents including different natural and synthetic carbon-based, organic, and mineral materials. Natural minerals of zeolite structure deserve special attention as available and cheap sorbents whose large reserves are found in Russia.

However, natural zeolites are characterized by relatively low adsorption capacity, selectivity, and hydrophobicity and, thus, need to be modified. Possible zeolite surface modifiers include nitrogen- and sulfur-containing compounds, which provide donor-acceptor binding of heavy metal ions into complex compounds. Strong immobilization of a modifier and the adsorbent hydrophobicity can be achieved using organosilicon compounds.

The present work aims to study the adsorption capacity of zeolite modified by organosilicon compounds toward Cu (II), Co (II), and Ni (II) ions in aqueous solutions. The object of study was calcium heulandite $Ca[Al_2Si_7O_{18}] \cdot 6H_2O$.

In this work, 1-(3-triethoxysilylpropyl)thiosemicarbazide was used as a modifier. It was synthesized from a mixture of 0.1 mol of 1-(3- aminopropyl)-triethoxysilane and thiosemicarbazide in the presence of 0.1 g of $(NH_4)_2SO_4$ catalyst at 150°C for 3 h.

The modifier was immobilized on the zeolite surface by mixing a modifier solved in hexane and natural zeolite for 1 h at the temperature of 50 °C. This process occurs with the formation of silanol from the modifier by its hydrolysis. The expedient

reaction performed only on the zeolite surface is provided by moisture bound in zeolite. At the same time, water-alcohol solution leads to a significant increase in hydrolytic polycondensation rate throughout the volume and the formation of a mechanical mixture of zeolite and the polycondensation product. The elemental analysis and electron microscopy data show full coverage of zeolite with a modifier layer.

The ion adsorption was studied using model aqueous solutions of $CuSO_4 \cdot 5H_2O$, $CoCl_2 \cdot 6H_2O$, and $NiSO_4 \cdot 7H_2O$. The initial metal concentration was 100 mg/L, the adsorbent weight was 1 g, the contact time was 1 h, pH=5, the temperature was 25°C. The equilibrium concentration of metal ions was determined by spectrophotometry. As can be seen from Table 1, where the adsorption capacities of natural and modified zeolite are reflected, the modification by organosilicon finishing agent leads to a significant increase in the adsorption capacity toward Ni (II), Cu (II), and Co (II) ions.

Table 1. Adsorption capacity values for natural and modified zeolite

HMI	Adsorption, mg/g	
	Natural zeolite [4,5]	Modified zeolite
Cu(II)	4.8	29.5
Co(II)	5.6	24.9
Ni(II)	5.9	16.6

The adsorption isotherms for heavy metal ions correspond to the Langmuir and Freundlich models. The ion adsorption occurs on a heterogeneous surface via a predominantly complex mechanism with the formation of a chelated adsorbate monolayer on the outer surface following the scheme shown in Fig. 1. The presented chemisorption mechanism is confirmed by the elemental mapping results and the IR and NMR spectroscopy data.

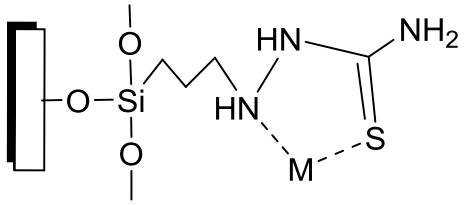

M = Cu(II), Co(II), Ni(II)

Fig. 1. Formation scheme of chelated complexes of metal ions on the surface of modified zeolite

Thus, the surface modification of natural heulandite by 1-(3-triethoxysilylpropyl)thiosemicarbazide increases the adsorption capacity of this zeolite toward copper, cobalt, and nickel ions with the formation of chelated complexes, which may be used in medicine as antiseptics.

References

1. Afroz R., Masud M.M., Akhtar R., Duasa J.B. Water pollution: Challenges and future direction for water resource management policies in Malaysia. Environ.Urban ASIA. (2014) **5**, 63.
2. Thomes M.W., Vaezzadeh V., Zakaria M.P., Bong C.W. Use of sterols and linear alkylbenzenes as molecular markers of sewage pollution in Southeast Asia. // Environ. Sci. Pollut. Res. (2019) 1-26.
3. Hoi H.T. Current situation of water pollution in Vietnam and some recommendations. IOP Conf. Ser. Earth Environ. Sci. (2020) N 442.
4. Pomazkina O.I., Filatova E.G., Pozhidaev Y.N. Adsorption of copper(II) ions by calcium heulandite. Prot. Met. Phys. Chem. Surf. (2015) **51**, 518
5. Filatova E.G., Pozhidaev Y.N., Pomazkina O.I. Investigation of adsorption of heavy metal ions by natural aluminosilicate Prot. Met. Phys. Chem. Surf. (2016) **52**, 438.

HIGH EFFICIENT CATALYTIC PLANTS FOR PURIFICATION OF INDUSTRIAL EMISSIONS OF PULP AND PAPER MILLS USING PAPER-LIKE COMPOSITE MATERIALS BASED ON MINERAL FIBERS

A.E. Smirnov [1], ***V.K. Dubovy*** [2], ***G.A. Suslov*** [2], ***N.A. Krinitsin*** [2], ***N.I. Bogdanovich*** [3]

[1]*Ltd. IG «Bezopasnye Tekhnologii», 197342, Saint Petersburg, Russia*
[2]*Saint Petersburg State University of Industrial Technologies and Design, 191186, Saint Petersburg, Russia*
[3]*Northern (Arctic) Federal University named after M.V. Lomonosov, 163002 Arkhangelsk, Russia*

The most common method for neutralizing volatile organic compounds (VOCs) has traditionally been thermal afterburning. In this case, the polluted stream is heated to 700-1200 ° C in the presence of oxygen, making it possible to neutralize the vast majority of pollutants. The disadvantage of this method is the cost of additional fuel and the formation of secondary pollutants such as NOX, SO2, etc.

The most effective way to solve this problem is the catalytic afterburning of VOCs, which allows the organic matter to be completely oxidized at temperatures from 100 ... 120 ° C. The most important elements of a catalytic purification unit are: 1) catalyst, 2) VOC concentration unit in case of its low content in the gas stream; 3) a heat recovery unit providing heating of the mixture before it is fed to the catalyst bed.

IG "Bezopasnye Tekhnologii" and the G.K. Boreskov Institute of Catalysis of SB RAS completed research and development work (R&D) on creating a model range of effective installations for the neutralization of VOCs. As a result, a unique ultra-low platinum content glass fiber catalyst has been developed.

The catalyst is characterized by nanometer-sized active platinum clusters located in the surface layer of the glass fiber. The structural features of the catalyst and the nature of the support ensure its high activity, increased resistance to poisons (S, Si,) and thermal stability (up to 1000 ° C).

An important element of the plants is a rotary concentrator, which is necessary for processing low-concentration gas streams of large volume. A rotary concentrator is a channel unit made of sorption material that replaces a system of several adsorbers

and operates continuously. Concentration is performed due to the difference between the flow rates of the processed gas and the regeneration gas.

Within the framework of R&D, a plate heat exchanger has also been developed; it can withstand high temperatures and has a low cost. In addition, the working samples of rotors based on ceramic honeycomb blocks (cordierite) coated with hydrophobic zeolite have also been created.

Promising non-combustible paper-like materials based on mineral fibers and synthetic zeolites have been developed in cooperation with the St. Petersburg State University of Industrial Technologies and Design. An important feature of the developed materials is the production method: the zeolite is introduced into the bulk of fibers already at the manufacturing stage. In comparison with existing methods of applying zeolites to finished structures made of ceramics or paper-like materials, this provides better retention of the zeolite on the support and lower thermal inertia of the material. In the foreseeable future, it is planned to manufacture prototypes of rotors for VOC concentrators based on the materials obtained with the aim of their subsequent testing and development in production.

Funding and acknowledgments

The work was carried out with the financial support of the Ministry of Education and Science of the Russian Federation. Resolution of the Government of the Russian Federation No. 218 dated 09.04.2010 (Agreement No. 03.G25.31.0221 dated 03.03.2017).

SORPTION RESPONSIVITY OF NATURAL NANOPOROUS LAYERED CLAYS TO THE TREATMENT IN ELECTROMAGNETIC FIELD OF ULTRA-HIGH FREQUENCY, WEAK PULSED MAGNETIC FIELD AND THEIR SUBSEQUENT ALTERNATION

L.I. Belchinskaya[1], K.V. Zhuzhukin[1], N.A. Khodosova[1], L.A. Novikova[1], A.V. Zhabin[2]

chem@vgltu.vrn.ru
[1] Voronezh State University of Forestry and Technologies named after G.F. Morozov, 394087 Voronezh, Russia
[2] Voronezh State University, Voronezh, Russia

The present work was aimed to study the sorption responsivity of aluminosilicates of layered (montmorillonite, Mt-type) and layered-tape (palygorskite, Pal-type) structures to the impact of a weak pulsed magnetic field (WPMF), microwave activation (UHF), and some other different sequential exposure to WPMF and UHF. Formaldehyde was used as a sorption indicator as we have absorbed it from a 1% solution. The peculiarities of the structure and the presence of charges are crucial for this particular study.

The main element of the crystal Mt structure is a three-story silicate package, which contains two articulated outer tetrahedral meshes and the inner octahedral one [1]. The pore size in the initial Mt was 4–7 nm. The main active centers of montmorillonite are exchangeable cations, hydroxyl groups, as well as coordinative unsaturated ions Al^{3+}, Mg^{2+}, Fe^{3+}. The intrinsic cations Na^{+}, Ca^{2+}, Mg^{2+}, K^{+} compensate for the negative charge and coordinately bind water molecules [2].

The excess positive charge of the octahedral mesh is balanced by the negative charge of the tetrahedral mesh due to the increased substitution of Si^{+4} by Al^{+3}. The sample under study contains 53% Mt and iron content, which can be represented as a sum Fe_2O_3 +FeO, it's value amounted to 2.93%. Palygorskite is an aqueous magnesium aluminosilicate, which has a layered-ribbon fibrous structure. In the structure of palygorskite, two silicon-oxygen elements are oppositely turned to each other by tetrahedron tops, which are connected in ribbons formed by Mg^{2+}, Al^{3+}, Fe^{3+} ions in the octahedral coordination. The octahedral ribbons are parallel to the tetrahedral layers. Active electronegative centers bind water in palygorskite in the

form of OH groups; oxygen atoms and exchange cations are located on the surface of the crystal channels.

The layered-tape crystal structure of palygorskite includes the zeolite-like channels with 0.64×0.37 nm dimensions. The exchange cations have almost no effect on the hydrophilicity of palygorskite since the hydration effect of the exchange cations is insignificant. The palygorskite sample is composed of 80% palygorskite and 20% quartz elements. In the sample, the content of iron in the form of Fe_2O_3 is equal to 8.23%.

For magnetic activation of layered aluminosilicates by a weak pulsed magnetic field (WPMF), we used a generator providing the amplitude of the magnetic field of 71mT with 30 seconds activation time. Adsorption occurred immediately after the exposure to WPMF and then 48 hours later after the treatment has finished. Microwave activation of the sorbents was carried out in a regular household 1100 W microwave at the 4 min time-set mode. X-ray diffraction and ultrasoft X-ray emission spectroscopy were used to detect possible changes in the atomic structure of powdered aluminosilicate samples. Formaldehyde sorption by the studied aluminosilicates was defined by the sulfite method.

During microwave treatment, the opposite processes occur: the structure changes upon dehydration and dehydroxylation, hydrogen bonds between neighboring water molecules are broken, and the bulk of water is removed from the inter-pack space in montmorillonite. In this case, the sorption activity of layered silicates increases. However, according to [2], under microwave exposure, the aggregation of particles and a decrease in the degree of dispersion and, accordingly, adsorption of formaldehyde on Mt and Pt are observed. As a result of the opposite processes, adsorption onto aluminosilicates increases to a greater extent on Mt (1.98 times more as compared to Pt, for which we observed just 1.5 times more adsorption).

The results of magnetic activation of Mt and Pt by WPMF are more significant for Mt (an increase in sorption by 2.3 and 1.7 times is observed). Using the treatment of Mt and Pt by WPMF we observe a dispersion of particles [2] and an increase of sorption capacity. The sorption process is greatly influenced by the non-equilibrium state of the magnetically treated structural systems of the investigated samples and the

different magnetic sensitivity of their atomic subsystems. The microwave and WPMF treatment sequence also leads to more intense sorption (2.86 times on Mt and 2.14 times on Pt). There is an extreme increase in sorption of up to 20.9 times after 48 hours of WPMF irradiation of Mt, while for Pt this process increases only by a factor of 1.97. There are very few substituted cations in Pt, and therefore, the surface charge on the particles is small, which is reflected by the less sorption response of Pt as compared to Mt.

In 48 hours after the exposure under microwave and WPMF, formaldehyde adsorption changed insignificantly (up to 21.6 times on Mt and up to 1.87 times on Pt.). Changing the sequence of exposure (first WPMF and then, microwave) leads to a smaller increase in sorption processes on both Mt (to 2.3 times), and on Pt (to 1.32 times). The effect of WPMF on the atomic subsystem were confirmed by the ultrasoft X-ray emission spectroscopy data [3]. It was found that the stoichiometry of silicon suboxides $SiO_{1.8}$ was restored in SiO_2 in Pt, and there is not any stoichiometry in Mt in the form of silicon suboxide $SiO_{1.8}$ with numerous oxygen vacancies, which probably serve as additional active sorption centers. No direct correlation was established between the quantitative content of iron oxides in clay magnetically activated samples and formaldehyde sorption.

The work was carried out within the framework of the Plan of the Scientific Council of the RAS on Physical Chemistry, theme no. in V.4 2.15.4.M

References

1. Tarasevich Y.I. “Adsorption as applied to clay minerals” / Y. I. Tarasevich, F. D.
2. Ovcharenko. - Kiev Naukova Dumka, 1975, pp. 351;
3. Belchinskaya L.I., Anisimov M.V., Khodosova N.A., et al, “Surface Characteristics of Magnetically Activated Clinoptilolite”, Fiziko Chemistry of Surface and Protection of Materials, 2020, Volume 56, No. 6, pp. 601-6063;
4. Belchinskaya L. I., Zhuzhukin K. V., Barkov K. A., et al. “Condensed media and interfacial boundaries”, 2020, 22(1), pp.18-27.

ASSESSMENT OF ANTIBACTERIAL PROPERTIES OF BENTONIT-LIKE CLAY OF BELGOROD REGION

A.I. Vezentsev, N.A. Volovicheva

vesentsev@bsu.edu.ru
Federal State Autonomous Educational Institution of Higher Education «Belgorod National Research University», 308015 Belgorod, Russia

The spread of human morbidity caused by further increasing environmental pollution can be significantly reduced by removing pathogens from the human organism. At the same time, from the practical and scientific point of view, it is advisable to jointly consider ecological issues to prevent the risk of infection with pathogens and pollution of environmental objects. Currently, sorption-active materials have been developed and introduced into practice, their effectiveness in detoxifying natural environments and the human organism was confirmed [1–3]. However, the expansion of the raw material base and improvement of the methods for increasing the activity of sorption materials continue to be relevant.

Within of this scientific research, we estimate the applicability of the local clay (the Belgorod region), containing a highly dispersed sorption-active hydroaluminosilicate montmorillonite in an amount of 60.0–67.0 wt. % for purification and disinfection of water from some pathogenic microorganisms. As model test systems, we used: E. coli 0III, Salmonella typhimurium, and Shigella sonnei. The samples of autoclaved tap water isolated from contaminating viruses and bacteria were used as the model aquatic environment. A certain dose of bacteria was introduced into the water under study to achieve the pollution, which actually develops near largely populated areas.

The introduced sorbent (native and acid-activated clays of the «Polyana» field, Shebekinsky district of the Belgorod region) was subjected to preliminary grinding and sterilization at a temperature of 160–170 °C for 60 minutes. The process was carried out under static conditions with subsequent sorbent separation from the aqueous medium during centrifugation. The content of bacteria in the aqueous medium was determined by the method of serial dilutions followed by the counting of colonies on solid selective media.

When studying the sorption activity of experimental materials in relation to bacterial cells of E. coli (initial content of $6.1 \cdot 10^8$ CFU / ml), it was found that the sorption efficiency is 57–62% for the native form and 96% for the acid-activated form of clay from the “Polyana” field.

The level of binding of Shigella sonnei was $1.63–1.95 \times 10^5$ CFU/mg of sorbent with an initial concentration of microorganisms in the suspension equal to 3.6×10^6 CFU/ml. At the same time, the highest activity against these microorganisms was also shown by clay with preliminary acid treatment. The efficiency of this material was 94.4%, while the native sample showed a result equal to 72%.

As in the experiments, the level of binding of Salmonella typhimurium was higher in acid-treated Polyanskaya clay: its value reached almost 99%.

Additional experiments were carried out for all studied microorganisms to assess the efficiency of bacterial cells binding when diluting the original clay suspensions. It was shown that dilution of suspensions led to an increase in the specific sorption activity of both native and acid-treated clay forms in relation to all studied microorganisms.

Thus, it was revealed that the studied clay field Polyana, which has montmorillonite as the main rock-forming mineral, has a sufficiently high sorption activity in respect to the studied pathogenic microorganisms. At the same time, the sample subjected to preliminary acid treatment showed the highest affinity for the cells of the bacteria of the intestinal group. The efficiency of sorption depends on both the quantitative content of cells of pathogenic microorganisms and the sorbent concentration in the suspension. The results obtained show the prospects of using clay from the specified deposit in the Belgorod region as a raw material for producing sorption materials with antibacterial properties.

References

1. I.V. Larionov, O. V. Rybalchenko, O. G. Orlova, I.L. Potokin, T.P. Sushko, T.A. Khrushchev, A.G. Boldyrev. Sorption and chromatographic processes. (2011) **11**. 792.
2. A.A. Novokshonov, N.V. Sokolov. Questions of modern pediatrics. (2011) **10,** 140.
3. V.I. Ilyin. Technological processes and methods of industrial wastewater treatment. M .: RKhTU im. D.I. Mendeleeva, 2014. 103 p. (in Russian)

SILICATE SORBENT FROM RICE STRAW

A.E. Panasenko, S.B. Yarusova, S.N. Somova, P.S. Gordienko, Yu.A. Parot'kina

yarusova_10@mail.ru
Institute of Chemistry, Far Eastern Branch of Academy of Sciences,
690022 Vladivostok, Russia

Among a variety of inorganic silicate sorbents used for extraction of various pollutants from water environments, in both Russian and foreign literature, attention is paid to materials based on calcium silicates $nCaO \cdot mSiO_2$ and hydrosilicates $nCaO \cdot mSiO_2 \cdot pH_2O$ [1–3]. As a silicon-containing raw material for obtaining calcium silicates, the wastes of rice production in the form of hulls and straw, formed during the production of rice in large quantities, are of particular interest.

In the review [4], an analysis of a large number of works related to obtaining sorbents by chemical and biological modification of rice hulls and straw was performed. In general, analysis of scientific and technical literature shows very few works on obtaining calcium silicates from rice straw (in comparison with rice husk). Recently, the methods to prepare wollastonite $CaSiO_3$ from rice straw were proposed [5,6].

The aim of the present work is to obtain a sorbent based on calcium silicate from rice straw and study the sorption properties of the obtained material in relation to Sr^{2+} ions.

The straw was cut into pieces 10–50 mm long, washed with water, and dried in the air. Then a weighted raw material was treated with 1 M sodium hydroxide solution at 90°C for 1 h. The solid residue of the straw (which can be further used as raw materials for producing cellulose) was separated from the solution, to which a solution of calcium chloride in the molar ratio of Ca/Si equal to 1:1 was added under vigorous stirring and the pH was adjusted to 7 by HCl solution. The resulting volumetric precipitate was washed with distilled water from soluble salts to a neutral reaction of the washing water, then filtered and dried in the air at 105°C.

The sorption experiments were performed under static conditions at a solid-liquid ratio of 1:400 and temperature of 20°C from aqueous solutions of strontium chloride ($SrCl_2 \cdot 6H_2O$) without salt background with various initial concentrations of

Sr^{2+} ions ranging from 0.016 to 1.22 mmol·L^{-1} under stirring on a magnetic stirrer "RT 15 power" (IKA WERKE, Germany) for 3 hours. To obtain a kinetic curve of sorption under similar conditions, sorbent suspensions were placed in a series of test tubes with an aqueous solution of $SrCl_2 \cdot 6H_2O$ with an initial concentration of Sr^{2+} ions of 1.22 mmol·L^{-1} and shaken from 1 to 180 min.

X-ray diffractograms were recorded on a Bruker D8 Advance diffractometer (Germany) in Cu Kα-radiation.

The content of Sr^{2+} ions in the initial solutions and filtrates after sorption was determined by atomic absorption spectrometry on a dual-beam spectrometer SOLAAR M6 (Thermo Scientific, USA) by the analytical line 460.7 nm. The detection limit of strontium ions in aqueous solutions is 0.002 μg·mL^{-1}. The error of determination of strontium in solutions is 10%.

According to X-ray diffraction analysis, the obtained sediment contains both the amorphous and crystal phases of calcite $CaCO_3$ whose formation is connected with carbonization of calcium hydroxide which is formed in small amounts at the interaction of calcium chloride solution with alkaline hydrolyzate of rice straw.

Based on the experimental data on the sorption of Sr^{2+} ions by the obtained material, the sorption isotherm was drawn (Fig. 1). To evaluate the sorption properties of the sample, the obtained sorption isotherm was analyzed in the appropriate coordinates of the Langmuir equation:

$$\frac{C_{eq}}{A_s} = \frac{1}{A_m \cdot k} + \frac{C_{eq}}{A_m},$$

where C_{eq} is the equilibrium concentration of Sr^{2+} ions in the solution, A_m is the maximum sorption capacity, k is the Langmuir constant. The value of A_m in the Langmuir equation was determined graphically by linearization of the isotherm. The parameters of the Langmuir equation were found: A_m value determined graphically was 0.26 mmol·g^{-1}, the Langmuir constant k = 2.1 L·$mmol^{-1}$, R^2 = 0.9896.

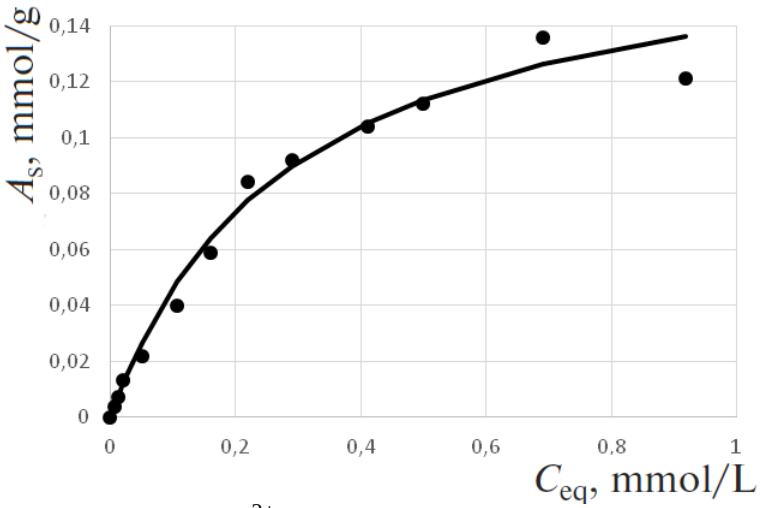

Fig. 1. Isotherm of sorption of Sr^{2+} ions from aqueous solutions of strontium chloride without salt background by calcium silicate obtained from rice straw

Figure 2 shows the kinetic curves of Sr^{2+} ions sorption at the temperatures of 20, 40, and 60°C.

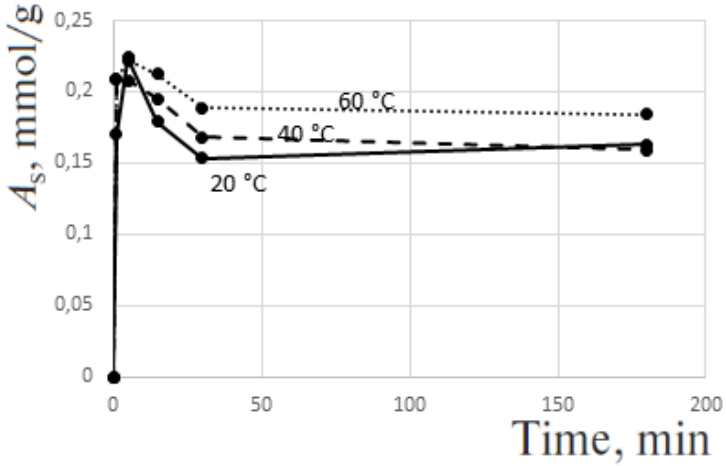

Fig. 2. Kinetic curves of sorption of Sr^{2+} ions from aqueous solutions of strontium chloride without salt background by calcium silicate from rice straw

As can be seen from the presented kinetic curves, the sorption capacity reaches a maximum within 5 minutes, after which some decrease is observed, which may be associated with both the presence of the organic component in the sorbent composition and with a change in pH over time. These results are planned to interpret in further studies. With an increase in temperature from 20 to 60°C, the sorption capacity slowly increases.

Funding and acknowledgments

The work was carried out within the framework of the State research №0205-2021-0002 of the Institute of Chemistry, FEB RAS.

The registration numbers of the research topics in the Plan of the Scientific Council of the Russian Academy of Sciences on Physical Chemistry (section "Adsorption phenomena") are 21-03-460-12 and 21-03-460-14.

References

1. Coleman, N.J., Brassington, D.S., Raza, A., Mendham, A.P. Sorption of Co^{2+} and Sr^{2+} by waste-derived 11 Å tobermorite. Waste Management (2006) **26**, 260.
2. Yarusova S.B., Gordienko P.S., Yudakov A.A., Azarova Yu.A., Yashchuk R.D. Kinetics of sorption of heavy metal ions by sorbent obtained from boric acid waste // Chemical Technology (2015) **16**, 620. *(In Russian).*
3. Maeda H., Ishida E.H. Hydrothermal preparation of diatomaceous earth combined with calcium silicate hydrate gels. J. Hazard. Mater. (2011) **185**, 858. DOI:10.1016/j.jhazmat.2010.09.099
4. Goodman B.A. Utilization of waste straw and husks from rice production: A review // JB&B (2020) **5**, 143. DOI: 10.1016/j.jobab.2020.07.001
5. Shamsudin R., Ismail H., Abdul Hamid M.A. The Suitability of Rice Straw Ash as a Precursor for Synthesizing β-Wollastonite Mater. Sci. Forum. (2016) **846**, 216.
6. Panasenko A.E., Yarusova S.B., Terminov S.A., Telushko M.S., Gordienko P.S., Zemnukhova L.A. Synthesis of wollastonite from alkaline extracts of rice straw. Materials of the Sixth Interdisciplinary Scientific Forum with international participation "New Materials and Advanced Technologies", Moscow, 23–27 November 2020. Volume II - M.: Center for Scientific and Technical Solutions (ANO CNTR), 2020. pp. 181–184. *(In Russian).*

NANOSTRUCTURED BARIUM-CONTAINING SILICATE SORBENT FROM PLANT RAW MATERIALS

A.E. Panasenko, S.B. Yarusova, P.S. Gordienko, S.N. Somova, Yu.A. Parot'kina

yarusova_10@mail.ru
Institute of Chemistry, Far Eastern Branch of Academy of Sciences,
690022 Vladivostok, Russia

All radioactive isotopes have a negative impact on the components of the environment. Active research is being conducted to create new sorption materials with a high sorption capacity, the high sorption selectivity for a particular element from solutions with complex ionic composition, and appropriate kinetic characteristics. The adequate time of sorption is of fundamental importance when using sorbents for decontamination of animal and human organisms.

A wide range of different materials is used for radionuclides extraction from aqueous media – ion exchange resins, natural and synthetic zeolites, materials based on titanate, vanadate, and tungsten, manganese oxides, hexacyanoferrates, ammonium molybdophosphates, hydroxyapatite, etc.

Some authors [1,2] pointed out the use of sorption-reagent systems based on amorphous barium silicate $BaSiO_3$, which is a result of sol-gel transition induced by adding Ba^{2+} ions into the Na_2SiO_3 solution.

In [3,4], the method was proposed to prepare a sorption material for selective extraction of strontium radionuclides, which was nanostructured barium aluminosilicate of composition $BaAl_2Si_nO_{(n+2)}\cdot 2mH_2O$, where n = 2, 4,...10; m takes both integer and fractional values greater than 1.

The purpose of this study was to synthesize and study the sorption properties of nanostructured barium aluminosilicate using rice straw as a silicon-containing raw material.

To obtain the sorbent, the rice straw (RS) of "Lugovoy" strain was cut into pieces <5 cm, treated with 1 M NaOH solution in the ratio solid:liquid = 1:15 at 90 °C for 1 hour. The hydrolysate was filtered off, and a solution of barium and aluminum chlorides was added to it with the ratio Al : Ba : RS = 1 : 2.6 : 17. The pH of the reaction mixture was adjusted to 7 by adding HCl, the precipitate was separated by

decantation, washed, and dried at 105 °C. The composition of the obtained material corresponds to the empirical formula $Na_{0.5}BaAl_{4.3}Si_{2.9}O_{13.5}$.

Sorption experiments were carried out under static conditions at a solid-liquid phase ratio of 1:400 and temperature 20 °C from aqueous solutions of strontium chloride ($SrCl_2 \cdot 6H_2O$) without salt background with different initial concentrations of Sr^{2+} ions ranging from 0.016 to 1.22 mmol·L^{-1} under stirring on a magnetic stirrer "RT 15 power" (IKA WERKE, Germany) for 3 hours. To obtain the kinetic curve of sorption, sorbent suspensions were placed in a series of test tubes with an aqueous solution of $SrCl_2 \cdot 6H_2O$ with an initial concentration of Sr^{2+} ions of 1.22 mmol·L^{-1} and shaken from 1 to 180 min.

The contents of Sr^{2+} and Ba^{2+} ions in the initial solutions and after sorption were determined by atomic absorption spectrometry on a SOLAAR M6 double-beam spectrometer (Thermo Scientific, USA): from the analytical lines at 460.7 nm and 553.6 nm, respectively. The detection limit of strontium ions in aqueous solutions was 0.002 μg·mL^{-1}, barium – 0.01 μg·mL^{-1}.

The sorption capacity (A_s, mmol·g^{-1}) of the studied samples was calculated by the formula:

$$A_s = \frac{(C_i - C_{eq})}{m} \cdot V,$$

where C_i is the initial concentration of Sr^{2+} ions in the solution, mmol·L^{-1}; C_{eq} is the equilibrium concentration of Sr^{2+} ions in the solution, mmol·L^{-1}; V is the solution volume, L; m is the sorbent mass, g.

Based on the experimental data obtained on the sorption of Sr^{2+} ions by barium aluminosilicate the sorption isotherm was drawn (Fig. 1).

The sorption properties of the sample were determined from the obtained sorption isotherm analyzed in the appropriate coordinates of the Langmuir equation:

$$\frac{C_{eq}}{A_s} = \frac{1}{A_m \cdot k} + \frac{C_{eq}}{A_m},$$

where C_{eq} is the equilibrium concentration of Sr^{2+} ions in the solution, A_m is the maximum sorption capacity, k is the Langmuir constant. The value of A_m in the Langmuir equation was determined graphically by linearization of the isotherm.

The parameters of the Langmuir equation were found: A_m value determined graphically was 0.4 mmol·g^{-1}, the Langmuir constant k = 27.0 L·mmol^{-1}, R^2 = 0.9153.

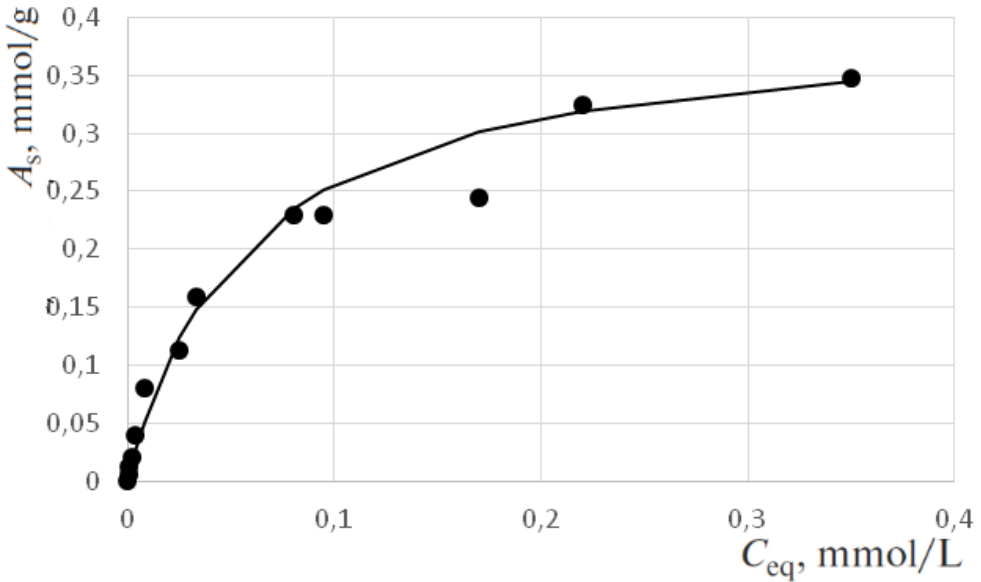

Fig. 1. Isotherm of sorption of Sr^{2+} ions from aqueous solutions of strontium chloride without salt background by barium aluminosilicate from rice straw

Fig.2 shows the kinetic curve of the sorption of Sr^{2+} ions at 20 °C.

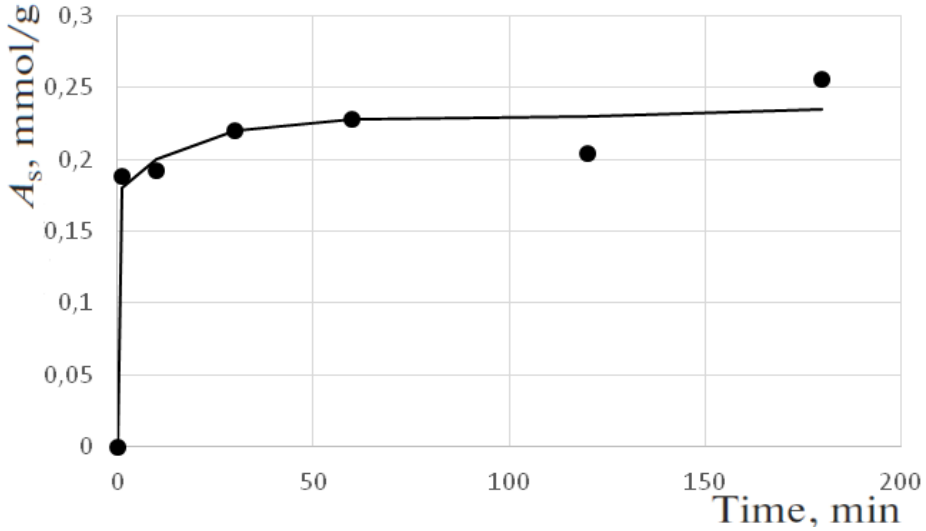

Fig. 2. Kinetic curve of the sorption of Sr^{2+} ions from aqueous solutions of strontium chloride without salt background by barium aluminosilicate from rice straw.

As can be seen from the figure above, the kinetic curve comes to a plateau after 30 min. In this case, the extent of extraction of Sr^{2+} ions reaches 45 %.

Analysis of Sr^{2+} and Ba^{2+} ions content in the filtrates after sorption shows that when the Sr^{2+} concentration in the solutions increases, the Ba^{2+} ion concentration in the filtrates after sorption increases from 0.01 to 0.19 mmol·L^{-1} relative to the control

experiment ions. This fact indicates that the primary sorption mechanism is the cationic exchange of Ba^{2+} ions for Sr^{2+} ions in the obtained aluminosilicate sorbent.

Funding and acknowledgments

The work was carried out within the framework of the State research №0205-2021-0002 of the Institute of Chemistry, FEB RAS.

The registration numbers of the research topics in the Plan of the Scientific Council of the Russian Academy of Sciences on Physical Chemistry (section "Adsorption phenomena") are 21-03-460-12 and 21-03-460-14.

References

1. Sokolnitskaya T. A., Avramenko V. A., Burkov I. S. et al. Sediment formation during absorption of strontium by sorption-reagent materials. J. Phys. Chem. (2004) **78**, 497. *(In Russian).*
2. Tananaev I.G., Avramenko V.A. Radiation Safety of the Far East: Problems and Solutions // Journal of Belarusian State University. Ecology (2017) № 4. 33. *(In Russian).*
3. Pat. 2680964 Russian Federation. Sorption material for selective extraction of strontium radionuclides from solutions with complex ionic composition and method of extraction of strontium radionuclides with it / P.S. Gordienko, I.A. Shabalin, S.B. Yarusova, S.B. Bulanova. - No. 2018113211 ; application. 11.04.2018 ; publ. 01.03.19, Bul. no. 7. *(In Russian).*
4. Gordienko P.S., Shabalin I.A., Yarusova S.B., Bulanova S.B., Kuryavy V.G., Zheleznov V.V., Somova S.N., Zhevtun I.G. Sorption of strontium ions by barium silicates from solutions of complex salt composition. J. Inorg. Chem. (2019) **64**, 1326. *(In Russian).*

CERAMIC MATRICES BASED ON WOLLASTONITE OBTAINED BY SPARK PLASMA SINTERING FOR IMMOBILIZATION OF COBALT-60

O.O. Shichalin, S.B. Yarusova, E.K. Papynov, P.S. Gordienko, I.Yu. Buravlev, S.B. Bulanova, A.A. Belov

yarusova_10@mail.ru
Institute of Chemistry, Far Eastern Branch of Academy of Sciences, 690022 Vladivostok, Russia

Among all artificial radioactive isotopes, ^{60}Co, with a half-life of about five years, has found wide application. The search for promising inorganic materials for sorption and immobilization of ^{60}Co, which is a source of gamma radiation, is an urgent problem in the context of radioactive waste management.

A number of studies pay attention to the sorption properties of amorphous and crystalline calcium silicates nCaO·mSiO$_2$. Industrial wastes from various industries based on silicon and calcium (for example, waste paper recycling, borohypsum, phosphogypsum, silica gel, fly ash, etc.) are used to synthesize these compounds. The maximum sorption capacity of the silicates under study with respect to Co^{2+} ions ranged from 0.18 to 4.1 mmol·g^{-1} [1–4]. Based on the scientific and technical literature analysis, it can be assumed that sorption materials based on calcium silicates can be used as effective matrices for cobalt immobilization.

This work aims to synthesize a material based on calcium silicate with sorption selectivity to cobalt ions and to produce on its basis solid matrices with high hydrolytic stability using the spark plasma sintering (SPS) technology.

To obtain the sorbent based on calcium silicate, we used boric acid production waste borohypsum with the content of the main components, mass %: SiO_2 – 32,2; CaO – 28,4; SO_3 – 31,3; Fe_2O_3 – 2,7. The main components of borohypsum are calcium sulfate dihydrate and amorphous silica. The specific surface area of borohypsum is 12.9 m^2·g^{-1}. Borohypsum was mixed with potassium hydroxide solution in a stoichiometric ratio. Synthesis was carried out in autoclave at the pressure of 1.7 atm. for two hours. The rate of the reaction under the above conditions of preparation is 81.2 %.

According to the X-ray diffraction analysis (XRD), the obtained sediment is amorphous, but crystalline phases of calcite and quartz were found in the composition. The specific surface area of the material obtained is 22.0 $m^2 \cdot g^{-1}$, density – 2.25 $g \cdot cm^{-3}$. The transition of amorphous calcium hydrosilicates to the crystalline phase of wollastonite of triclinic modification occurs due to sample's burning, as evidenced by XRD data of the sample after burning at 850 °C and thermogravimetric analysis.

The precipitate obtained by drying to a constant mass at 105°C was treated under static conditions with an aqueous solution of $CoCl_2 \cdot 6H_2O$ with a concentration of Co^{2+} ions of 110.1 $mmol \cdot L^{-1}$ until its saturation, at a solid-liquid phase ratio equal to 1:40 and temperature 20 °C for 3 hours with stirring at 150 rpm using an RT 15 power magnetic stirrer (IKA WERKE, Germany). The sorption capacity by Co^{2+} ions at the indicated conditions was 1.98 $mmol \cdot g^{-1}$. Cobalt content in the saturated sample is 31.5 mass%.

Synthesis of ceramic matrices was carried out by Spark Plasma Sintering (SPS), by the consolidation of the obtained powder on SPS 515S unit by "Dr. Sinter LAB™" (Japan): 1 g of powder was placed in a graphite mold (diameter 10.5 mm), then the blank was placed in a vacuum chamber (10^{-5} atm.), then sintered. Geometric dimensions of the obtained samples of cylindrical matrices: diameter 10.3 mm, height 4-5 mm (depending on the type of mold and sintering modes).

According to XRD data, the phase composition of the consolidated samples is characterized by the presence of phases $CaCoSi_2O_6$, wollastonite $CaSiO_3$, and quartz SiO_2.

The hydrolytic stability of the received samples, which is the primary indicator of their efficiency for immobilization of a radionuclide of cobalt, is carried out. Hydrolytic stability of matrices was estimated based on desalination rate of cobalt under long-term contact (30 days) with the distilled water (pH 6.8) at room temperature (25°C) in static condition according to well-known Russian Government Standard (GOST R 52126-2003), closely related to the ANSI/ANS-American National Standards Institute /American Nuclear Society 2019 (ANSI/ANS 16.1) that was updated according to the older procedure recommended by IAEA (ISO 6961:1982).

It was found that the lowest cobalt leaching rate is observed for samples obtained at 1000 °C (Fig. 1). This parameter reaches $2.03 \cdot 10^{-7}$ $g \cdot cm^{-2} \cdot d^{-1}$, which corresponds to the requirements of GOST R 50926-96 for solidified high-activity wastes.

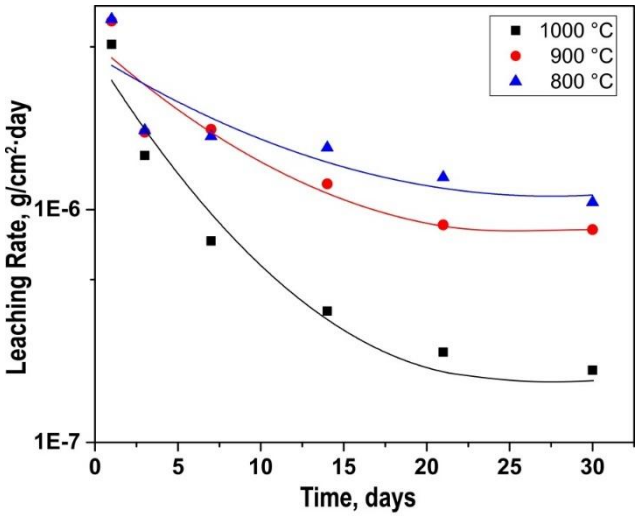

Fig. 1. The leaching rate of cobalt from wollastonite-containing matrices obtained with different SPS temperatures (800, 900, 1000 °C)

Thus, the ceramic wollastonite-containing matrices obtained by the IPS method using technogenic raw materials and data on their hydrolytic stability are of scientific and practical interest and the basis for further research.

Funding and acknowledgments

The work was carried out within the frames of the state research №0205-2021-0002 of the Institute of Chemistry, FEB RAS. This work was supported by a grant from the Government of the Primorye Territory (Russia) (2020–2021).

The registration number of the topic in the Plan of the Scientific Council of the Russian Academy of Sciences for Physical Chemistry (section "Adsorption Phenomena") is 21-03-460-11 and 21-03-460-14.

References

1. Coleman N. J., Brassington D. S., Raza A., Mendham A. P. Sorption of Co^{2+} and Sr^{2+} by waste-derived 11 Å tobermorite. Waste Management (2006) **26**, 260.
2. Akatyeva L.V. Synthesis and physicochemical properties of xonotlite and wollastonite. Ph.D. Thesis. / Institute of General and Inorg. Chem. N.S. Kurnakov RAS. - M., 2003. - 233 p. *(In Russian).*

3. Gordienko P.S., Yarusova S.B., Bulanova S.B., Suponina A.P., Zarubina N.V., Mayorov V.Y. Sorption properties of materials based on calcium silicates in relation to ions Co^{2+} . Chem. Techn. (2011) **12**, 282. *(In Russian).*
4. Qi G., Lei X., Li L., Yuan C., Sun Y., Chen J., Chen J., Wang Y., Hao J. Preparation and evaluation of a mesoporous calcium-silicate material (MCSM) from coal fly ash for removal of Co(II) from wastewater. Chem. Eng. J. (2015) **279**, 777. **DOI:** 10.1016/j.cej.2015.05.077

STUDY OF THE SORPTION-DESORPTION PHENOMENA OF MYCOTOXINS ON THE NATURAL LIGNINS SURFACE

L.S. Kocheva [1], ***A.V. Kanarsky*** [2], ***A.P. Karmanov*** [3, *], ***N.I. Bogdanovich*** [4, **]

**apk0948@yandex.ru; **n.bogdanovich@narfu.ru*

[1] *Institute of Geology of the Komi Science Center UB RAS, 167982 Syktyvkar, Russia*

[2] *Kazan National Research Technological University, 420015 Kazan, Russia*

[3] *Institute of Biology of the Komi Science Center UB RAS, 167982 Syktyvkar, Russia*

[4] *Lomonosov Northern (Arctic) Federal University, 163002 Arkhangelsk, Russia*

As shown by the research of recent years, conducted at the Ioffe Physico-Technical Institute RAS and the Unitary Enterprise "S.V. Lebedev Institute of the Synthetic Rubber", natural lignins can be successfully used for the SVS synthesis of new nanocarbon materials. However, the results of synthesis largely depend on the choice of lignins since their structure and properties depend on the taxonomic origin of lignins. In the presented work, comprehensive studies of various properties, including sorption, of a number of natural lignins were carried out: SL-1 (*Junglas regia*), SL-2 (*Picea abies*), SL-3 (*Helianthus tuberosus*), SL-4 (*Ledum*), SL-5 (*Lavatera*), SL-6 (*Secale*), as well as nanocarbon materials (NCM) based on lignins.

One of the sections of the work is devoted to the study of sorption-desorption of mycotoxins aflatoxin B1 and ochratoxin A. The SL-3 sample has the best characteristics (adsorption capacity S>64 %, desorption value D<6 %). The lowest results were obtained for SL-5 (S~30 %). Since the sorption capacity of materials can depend both on the surface-porous structure of adsorbents and on their structural and chemical features, we have studied and analyzed both of these aspects. To characterize the surface of adsorbents, the method of low-temperature nitrogen adsorption was used (Table, Figure).

Table. Surface characteristics of lignin and NCM samples[1]

Samples	SSA-BET, m^2/g	SSA_{m-m}, m^2/g	Pore width, nm	SSA_{meso}, m^2/g	SSA_{micro}, m^2/g	V_{Σ}-BET, m^2/g	$V_{\Sigma meso}$, m^2/g
SL-1	9.9	–	1.6	–	–	0.019	–
SL-2	28.4	24.9	1.4	14.9	3.5	0.06	0.03
SL-3	24.5	22.9	1.8	15.8	1.6	0.13	0.07
SL-4	10.6	9.4	1.8	7.0	1.2	0.02	0.02

SL-5	17.8	17.8	1.8	10.8	–	0.09	0.04
SL-6	36.0	34.8	1.5	0.2	1.2	0.26	0.15
NCM2	288.0	–	3.3	–	–	0.236	–

[1] SSA-BET – specific surface area according to Brunauer-Emmet-Teller; SSA_{m-m} – specific surface area of meso and macropores; SSA_{meso} – specific surface area of mesopores; SSA_{micro} – specific surface area of micropores; V_{Σ}-BET – total pore volume according to Brunauer-Emmet-Teller; $V_{\Sigma meso}$ – mesopore volume. [2]-based on Betula verrucosa lignin

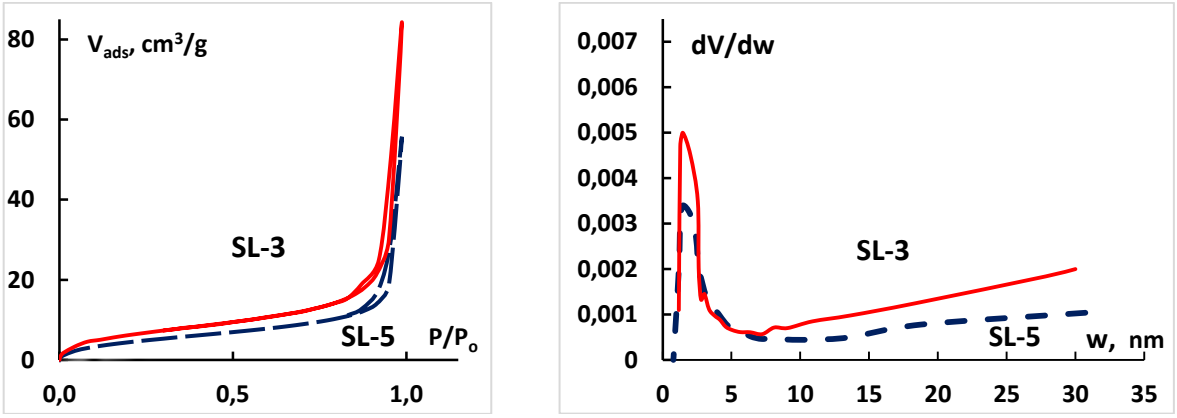

а б

Figure. Nitrogen adsorption isotherms (a); pore size distribution (b).

The establishment of correlations between the adsorption capacity and the parameters of the surface-porous structure and chemical structure of various lignins leads to the conclusion that the chemisorption mechanisms and the formation of chemical bonds played the most important role in the implementation of strong adsorption of mycotoxins. At the same time, the contribution of physical phenomena is not significant.

It was found that the SSA-BET index for the obtained carbon nanomaterials is 10–30 times greater than for lignins. It is concluded that the main role in sorption processes involving NCM is played by surface physicochemistry.

PREDICTIVE LATTICE MODELS OF SURFACE-CONFINED METAL-ORGANIC NETWORKS

V.A. Gorbunov*, *A.I. Fadeeva

vitaly_gorbunov@mail.ru
Omsk State Technical University, 644050 Omsk, Russia

Surface confined metal-organic networks (SMONs) are two-dimensional materials resulting from the self-assembly of organic molecules and metal atoms on solid surfaces. The most important application of SMONs relies on their relative thermal stability and ability to control the nanostructure of the adsorption layer using its composition and external conditions. Many papers have been published on the synthesis and physicochemical properties of such materials, demonstrating many potential applications [1-4].

Usually, SMONs are obtained by the molecular beam epitaxy of organic molecules and metal atoms. Further, the structure of the monolayers or thin films is studied with a complex of experimental and theoretical methods. The main research tool is scanning tunneling microscopy, which is supplemented by different spectral methods to understand the detailed chemical structure of the adsorption layer. Theoretical studies in most cases focus on the electron density functional theory calculations and analyzing the structural properties of a single adsorption complex. While maintaining the set of suitable experimental techniques, the study of self-assembly of surface confined metal-organic structures requires other theoretical approaches. The statistical simulation, in particular [5–10].

We demonstrate that the rigidity and directional character of the coordination bonds makes the lattice models a natural and effective tool for solving problems of the equilibrium self-assembly of surface-confined metal-organic networks. Summarizing our recent results, we can conclude:

1) The level of model specification is determined by the number of considered adsorption complexes differing in the position of molecules on the surface and by the theory level of model parameterization (molecular or quantum mechanics).

2) Depending on the level of specification, the lattice models allow one to reveal common features of the phase behavior of different SMONs or can be used to analyze the driving forces of self-assembly in specific metal-organic layers.

3) Applying several complementary methods for the same lattice model, such as the Monte Carlo method and tensor renormalization networks, one can reproduce the SMONs already found experimentally and predict new SMONs.

Acknowledgments

This study was supported by the Ministry of Science and Higher Education of the Russian Federation on a budget-funded basis for 2020–2022 (project No FSGF-2020-0001).

References

1. L. Dong, Z. Gao, N. Lin, Prog. Surf. Sci. (2016) **91**, 101.

2. Y. Geng, P. Li, J. Li, X. Zhang, Q. Zeng, C. Wang, Coord. Chem. Rev. (2017) **337**, 145.

3. R. Sakamoto, K. Takada, T. Pal, H. Maeda, T. Kambe, H. Nishihara, Chem. Commun. (2017) **53**, 5781.

4. S. Xing, Z. Zhang, X. Fei, W. Zhao, R. Zhang, T. Lin, D. Zhao, H. Ju, H. Xu, J. Fan, J. Zhu, Y. Ma, Z. Shi, Nat Commun. (2019) **10**, 70.

5. T. Lin, Q. Wu, J. Liu, Z. Shi, P.N. Liu, N. Lin, J. Chem. Phys. (2015) **142**, 101909.

6. T. Lin, X.S. Shang, P.N. Liu, N. Lin, J. Phys. Chem. C. (2013) **117**, 23027.

7. D. Nieckarz, P. Szabelski, J. Phys. Chem. C. (2013) **117**, 11229.

8. A.I. Fadeeva, V.A. Gorbunov, P.V. Stishenko, A.V. Myshlyavtsev, J. Phys. Chem. C. (2019) **123**, 17265.

9. A.I. Fadeeva, V.A. Gorbunov, O.S. Solovyeva, P.V. Stishenko, A.V. Myshlyavtsev, J. Phys. Chem. C. (2020) **124**, 11506.

10. A.I. Fadeeva, V.A. Gorbunov, P.V. Stishenko, S.S. Akimenko, A.V. Myshlyavtsev, Appl. Surf. Sci. (2021) **545**, 148989.

SYNTHESIS AND INVESTIGATION OF THE ADSORPTION PROPERTIES OF THE Ce-BTC METAL-ORGANIC FRAMEWORK STRUCTURE

A.E. Grinchenko*, *M.K. Knyazeva, A.A. Fomkin, A.V. Shkolin, A.L. Pulin

s-grinchenko@mail.ru
A.N. Frumkin Institute of Physical Chemistry and Electrochemistry, Russian Academy of Sciences (IPCE RAS), 119071 Moscow, Russia

Metal-organic frameworks (MOF) are ordered porous structures in which molecules of polydentate organic ligands are connected using metal ions. Studies of the last decade have shown that the use of polydentate organic ligands with various physicochemical properties and metal ions allows us to obtain a wide range of porous structures that can be used in various processes of adsorption, catalysis, medicine, and photonics [1]. Recently, rare-earth metals-based MOF with luminescent and sensory properties, such as Tb-BTC and Eu-BTC [2,3], have attracted much attention due to their applications for adsorption desulfurization [4] and hydrogen accumulation [5].

In this work, MOF of the Ce-BTC composition was synthesized by the method of solvothermal synthesis. Cerium nitrate hexahydrate ($Ce(NO_3)_3 \cdot 6H_2O$) was used as a metal ion source, 1,3,5 – benzenetricarboxylic acid ($C_9H_6O_6$) was used as an organic ligand, and N,N'-dimethylformamide was used as a solvent.

The parameters of the porous structure of the synthesized sample were derived from the adsorption isotherm of standard N_2 vapor at 77 K measured using the Micromeritics ASAP 2020 analyzer. The adsorption-desorption isotherms on the Ce-BTC sample are shown in Fig.1.

As follows from Fig. 1, the nitrogen adsorption isotherm increases sharply in the region up to 10 kPa, attaining the relatively high value of adsorption (~ 9–10 mmol/g), and the hysteresis loop is not pronounced, which indicates the absence of capillary condensation. Therefore, one can conclude that the Ce-BTC sample has a developed microporous structure, which is confirmed by the relatively large specific surface area evaluated by the standard BET method. The Dubinin theory of volume filling of micropores (TVFM) was employed to evaluate the structural and energy characteristics of the porous structure (see Table) and compared with the data obtained by the NLDFT method for a cylindrical pore model (Fig. 2).

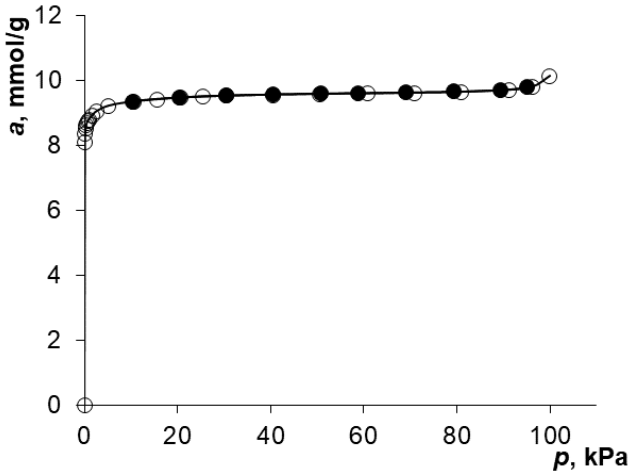

Fig. 1. Nitrogen adsorption isotherm at 77K on the Ce-BTC sample. Light symbols – adsorption, dark symbols-desorption.

Table 1. Structural-energy characteristics of the Ce-BTC sample determined from the isotherm of adsorption of standard nitrogen vapor at 77 K by the .

Characteristic, Dimension	Value
Specific surface area, S_{BET}, m^2/g	770
Specific volume of micropores, W_0, cm^3/g	0.32
Effective diameter of micropores by Dubinin theory, $2x_0$, nm	0.43
Limiting value of adsorption in micropores, a_0, mmol/g	9.4
Characteristic energy of adsorption of standard benzene vapors, E_0, кJ/mol	36.6

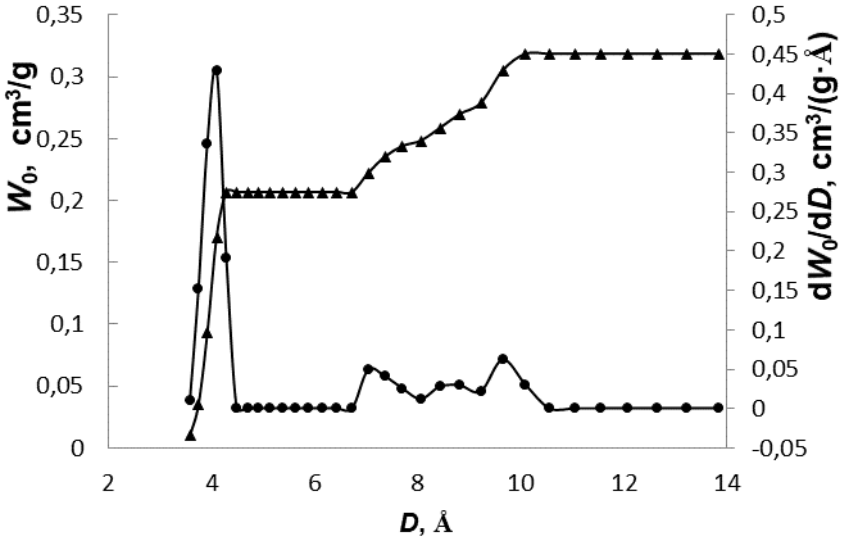

Fig. 2. Cumulative (triangle) volume and pore size distribution (circle) in the Ce-BTC MOF sample determined by the NLDFT method for a cylindrical pore model from the isotherm of adsorption of standard nitrogen vapor at 77 K.

As follows from Fig. 2, the porous structure of Ce-BTC is characterized by a monomodal pore size distribution with a maximum at the pore diameter of about 4 Å, which coincides with the value of $2x_0$ (0.43 nm) determined by the TVFM equations. Thus, in our opinion, the developed monoporous structure of the Ce-BTC MOF sample opens up the possibility of using it for adsorption systems of molecular sieve separation of gas mixtures.

Funding and acknowledgments

The work was performed within the framework of the State Task No. 0081-2019-0018

References

1. Tsivadze A. Yu., Aksyutin O. E., Ishkov A. G., Knyazeva M. K., Solovtsova O. V., Menshchikov I. E., Fomkin A. A., Shkolin A.V., Khozina E. V., Grachev V. A. Metal-organic frame structures as adsorbents for natural gas accumulation / / Uspekhi Khimii. 2019. Vol. 88, №. 9. P. 925-978.
2. Chen, L. Wang, F. Zapata, G. Qian, E. B. Lobkovsky / / J. Am. Chem. Soc. 2008. V. 130. P. 6718-6719.
3. Kreno, L.E., Leong, K., Farha, O.K., Allendorf, M., Van Duyne, R.P., Hupp, J.T.: Metal–organic framework materials as chemical sensors. Chem. Rev. 2011. V. 112. P.1105–1125.
4. L. Xiang, W. Jingyan, L. Qingyuan, J. Sai, Z. Tianhao, JI Shengfu Synthesis of rare earth metal-organic frameworks (Ln-MOFs) and their properties of adsorption desulfurization // Journal of Rare Earths. 2014. V.32. I.2. P.189-194.
5. J. Luo, H. Xu, Y. Liu, Y. Zhao, L. L. Daemen, C. Brown, T. V. Timofeeva, S. Ma, H.-C. Zhou // J. Am. Chem. Soc. 2008. V. 130. P. 9626–9627.

CARBON DIOXIDE ADSORPTION ONTO THE Al-BTC METAL-ORGANIC FRAMEWORK

***M.K. Knyazeva*, A.A. Fomkin, A.V. Shkolin**

knyazeva.mk@phyche.ac.ru
A.N. Frumkin Institute of Physical Chemistry and Electrochemistry, Russian Academy of Sciences (IPCE RAS), 119071 Moscow, Russia

Greenhouse gases that appear because of human activity contribute to a change in the Earth's climate. Effective methods of carbon dioxide absorption are required to protect the environment and improve the ecological situation. In addition, the captured CO_2 can potentially be used for many applications. The tasks of CO_2 capturing and accumulating can be successfully solved using the methods based on reversible physical adsorption.

Metal-organic frameworks (MOF) are promising adsorbents in comparison with other porous materials due to their 3D porous structure characterized by high values of the specific surface area and micropore volume [1]. These properties make MOF attractive porous materials with the possibility of use in various fields, such as biomedicine, catalysis, as well as adsorption. The structure and energy characteristics of the Al-BTC metal-organic porous structure make them promising adsorbents for the adsorption-based storage system for energy gases, for example, methane [2]. The use of aluminum-based MOF is also of great interest for the adsorption-based CO_2 capture since the Lewis centers of Al^{3+} and hydroxyl groups located in the structure are characterized by the high-energy interactions with CO_2 molecules [3].

In the present work, Al-BTC was synthesized by the solvothermal method described in [4]. The data on its porous structure were evaluated from the isotherm of standard nitrogen vapor at 77 K measured by the Quantochrome iQ analyzer. The nitrogen adsorption isotherm has a reversible part and a hysteresis loop, which indicates the presence of micro - and mesopores in the porous structure.

The results of the analysis of the low-temperature N_2 adsorption onto Al-BTC are listed in Table. The structure and energy characteristics of the MOF sample were determined using the Dubinin theory of volume filling of micropores (TVFM), the Kelvin equation was used to calculate the parameters of mesopores, and the standard

BET formula was used to evaluate the specific surface area. According to Table, Al-BTC MOF has a highly developed porous structure predominantly composed of mesopores.

Table. Structure and energy characteristics of Al-BTC.

Adsorbent	W_0, cm^3/g	E_0, кJ/mol	x_0, nm	a_0, mmol/g	E, kJ/mol	S_{BET}, m^2/g	W_{me}, cm^3/g	S_{me}, m^2/g
Al-BTC	0.53	15.7	0.76	15.1	5.2	1530	1.22	440

In the present work, the CO_2 adsorption onto Al-BTC MOF regenerated at a temperature of 403 K under thermal vacuum conditions was studied. The isotherms of carbon dioxide adsorption at temperatures from 216.6 to 393 K and pressures up to 120 kPa are shown in Fig.1.

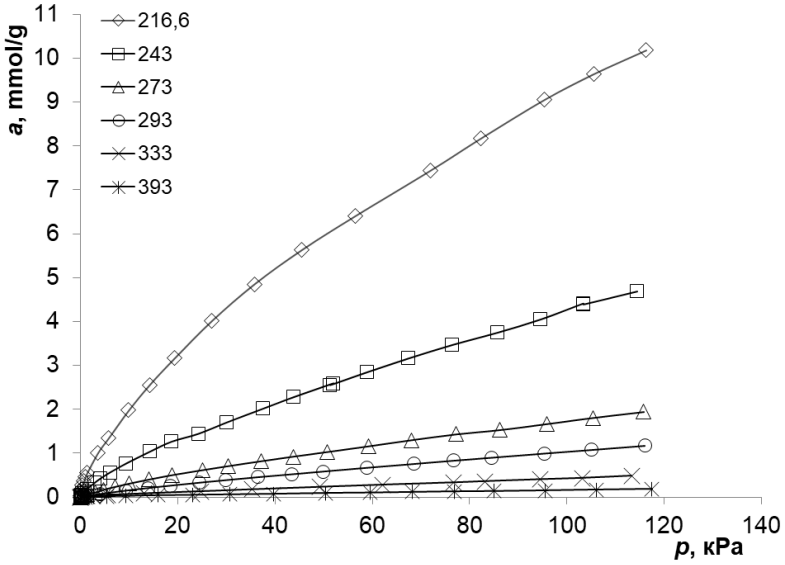

Fig. 1. Isotherms of CO_2 adsorption on the Al-BTC MOF sample at temperatures from 216.6 to 393 K and pressures up to 120 kPa.

As follows from Fig. 1, the adsorption of carbon dioxide on the Al-BTC sample under standard conditions (T = 273 K and P = 100 kPa) reaches a=1.8 mmol/g or 11.5 wt.%. A decrease in temperature leads to a sharp increase in CO_2 adsorption up to 44.8 wt.% at 216.6 K and 120 kPa.

It was found that the Al-BTC MOF sample can be considered a promising adsorbent for carbon dioxide at pressures up to 120 kPa, which allows it to be used in storage systems.

Funding and acknowledgments

The work was performed within the framework of State Task No. 0081-2019-0018.

References

1. T. Ghanbari, F. Abnisa, W. M. A. W. Daud. A review on the production of metal-organic frameworks (MOF) for CO_2 adsorption. Science of the Total Environment. (2020) **707**, 135090.
2. Batrakova M.K., Solovtsova O.V., Fomkin A.A., Tsivadze A.Yu, Shkolin A.V., Shiryaev A.A., Vysotskii V.V. Synthesis and structure-energy characteristics of an MOF Al-BTC organometallic framework structure. Prot. Met. Phys. Chem. Surf. (2017) **53**, 961.
3. Miguel A. Andrés, M. Benzaqui, S. Serre, N. Steunou, I. Gascóna. Fabrication of ultrathin MIL-96(Al) films and study of CO_2 adsorption/desorption processes using quartz crystal microbalance. J. Colloid Interf. Sci. (2018) **519**, 88.
4. Knyazeva M.K., Tsivadze A.Yu, Solovtsova O.V., Fomkin A.A., Pribylov A.A., Shkolin A.V., Pulin A.L., Men'shchikov I.E. Methane adsorption on the metal-organic framework structure Al-BTC Prot. Met. Phys. Chem. Surf. (2019) **55**, 9.

THE EFFECT OF STRUCTURAL DEFECTS AND FRAMEWORK FLEXIBILITY ON THE WATER ADSORPTION IN CAU-10-H

I.V. Grenev [1,2], ***A.A. Shubin*** [1,2], ***M.V. Solovyeva*** [1], ***L.G. Gordeeva*** [1]

greneviv@catalysis.ru
[1]*Boreskov Institute of Catalysis SB RAS, 630090 Novosibirsk, Russia*
[2] *Novosibirsk State University, 630090 Novosibirsk, Russia*

Porous metal-organic frameworks (MOFs) are a promising class of crystalline materials for a wide range of applications, such as gas storage [1], separation [2], catalysis [3], drug delivery [4], and water harvesting [5]. The variation of organic linkers and inorganic building units allows us to regulate their adsorption properties, surface area, pore size, and volume and adjust their physical and chemical properties according to the requirements of specific technological applications. The water adsorption in MOFs is of special interest for heat transformation applications [6,7]. Potential MOFs for such applications have to match three criteria [8]: the water adsorption isotherm has to be of S-type with a steep adsorption rise in relative pressure P/P_0 range of 0.1 - 0.3, the adsorption capacity should be sufficiently high, and the structure of the MOF should be stable during a large number of adsorption-desorption cycles.

Aluminum-based metal-organic framework CAU-10-H is a promising candidate for heat transformation applications due to its hydrothermal stability, appropriate adsorption properties, and low toxicity. The CAU-10-H framework consists of *cis*-corner-sharing AlO_6 polyhedra forming four-fold helical chains and isophthalate linkers (1,3-benzenedicarboxylate) connecting each helical chain with four neighboring chains. In this work, the effect of the framework flexibility and structural defects on the mechanism of water adsorption in CAU-10-H was studied by the grand canonical Monte Carlo (GCMC) method. It was shown by the simulations that the rigid ideal MOF framework is hydrophobic. Consideration of the framework flexibility in adsorption simulation showed that CAU-10-H becomes more hydrophilic due to the unblocking of bridging μ-OH hydroxyl groups, previously inaccessible to water. The adsorption of one water molecule on such a μ-OH group leads to a tilt of the 4 nearest linkers (Fig. 1), resulting in two different linker configurations. In the first configuration, the plane of the

aromatic ring is almost perpendicular to the channel axis, and in the other, it is almost parallel to the channel axis. This observation was confirmed by X-ray powder diffractometry [9] for the wet CAU-10-H structure. Nevertheless, taking into account the framework flexibility in simulations did not allow us to reproduce the experimental pressure where the water adsorption begins, the adsorption capacity and the heat of adsorption at low coverage.

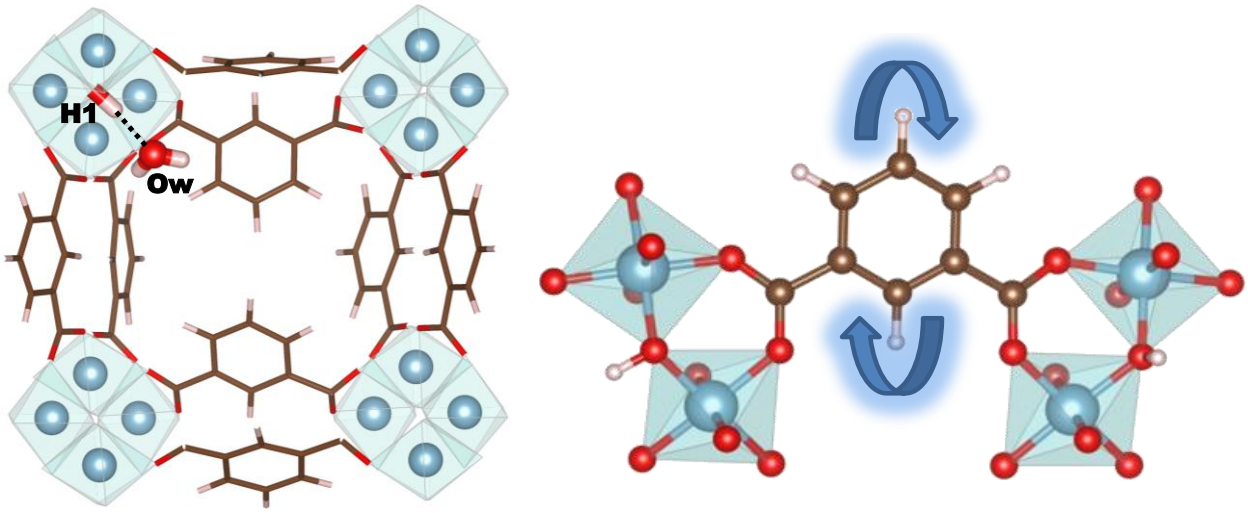

Fig.1. Simulation snapshot of water molecule adsorption on the bridging μ-OH hydroxyl group in flexible ideal CAU-10-H structure model at low loading (left). Schematic representation of the "flapping" linker motion (right).

In this study, we suggested that structural defects could be factors leading to the increase of the MOF hydrophilicity. The investigation of water adsorption for several CAU-10-H structures models with different concentrations and locations of structural defects demonstrated that even a small number of defects shifts the calculated adsorption “step” to experimental values and increases the adsorption capacity of the structure. It is shown that the heat of adsorption at low coverage exceeds the water heat of vaporization and is 50 - 53 kJ/mol, which is in good agreement with the experimental data [9,10]. It should be noted that the presence of defects in the structure also affects to the initial region of the adsorption isotherm.

Thus, the investigation of the water adsorption in CAU-10-H demonstrated that both factors, the framework flexibility and the structural defects, have significant effects on the shape of the adsorption isotherm. Defects are primary hydrophilic sites where adsorption of water molecules at low P/P_0 takes place. At the further increase of the water pressure in the system, the adsorption of water on the bridging hydroxyl μ-

OH groups occurs, causing structural changes, which leads to the subsequent filling of the whole pore space. The results obtained in this study reveal that the adsorption properties of MOFs for heat pump applications can be regulated not only by the linker functionalization but also by controlling the concentration and location of defects in the MOF structure.

Funding

The reported study was supported by Russian Foundation for Basic Research, projects number 19-33-60087 and 18-29-04033.

References

1. Li H. et al. Recent advances in gas storage and separation using metal–organic frameworks. Materials Today (2018) **21**, 108.
2. Adatoz E., Avci A.K., Keskin S. Opportunities and challenges of MOF-based membranes in gas separations. Sep. Purif. Technol. (2015) **152**, 207.
3. Chen Y.-Z. et al. Metal–organic framework-derived porous materials for catalysis. Coord. Chem. Rev. (2018) **362**, 1.
4. Wu M.-X., Yang Y.-W. Metal-Organic Framework (MOF)-Based Drug/Cargo Delivery and Cancer Therapy. Adv. Mater. (2017) **29**, 1606134.
5. Kalmutzki M.J., Diercks C.S., Yaghi O.M. Metal-Organic Frameworks for Water Harvesting from Air: 37. Adv. Mater. (2018) 30, 1704304.
6. de Lange M.F. et al. Adsorption-Driven Heat Pumps: The Potential of Metal–Organic Frameworks. Chem. Rev. 2015. Vol. 115, № 22. P. 12205–12250.
7. Henninger S.K. et al. New materials for adsorption heat transformation and storage. Renew. Energy (2017) **110**, 59.
8. Henninger S.K. et al. MOFs for Use in Adsorption Heat Pump Processes. Eur. J. Inorg. Chem. (2012) **2012**, 2625.
9. Fröhlich D. et al. Water adsorption behaviour of CAU-10-H: a thorough investigation of its structure–property relationships: 30. J. Mater. Chem. A. (2016) **4**, 11859.
10. Solovyeva M.V. et al. Water Vapor Adsorption on CAU-10-X : Effect of Functional Groups on Adsorption Equilibrium and Mechanisms. Langmuir (2021) 37, 693.

PREPARATION AND BULK PHYSICOCHEMICAL PROPERTIES OF NEW ADSORBENTS BASED ON THE InSb-ZnS SYSTEM

I.A. Kirovskaya

kirovskaya@omgtu.ru
Omsk State Technical University, 644050 Omsk, Russia

The present work is focused on the new adsorbents, which are multicomponent diamond-like semiconductors – solid solutions based on the reputable binary semiconductors of the $A^{III}B^{V}$, $A^{II}B^{VI}$ (InSb, ZnS) type [1]. It may be expected both the predictable effects caused by the unique physical, physical and chemical properties of the binary semiconductors and the unanticipated effects due to the complexity of the internal processes accompanying the formation of solid solutions.

Solid solutions $(InSb)_x(ZnS)_{1-x}$(x=4, 8, 18, 23, 90, 95, 98 mol.%) were prepared following the practicable technology, involving the particular temperature heating program, the synthesis completion at a reasonably chosen temperature – 1000 K, in evacuated, sealed quartz ampoules [2]. The completion of the synthesis and the formation of the structure of solid solutions were estimated by the results of X-ray studies which were later used in combination with the electron microscopical data for certification, determination of the structure, and basic structural characteristics of solid solutions.

X-ray studies were carried out on a D8 Advance diffractometer "Bruker" (Germany) in CuKα-radiation (λ = 0,15406 nm, T = 293 K) according to the wide-angle survey technique [1] with a position-sensitive detector Lynxeye. The decoding of the obtained X-ray patterns (diffractograms) was performed using the ICDDIPDF-2 powder diffraction database; the lattice parameters refining was conducted using the TOPAS 3.0 (Bruker) software by the least-squares method.

Electron microscopic studies were carried out on a JCM-5700 scanning electron microscope equipped with a nitrogen-free X-ray energy-dispersive spectrometer [2].

The results of the X-ray studies (Fig. 1, 2) prove the formation of the substitutional solid solutions with the cubic structure of sphalerite in the InSb-ZnS system, according to the following criteria: relative position and intensity distribution of the main lines in the X-ray diffraction patterns of the binary components and solid

solutions, depending on the composition of the lattice parameter values (a), interplanar distances (d_{hkl}), density (ρ_r). Deviations from the smooth or linear dependences $a = f(x_{ZnS})$, $d_{hkl} = f(x_{ZnS})$ at the boundary content in the ZnS system (77 mol.%), allowing unlimited mutual solubility of binary components (InSb, ZnS), i.e., the formation of substitutional solid solutions can be explained by some not clearly manifested structural change [3].

The solid solutions formation is also indicated by the absence of additional lines in the X-ray diffraction patterns corresponding to the unreacted binary components and the blurring of the main.

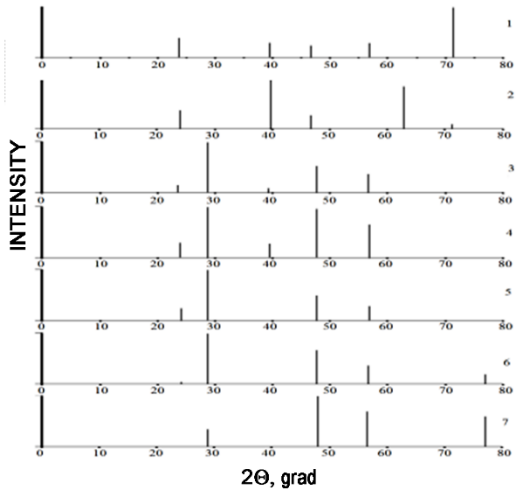

Fig. 1. X-ray patterns of the InSb-ZnS system components: 1 – InSb, 2 – $InSb_{0,90}ZnS_{0,10}$, 3 – $InSb_{0,23}ZnS_{0,77}$, 4 – $InSb_{0,18}ZnS_{0,82}$, 5 – $InSb_{0,08}ZnS_{0,92}$, 6 – $InSb_{0,04}ZnS_{0,96}$, 7 – ZnS

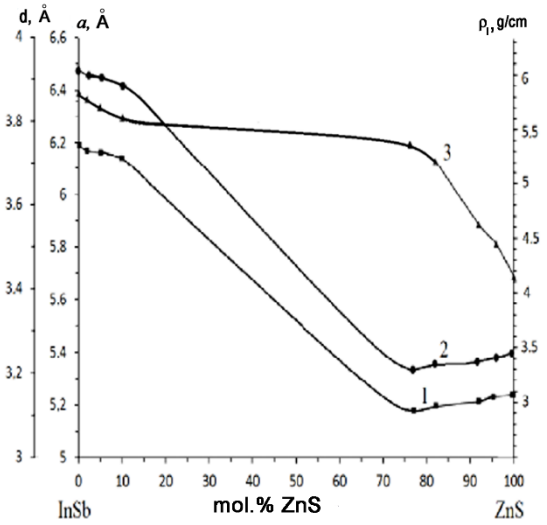

Fig. 2. Dependences of the parameter of the crystal lattices a (2), interplanar space d_{111} (1) theoretical calculated crystal density ρ_r (3) on the composition of the components of the system InSb-ZnS

According to the results of the electron microscopic studies (Fig. 3) the elemental compositions, surface structure, average particle sizes (l_{av}) of the system components, concentration dependences of the number of particles of a certain (average) size ($n_{av} = f(X_{ZnS})$) were determined.

It was concluded that the elemental composition of all components is in satisfactory agreement with the molar composition; the surfaces had a polycrystalline structure with the nonuniformly distributed crystallites, which are capable of forming agglomerations consisting of grains of various sizes.

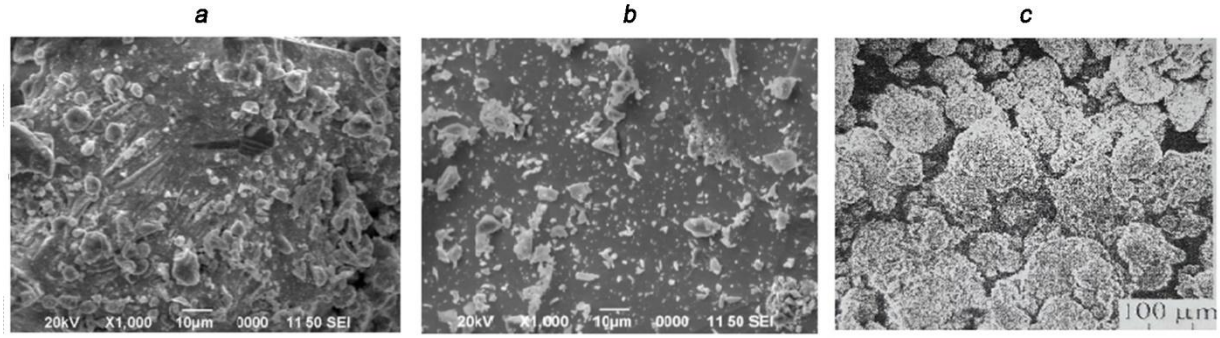

Fig. 3. SEM-images of the InSb (*a*); $InSb_{0,90}ZnS_{0,10}$ (b); ZnS (*b*) powders (*c*) in phase contrast mode.

Noting the extreme nature of changes with the parameter composition (*a*), interplanar distances (d_{hkl}) of the crystal lattices of the InSb-ZnS system components, one cannot fail to mention a gradual decrease in density (ρ_r) with an increase in the zinc sulfide content in the system with a smooth forbidden bandwidth increase – ΔE (from 0.18 to 3.67 eV) and the electronegativity difference ΔX (from 0.1 to 0.9) (Fig. 2). Thus, we observed an inevitable competition between the increase in the surface atoms coordinative unsaturation, respectively, the contribution of Lewis sites, and an increase in the ionic bond character, degree of surface hydration, consequently the contribution of Bronsted sites. With an increase in the relative contribution of the latter, an increase in the hydrogen index of the isoelectric state of surfaces (pH_{iso}) in the sequence InSb → $(InSb)_x (ZnS)_{1-x}$ → ZnS is expected.

Conclusion

The practicable technology was used to obtain the solid solutions of the InSb-ZnS system, certified based on the results of X-ray and electron microscopic studies as substitutional solid solutions with a sphalerite structure. Based on the results of electron microscopic studies, the elemental composition of the InSb-ZnS system components was determined, which practically coincides with the molar composition, the average sizes (l_{av}) and average numbers (n_{av}) of the dominant particles and the surface structure.

The consistent patterns in the composition of the studied properties were revealed, which are of both extreme ($a = f(x_{ZnS})$, $dhkl = f(x_{ZnS})$) and smooth ($n_{av} = f(X_{ZnS})$, $\rho_r = f(X_{ZnS})$) character.

The inevitable competition on the surfaces of the system components between the relative contributions of the acid Lewis and Bronsted sites was substantiated. Projections were

made on the nature of the pH_{iso} change in the sequence InSb → $(InSb)_x$ $ZnS)_{1-x}$ → ZnS and, thus, on the activity of surfaces towards gases of a certain electronic nature.

Funding and acknowledgments

The work was carried out following the plan of the Russian Academy of Sciences Council on Physical Chemistry, the theme no.20-03-460-02.

References

1. I.A. Kirovskaya Physical and chemical properties of binary and multicomponent diamond-like semiconductors. Novosibirsk: Siberian Branch of the Russian Academy of Sciences publishing house, 2015. p. 367.

2. I.A. Kirovskaya and etc. Adsorbents based on systems of the $A^{II}B^{VI}$-$A^{II}B^{VI}$ type - materials for semiconductor gas analysis. Novosibirsk: Siberian Branch of the Russian Academy of Sciences Publishing House, 2018. p.267.

3. M.V. Kot, V.G. Tyrziu Semiconductor compounds and their solid solutions. Kishenev: Publishing house Moldavian Academy of Sciences of the SSR, 1970. p. 31.

SURFACE PROPERTIES OF THE NEW ADSORBENTS $(InSb)_x(ZnS)_{1-x}$

I.A. Kirovskaya

kirovskaya@omgtu.ru
Omsk State Technical University, 644050 Omsk, Russia

The surface properties of solid bodies - adsorbents, materials undoubtedly are central to many technological processes, operation of devices, catalysts.

In the present work, the chemical composition and acid-base properties of the new adsorbents - solid solutions $(InSb)_x(ZnS)_{1-x}$ based on the relatively studied binary semiconductor compounds InSb and ZnS were studied.

Solid solutions $(InSb)_x(ZnS)_{1-x}$ (x = 4, 8, 18, 23, 90, 95, 98 mol%) *were obtained* using the practicable technology involving isothermal diffusion of the initial binary compounds (InSb, ZnS) and the fundamental available information on their bulk physical and physical and chemical properties [1].

The *chemical composition* of the surfaces of solid solutions and binary components of the InSb-ZnS system was evaluated using the IR spectra recorded on an Infra-LUM FT-02 infrared Fourier spectrometer with a multiply attenuation total reflectance attachment [1, 2]; *acid-base properties* - by the methods of hydrolytic adsorption (determination of the hydrogen index of the surfaces' isoelectric state - pH_{iso}), non-aqueous conductometric titration, mechanochemistry, IR spectroscopy multiply attenuation total reflectance attachment [1-3].

According to the results of IR spectroscopic studies, the ***chemical composition of the initial*** (exposed to air) ***surfaces*** of the InSb-ZnS system components is represented mainly by adsorbed (coordination-bound) water molecules (3500-3640, 1630-1680 cm^{-1}), OH^-groups (3700-3750 cm^{-1}), carbon-containing compounds (2360, 2850, 2900-2920 cm^{-1}) and surface atoms oxidation products [1]. After vacuum heat treatment ($P = 5 \cdot 10^{-4}$ Pa, T=573–673 K), the surfaces are freed from the adsorbed impurities to a large extent from their oxide phase, reaching the stoichiometric [1, 3].

Following the results of comprehensive research of the ***acid-base properties of the system components surfaces***, the average strength, the nature of active (acid) sites

of various origins, their relative contribution, and the mechanisms of acid-base interactions were determined.

The average strength of acid sites (pH_{iso}) of the system components' initial surfaces fits into the range of 6,3-6,6, conforming to the weak acidic region and growing in the sequence InSb → $(InSb)_x(ZnS)_{1-x}$ → ZnS.

During the identification of the acid sites nature, the results of non-aqueous conductometric titration and mechanochemical studies proved to be helpful. *Curves of non-aqueous conductometric titration* having three or more peaks (Fig. 1) indicate the presence of various types of acid sites on the specified surfaces. In line with the previously stated considerations (see, for example, [1]), coordination-unsaturated atoms (Lewis sites), adsorption water molecules, OH^- groups (Bronsted sites) can act as such. This is confirmed by the IR spectra of surfaces exposed to air: we note not only the presence of stretching vibration bands of the adsorbed water, OH^- groups (Bronsted sites), but also the formation of donor-acceptor (coordination bonds) $H2O^{+\delta}$ - $Me^{-\delta}$, $CO2^{+\delta}$ - $Me^{-\delta}$ with coordination-unsaturated atoms (Lewis sites) [1].

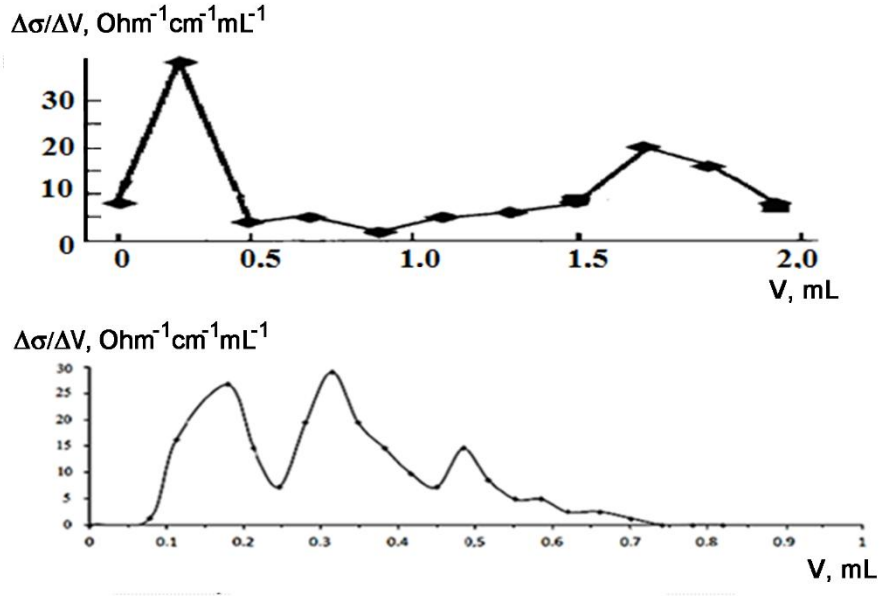

Fig. 1. Differential curves of non-aqueous conductometric titration of the InSb-ZnS system components exposed to air: *a* – InSb, *b* – ZnS.

The results of mechanochemical studies clarified the role of coordination-unsaturated atoms (Lewis sites). In the IR spectra of aqueous suspensions of dispersed components of the InSb-ZnS system, absorption bands were found, for which the ions

SbO_4^{3-}, SO_4^{2-}, SO_3^{2-} are most probably responsible - residues of H_3SbO_4, H_2SO_4, H_2SO_3 [3] acids. The latter, as shown, in particular, in [3], are of surface origin, being the products of the interaction of water with coordination-unsaturated atoms located on the newly created surfaces, and in the process of mechanochemical action turn into the bulk, splitting off their residues (SbO_4^{3-}, SO_4^{2-}, SO_3^{2-}). Hydrolysis of the weak acid residues (SO_3^{2-}) can lead to alkalinization of the medium, which is in evidence.

The connection between the surface and bulk properties comes under notice. Thus, the noted tendency of an increase in the basicity (pH_{iso}) of the surfaces with an increase in the content of a more ionic component ZnS in the system corresponds to a similar tendency (an increase in pH_{iso}) with an increase in such bulk properties as melting point (T_m), forbidden bandwidth (ΔE), a difference of electronegativities (Δx).

Thus, it is possible to predict acidity and activity of the surfaces toward gases of a certain electronic nature at the stage of studying volumetric (physical and physicochemical) properties and even at the stage of analyzing the available information on them, which facilitates the search for the requested materials of the advanced, in particular, sensor technology.

Funding and acknowledgments

The work was carried out according to the plan of the Russian Academy of Sciences Council on Physical Chemistry, the theme no.20-03-460-02.

References

1. Kirovskaya I.A. Physical and chemical properties of binary and multicomponent diamond-like semiconductors. Novosibirsk: Siberian Branch of the Russian Academy of Sciences publishing house, 2015. p. 367.
2. Little L. Infrared spectra of adsorbed molecules. M.: Mir, 1969. p. 514.
3. Kirovskaya I.A. Surface phenomena. Omsk : OmSTU publishing house, 2001. p.175

DEVELOPMENT OF SUBSTITUTED ZINC FERRITE NANOPARTICLES: SYNTHESIS AND CHARACTERIZATION

M. Ignat [1,2], P. Samoila [2], E. Mahu [1,2], T.F. Kouznetsova [3], A. Ivanets [3], V. Harabagiu [2]

tatyana.fk@gmail.com, maria.ignat@uaic.ro
[1] Laboratory of Materials Chemistry, Department of Chemistry, "Alexandru Ioan Cuza" University, Iaşi 700506, Romania
[2] Laboratory of Inorganic Polymers, "Petru Poni" Institute of Macromolecular Chemistry, 700487 Iasi, Romania
[3] State Scientific Institution, "The Institute of General and Inorganic Chemistry of the National Academy of Sciences of Belarus", 220072 Minsk, Republic of Belarus

Due to several advantages over other developed methods, the spinel ferrites have been prepared by a sol-gel auto-combustion method using metal nitrates and citric acid as reactants. As a result, ultrafine nanopowders with a good homogeneity and narrow particle size distribution were obtained, exhibiting different structural and morphological properties of spinel ferrites. Thus, spinel ferrites with the general formula $ZnFe_{0.5}Cr_{1.5-y}Gd_yO_4$ (y=0.02 and 0.08) were prepared using a stoichiometric ratio of the metal nitrates and the citric acid as the combustion agent. In order to achieve a pure spinel-phase formation, the samples were thermally treated at 500˚C and 700˚C. Thus, four samples have been obtained and characterized: ZFCG2-500, ZFCG2-700, ZFCG8-500, and ZFCG8-700, respectively.

The prepared iron-based nanoparticles were characterized using various physical techniques. Thus, structural features were investigated by X-ray diffraction, and the registered patterns are shown in Fig. 1, showing a cubic spinel structure confirmed by (111), (311), (400), (422), (511) (400), (533) diffraction planes. The broadening of diffraction peaks indicates the presence of nanocrystallites of substituted zinc ferrites, whose size was estimated by using the Debye-Scherer formula and Williamson–Hall plot. The calculated crystallite sizes for the prepared samples are given in Table 1. An increase in the crystallite size has been observed as calcination temperature increases and Gd^{3+} concentration decreases. The last fact is most probably due to the substitution of Fe^{3+} ions that have a smaller ionic radius (0.645 Å) by Gd^{3+} ions in the host spinel matrix, the last one having a higher ionic radius (0.938 Å) [1,2],

thus the substitution of Gd^{3+} ions into spinel ferrite nanoparticles stopping the lattice growth of nanocrystalline particles [3].

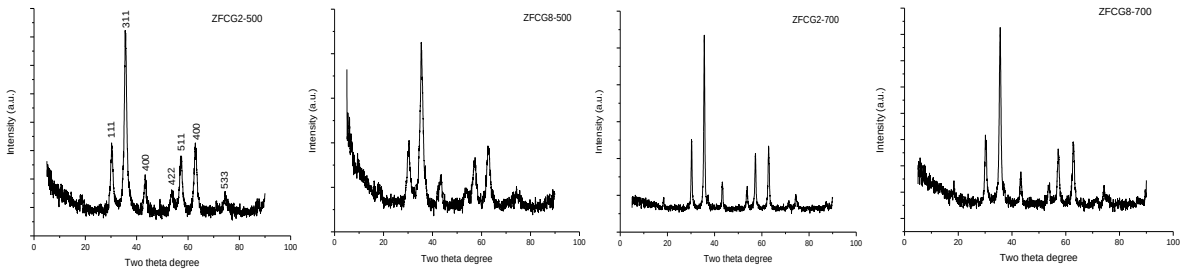

Fig. 1. X-ray diffraction patterns of the synthesized iron-based nanoparticulate materials.

Table 1. Textural and structural features of synthesized $ZnFe_{0.5}Cr_{1.5-y}Gd_yO_4$ (y=0.02 and 0.08) spinel ferrite nanoparticles.

Sample	$D_{Scherrer}$ (nm)	δ (nm^{-2}) (Scherrer method)$\times 10^{-2}$	D_{W-H} (nm)	ε (W–H method) $\times 10^{-3}$	S_{BET}, m^2/g	V_t, cc/g STP	S_μ, m^2/g	V_μ, cc/g STP	d_{BJH}, nm
ZFCG2-500	9.2	1.18	6.0	− 3.4	50.8	0.128	0	0	12.1
ZFCG2-700	19.5	0.26	13.3	− 1.7	16.7	0.023	3.6	0.002	3.0
ZFCG8-500	6.8	2.16	3.9	− 6.6	56.1	0.119	1.7	0.002	10.0
ZFCG8-700	13.9	0.51	9.0	− 2.3	22.6	0.037	3.8	0.002	3.2

Textural properties of the prepared substituted zinc ferrite nanoparticles have been investigated by N_2-sorption measurements (Fig. 2). The registered isotherms allowed us to calculate the BET specific surface (S_{BET}), the total pore volume (V_t), the micropore specific surface area (Sμ), micropore volume (Vμ), and the mean pore size diameter ($d_{mean\ pore}$) (Table 2). Ferrites synthesized at 500°C, show a type IV isotherm (according to IUPAC), characterizing mesoporous materials, accompanied by a H2 type hysteresis loop, showing a pore-blocking effect. On the other hand, higher calcination temperatures lead to ferrites characterized by Type II isotherms, indicating a nonporous or macroporous adsorbent.

Tauc plots allowed one to evaluate the optical properties of the synthesized spinel ferrite nanoparticles (Fig. 3). Thus, the optical band gaps (E_g) were estimated. One can be concluded: the gadolinium and calcination temperatures lead to a slight increase in the bandgap energy of the prepared ferrites. Thus, the obtained results recommend the synthesized spinel ferrite nanoparticles as suitable materials for visible-light photocatalysis applications. Thus, as an expanding field of applications,

the investigation of photocatalytic properties of the prepared samples will be focused further.

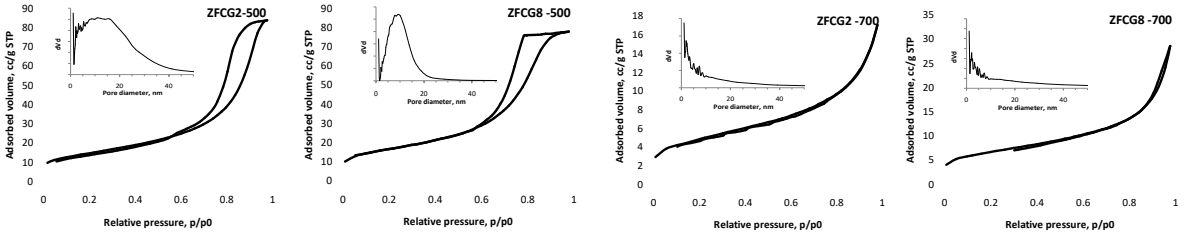

Fig. 2. Nitrogen adsorption-desorption isotherms for the prepared spinel ferrite nanoparticles and corresponding BJH pore size distributions.

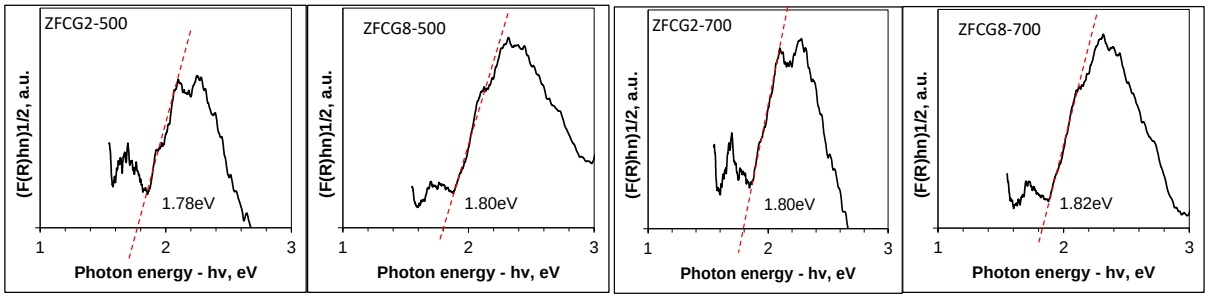

Fig. 3. Tauc plots and direct bandgap energies for the synthesized spinel ferrite samples.

Funding and acknowledgments

This work is part of the Joint Research Project AR-FRBCF-2020-2021, Romanian Academy – National Academy of Sciences of Belarus, Belarusian Republican Foundation for Fundamental Research.

References

1. P. Samoila, L. Sacarescu, A.I. Borhan, D. Timpu, M. Grigoras, N. Lupu, M. Zaltariov, V. Harabagiu, J. Mag. Magn. Mat. (2015) **378**, 92.
2. J. Angadi, B. Rudraswamy, K. Sadhana, S. Ramana Murthy, K. Praveena, J. All. Comp. (2015) **656**, 5.
3. A. Kumar, P.S. Rana, M.S. Yadav, R.P. Pant, Ceram. Int. (2015) **41**, 1297.

SYNTHESIS OF A HYDROGENATION CATALYST SUPPORT BASED ON ALUMINUM OXIDE

Yu.E. Romanenko*, *M.M. Klimushina*, *R.N. Rumyantsev

Romanenko@isuct.ru.
Ivanovo State University of Chemistry and Technology,
153000, Russian Federation, Ivanovo, Sheremetevsky ave., 7

γ-alumina is widely used in various industries as a desiccant, catalyst support, and a component of many catalysts. This is due to the high values of the specific surface area and strength of the granules, as well as their inertness. When obtaining a hydrogenation catalyst, γ-oxide is often supported by metals: platinum, copper, and nickel.

The aim of this work was the synthesis of hydrogenation catalyst support based on γ-alumina with high specific surface area, pore volume and granule strength.

In this work, the support was obtained by molding from hydrargillite $Al(OH)_3$, pseudoboehmite AlOOH, and γ-aluminum oxide γ-Al_2O_3 with a 20% nitric acid solution to a moisture content of 30÷50%. The resulting granules with a size of ~0.5 mm were dried for at least a day at room temperature and 8 hours at 100 °C. The dried granules were fired for 3 hours at a temperature of 500 °C with a heating rate of 3 °C/min.

Additives of starch and polyvinyl alcohol (PVA) were added to the molding mass in the amount of 5% by weight of dry matter to increase the porosity and strength of the granules. The additives affect the structure of the solvation shell of the dispersed phase and the structural and bulk mechanical properties.

The specific surface area and pore volume were determined using low-temperature nitrogen adsorption according to the BET method on the "Sorbi MS" hardware complex. Granules with additives of starch and PVA have pore volumes of 0.163 cm^3/g and 0.174 cm^3/g, respectively. The specific surface of the samples is given in Table 1.

Granules with a high specific surface area obtained from the coarse γ-Al2O3 fraction had low strength even with 5% polymer additions. On the contrary, the fine fraction had high strength and low specific surface area. The optimal support was

found to be a sample of a fine fraction of hydrargillite, whose strength was sufficient even without additives.

Table 1. Specific surface of the samples.

Starting compound		without additives	+ 5% starch	+ 5% PVA
γ-Al_2O_3	Fine fraction ~ 2 μm	208.9±3.3	167.9±1.5	176.5±1.1
	Coarse fraction ~ 30 μm	–	267.0±18.0	296.6±27.1
$Al(OH)_3$	Fine fraction ~ 2 μm	229.0 ± 5.1	209.7 ± 6.4	203.6 ± 6.0

The granules obtained from the pseudoboehmite and the coarse hydrargillite fraction fell apart during the drying process. The compressive strength of the remaining granules was measured on a balance by a static method. The results obtained for samples with sufficient strength are shown in Table 2.

Table 2. Compressive strength of samples, kg.

Starting compound		without additives	+ 5% starch	+ 5% PVA
Al_2O_3	Fine fraction ~ 2 μm	0.2±0.2	3.9±0.2	1.5±0.2
	Coarse fraction ~ 30 μm	–	0.5±0.2	0.4±0.2
$Al(OH)_3$	Fine fraction ~ 2 μm	1.2±0.2	1.1±0.2	0.7±0.2

Funding and acknowledgments

The study was supported by a grant from the Russian Science Foundation №21-73-10210, https://rscf.ru/project/21-73-10210/

The study was carried out using the resources of the Center for Shared Use of Scientific Equipment of the ISUCT (with the support of the Ministry of Science and Higher Education of Russia, grant No. 075-15-2021-671)

EXPERIMENTAL STUDY OF NITROGEN ADSORPTION ON ALUMINUM POWDER MODIFIED WITH COPPER FORMATE

A.V. Ryabina, V. G. Shevchenko, V.N. Krasilnikov

anna-ryabina@yandex.ru
Institute of Solid State Chemistry of the Ural Branch of the Russian Academy of Sciences, GSP-145. 620219 Yekaterinburg, Russia

In its pure form, aluminum has low strength characteristics and is used as the basis of structural materials in the form of alloys with other metals. In particular, with the addition of copper, the properties of aluminum change significantly: strength increases, plasticity remains [1]. Since, according to the state diagram, the maximum solubility of copper in a solid aluminum solution is slightly more than 4%, it is impractical to introduce copper in an amount greater than 4–5%. Copper formates can be used to obtain copper powders or copper coatings on the surface of metals and oxides. When they are thermally decomposed, metallic copper is formed at the temperatures of 220–2500 °C [2].

The objects of the experimental study were the aluminum powder of the ASD-4 brand, obtained by spraying molten metal with nitrogen, with an active metal content of 98.7±0.5%, and the ASD-4 powder impregnated with copper formate in a concentration of 1, 2, 3, 5% by weight. Adsorption measurements were carried out on the Gemini VII 2390 adsorption analyzer (USA), the principle of operation of which is based on the adsorption and desorption of gas on the external and internal surfaces (in the pores) of the studied samples of dispersed and porous substances and materials at the temperature of liquid nitrogen. The adsorption isotherms were measured, and the specific surface area and porosity of the powders were calculated. The results of the morphology study are presented. The average adsorption and desorption diameters of the pores and the differential distribution of the mesopore volume by diameter were calculated using the Barrett-Joyner-Halenda (BJH) method. The analysis of the porosity of materials by adsorption isotherms was based on the accepted interpretation of capillary condensation and evaporation mechanisms and related hysteresis phenomena [3]. According to the experiment, with an increase in the concentration of copper formate in the samples, the specific surface area increases, mesopores are

formed. Thus, for the sample ASD-4-1% Cu, the specific surface area was 0.9331 m^2/g, for the sample ASD-4-5%Cu – 12 m^2/g. The average pore diameter is 50Å. It was shown that the type of hysteresis loop formed by adsorption/desorption isotherms was determined by various mechanisms of condensation and evaporation and depended on the shape and size of the pores. The isotherms of samples with a copper formate content of 3, 5% are characterized by a vertical adsorption branch near the saturation pressure and a steep desorption branch in the region of intermediate pressures (P/P_0 =0.4–0.5). According to the De Boer classification, hysteresis loops of this form are typical for samples containing a certain number of micropores. Thus, the area of micropores calculated by the Garkins-Yura method was 1.3084 m^2/g for the ASD-4 sample of 5% Cu. The stepped shape of the hysteresis loop with a closing point in the range from $P/P_0 \approx 0.49$ to ≈ 0.47 may also indicate cavitation evaporation. The differential distribution of the pore volume over the effective diameters is characterized by one clear peak for the ASD-4 samples with 3, 5% Cu. A polymodal distribution was found for the ASD-4 samples with 1, 2% Cu. Since the activity and selectivity of the adsorbent affect both the dynamics and the rate of adsorption processes, knowledge of the structure of the adsorbent, the chemical nature of its surface, as well as the nature of the absorbed substance, contributes to more efficient use and expansion of their practical applications.

Funding and acknowledgments

The work was performed in accordance with the state task AAAA-A19-119031890028-0.

References

1. V.S. Zolotorevsky, N. A. Belov. Technology of light-metal alloy (Technologiya legkih splavov), 1997, No. 4, 20. (*in Russian*)
2. V. Rosenband, A. Gany. J. Mater. Process. Techn. (2004), **153–154**, 1058.
3. Greg S., Sing K. Adsorption, surface area, porosity. Academic Press; 1st Edition, 1967, 371p.

ADSORPTION IN CATALYTIC PROCESSES WITH THE PARTICIPATION OF HYDROGEN-CONTAINING GASES

Prozorov D.A.*, *Afineevskii A.V.*, *Smirnov D.V.

prozorovda@mail.ru
ISUCT, 153000 Ivanovo, Russia

Hydrogenation of various classes of organic compounds is an obligatory stage in the main large-scale chemical industries. Knowledge and the ability to control the regularities of hydrogen adsorption on transition metals will allow one to understand the mechanisms of catalytic processes and create catalytic systems with predictable performance properties (activity, selectivity, stability of operation). Processes of different nature with the participation of hydrogen proceed under different conditions (pressure, temperature), while transition metals, most often nickel, cobalt, molybdenum, and copper, are used as catalysts. Methods for the synthesis of catalytic systems for processes such as methanation, hydrogenation, methanol synthesis, natural gas conversion, hydrofining of light oil products, etc., have a number of stages of the same type (sometimes their different sequence). The listed facts allow us to assert that the determining factor in the operation of a catalyst in a particular process is precisely the regularities of the adsorption of reactants. In this case, it is advisable for the reduction processes to consider the adsorption of hydrogen primarily; it is known that a completely dehydrogenated catalyst completely and often irrevocably loses its activity.

The aim of this work was to study the hydrogen adsorption properties of bulk and supported catalysts for methanation, hydrogenation, methanol synthesis, and hydrofining of light petroleum products, including industrial samples.

Skeletal nickel, skeletal copper, methanol synthesis catalyst (Cu 54.95 wt.%; Zn 21.96 wt.%; O 19.75 wt.%; Al 2.9 wt.%; Mg 0.43 wt%) were used as samples of bulk catalysts. γ-Al2O3 with a specific surface area of 294 $m^2 \cdot g^{-1}$ was used as a substrate for the supported catalysts under study, including industrial samples.

The adsorption properties of the catalyst were studied using a complex for simultaneous thermal analysis and mass spectrometry, which includes: a STA 449 F3 Jupiter® NETZSCH synchronous thermal analysis device and a QMS 403 C Aëolos®

mass spectrometer, a PulseTA® reaction gas dosing system, an evacuation system, and high-temperature furnace and sensor for STA 449 F3 Jupiter®. The analysis of catalyst samples was carried out at temperatures from 30 to 950 °C in an argon atmosphere.

The reduction of the catalysts was carried out in a stream of hydrogen under industrial conditions. Conditions for simultaneous thermal analysis and mass spectrometric analysis: heating rate 5 °C per min, ionization current 70 V, measurement resolution 5 pcs per s. The data on the molecular weights of the fragments were taken from the NIST international database.

The data obtained make it possible to assert that molecular forms of hydrogen leave the surface of all catalytic systems already at room temperature; the maximum temperature of hydrogen desorption was observed at a temperature of 850 °C on an industrial sample of a methanation catalyst. The complex of the obtained data confirms the idea of the existence of the most reactive form of adsorbed hydrogen for each specific reaction.

Funding and acknowledgments

This work was supported by a grant from the Russian Science Foundation No. 21-73-10210.

STUDY OF THE INFLUENCE OF MgCo/AlFe-LDH SYNTHESIS METHODS ON THE CHANGE OF SORPTION PROPERTIES

***Nestroinaia O.V.*[1], *Goncharov I.Yu.*[2], *Lebedeva O.E.*[1]**

nestroynaya91@gmail.com
Belgorod State University, 308015, Belgorod, Russia
[2] *CCP "Technologies and Materials of "BelSU",308033, Belgorod, Russia*

In recent years, sorption-active materials with magnetic properties have been of particular interest to researchers. Basically, magnetic sorbents are used for water purification from pollutants of various nature [1]. The increased interest in magnetic materials is due to the possibility of using magnetic separation to remove the sorbent.

The present work is devoted to the study of the influence of the conditions for the synthesis of magnetic materials based on layered double hydroxides on their physicochemical and sorption properties.

Layered double hydroxides (LDH) are a class of natural and synthetic layered materials with high sorption activity with respect to organic and inorganic anions [2,3], as well as to metal cations [4,5].

The synthesis of samples of layered double hydroxides of the composition $Mg_{5.7}Co_{0.3}Al_{1.7}Fe_{0.3}(OH)_{16}CO_3$ $4H_2O$ was carried out by different methods: by coprecipitation at variable pH with different deposition rates (2,5; 4 и 15 ml/min) (MgCo/AlMg-c-2,5; MgCo/AlMg-c-4; MgCo/AlMg-c-15), by coprecipitation followed by microwave treatment (MgCo/AlMg-mw) and coprecipitation with hydrothermal treatment (MgCo/AlMg-ht).

The samples were studied in detail using a complex of methods of physical and chemical analysis. The MgCo/AlMg-c-2,5 sample was subjected to heat treatment (MgCo/AlMg-ox) in a muffle furnace for 2 hours at 600°C in an air atmosphere.

According to X-ray diffractograms, all samples have a highly crystalline structure characteristic of the LDH class. For all materials, the presence of an extraneous phase was recorded, which presumably represents $CoFe_2O_4$ spinel. TEM micrographs of all samples show both the presence of hexagonal scales, typical of layered double hydroxides and elongated aggregates of lamellar particles, as well as crystals of a different shape, which are most likely the spinel phase.

The values of the texture characteristics of the sorbents are presented in Table 1. At room temperature, the samples exhibit magnetic properties. The values of magnetization in a saturated magnetic field for materials are approximately the same and vary in the range from 2 to 6 emu/g.

Table 1. Textural characteristics of synthesized materials

Sample	Specific surface area, m^2/g	Pore volume, cm^3/g	Average pore size, A
MgCo/AlFe-c-2,5	28.29	0.0840	118.198
MgCo/AlFe-c-4	43.1845	0.1653	145.519
MgCo/AlFe-c-15	55.90990	0.18312	115.923
MgCo/AlFe-mw	47.3658	0.15899	130.042
MgCo/AlFe-hd	48,9039	0.2684	296.008
MgCo/AlFe-ox	75.3759	0.394463	210.130

The sorption capacity of the samples was studied with respect to the congo red anionic dye at two temperatures (25 and 35 ° C). Sorption capacity was also studied for the MgCo/AlMg-ox sample after the sorption-thermal regeneration cycle at 600 °C.

The maximum sorption rate at 25 °C has a sample obtained by the method of coprecipitation deposition with hydrothermal treatment (Fig. 1). According to the data obtained, the sorption equilibrium for the Congo red dye is reached on the MgCo/AlMg-hd sample after 60 minutes, and for other samples, it takes longer – from 360 to 480 minutes. When the temperature rises to 35°C, the sorption equilibrium for the dye is reached from 40 to 200 minutes.

Isotherms of sorption of Congo red by synthesized materials are constructed (Fig.2). The isotherms for all samples are similar, and they can be attributed to type IV (according to the BDDT classification), which characterizes the samples as mesoporous bodies [6]. The sorption capacities of the samples differ insignificantly. The Langmuir model well describes the sorption isotherms for all samples in a given concentration range.

After sorption, a decrease in crystallinity was recorded for all samples, which is most likely due to the gradual destruction of the LDH structure and partial introduction of the dye into the interlayer space (Fig.3).

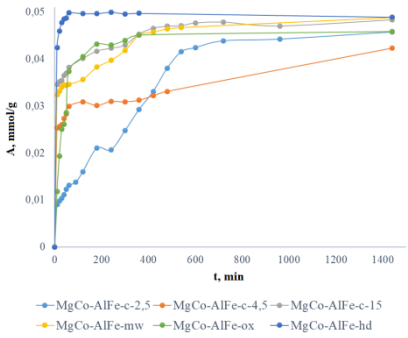

Fig. 1. Kinetic curves of congo red sorption on synthesized materials

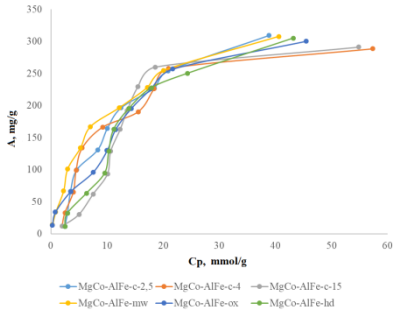

Fig. 2. Isotherm of sorption of congo red on synthesized materials

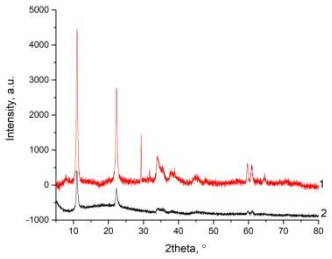

Fig. 3. X-ray powder diffractograms of the MgCo/AlMg -hd sample before (1) and after (2) sorption

Funding and acknowledgments

The work was carried out within the framework of the RFBR grant No. 18-29-12103 mk.

References

1. Ruthiraan M., Mubarak M.N., Abdullah E.C., Khalid M., Nizamuddin S., Walvekar R., Karri R.R. An *Magnetic Nanostructures. Nanotechnology in the Life Sciences.* Springer, Cham. (2019), 131.

2. Chaara, D., Pavlovic, I., Bruna, F., Ulibarri, M.A., Draoui, K., Barriga, C., Appl. Clay Sci. (2010) **50**, 292.

3. Koilraj P., Sasaki K. J. Environ. Chem. Eng. (2016) **4.** I. 1. 984.

4. Lei, C., Zhu, X., Zhu, B., Jiang, C., Le, Y., & Yu, J. J Hazard Mater. (2017). **321,** 801.

5. Ryltsova I.G., Piskareva V.A., Vorontsova O.A., Lebedeva O.E. Butlerovskie soobsheniia. (2016) **48,** 77.

6. Greg S., Sing K. Adsorption, specific surface area, porosity. Translated from the English 2nd ed. Moscow, Mir.1984. 306 c.

THE STUDY OF Si DISTRIBUTION IN THE SAPO-11 STRUCTURE: COMBINING SIMULATION AND EXPERIMENTAL ADSORPTION METHODS

I.V. Grenev [1,2], V.Yu. Gavrilov [1]

greneviv@catalysis.ru
[1]Boreskov Institute of Catalysis SB RAS, 5 Lavrentieva St., Novosibirsk 630090, Russia
[2] Novosibirsk State University, 1 Pirogova St., Novosibirsk 630090, Russia

Microporous crystalline silicoaluminophosphate molecular sieves (SAPOs) are of great interest both for academic studies and industrial applications due to the presence of ordered molecular-size microchannels and the diversity of their topology and chemical composition. SAPO-n are widely applied in catalytic and membrane technologies. Crystalline silicoaluminophosphates are often called zeolite-like materials due to the primary structural unit of SAPO-n is a tetrahedral complex, in which the T-atom (Si^{4+}, Al^{3+} or P^{5+}) is located in the center, and four oxygen atoms are located in the vertices. Partial isomorphous substitution of T-atoms (Al or P atoms) for Si atoms changes the chemical composition of these microporous materials making it possible to vary their acid, ion-exchange and catalytic properties.

There are several isomorphous substitution mechanisms of T-atoms in the SAPO framework for Si atoms [1]: substitution of an aluminum atom for a silicon atom (SM1), the substitution of a phosphorus atom for silicon and a proton (SM2), substitution of adjacent atoms of aluminum and phosphorus by two atoms silicon (SM3). The information about the concentration and the distribution type of Si in the SAPO-n framework can be obtained using a combination of experimental physicochemical characterizing methods. For example, determination of the silicon fraction with different local environments (^{29}Si MAS NMR), determination of the number and strength of acid sites (TPD of ammonia), determination of the bulk chemical composition (ICP-AES), determination of the surface chemical composition (XPS). However, all these methods give only bulk results and cannot allow distinguishing Si in the SAPO framework from Si in amorphous SiO_2.

In this work, it is shown that the hydrogen adsorption at 77 K in the low-pressure range in the microporous SAPO-11 is sensitive not only to the Si concentration but

also to the Si distribution in the structure. We considered models of the “isolated” type of Si distribution, formed only by the substitution mechanism SM2, for cases of 1, 2, and 3 Si atoms per SAPO-11 unit cell and the model of “island” type of Si distribution formed by a combination of substitution mechanisms SM2 and SM3 for 5 Si atoms per unit cell. At the first stage, the geometry optimization and the energy calculation of the obtained structures was carried out by the molecular modeling method. The obtained results were refined by the DFT method for the most stable structures. The Henry constants of H_2 adsorption were calculated by the Monte Carlo simulation method for the most probable structures. It is shown that Henry's constants increase with an increase in the Si concentration per unit cell substituted by SM2 and practically do not depend on the Si concentration per unit cell substituted by SM3. The dependence of Henry's constants on the Si concentration per unit cell of SAPO-11 substituted by SM2 was calculated (Fig. 1). The obtained result can be used to solve the inverse problem of determining the Si concentration substituted by SM2 from experimental H_2 adsorption data at 77 K in SAPO-11.

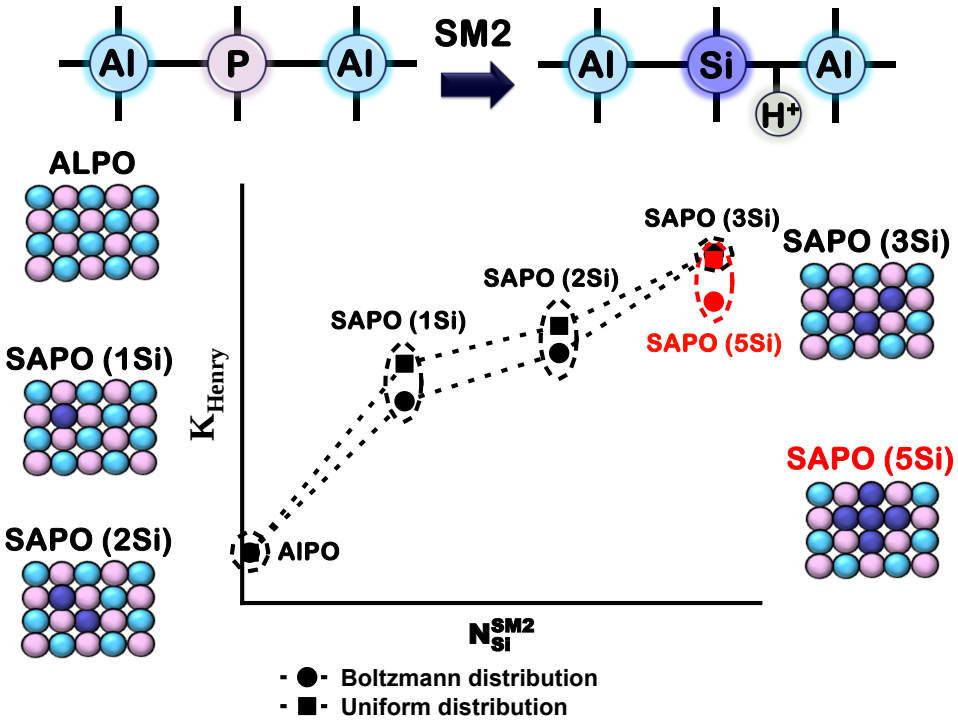

Fig. 1. Schematic representation of the dependence of Henry's constants on the silicon concentration substituted by SM2 per unit cell of SAPO-11.

The work also demonstrates the practical application of the obtained dependence for determining the silicon concentration substituted by SM2 for 3 samples of SAPO-11 with different bulk Si concentration. The advantages of combining the proposed adsorption-based method with experimental physicochemical methods for determining the surface chemical composition, the bulk chemical composition, and determination of the number of acid sites are shown. The proposed approach can be adapted for any other heteroatom-containing aluminophosphate molecular sieves and can be applied to aluminosilicate zeolites.

Funding

The reported study was funded by RFBR and the Government of the Novosibirsk Region according to the research project 19-43-543039.

References

1. Sastre G., Lewis D.W., Catlow C.R.A. Structure and Stability of Silica Species in SAPO Molecular Sieves. The Journal of Physical Chemistry (1996) **100**, 6722.

ADSORPTION OF 137Cs AND 90Sr RADIONUCLIDES FROM ELECTROLYTES SOLUTIONS BY COMPOSITE Zr-Ca-Mg PHOSPHATES

A.I. Ivanets[1], N.V. Kitikova[1], I.L. Shashkova[1], V.V. Milyutin[2], N.A. Nekrasova[2]

Andreiivanets@yandex.ru

[1] Institute of General and Inorganic Chemistry of National Academy of Sciences of Belarus, 220072 Minsk, Belarus

[2] A.N. Frumkin Institute of Physical Chemistry and Electrochemistry of the Russian Academy of Sciences, 199071 Moscow, Russia

Inorganic adsorbents are widely used for the selective removal of long-lived ^{137}Cs and ^{90}Sr radionuclides from liquid radioactive waste. Zirconium phosphates are a well-studied class of inorganic ion exchangers characterized by high affinity for ^{137}Cs and ^{90}Sr radionuclides [1]. Sodium-zirconium phosphates $NaZr_2P_3O_{12}$ and calcium-zirconium phosphates $CaZr_4P_6O_{24}$, also known as NZP materials, are promising matrices for the long-lived radionuclides immobilization [2].

The purpose of this work is to develop a heterogeneous method for the synthesis of composite Zr-Ca-Mg phosphates and to study their adsorption characteristics to 137Cs and 90Sr radionuclides in the presence of electrolytes. The relevance of the work is due to the possibility of subsequent immobilization of radionuclides into solid-state NZP matrices by heat treatment of spent adsorbents [3].

Samples of phosphatized dolomite $Ca_{0.7}Mg_{0.3}HPO_4 \cdot 2H_2O$ (PD-1) and Ca2.65Mg3 $Ca_{2.65}Mg_3(NH_4)_{1.3}(PO_4)_4(CO_3)_{0.3} \cdot 6H_2O$ (PD-2) were used for the synthesis of composite Zr-Ca-Mg phosphates by their heterogeneous interaction with a given volume of 2.0 wt. % $ZrO(NO_3)_2$ aqueous solution. The ratio of $ZrO(NO_3)_2$ /PD-1(PD-2) was 2.2 and 6.6 mmol/g for PD-1 (PD-2)-2 and PD-1 (PD-2)-4 samples, respectively. The adsorption characteristics of the samples were determined under static conditions by continuously mixing a sample of 0.1±0.0001 g of adsorbent with 20.0 cm^3 of the solution for 24 h. The following solutions were used as the liquid phase during ^{137}Cs adsorption: 0.1 and 1.0 mol/dm^3 $NaNO_3$, pH 6.0; tap water of Moscow city the following composition, mg/dm^3: Na^+- 6–8; K^+- 4–5; Mg^{2+} - 15–17; Ca^{2+} - 52–56; Cl^- - 6–8; SO_4^{2-} - 36–38; HCO_3^- - 200–205; total salinity - 310–330; total hardness – 3.6–3.8 mg-eq/dm^3, pH 7.6; and seawater sampled from Sevastopol Bay of

the Black Sea (total salinity – 21.2 g/dm^3, pH 7.8). During ^{90}Sr adsorption, the following model solutions were used: 0.1 mol/dm^3 $NaNO_3$, pH 6.0; 0.01 mol/dm^3 $CaCl_2$, pH 6.0, as well as tap water and seawater of the above composition.

All synthesized adsorbents are mesoporous, differing in specific surface area, volume, and pore size depending on the composition (Table 1). The highest values of the specific surface area of ~80-86 m^2/g and the total pore volume of ~0.166-0.208 cm^3/g are characterized by PD-1-2 and PD-2-2 samples with the lowest zirconium content. At the same time, the average pore size varies slightly from 7.6 to 11.2 nm.

Table 1 – Texture characteristics and chemical composition of adsorbents.

Sample	$A_{sp.}$, m^2/g	$V_{des.}$, cm^3/g	$D_{av.}$, nm	Chemical composition (EDX analysis), at. %				
				Ca	Mg	Zr	P	O
PD-1-2	80	0.166	7.6	6.0	2.5	7.8	12.9	70.8
PD-1-4	29	0.082	9.3	0.7	0.4	15.1	12.7	71.1
PD-2-2	86	0.208	8.1	5.5	8.7	3.6	13.5	68.7
PD-2-4	21	0.075	11.2	1.3	1.4	15.2	12.4	70.0

The selective properties of composite phosphates to ^{90}Sr and ^{137}Cs radionuclides in various salt solutions are presented in Table 2.

Table 2 – Distribution coefficient values (K_d) ^{90}Sr and ^{137}Cs on various adsorbents during adsorption from model solutions.

Sample	K_d values, cm^3/g in solution:			
	0.01 mol/dm^3 $CaCl_2$	0.1 mol/dm^3 $NaNO_3$	Tap water	Seawater
^{90}Sr				
PD-1-2	1.1×10^3	1.5×10^3	4.0×10^3	275
PD-1-4	195	180	1.5×10^3	24
PD-2-2	1.7×10^3	4.1×10^3	4.9×10^3	540
PD-2-4	820	1.5×10^3	2.4×10^3	150
^{137}Cs				
PD-1-2	6070	280	4050	1950
PD-1-4	5200	498	2.2×10^4	1350
PD-2-2	920	22	430	141
PD-2-4	980	118	1260	363

The values of the ^{90}Sr distribution coefficients (K_d) for all adsorbents have sufficiently high values when using tap water and 0.1 M $NaNO_3$ solution as background solutions, while the sorbents PD-1-2 and PD-2-2 are not inferior to known natural and synthetic adsorbents. In calcium-containing solutions, the values of K_d ^{90}Sr decrease on all the studied adsorbents, while the adsorbents with the highest Ca and Mg content (PD-1-2 and PD-2-2) demonstrate the best selective properties.

Comparative studies of a number of commercially available adsorbents with synthesized Zr-Ca-Mg phosphates have been carried out. Thus, for most adsorbents, K_d ^{137}Cs decreases with increasing total salinity in the series tap water > 0.1 M $NaNO_3$ > seawater > 1.0 M $NaNO_3$. The highest K_d values are characterized by samples based on Ca-Mg hydrogen phosphates (PD-1-2 and PD-1-4), which are noticeably inferior only to ferrocyanides-containing adsorbents and titanosilicates.

Thus, the composite adsorbents based on mixed Zr-Ca-Mg phosphates (PD-1-2 and PD-1-4) can be used for effective ^{137}Cs and ^{90}Sr radionuclides removal in one stage with K_d from 1.5×10^3 up to 2.2×10^4 cm^3/g.

Funding and acknowledgments

The work was carried out with the financial support of the BRFFI (grant X20MC-022).

References

1. Maslova M.V., Gerasimova L.G., Motina N.V., 2008. Sorption of Cs^+ and Sr^{2+} by ion exchanger based on titanium phosphate. Russ. J. Appl. Chem. (2008) **81**, 771.
2. Orlova A.I., Volgutov V.Yu., Mikhailov D.A. et al., 2014. Phosphate $Ca_{1/4}Sr_{1/4}Zr_2(PO_4)_3$ of the $NaZr_2(PO_4)_3$ structure type: Synthesis of a dense ceramic material and its radiation testing. J. Nucl. Mater. (2014) **446**, 232.
3. Ivanets A., Shashkova I., Kitikova N. et. al., 2021. Facile synthesis of calcium magnesium zirconium phosphate adsorbents transformed into $MZr_4P_6O_{24}$ (M: Ca, Mg) ceramic matrix for radionuclides immobilization. Separ. Pur. Technol. (2021) **272**, 118912.

UV DECOLORIZATION OF NITROPHENOL AND METHYL ORANGE SOLUTIONS WITH TITANIUM DIOXIDE DOPED BY Co, Rh, Ir IONS

***I.I. Mikhalenko*, D.A. Zaev**

mikhalenko_ii@pfur.ru
Department of Physical and Colloidal Chemistry, RUDN-University,
117198 Moscow, Russia

Many works have been devoted to the study of the photocatalytic properties of titanium dioxide with various additives and the number of which continues to increase. Based on TiO_2 technologies, industrial methods for water and air purification using UV and visible range radiation have been created. The introduction of additives changes the course of the main stage of photo-stimulated processes (the absorption of a quantum of light and the appearance of electron-hole pairs), which is important for the adsorption and light driven reactivity of the reactants.

This work aims to determine the effect of Co^{+2}, Rh^{+3} and Ir^{+3} ions presence on the surface of anatase and TiO_2 xerogel powders on the rate of photodecolorization of aqueous solutions of methyl orange and 4-nitrophenol anions as model pollutants.

Anatase (Aldrich, USA, ≥ 99%) and amorphous xerogel obtained from organogel (ACROS Organics $C_{16}H_{36}O_4Ti$, $C_6H_{14}O_4$, n-butanol) were dried at 120 ^{0}C and kept for 24 h in solutions of cobalt, rhodium, and iridium chlorides with salt`s content corresponded to atomic ratio M:Ti = 1:1000 in case of mono, binary and ternary modifiers M. The control sample was kept in water. Then the powders were calcined for 3 h at 450^{0}C. Photodecolorization (PDC) of tested substances was controlled by photometric method at the maxima of 465 nm (MO) and 403 nm (4NP). The dependences of the decrease in the optical absorption of solutions on the UV irradiation time t* (Hg-lamp 350) were represented as PDC degree β–t* or n–t* (Fig.1). Initial photoactivity as PDC rate, normalized by t*=1 min (W_1), was calculated via bilogarithmic anamorphose of n–t* plot. A linear increase of the extinction E_{4NP} with an t* increase was observed in homogeneous system due to 4NP dimers splitting and this fact was taken into account in calculation of the number of moles (n) of photo degraded 4NP ions. The photoactivity testing data were added by the analysis of the IR spectra and SEM data of the samples.

(a) M/xerogel TiO_2 ***(b)*** M/anatase

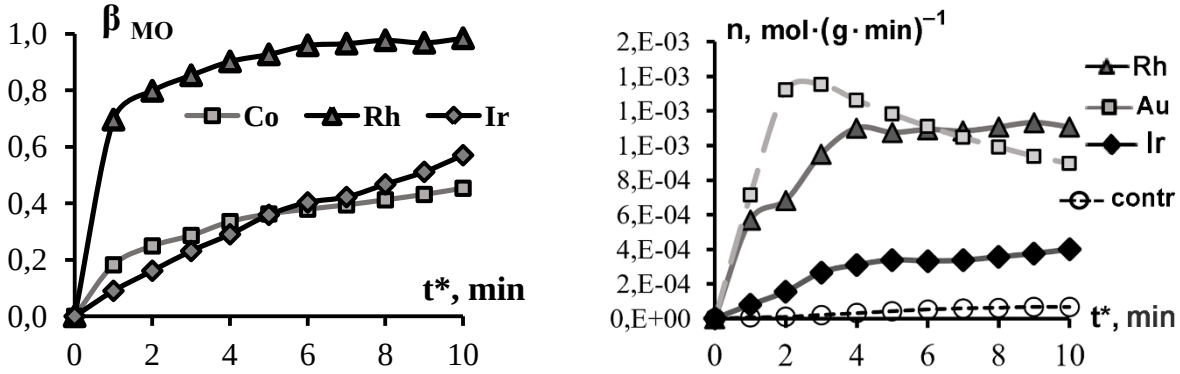

Fig.1. The effect of the duration of UV irradiation on the photodegradation of MO (*a*) and 4NP (*b*) in an aqueous solution

Among M^{+n} modifiers, rhodium ion is the most active (Fig. 1, Table 1,2), and it is not inferior to Au^{+3}. In MO photodegradation kinetics, the activity of Rh^{+3}/ xerogel TiO_2 is 2 times higher than that of Au^{+3} (W_1= 0.055 $g^{-1}\cdot min^{-1}$). Note, photo decolorization of 4NP ions does not decrease with irradiation time t* increasing, as in the case of Au^{+3} and Co^{+2}.

Table 1. Photo degradation rates W_1 ($g^{-1}\cdot min^{-1}$) for Methyl Orange solution with xerogel powders M^{+n}/TiO_2

MO solution	without **M**	**Co**	**Rh**	**Ir**
0.013	0.037	0.036	**0.108**	0.029

Table 2. Photo degradation rates for 4NP anions with M^{+n}/anatase powders W_1, $mmol\cdot g^{-1}\cdot min^{-1}$

Без M	**Co**	**Rh**	**Ir**	**Co : Rh**			**Co : Ir**			**Rh:Co:Ir**		
				1:3	2:2	3:1	1:3	2:2	3:1	1:1:2	1:2:1	2:1:1
0.007	-0.02	**0.18**	0.07	**36.9**	8.1	10.5	14.4	11.9	9.9	10.8	8.3	**12.4**

Mono-additives in M^{+n}/anatase samples are not active in 4NP photodecolorization compared to the double and ternary modifiers (Table 2), the composition of which affects the TiO_2 photoactivity. The best are CoRh and CoIr pairs with a 3-fold excess of platinum metal ions and RhCoIr with an atomic element ratio of 2Rh : 1Co : 1Ir. So, the efficiency of titania surface doping by cations with an increase of photoactivity in a row $Co^{+2} < Ir^{+3} < Rh^{+3}$ is shown, and it can be enhanced by a combination of ions with the greater activity for the samples with a higher rhodium content.

INFLUENCE OF MICROWAVE TREATMENT ON THE ADSORPTION CAPACITY OF ALZR(YB) OXIDE POWDERS WITH POLYMER

N.E. Vakhrushev [1], ***I.I. Mikhalenko*** [2], ***A.A. Ilyicheva*** [1], ***L.I. Podzorova*** [1]

mikhalenko_ii@pfur.ru
[1]*Institute of Metallurgy and Materials Science, Russian Academy of Sciences, 119334 Moscow, Russia*
[2]*Peoples' Friendship University of Russia (RUDN University), 117198 Moscow, Russia*

AlZr-xerogels, which are precursors of alumina ceramics, attract attention as environmentally friendly materials with high sorption properties. An important step in the sol-gel technology of oxide ceramics preparation is the primary heat treatment (hydrogel drying), because of the great influence of its conditions on the texture and morphology of the material after calcination. In order to obtain a high specific surface area after high-temperature treatments and other optimal performance of the Al_2O_3-$ZrO_2(Yb_2O_3)$ system, a polymer structure-forming agent is added into the sol-gel synthesis in which the traditional drying stage at 180^oC is 2-3 h of duration [1].

The aim of this work is to compare mixed alumina-zirconia oxides prepared by the sol-gel method at 10^0C and subsequent long thermal (1) or rapid microwave drying (2) of the hydrogel with and without xerogel calcination in terms of specific surface area, porosity, and adsorption of test pollutants – methyl orange and dichromate ions.

The hydrogels were synthesized by the hydrolysis-condensation reaction by reverse precipitation of salts ($Al(NO_3)_3•9H_2O$; $ZrOCl_2•8H_2O$; $Yb(NO_3)_3•5{,}44H_2O$) with ammonia solution and surfactant-polymer addition ($NH_3•H_2O$; polyvinylpyrrolidone PVP) for 1 h at 10^oC sol-gel synthesis temperature. The salt suspensions corresponded to molar percentages of $35\%Al_2O_3$-$65\%ZrO_2(3\%Yb_2O_3)$-PVP. One part of the hydrogel (1) was subjected to ordinary drying (180^oC; 2 h) and the other (2) to microwave drying (W = 600W, 6 min). All samples were then calcined for 1 h at 500^oC.

The specific surface area and porosity of the obtained materials were analyzed (Tristar-3000). The adsorption capacity of two series of samples was compared in steady-state and kinetic mode by values of the degree of substance extraction (1), Gibbs adsorption per unit mass of sorbent G_m (2), and per unit surface G_S (3) using

spectrophotometry (EcoView UV-Vis 1200). The analytical wavelength, extinction and concentration of sorbate anions were 462 nm; 18800 cmM-1; 0.075 mM for methyl orange (MO) and 368 nm; 4890 cmM^{-1}; 0.330 mM for potassium dichromate (DCH).

The xerogels had a mesoporous structure (Table 1). The samples with microwave drying were of the same pore diameter 3 and 6 nm respectively before and after calcination at 500^0C. The specific surface area of the material after microwave treatment was 3.5 times less than that of sample 1, implying that the structure of xerogels 1 and 2 differed at the stage of their primary dehydration. The calcination of sample 1 resulted in a surface reduction of 2.4 times, while the surface of sample 2 remained practically unchanged. The texture and particle shape of the microwave dried samples differ when compared to control sample 1 (SEM data).

Table 1. Specific surface area and porosity of powders AlZr(Yb)-PVP

1	S_{BET}, m^2/g	V_{pores}, cm^3/g	d_{pores}, nm	2	S_{BET}, m^2/g	V_{pores}, cm^3/g	d_{pores}, nm
180°C	427	0,326	3	MW	125	0,085	3
500°C	176	0,242	6	500°C	131	0,162	5

Despite the reduced specific surface area of the microwave treated samples, their adsorption characteristics, investigated under the same conditions, are no worse and, for MO, even better than those of the samples dried at 180^0C.

Table 2. Adsorption of methyl orange (MO) and dichromate ions (DCR), where β in %; G_m in μmole/g, G_S in μmole/m^2 (adsorption time – 24h, 25 ^{0}C)

Способ	Drying				After calcination (500°C)					
	MO		DCR		MO			DCR		
	β	G_m	β	G_m	β	G_m	G_S	β	G_m	G_S
1. 180^0	62	11,6	70	114	76	14,2	81	71	119	0,675
2. MW	75	13,9	70	114	85	15,9	121	79	129	0,870

The kinetic dependences of adsorption of test molecules (Fig. 1) are non-linear and correspond to fast and slow adsorption stages. The rates of W_0 (at t=0) and W respectively can be calculated from linear regression $G_m = W_0 + W \cdot t$. The ratio W_0/W shows the heterogeneity of the adsorption sites of the complex Al-Zr oxide sorbent.

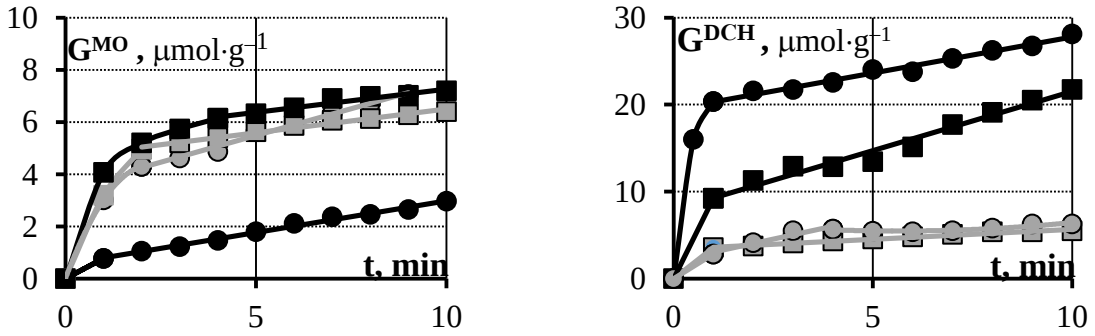

Figure 1. Adsorption kinetics for the dye methyl orange and dichromate ions on AlZr(Yb) sorbents after heat treatment at 180 °C (●), microwave drying (■), and the same samples after calcination at 500 °C (● and ■).

The data in Table 3 show that sample 1 loses its activity with respect to the adsorption of MO after calcination: the rates of W_0 and W decrease by a factor of 7 and 2, whereas in the sample with microwave drying W_0 increases, and W does not change. The W_0/W ratio is significantly higher for the microwave-treated sample.

Table 3. Adsorption rates (min^{-1})

Sorbate	Methyl orange				Dichromate ion			
Sample	1	2	1-500	2- 500	1	2	1-500	2- 500
W_0	3.3	4.7	0.5	5.5	2.0	3.4	19.5	8
W	0.4	0.2	0.2	0.2	1.0	0.2	0.8	1.4
W_0/W	8	26	2.5	28	2	17	24	6

The same result is observed qualitatively for the adsorption of dichromate ions but with a more significant increase in the sorbent activity when using microwave drying.

Thus it is possible to recommend microwave treatment before calcination of mixed oxide material in the technological process of AlZr(Yb)-PVP nanopowders production at low sol-gel synthesis temperature.

Funding and acknowledgments

This work is carried out as a part of collaboration between RUDN and the Institute of Metallurgy and Materials Science RAS according to the Plan of the Adsorption Phenomena section of the RAS Research Council on Physical Chemistry 2021, V.1 2.15.1.T, No. 21-03-60–01.

References

1. A.A. Ilyicheva, M. Do, N.A. Mikhailina, I.I. Mikhalenko, L.I. Podzorova, S.V. Kutsev. V All-Russian Conference on Nanomaterials - Moscow: IMET RAS, 2013, p.520.

HIGHLY SELECTIVE SORPTION OF BIOLOGICALLY ACTIVE SUBSTANCES BY MOLECULAR IMPRINTED POLYMER SORBENTS

I.S. Garkushina

irin-g16@yandex.ru
Institute of Macromolecular Compounds of the Russian Academy of Sciences, 199004 St. Petersburg, Russia

According to the classification, highly selective polymeric sorbents as chromatographic carriers for the sorption of biologically active substances are subdivided by shape, divided into a block, monolithic, and granular. The selectivity of sorbents is primarily due to the synthesis method, for example, molecular imprinting. The essence of the molecular imprinting method lies in the self-organization of functional monomers around the target molecule (template).

The study of the sorption of the target object (erythromycin) by molecularly imprinted polymer-carriers (MIPs) based on methacrylic acid, ethylene glycol dimethacrylate, and erythromycin methacrylate and synthesized in the form of a block with subsequent fractionation showed selective polyfunctional binding of the antibacterial antibiotic erythromycin. However, a large contribution of nonspecific binding was established due to the carboxyl groups of methacrylic acid and the hydrophobic polymer matrix [1]. To minimize nonspecific binding and, accordingly, increase the selectivity of sorbents, methacrylic acid was replaced by 2-hydroxyethyl methacrylate, which lacks ionic functional groups, and the presence of hydroxyl groups promotes the hydrophilization of the polymer matrix [2]. The ionic strength of the external solution did not affect the sorption of erythromycin by the hydrophilic MIPs, in contrast to the sorption on the control polymer. Therefore, it was carried out with the prevalence of non-ionic, in particular, hydrophobic interactions. A comparative study of the equilibrium and kinetics of sorption of erythromycin by synthesized sorbents shows that the equilibrium sorption capacity of hydrophilic MIPs for erythromycin exceeds those for hydrophobic MIPs, even though functional groups in polymers are located not only at imprint sites [3]. The kinetics of sorption of erythromycin on all studied sorbents was limited by internal diffusion, and the

effective diffusion coefficients increased with an increase of the erythromycin amount introduced during the synthesis.

Monoliths traditionally have a prevailing contribution of convective mass transfer to the total sorption rate. The frontal sorption of erythromycin occurs not only in the interglobular space in the macropores but also in the intraglobular space due to the diffusion of small target molecules into the polymer matrix [4]. The flow rate of the mobile phase influenced the mass transfer of erythromycin molecules in the imprinted polymer matrix both during convection and diffusional mass transfer, in contrast to the control polymer (CP), in which the effect of the flow rate is traced only during diffusional mass transfer. Moreover, the imprinting of a polymer matrix by erythromycin molecules, regardless of the shape (architecture) of the sorbent, leads to the implementation of a quasi-equilibrium mode of sorption from a constantly renewed solution [5].

The study of the frontal sorption of uremic toxin (uric acid) on a granular MIP based on 2-hydroxyethyl methacrylate and ethylene glycol dimethacrylate also showed the implementation of the selective process in a more regular mode as compared to KP [6].

Granular sorbents potentially have better kinetic characteristics when sorption is carried out from a constantly renewed solution since they are uniform in shape and have a large surface area. However, the synthesis of granules is carried out using stabilizers or emulsifiers, which are often toxic, and the resulting polymer is practically not washed away from them. The solution to this problem can be the synthesis of granules by emulsion polymerization according to the type of Pickering emulsions, in which nanoparticles are used as stabilizers of polymer-monomer droplets, which are less toxic and are capable of imparting additional properties (for example, biological) to the polymer matrix.

Surface MIPs based on 2-hydroxyethyl methacrylate and ethylene glycol dimethacrylate with respect to glucose [7] and cholesterol using Se nanoparticles as a stabilizer were synthesized via free-radical emulsion polymerization of the Pickering emulsion. The study of equilibrium sorption was shown that sites binding retain their complementarity to the target molecule only when sorption is carried out under

synthesis conditions. This leads to an increase in the affinity of the sorption surface and an improvement in the availability of sites binding, and simultaneously with the implementation of monolayer sorption, which will subsequently lead to an increase in selectivity.

Thus, the solution to the problem of extracting small molecules from multicomponent mixtures can be the use of granular MIPs capable of efficiently and selectively extracting the target object from the solution.

References

1. I.S. Garkushina, N.M. Ezhova, O.A. Pisarev The interaction of erythromycin with polymeric sorbents adjusted to the antibiotic molecule. Russ. J. Phys. Chem. A (2009) **83**, 125.
2. N.M. Ezhova, I.S. Garkushina, O.A. Pisarev Molecularly imprinted hydrophilic polymer sorbents for selective sorption of erythromycin. Appl. Biochem. Microbiol. (2011) **47**, 635.
3. I.S. Garkushina, N.M. Ezhova, O.A. Pisarev Molecularly imprinted polymeric sorbents for selective sorption of erythromycin. Russ. J. Appl. Chem. (2014) **87**, 1126.
4. I.S. Garkushina, I.V. Polyakova, O.A. Pisarev Frontal dynamics of erythromycin sorption on monolithic molecularly imprinted polymer sorbents. Russ. J. Phys. Chem. A (2017) **91**, 2225.
5. I.S. Garkushina, O.A. Pisarev Sorption of erythromycin by molecular imprinted sorbents with different architecture. AIP Conf. Proc. (2020) **2280**, 50020.
6. I.S. Garkushina, I.V. Polyakova, O.A. Pisarev Dynamics of Uric Acid Sorption on Molecularly Imprinted Sorbent. Russ. J. Appl. Chem. (2019) **92**, 437.
7. I.S. Garkushina, P.Y. Morozova, A.A. Osipenko Equilibrium Sorption of Glucose by Surface Imprinted Organo–Inorganic Sorbents. Russ. J. Phys. Chem. A (2021) 95, 1918.

SURFACE-IMPRINTED ORGANIC-INORGANIC AND POLYMERIC SORBENTS FOR SELECTIVE EXTRACTION OF CHOLESTEROL

A.A. Osipenko*, *I.S. Garkushina

osipeno4kalexa@mail.ru
[1] Institute of macromolecular compounds Russian Academy of Sciences, 199004 Saint-Petersburg, Russia

The problems associated with excessive accumulation of metabolites in the body are solved by employing efferent methods of treatment (hemo- and plasmasorption) using hemosorbents. Hemosorbents must meet a number of requirements, one of which is high selectivity in relation to the target metabolite. Currently, immunoaffinity sorbents are used as highly selective hemosorbents; their production and use are expensive and unsafe. The creation of highly selective polymeric hemosorbents will make it possible to reduce the cost of both production and their further use. Taking into account the practical interest in highly selective sorbents, the development of a method for the synthesis of new surface-imprinted organic-inorganic sorbents, and the identification of the effect of the synthesis method on their physicochemical and sorption properties are relevant.

Organo-inorganic sorbents surface-imprinted by molecules of cholesterol (Ch), were synthesized by Pickering emulsion polymerization (series 1, Ch-MIP-1) and precipitation polymerization in n-propyl alcohol (series 2, Ch-MIP-2). The synthesis was carried out by free radical polymerization of 2-hydroxyethyl methacrylate (HEMA) and ethylene glycol dimethacrylate (EGDMA) similarly to [1], except reducing the amount of EGDMA to 14 mol.% to reduce the nonspecific binding of cholesterol with sorption sites. Cholesterol was added as template molecules at the final stage of granule formation for molecular imprinting in the surface layer. The amount of cholesterol was 2 mol.% (Ch-MIP-1-2, Ch-MIP-2-2), 4 mol.% (Ch-MIP-1-4, Ch-MIP-2-4) and 6 mol. % (Ch-MIP-1-6, Ch-MIP-2-6) calculated with respect to the mass of monomers. Control polymers (CP-1 and CP-2) were synthesized without the addition of template cholesterol molecules. An increase in the amount of cholesterol added during the synthesis of Ch-MIPs led to an increase in the yields of both organic-inorganic and polymeric sorbents.

The morphology of the polymers was investigated using scanning electron microscopy. The addition of the Ch template in an amount of 6 mol.% led to the creation of more segregated Ch-MIP-6 matrices by both synthesis methods. Transmission electron microscopy showed the presence of Se^0 nanoparticles in the matrix of organic-inorganic sorbents. The addition of Ch as template molecules promoted the formation of more homogeneous and structurally stable sorbent matrices, and an increase in the amount of template in the polymerization mixture led to an increase in the areas of accessible sorption surfaces in the solvated state for the target Ch molecule at a temperature of 37°C, corresponding to the synthesis temperature.

In the study of the equilibrium sorption of Ch by synthesized sorbents (fraction 160-315 μm) at temperatures of 25°C and 37°C, it was shown that the addition of 6 mol.% Ch into the polymerization mixture promoted the formation of sorption surfaces of polymers of both series with high affinity for Ch molecules at the sorption temperature 25°C. The synthesis of polymer sorbents by the Pickering emulsion polymerization led to the formation of a sorption surface of Ch-MIP-1-6 with a high affinity for Ch both at the synthesis temperature (the temperature of the formation of imprint-sites) and at room temperature. The synthesis of Ch-MIPs by the Pickering emulsion polymerization led to an improvement in the availability at 37°C of sorption centers Ch-MIP-1-2 and Ch-MIP-1-4 compared to Ch-MIP-2-2 and Ch-MIP-2-4.

Differences in cholesterol binding between imprinted and control polymers were established by IR spectroscopy. The registration of an additional peak in the IR spectra after sorption on Ch-MIP-1-6 indicated a change in the nature of cholesterol-binding by imprint-sites formed by the Pickering emulsion polymerization.

The dynamics of Ch sorption was carried out by surface-imprinted organo-inorganic sorbents (fraction 160-315 μm) at 25°C. The optimal conditions for the implementation of the dynamic sorption process of cholesterol extraction were identified: the height of the sorption layer is 3.0 cm, the inner diameter of the column is 1.0 cm, and the flow rate is 0.25 ml/min, and the optimal sorbent with the highest *IF* is Ch-MIP-1-6. Under these conditions for the structural analog, cholic acid, a nonequilibrium mode of sorption dynamics was observed.

Extraction of cholesterol from blood plasma with Ch-MIP-1-6 synthesized by the Pickering emulsion polymerization was carried out more efficiently (29%) compared to CP-1 (14%).

Thus, the imprinting of polymer matrices with 6 mol.% cholesterol led to: the highest yields after synthesis, the creation of more segregated Ch-MIP-6 matrices, as well as the largest values of the areas of available sorption surfaces for the target molecule at 37°C (corresponding synthesis temperature), to the formation of sorption surfaces of polymers with high affinity for Ch molecules at a sorption temperature of 25°C, both organic-inorganic and polymer sorbents. The synthesis of Ch-MIPs by Pickering emulsion polymerization with the addition of 2 mol.% and 4 mol.% improved the accessibility of sorption sites; with the addition of 6 mol.% cholesterol into the polymerization mixture, it promoted the formation of a sorption surface with high affinity at 25°C and 37°C.

References

1. I.V Polyakova, A.A. Osipenko, L.N. Borovikova. Rus. J. Appl. Chem. (2015) **88**, 1617.

SYNTHESIS OF A HYDROGENATION CATALYST SUPPORT BASED ON SPECTRAL CHARACTERISTICS OF THE ANTITUMOR ANTHRACYCLINE ANTIBIOTICS BY SELENIUM NANOPARTICLES

L.N. Borovikova, I.S. Garkushina

diadora3@mail.ru
Institute of Macromolecular Compounds of the Russian Academy of Sciences, Bolshoi Pr. V.O. 31, 199004 Saint-Petersburg, Russia

Principle limitations concerning the wide use of antitumor anthracycline antibiotics in oncologic practice relate to their resistance and side effects [1]. Great attention has been paying in recent years to modification of the antibiotics in use for the creation of better preparations for clinical use with various modes of action [2]. Different approaches, one of which is the modification of anthracycline antibiotics by nanoparticles, are used for this purpose. Metal and non-metal nanoparticles represent an effective solution to overcome bacterial resistance and to improve the efficiency of the antibiotics due to their antibacterial activity [3]. Selenium represents interest from this point of view as well due to its own antitumor activity [4]. Compared to other Se-containing compounds, the nanoparticles of Se have much less toxicity and prevent the formation of cancerous tumors [5].

The purpose of this paper is to study spectral characteristics and intermolecular interactions in the synthesized nanocomplexes of the daunomycin antitumor anthracycline antibiotics (DM) and doxorubicin (DOX) by Se nanoparticle stabilized by polyvinyl pyrrolidone (PVP).

DM and DOX anthracycline antibiotics consist of chromophore-tetracyclic anthraquinoid aglycon linked by a glycosidic bond with aminosugar of daunosamine. It is generally accepted that aglycon is a hydrophobic part of the antibiotic molecule, while the aminosugar of daunosamine represents its hydrophilic part. These antibiotics differ from each other by the presence of hydroxyl group in DOX instead of the methyl group in DM. The presence of hydroxyl group results in redistribution of electron density of the molecule, and this makes an influence on spectral characteristics of the molecule, so DM displays 6 absorption spectrum peaks (234, 252, 290, 480, 495, and 532 nm), while DOX shows 5 peaks

(248, 290, 485, 496, 535 nm). Absorption in UV is connected with absorption of aglicone groups, while aminosugar absorbs in the visible range due to electron transition between valent molecular orbitals of the oxygen atom embedded into a ring and amino group. The presence of the hydroxyl group also suggests that hydrogen bonds can be formed in addition to hydrophobic bonds. Triple complexes have been synthesized in water medium according to the method described in detail in [6]: the method involves that Se nanoparticles have been synthesized preliminary in the presence of PVP with follow-up introduction of DOX/DM. Concentrations C_{Se} = 0.025 mg/ml and $C_{DOX/DM}$ =0.05 mg/ml, concentration of PVP remains constant C_{PVP} = 1.0 mg/ml. Antibiotic concentration values when synthesizing triple complexes corresponded to the values at which they are used in medical practice (60 -75 mg/kg). The synthesized complexes were sedimentation stable during 6 months. The region of the visible spectrum on the absorption spectrum {Se+PVP} + DM (Fig. 1a, curve 3) is practically identical to DM (Fig. 1a, curve 1) that testifies the absence of interaction in the nanocomplex by DM aminosugar fragment. UV region of the spectrum of the complex differs from the UV region of the DM spectrum: there is no 290 nm peak, and hypochromic effect is observed at 232 nm and 252 nm, which testifies interaction with the components by aglicone due to hydrophobic interactions. The hyperchromic effect is observed in the absorption spectrum {Se+PVP} + DOX in the visible part of the spectrum compared to DOX spectrum (Fig. 1a, curves 1 and 3) that testifies interaction in the nanocomplex by DOX aminosugar fragment. All characteristic peaks of DOX are observed in the UV part of the spectrum, and a hyperchromic effect is also observed that demonstrates the presence of interaction with the components of the complex by aglicone.

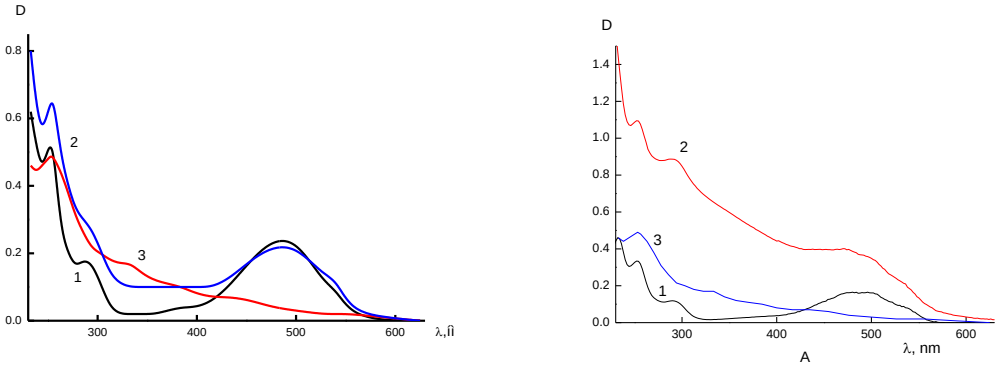

Figure 1. DM (a) and DOX (b) nano-complexes absorption spectra: 1 – DOX/DM; 2 - {Se+PVP} + DOX/DM; 3 - Se+PVP.

Hence, the study of the absorption spectra of the {Se+PVP} + DOX and {Se+PVP} + DM systems demonstrated that, in the case of DM, the interaction proceeds through aglicone via hydrophobic bonds, while, in the case of DOX, it proceeds both through agclicone and aminosugar fragment of the molecule.

References

1. Corrie G.P. Cytotoxic Chemotherapy: Clinical Aspects. Medicine (2008) **36**. 24.
2. Cuihua H., Chen X., Z., C., Huang Y. Design and Modification of Anticancer Peptides. Drug Des. (2016) **5**, 1
3. Zunino F., Capranico G. DNA Topoisomerase II as the Primary Target of Anti-Tumor Anthracyclines..Anti-Cancer Drug Design. (1990) **5**, 307.
4. Khurana A., Tekula S., Saifi M. A., Venkatesh P., Godugu C. Therapeutic applications of selenium nanoparticles. Biomedicine & Pharmacotherapy. (2019) **111**, 802
5. Li Q., Chen T., Yang. F. Facile and controllable one-step fabrication of selenium nanoparticles assisted by l-cysteine. Mater. Lett. (2010) 64, 614.
6. Kipper A.I., Borovikova L.N., Pisarev O.A., Yakovlev I.V. Synthesis and properties of organo-inorganic composites based on daunomycin, polyvinylpyrrolidone, and selenium nanoparticles. Russ. J. Appl. Chem. (2018) **91**, 131.

THE STUDY OF AMMONIA ADSORPTION FROM GAS-AIR MIXTURES ON FIBROUS SORBENTS MODIFIED WITH COPPER (II) AND NICKEL (II) IONS

S.E. Plotnikova, Yu.S. Peregudov, N.V. Voikina, S.I. Niftaliev

post@vsuet.ru
Voronezh State University of Engineering Technologies
394036 Voronezh, Russia

To separate ammonia from gas-air mixtures, condensation, absorption, and adsorption are used. The first two methods have significant disadvantages: they do not provide the required reduction of ammonia content in waste gases; they involve the use of complex equipment, and they are multi-stage. The ammonia adsorption by different sorbents is of interest. The use of ion-exchange polymer fibers has advantages in sorption rate, developed surface, and low resistance of the filtering layer compared to inorganic sorbents.

To study ammonia sorption, chemisorption fibers VION KN-1 containing carboxyl groups and FIBAN K-1 including sulfogroups were used. Modification of fibrous sorbents with ions of metal complex formers, such as Cu, Ni, Co, Cd, etc., increases the sorption capacity for ammonia by 2-3 times. Therefore, Cu^{2+} and Ni^{2+}cations were chosen as fiber modifiers.

To study sorption in the desiccators, we created atmospheres with a volume concentration of ammonia ranging from 5 to 250 mg/m^3. The pressure of ammonia in the gas phase was determined from literature data; the volumetric concentrations were calculated using the Mendeleev-Clapeyron equation for a temperature of 293 K.

The fibers were modified with Cu^{2+} and Ni^{2+}ions by saturating the fibers in salt solutions with a concentration of 0.1 mol/dm^3 for 24 h. Then, the fibers were dried to constant weight and weighed in cups with lids. The weight of the fibers was 0.15±0.001 g. The cups with fibers were placed in desiccators and kept at a temperature of 293 K for 24 h. After the ammonia sorption process on copper and nickel samples, the fibers acquired the colors characteristic of amino complexes. The fibers were extracted, and the ammonia absorbed by the fiber was desorbed with 0.1 mol/dm^{3}hydrochloric acid solution. Desorption was performed under static conditions

at a temperature of 293 K for 1.5 h. In this case, the fiber took its original color, which indicates the destruction of the complexes and the transition into the solution of the complex former cations and ligands. In an acidic medium, ammonia transfers to ammonium cation. To determine the concentration of ammonium ions, I-130 ionometer with an ion-selective electrode was used. The amount of the sorbed substance (mol/g) was calculated by the formula:

$$A = \frac{C \cdot V}{m},$$

where m is the weight of the fiber sample, g; V is the volume of the hydrochloric acid solution, dm^3; C is the concentration of ammonium ions, mol/dm^3.

The results of the studies are presented as a graphical dependence of the amount of sorbed ammonia on the volume concentration of ammonia in the gas phase (Fig. 1a, b).

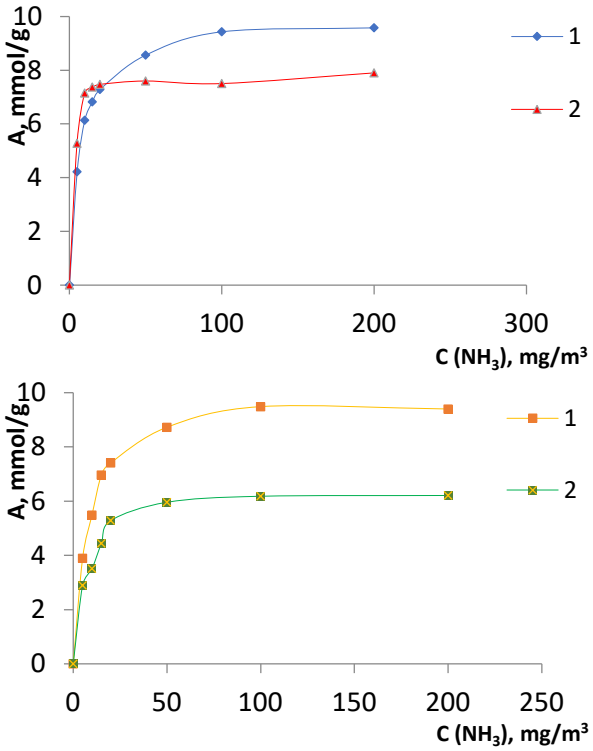

Fig. 1. Isotherms of ammonia sorption on VION KN-1 (a) and FIBAN K-1 (b) fibers modified withNi^{2+} ions - 1, Cu^{2+} ions - 2.

The shape of isotherms is described by the Langmuir theory. At low concentrations, sorption increases linearly with increasing concentration. At high

concentrations of the sorbate, the saturation of the adsorbent surface is achieved.In this case, the amount of adsorbed substance no longer depends on the concentration; it is constant and corresponds to the limiting adsorption.

The sorption isotherm can be represented in the Langmuircoordinates for calculating the quantitative characteristics of sorption. The dependence graphs of the ratio P/A = f(P) are a straight line. According to the straight-line equations, the limiting adsorption value A and the sorption equilibrium constant can be calculated (Table).

The Langmuir equation describes the shape of isotherms. The sorption isotherms presented in the Langmuir coordinates have a coefficient of determination R^2 close to 1.

Table. Quantitative characteristics of ammonia sorption on modified fibers

Fiber	Fiber modifier	Monolayer capacity, A_∞	Sorption equilibrium constant, K	Coefficient of determination,R^2
VION KN-1	Ni^{2+}	9.930	1.029	0.9998
	Cu^{2+}	9.775	1.081	0.9994
FIBAN K-1	Ni^{2+}	7.918	3.538	0.9994
	Cu^{2+}	6.431	1.205	0.9994

The monolayer capacity determined from the isotherms shows that the fiber modified with nickel ions is a more efficient sorbent than the fiber modified with copper ions. At the low content of ammonia in the gas phase, the fiber VION KN-1 in the copper form has an increased sorption affinity to ammonia.

The results of the study can be used to develop systems for gas emissions after treatment and to control the ammonia content in the air.

ADSORBED PALLADIUM (II) CHLORIDE COMPLEXES ON POLYVINYLENES AS CATALYST SUPPORTS

E.S. Zapevalova [1], ***O.B. Belskaya*** [1], ***I.V. Anikeeva*** [1], ***Yu.G. Kryazhev*** [1]

zapevalova@ihcp.ru
[1]*Center of New Chemical Technologies BIC,*
Boreskov Institute of Catalysis, 644040 Omsk, Russia

In the previous studies [1], we have shown the possibility of fixing anionic palladium complexes $[PdCl4]^{2-}$ on a polymer support with a conjugation system. Polyvinylene (PV) as a support was used. It was formed during the alkaline dehydrochlorination of polyvinyl chloride (PVC) under the bases action [2]. The formation of dispersed palladium particles on the PV in a result of sorption was observed.

In this work, two types of polymer supports are compared: 1) PV and 2) alkaline complexes of PV, which are formed during the interaction of PV with NaOH (PV-OH). Earlier in our work, the ability of PV to form complexes with alkalis was noted [3]. To assess the effect of the –OH active centers on sorption of the palladium chloride complexes, the PV-OH support was chosen. The selected method of PV treatment provided the content of the centers of 6.6 mmol-eq / g or 263 mgNaOH / gPV on the PV-OH.

Adsorption isotherms of palladium complexes on the studied supports were plotted. The isotherms were described using the Langmuir equation in the following form:

$$\frac{C}{a} = \frac{1+kC}{a_m k} = \frac{1}{a_m k} + \frac{C}{a_m}$$

, where

a_m- the value of adsorption, which corresponds to the capacity of the layer

k- constant of adsorption equilibrium

Fig. 1 is shown a linear view of the obtained isotherms.

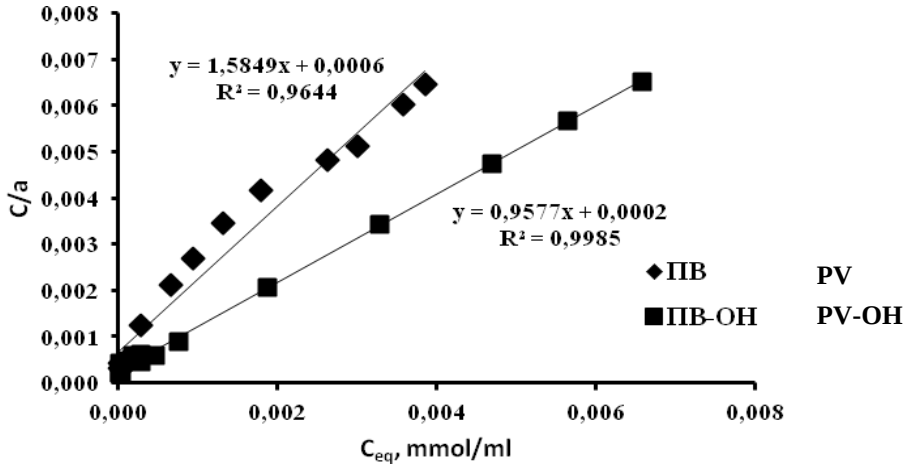

Fig.1. Linear view of palladium adsorption isotherms on PV and PV-OH

The value of the determination coefficient (R^2) for both isotherms is close to 1. This confirms the correctness of the adsorption description by Langmuir's model. According to obtained data (Tabl.1) the adsorption processes for PV and PV-OH are different. The values of a_m and k for PV-OH are twice as many as for PV. The maximum amount of adsorbed Pd reaches 6 wt. % for PV and 9.7 wt. % for PV-ON. The higher adsorption capacity of PV-OH can be related to the interaction of the -OH groups of the surface PV-OH with $[PdCl4]^{2-}$. As a result, the formation of hydrolyzed polynuclear forms of palladium occurs. The adsorption of palladium on PV probably occurs as a result of the interaction of $[PdCl4]^{2-}$ complexes with the PV's conjugation system.

Table 1. Absorption characteristics of supports, which were formed by dehydrochlorination of PVC

Support	k, l/mmol	a_m, mmol Pd/g	C_{max} Pd, wt %.
PV	2.6	0.63	6.0
PV-OH	4.8	1.04	9.7

Catalysts Pd/PV and Pd/PV-OH were obtained by reduction of palladium with sodium formate. And then, they were tested in the hydrogenation reaction of

nitrobenzene (50 ^{O}C, 1.0 MPa, solvent C2H5OH). All catalysts are ensured complete conversion of the nitrobenzene in hydrogenation reaction, but the PV-OH catalysts is outperformed the PV-based catalysts in activity. Hydrogenation reaction rates for samples with the same metal content (of 5.8 wt.% Pd/PV and 5.9 wt.%Pd/PV-OH) are 1.9 and 5.8 mmol $H_2/(g_{cat}$*min), respectively.

Thus, the use of PVC-based polymer supports makes it possible to obtain effective nitrobenzene hydrogenation catalysts. Modifying the PV surface with alkali contributes to an increased adsorption capacity and a strong fixation of palladium on the support.

Funding

This work was supported by the Ministry of Science and Higher Education of the Russian Federation within the governmental order for Boreskov Institute of Catalysis (project AAAA-A21-121011490008-3)

References

1. O. B. Belskaya, I. V. Anikeeva, M. V. Trenikhin, R. R. Izmailov, Yu. G. Kryazhev, Investigation of adsorption of the Pd(II) chloride complexes on polyvinylene for the selective hydrogenation catalysts synthesis, Phys. and chem.. problems of adsor. in nanopor. mat.: mat. Russ. Internet-symp., IPCE RAS, Moscow, 2019, p. 205
2. V. S. Solodovnichenko, Yu. G. Kryazhev, A. B. Arbuzov, V. P. Talzi, N. V. Antonicheva, V. A. Drozdov, E. S. Zapevalova, V. A. Likholobov, Polyvinide chloride as a precursor for low-temperature synthesis of carbon materials, Rus. Chem.Bul, (2016) **65**, 27
3. E. S. Martynenko, V. S. Solodovnichenko, Yu. G., A. B. Arbuzov, A. A. Kalinina, Yu. G. Kryazhev, Alkaline complexes of polyvinylene chlorides and their capacity for reversibly sorbing phenol, Sol. Fuel Chem. **49**, 387.

ABOUT THE DIVERSITY OF SURFACE EFFECTS ON THE COASTAL SANDS OF NORTHERN AND CENTRAL VIETNAM IN THE CONDITIONS OF AGGRESSIVE IMPACT

A.A. Yakovleva, Trung Thuy Nguyen

ayakovistu@mail.ru, nguyentrungthuy_irk@mail.ru
Irkutsk National Research Technical University, 664074 Irkutsk, Russia

Environmental pollution is an urgent problem in modern society. The role of a comprehensive analysis of changes in the environment and its potential for self-recovery and self-purification is important. In this paper, coastal sands are selected as objects of research to assess the adsorption characteristics and their functions in protecting groundwater and underlying soils from pollutants. The aim of the work is to study the mechanisms of surface phenomena in the sands by considering their adsorption-desorption characteristics in relation to iron (III), nickel (II) ions, petroleum products, and surfactants.

The samples of sand used A, B, G and K are selected on the banks of the rivers and Bacbo Bay in Vietnam. The physical and chemical characteristics of the sands are presented earlier [1–4]. The preparations $FeCl_3 \cdot 6H_2O$ (mark “Pure” GOST 4147-74), $NiCl_2 \cdot 6H_2O$ (mark “Pure for analysis” GOST 4038-79), gasoline A-92 (GOST 32513-2013) and engine lubrication (“Demand drive plus” by company “Pure Polaris”, USA), surfactants ($C_{14}H_{29}SO_4Na$, $C_{16}H_{33}SO_4Na$, $C_{17}H_{33}COONa$ mark “Pure”) were used to simulate pollutants. The adsorption properties were studied by classical methods of colloid-chemical studies. Standard methods were used to determine the concentrations of the studied solutions. Fig. 1 shows some results of generalization of processes adsorption-desorption of iron (III) ions under different conditions.

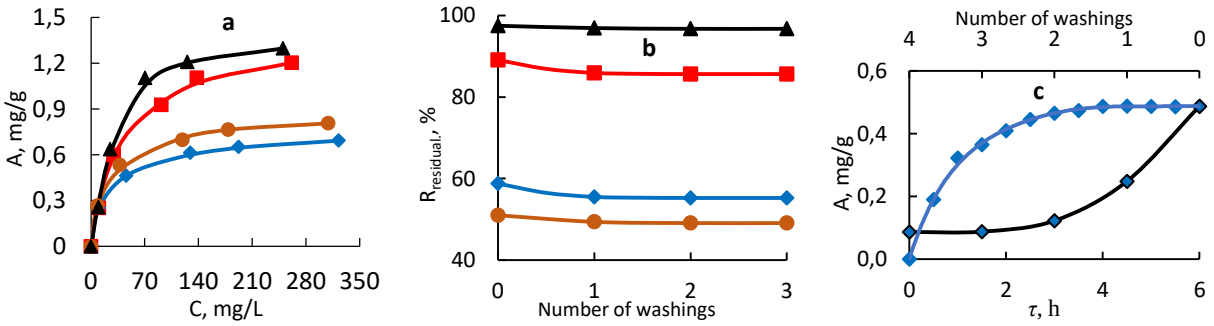

Fig. 1. Adsorption-desorption of iron (III) ions on the surface of sands:
■–A; ◆–B; ▲–G; ●–K.

Figure 1a shows the isotherms of the adsorption of iron (III) ions on the surface of sands at a temperature of 298 K. Figure 1b shows the process of desorption in dynamic conditions, and on Fig. 1c, this process occurs under static conditions (for example, sand B is shown).

Figure 2 presented the kinetic regularities of the processes of adsorption and desorption of nickel (II) ions at a temperature of 298 K; in Fig. 3, the features of the adsorption-desorption processes of surfactants on the example of tetradecyl sulfate sodium are shown, and Figure 4 demonstrates the dependence of the retention of petroleum products on the experimental conditions (the height of the sand layer in the column).

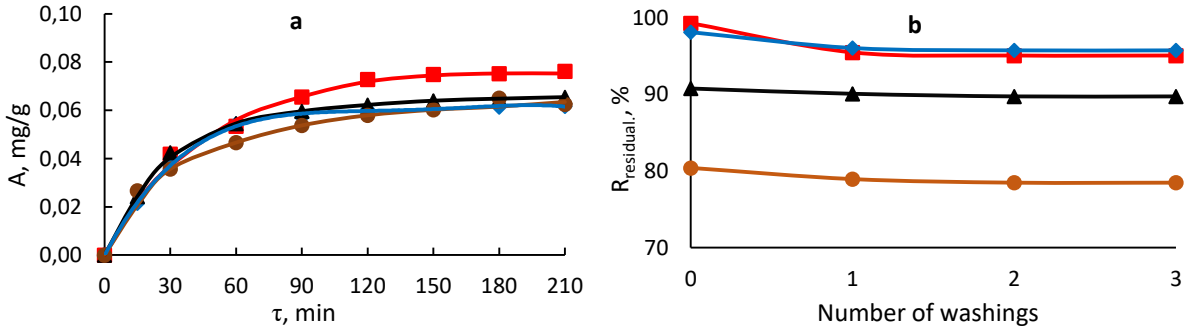

Fig. 2. Adsorption-desorption of nickel (II) ions. Sand designations are the same

It can be seen that the adsorption equilibrium in the system occurs in ~ 180 min; the adsorption process is irreversible (fig. 2b).

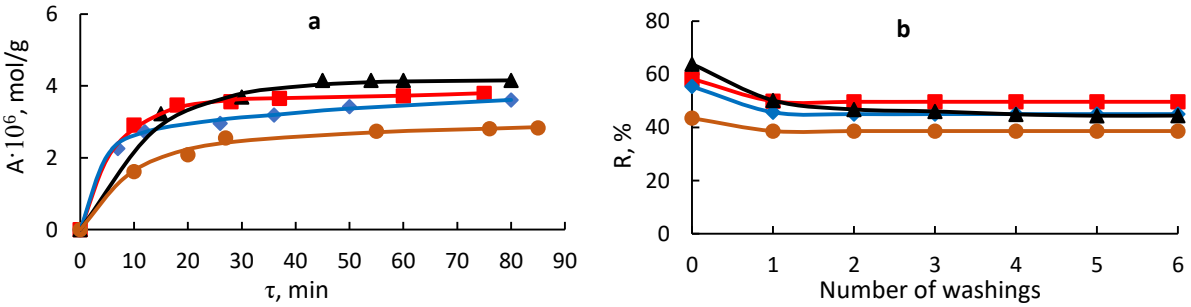

Fig. 3. Adsorption-desorption $C_{14}H_{29}SO_4Na$. Sand designations are the same

It can be seen that the sand retains a significant part of surfactants and petroleum products from solutions. The research results showed that the surface processes are of a different nature and are accompanied by molecular adsorption, ion exchange, film formation, and other effects.

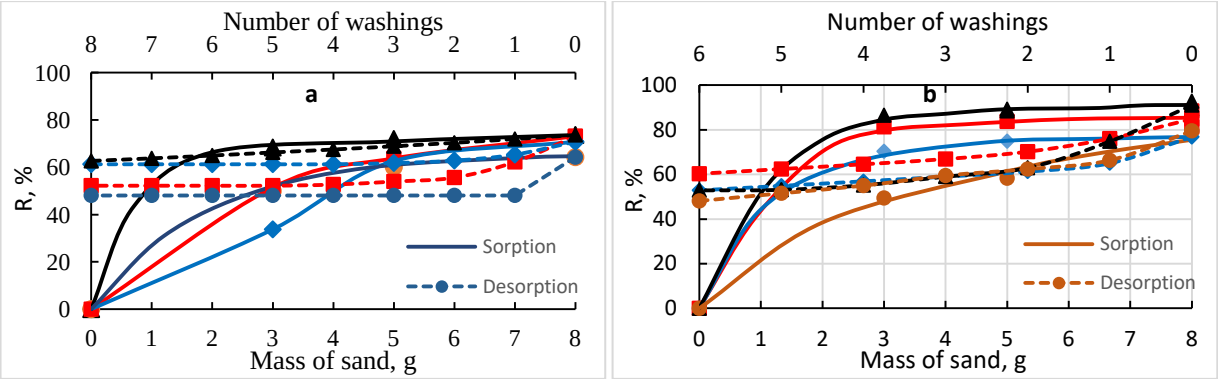

Fig. 4. Adsorption-desorption of petroleum products:
a – gasoline A-92; b – engine lubrication. Sand designations are the same

Thus, the studied sands, like many other mineral materials, can play an important role as barriers in protecting groundwater and underlying soils due to their adsorption characteristics.

References

1. Yakovleva A.A., Nguyen T.T. Characteristics of Sorption on Surfaces of River Sands with the Participation of Iron (III) Ions. Russ. J. Phys. Chem. A. (2021) **95**, 1216.
2. Yakovleva A.A., Nguyen T.T. On the question of the barrier qualities of the sands of northern and central Vietnam. Sorption of iron (III) ions Russ. J. Phys. Chem. A. (2020) **64**, 80.
3. Yakovleva A.A., Nguyen T.T. Barrier qualities of the sands of Northern and Central Vietnam. Sorption of the engine oil emulsion. Russ. Chem. J. (2021) **65**, 116.
4. Yakovleva A.A., Nguyen T.T. Adsorption of surfactants on sands and their role in environmental barriers. Chem. Saf. Sci. (2021) **5**, 237.

MODERN PHYSICOCHEMICAL METHODS FOR REMOVING TOXIC IMPURITIES FROM AQUEOUS SOLUTIONS

V.V. Milyutin

vmilyutin@mail.ru
Frumkin Institute of Physical Chemistry and Electrochemistry of the Russian Academy of Sciences (IPCE RAS), 119071 Moscow, Russia

In the process of industrial, household, and other human activities, the formation of various types of dangerous wastes inevitably occurs. Industrial wastewaters generated by various enterprises are the most significant environmental hazard to human health and the environment. Since most of the production processes occur in the aquatic media, the main part of toxic impurities enters the environment with wastewater. The main toxicants contained in industrial wastewater are: compounds of non-ferrous and heavy metals (Ni, Cu, Zn, As, Sr, Cd, Ba, Hg, Tl, Pb, etc.); organic compounds (petroleum products; surfactants; dyes; pesticides, etc.), as well as radioactive elements, both natural and technogenic origin (radionuclides of uranium, thorium, radium, cesium, strontium, plutonium, etc.)

Depending on the phase-dispersed state of impurities in aqueous solutions, various physic-chemical methods of wastewater treatment are used: thermal, precipitation, sorption, membrane. The choice of the most effective treatment method depends on the chemical composition of the effluent, the requirements for the quality of treatment, and economic factors.

In accordance with the modern classification, impurities present in aqueous solutions by phase-dispersed composition are divided into two large groups: insoluble (heterogeneous systems) and soluble (homogeneous systems). The insoluble state of impurities is represented by coarse, finely dispersed, and colloidal particles. The soluble state is represented by various ionic forms, uncharged complexes, neutral molecules of high molecular weight compounds, surfactants, etc.

Methods of sedimentation, mechanical filtration, membrane filtration (micro- and ultrafiltration), coagulation are used to remove insoluble forms of impurities. Mechanical filtration is used for purification from coarse particles, from fine and

colloidal impurities - membrane filtration. The coagulation method is universal and allows one to purify wastewater from all types of insoluble forms of radionuclides.

Membrane filtration methods (nanofiltration and reverse osmosis) and sorption processes are used to remove soluble forms of impurities. The reverse osmosis and nanofiltration processes provide the purification from all singly and multiply charged ions and molecules with a molecular weight above 100. Sorption methods for removing soluble forms of impurities are based on physical adsorption or ion exchange processes. In physical adsorption, the removal of impurities occurs due to the adsorption of the components of the solution on the surface of the solid (adsorbent). Solids with a high specific surface area and a branched pore system (active carbons, silica gels, polymer adsorbents, natural and synthetic aluminosilicates, etc.) usually use as an adsorbent. Physical adsorption methods are mainly used to purify wastewater from impurities of organic compounds (oil products, surfactants, dyes, etc.).

In wastewater treatment by ion exchange, organic ion exchange resins and inorganic sorbents are used as ion exchangers. Organic ion-exchange resins are used mainly for the complete or partial demineralization of water and the removal of multiply charged heavy metal ions. Inorganic sorbents based on natural and synthetic aluminosilicates and zeolites, titanates, and titanosilicates of alkali metals, phosphates of titanium and zirconium, ferrocyanides of transition metals are used mainly for the sorption of long-lived radionuclides of cesium and strontium. Inorganic sorbents have high chemical, thermal and radiation resistance, as well as increased, in comparison with organic ion exchangers, selectivity to certain ions.

Thus, modern technologies using various physical and chemical methods make it possible to effectively purify industrial waste and natural waters of various chemical compositions from a wide range of toxic impurities.

COMPLETE PURIFICATION OF WATER FROM METAL CATION WITH A FIBROUS ION EXCHANGER

Yu.S. Peregudov, L.P. Bondareva, S.I. Niftaliev

inorganic_033@mail.ru
The Voronezh State University of Engineering Technologies,
394036 Voronezh, Russia

Ion-exchange fibers VION are used to purify gaseous media from toxic and corrosive components: SO_2, SO_3, NH_3, to extract metal cations Cu^{2+}, Ni^{2+}, Co^{2+}, Pb^{2+}, Zn^{2+}, Cd^{2+}, Mn^{2+}, Fe^{2+} from aqueous media. Major advantages of fibers are highly ion exchanger purification, adsorption and regeneration rate is 10–15 times higher than for granular materials, a high exchange capacity enough large chemical resistance, and ability to maintain the exchange capacity of more than 100 cycles after "sorption-regeneration."

Fiber VION KN-1 is a cation-exchange, carboxyl-containing, chemisorption, weakly acidic fiber with a three-dimensional mesh. The polymer has a high exchange capacity of carboxyl groups (6.5-6.8 mmol/g), characterized by a high adsorption rate, hygroscopic resistance, hydrophilicity, and high surface area. The VION KN-1 synthesis technology is well-known and easily implemented in polyacrylonitrile fiber factories, which will make this fiber available for use.

Carboxyl cation exchangers are highly selective towards ions with a small radius of the non-hydrated ion. The intense forcefield of carboxyl groups in ion exchangers leads to increased electrostatic interaction with the counter-compensates for the energy costs of their dehydration. Literature data on the selectivity of carboxyl ion exchangers to metal cations are very contradictory [1–4]. There is reason to assume that for a fibrous carboxyl ion exchanger, the most probable series of cations selectivity is $Cu^{2+} > Pb^{2+} > Ni^{2+} > Zn^{2+} > Cd^{2+} > Ca^{2+} > Mg^{2+} > Na^{+}$.

In this work, we studied the exchange of doubly charged cations Cu2 Cu^{2+}, Pb^{2+}, Mg^{2+}, Ca^{2+} etc. on fibrous carboxylic sorbent VION KN-1 in sodium form using the method of variable concentrations to obtain sorption isotherms, the calorimetric method used to establish the thermal effects of sorption and the IR spectroscopic method to determine the type of sorption centers formed in the polymer. Ion exchange

isotherms have a typical form corresponding to the Langmuir isotherms. The sorption exchange capacity increases in the order Cu^{2+} > Ni^{2+}> Pb^{2+} > Zn^{2+} > Cd^{2+} > Ca^{2+} > Mg^{2+} > Na^{+} and ranges from 5.3 mmol / g to 2.9 mmol/g.

The affinity of copper (II) cations for carboxyl fiber is significantly higher than other transition metal cations and lead (II) cations with comparable selectivity. This is probably due to the difference in the positions of the cations Ni^{2+}, Pb^{2+}, Zn^{2+}, Cd^{2+} in the series of selectivity.

It was found by IR spectroscopy and sorption analysis that an ion-coordination bond is formed in the polymer between the counterions of transition metals and the carboxyl groups of VION KN-1. Ion exchange is accompanied by absorption of heat, wherein the sorption enthalpies have low values of 2.5 to 21 kJ / mol, increasing with a rise in the degree of filling fiber sorbate.

Based on the results of the study, a technological scheme for wastewater treatment using ion-exchange fiber has been proposed, including units for reagent treatment, thin-layer sedimentation of wastewater, sludge dehydration, deep clarification on mechanical filters, and additional wastewater treatment on ion-exchange filters.

References

1. Soldatov V.S., Zelenkovskii V.M., Kosandrovich E.G. Reactive and Functional Polymers. (2016). No. 102. P. 147.

2. B. Treimion Separation on ion exchange resins. / Per. from French ed. Chmutova K.V., Kremer N.A.M. 1967.432 s.

3. Ion Exchange Technology I Theory and Materials / Ediors Luqman I. M., Springer Dordrecht Heidelberg New York London, 2012.550 p.

4. Pehlivan E., Altun T. Journal of Hazardous Materials. (2007). No. 140. P. 299.

NOVEL MF-4SC/PTMSP BILAYER MEMBRANES, ASYMMETRY OF THEIR TRANSPORT PROPERTIES, AND MODELING

A.N. Filippov [1], ***N.A. Kononenko*** [1,3], ***N.V. Loza*** [3], ***V.I. Ivanov*** [1], ***D.A. Petrova*** [1,2]

filippov.a@gubkin.ru
[1] *Gubkin University, 119991 Moscow, Russia*
[2] *Faculty of Chemistry, Lomonosov Moscow State University, Moscow, Russia*
[3] *Department of Physical Chemistry, Kuban State University, Krasnodar, Russia*

The asymmetry of transport properties is an important feature of bilayer membranes. When the direction of the driving force (pressure gradient or concentration gradient, electric field) changes, the flux of solvent, solute, and electric current correspondingly can change significantly. In the latter case, an asymmetry of the current-voltage characteristic is observed. It leads to a significant difference in the limiting current density when the orientation of the membrane in the measuring cell changes. This property can be promising while creating membrane diodes when a bilayer membrane passes current well in one direction and practically does not pass it in the other.

The aim of the work was to establish and quantify the asymmetry of the current-voltage curve of a bilayer composite membrane based on a thick layer (280 μm) of cation-exchange perfluorinated membrane MF-4SC and a thin (1 μm) non-conducting layer of poly(1-trimethylsilyl-1-propyne) (PTMSP) depending on the direction of the external electric field.

The current-voltage characteristics (CVC) were measured in a 0.05 M solution of HCl and NaCl, which was pumped at a volume rate of 15 ml/min. A constant electric current was applied to the polarizing electrodes with a given sweep speed of $1 \cdot 10^{-4}$ A/s or $5 \cdot 10^{-5}$ A/s using a current source. The voltage drop ΔE on the test membrane was measured using Luggin-Haber capillaries, connected on both sides to the surface of the membrane and attached to silver-chloride electrodes linked to a multimeter, from where the signal was fed to a computer. The CVC of this sample has a characteristic form for ion-exchange membranes: typical areas (ohmic, limiting current plateau, and overlimiting) are well distinguished on curves (Fig. 1).

As can be seen from Fig.1, there is a significant CVC asymmetry, which we described quantitatively using our homogeneous model of fine porous bi-layer membrane [1]. The homogeneous model was applied successfully to bi-layer

membranes consisting of a pure MF-4SC layer and a layer modified by halloysite nanotubes functionalized with polyaniline [2].

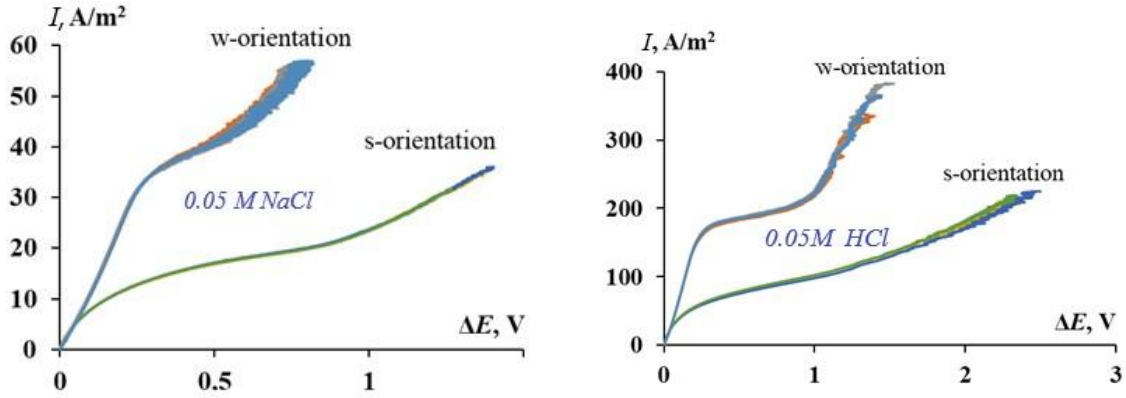

Fig.1. CVCs of bi-layer MF-4SC/PTMSP membrane in 0.05M NaCl (left) and HCl (right) electrolyte solutions.

Thus, with the orientation "w", that is, by the MF-4SC layer faced to the counterion flux, the value of the limiting current density is 2.5 and 2.8 times higher in the case of the NaCl and HCl solutions, respectively. The conductivity in the ohmic region and in the region of overlimiting currents is also higher in the case of the "w" orientation. At the same time, in the ohmic section, the difference between these values is approximately 1.8 times for both solutions, and in the overlimiting mode – 3.8 times for an acid solution and 2 times for a sodium chloride solution. In addition, the extent of the limiting current plateau also depends on the orientation of the sample to the counterions flux: a more extended plateau is observed in the case of the orientation "s", that is, by a layer of non-conducting polymer PTMSP faced to the flux of counterions. The obtained layered composite is important for potential applications as membrane sensors and diodes [3].

Funding

This work was supported by the Russian Science Foundation, Project # 20-19-00670.

References

1. A.N. Filippov, Colloid J. (2016) **78**, 397.
2. A.N. Filippov, N.A. Kononenko, N.V. Loza, D.S. Kopitsyn, D.A. Petrova, Electrochimica Acta (2021) **389**, 138768.
3. D. Du, X. Wei, Y. Tu, J. Huang, J. Electroanal. Chem. (2021) **889**, 115230.

KINETIC MODEL OF THERMAL DECOMPOSITION OF ANIONITES ON THE EXAMPLE OF AV-17×8 IN NITRATE FORM

V.V. Kalistratova [1], ***V.V. Milyutin*** [2], ***E.V.Belova*** [1]

vera.kalistratova@gmail.com
[1]*Laboratory of Radiation and Radioecological Problems, IPCE RAS,*
[2]*Laboratory of Chromatography of Radioactive Elements, IPCE RAS,*
119071 Moscow, Russia

Chromatographic methods are widely used for the separation and isolation of radioactive elements in radiochemical technology, using strongly basic anion exchangers. The operating conditions of ion-exchange materials, as a rule, are rather harsh and are associated with the effect of ionizing radiation, oxidants and temperature on the ion exchangers. In this regard, it is of great importance to ensure the reliability, stability and safety of technological operations with sorbents. During the period of operation of radiochemical plants, a number of accidents occurred in sorption systems using anion exchangers [1,2,3], which led to the release of radioactive substances into the environment and significant material costs for eliminating the consequences. The analysis of these accidents shows that the cause of the destruction of the sorption columns and the release of their contents were exothermic processes of interaction of the anionite with nitric acid oxidants, accompanied by significant heat and gas release..

An attempt to create a model of thermal oxidation of anion exchanger, using the example of AB-17×8 in nitrate form, has been made in this work. It done with the aim of further using the results obtained for a comparative assessment of the safety of technological processes with promising brands of sorbents. To obtain the initial calorimetric data, we used a combined method of differential scanning calorimetry and thermogravimetry (DSC-TG) using a synchronous thermal analyzer STA 449 F1 Jupiter (manufactured by NETZSCH).

Before the experiment, the ion exchanger was preliminarily converted into the nitrate form and dried in air at room temperature to constant weight. A sample of the substance was placed in a corundum crucible with a lid; aluminum oxide was used as a reference sample. To obtain the initial calorimetric data on heat release

versus temperature, a dynamic heating mode was used at a rate of 1.2 and 4 K / min from room temperature to 800 ° C in an air atmosphere and nitrogen atmosphere. Experimental baselines were obtained to calculate the total thermal effect.

Figure 1 shows the curves of the dependence of the heat rate production and weight loss on temperature for AV-17×8 in nitrate form. There are several peaks on the heat release curve, which indicate the occurrence of oxidation reactions. The most interesting for further detailed consideration for us are the reactions occurring in the temperature range up to 400 ° C.

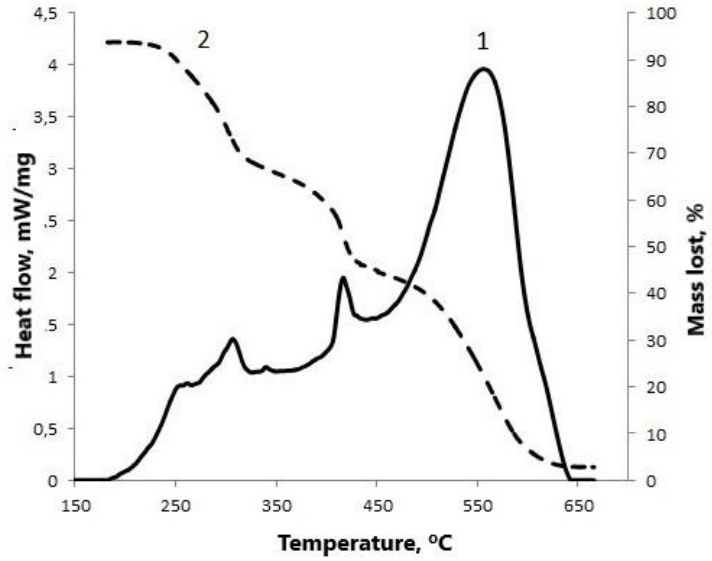

Fig.1. Dependence of heat flow (1) and change in mass (2) on temperature for the sorbent AV-17×8

Based on the analysis of the results of DSC-TG experiments, kinetic equations were proposed for the processes occurring in the temperature ranges 170-250 ° C (stage 1), 250-300 ° C (stage 2):

Stage 1 (n1-order reaction):

$$w_1 = k_{0_1} * \exp\left(-\frac{Ea_1}{RT}\right) * (1-\alpha)^{n_1}$$

Stage 2 (n2-order reaction):

$$w_2 = k_{0_2} * \exp\left(-\frac{Ea_2}{RT}\right) * (1-\alpha)^{n_2}$$

where w_i is the reaction rate (heat release), sec^{-1}; T is temperature, K; k_0 – preexponential factor, 1/sec; R is the universal gas constant, 8.31 J / (mol K); a – the

depth of transformation at this stage; E_{ai} — activation energy, kJ / mol; n_i is the order of the reaction.

Additional DSC-TG experiments in an inert atmosphere (nitrogen) showed that the air oxygen present acts as a catalyst for the decomposition of the nitrate form AB-17 × 8 and increases the total thermal effect of the second stage of the process, while the exothermic effect of the first stage of the process does not affect the composition of the atmosphere.

Experiments in an inert atmosphere made it possible to refine the kinetic parameters of the second exothermic effect, which amounted to lnk0 = 35.4 ± 1.4ln (1/sec); Ea = 185.2 ± 5.2 kJ / mol; n = 1 ± 0.09; Q = 660 ± 45 kJ / kg. Calculations carried out using the refined parameters show that the value of the critical temperature for the AB-17×8 anionite in nitrate form under the experimental conditions is in the range of 247-252 ° C. At a thermostat temperature of 255 ° C, a thermal explosion is predicted in ~ 2300 sec. The experiment carried out showed that the ignition of the anionite occurred after ~ 2600 sec, which, taking into account a number of uncertainties in the initial parameters of the system, can be considered a quite acceptable estimate. At temperatures of 220 and 235 ° C, both the model and the experiment show the absence of a thermal explosion.

Thus, the developed model using the results of DSC-TG experiments on samples of theAV-17×8 anionite of small mass (about 10 mg) allows describing processes using gram amounts of sorbent and can be used to assess the safety of various technological processes using anioniteAB-17×8 in nitrate form.

References

1. Milest F.W. «Lon-Exchange-Resin System Failures in Processing Actinides», Isotopes and Radiation Technology (1969) **6**, 428.
2. Calmon C. «Explosion hazards of using nitric acid in ion-exchange equipment», Chem. Eng. (1980), 271 p.
3. Glagolenko Yu. V. "Analysis of the causes of depressurization of the sorption column at the plant for the production of plutonium-238 of the radioisotope plant" PO "MAYAK", V. G. Khlopin Radium Institute, Tsniiatominform, 1996

ADSORBENTS APPLICATION PRACTICE FOR FORMING A RANGE OF MODERN FILTERS FOR GAS MASKS AND RESPIRATORS. REPORT 3.

M.V. Talipova, A.V. Liang

talipova@sorbent.su; avl@sorbent.su
Sorbent JSC, 614042 Perm, Russia

Due to the development of technology and the intensive growth of industry, the requirements for respiratory personal protective equipment (RPE), including filters for gas masks and respirators, are becoming more stringent.

Earlier, we have shown that due to the improvement of working conditions and labor protection, there is a need for compact, lightweight filters, which have low breathing resistance, high efficiency of protection against particles, as well as effective protection against gases and vapors at their low concentration up to 3 permissible exposure limits (PEL) in accordance with GOST 12.1.005-88. Creating such a filter, equipped with a united gas and particle element with a low resistance to airflow during breathing, is an urgent task [1].

The practice analysis and research of using adsorbents showed that the element can be used in flat or corrugated forms, and the element shall be obtained either from filtering material used together with an adsorbent for protection against particles or the adsorbent in the form of a filtering adsorbing material. As a rule, microporous activated carbon based on a coconut shell with different adsorbent activity and particle size is used as adsorbent particles [2].

It has been established among the range of adsorbents for co-use with filtering material, the most promising, in our opinion, is a bulk material enclosed between two non-woven substrates, in the form of polymer fibers deposited with activated carbon particles, which makes it possible to achieve a sufficiently high level of breakthrough time, presumably due to the creation of local zones of high turbulence around activated carbon particles.

An experimental number of studies based on the use of filtering adsorbing material with various types of adsorbents obtained by applying chemical ingredients to the surface of activated carbon pores have been set. The comparative tests of filtering

adsorbing material, simulating test conditions of compact, lightweight filters have been performed. Based on the analysis results, the optimal filtering adsorbing materials have been determined.

As follows from the research:

(1) The combination of the filtering material and the activated carbon impregnated with chemical additives has been tested and evaluated in the compact lightweight filters. The essential physicochemical and sorption parameters of adsorbents are determined: activated carbon and activated carbon impregnated with chemical additives.

(2) It has been revealed that the combination of filtering material and adsorbents with a low depth of layer is identical in comparison with gas and combined filters for gas masks and respirators, equipped with adsorbents with a high depth of the layer of the chemical filling. Specifically, the compact lightweight filters with the required increased degree of genericity action are possible in case of using the principle of a multifunctional two-layer chemical filling with immiscible layers, when one layer is a multicomponent absorber obtained after the process of using the principle of chemical indifference or impregnating salts of acidic and basic nature. The choice of the second layer is due to the requirements for the degree of genericity action of the compact lightweight filters (ammonia absorber, activated carbon, etc.). The principle of chemical indifference is fulfilled when the salts with the same anions are used as impregnating additives. Or the two multicomponent absorbers in the multifunctional chemical filling are used: the first when using the principle of chemical indifference, and the second using salts of acidic and basic nature [3].

(3) It has been revealed when selecting the combination of filtering material and adsorbent in the RPE against particles upon reaching the highest possible breakthrough time, the determining factor is the adsorbent grains degree of freedom from the binding substance and the increased intensity of their interaction with the gas-vapor flow, presumably due to the creation of local turbulence in the layer.

In general, the methods of combining filtering materials and adsorbents have been studied and systematized as a prerequisite for creating a new class of the lightweight particle RPE - gas masks and respirators with additional protection against

gases and vapors, which shall result in standardization of the requirements for such RPE and relevant filters.

On practical grounds, the development of the filtering adsorbing material obtained by different methods, with chemical ingredients applied on the surface of activated carbon pores, will expand the range of lightweight RPE with improved ergonomic properties and will make it possible to select the compact lightweight filters for protection against various harmful chemicals and its combinations. Industrial personnel working in areas with high concentrations of particles and low concentrations of harmful chemicals in the air will have additional opportunities to preserve their health and life.

References

1. M.V. Talipova, A.V. Liang. Combination of the filter material with sorbents for air purification in respiratory personal protective equipment: Proceedings of the 5th International Scientific and Technical Conference dedicated to the memory of Professor V.I. Komarov, September 11-14, 2019 / Ministry of Science and Higher Education of the Russian Federation, Federal State Autonomous Educational Institution of Higher Education "Northern (Arctic) Federal University named after M.V. Lomonosov". - Arkhangelsk: 2019. – 368 p.

2. M.V. Talipova, A.V. Liang. Adsorbents application practice for forming a range of modern filters for gas masks and respirators. Report 1: Proceedings of the Internet Symposium. - Physicochemical problems of adsorption and technology of nanoporous materials: All-Russian Internet symposium with international participation. October 19 - November 15, 2020, Moscow, Russia / Ministry of Science and Higher Education of Russia, Russian Academy of Sciences “Institute of Physical Chemistry and Electrochemistry named after A.N. Frumkin, RAS". - Moscow: IPCE RAS, 2020. – 328 p.

3. A.V. Liang. Adsorbents application practice for forming a range of modern filters for gas masks and respirators. Report 2: Proceedings of the Internet Symposium. - Physicochemical problems of adsorption and technology of nanoporous materials: All-Russian Internet symposium with international participation. October 19 - November 15, 2020, Moscow, Russia / Ministry of Science and Higher Education of Russia, Russian Academy of Sciences “Institute of Physical Chemistry and Electrochemistry named after A.N. Frumkin, RAS". - Moscow: IPCE RAS, 2020. – 328 p.

RECORDING OF SINGLE AND MULTI-COMPONENT ISOTHERMS USING DYNAMIC METHODS

S. Ehrling, R. Eschrich, A. Möller, C. Blum

Sebastian.ehrling@3P-instruments.com
3P Instruments GmbH, Odelzhausen, Germany

Climate change is a widely discussed topic, and therefore, both scientific and industrial researchers are working in this field. Carbon dioxide plays a crucial role within this challenge since CO_2 is mainly responsible for the blanket, trapping the heat in the atmosphere.

Simple literature research reveals that in the last 4 years, around 18,000 different papers were published dealing with the topic of CO_2 adsorption. Often new materials are discussed, highlighting the strong interest [1].

For the characterization or the suitability testing of new materials, single-component isotherms are classically recorded. With the help of common adsorption models, such as the Ideal Adsorbed Solution (IAS) theory, the ideal separation behavior is then calculated [2]. The IAS theory is only applicable to "ideal adsorption processes", since the original theory is based on hypotheses, e.g., that the framework is thermodynamically inert [3]. Therefore, this theory has limitations for materials such as zeolites [4], MOFs [5], or carbon-based materials, which mostly result in an over-evaluation of the material. A prediction of real competitive adsorption behavior based on only pure component isotherms is hard to realize but highly desirable [6]. The alternative way for experimental characterization is to include co-adsorption processes. However, this process can be very complicated since numerous parameters such as temperature, total pressure, and the composition of the gases, and thus the partial pressure, must be taken into account.

With the mixSorb S and the mixSorb SHP devices from 3P Instruments, it is now possible to record both single-component isotherms up to a pressure of 8 bar (mix Sorb S) / 50 bar (mixSorb SHP) and multi-component isotherms on one instrument.

In this study, different approaches are compared to prove the robustness of this method. For this purpose, isotherms of CO_2 and CH_4 were recorded using dynamic

manometry, classical gravimetric adsorption, and so-called step breakthroughs on a mixSorb SHP.

References

1. R. Ben-Mansour, M.A. Habib, O.E. Bamidele, M. Basha, N.A.A. Qasem, A. Peedikakkal, T. Laoui and Majid Ali "Carbon capture by physical adsorption: materials, experimental investigations and numerical modeling and simulations–a review." *Applied Energy* 161 (2016): 225-255.
2. K. S. Walton and David S. Sholl. "Predicting multicomponent adsorption: 50 years of the ideal adsorbed solution theory." *AIChE Journal* 61.9 (2015): 2757-2762.
3. A. L. Myers and John M. Prausnitz. "Thermodynamics of mixed-gas adsorption." *AIChE journal* 11.1 (1965): 121-127.
4. R. Krishna and J. M. van Baten. "Investigating the non-idealities in adsorption of CO_2-bearing mixtures in cation-exchanged zeolites." *Separation and Purification Technology* 206 (2018): 208-217.
5. G. H. Fuchs and F-X. Coudert "On the use of the IAST method for gas separation studies in porous materials with gate-opening behavior." *Adsorption* 24.3 (2018): 233-241.

SURFACE MASS SPECTROMETRY AND ITS APPLICATION IN MODERN RESEARCH

E.S. Kuznetsova, I.S. Pytskii, A.K. Buryak

ivanpic4586@gmail.com
Federal State Budgetary Institution of Science Institute of Physical Chemistry and Electrochemistry RAS, 119071, Moscow, Russia

Surface mass spectrometry is a group of mass spectrometric techniques that uses different methods to ionize compounds from different surfaces. Most often, accelerated atoms (fast atom bombardment, FAB), field-accelerated ions of heavy elements (secondary ions mass spectrometry, SIMS), or high-energy photons generated by lasers of various types (surface assisted laser desorption / ionization, SALDI) are used for ionization. Unlike other methods of surface research, SALDI has a much simpler device, a set of many sample preparation methods depending on the task and a large set of parameters for regulating ionization conditions. Typically, the method is used to study samples crystallized on the surface or thin films in the imaging mass spectrometry (IMS) mode. In this mode, it is possible to search for target compounds on the surface of thin films and build diagrams of their distribution over the surfaces. The authors have shown that the use of this method is not limited only to thin films, and with a slight modification of the equipment, it is possible to study surfaces of any thickness. It is shown that the modified method can be used to assess the contamination of surfaces of structural materials made of stainless steel, galvanized, copper, bronze, brass and others. The method perfectly detects organic impurities, inorganic compounds, oxides of the base metals of the alloy, which makes it possible to assess the damage to the surface during the operation of the material. In this case, it is also possible to qualitatively determine the impurities of other metals that affect the performance of the material. In addition, the fundamental possibility of studying polymer compounds of great thickness is shown. In this case, it is possible to determine not only impurities (salts, by-products of synthesis, plasticizers, and others), but also the degree of polymerization and the type of polymer in one experiment with a combination of surface and matrix ionization. It should be especially noted that the method is capable of studying the surface morphology of various materials. For this, a

marker substance (aromatic or heterocyclic compound or cluster-forming inorganic salts) is applied to the surface under study, according to the distribution of which on the surface microscopic damage or chemical inhomogeneities can be detected. The method is indispensable in itself as an express control of exploited surfaces, as well as in combination with chromatography, fluoroscopy and thermal desorption mass spectrometry to obtain information on the effect of environmental components on various materials and to develop the physicochemical bases of these processes.

CONTENT

1	***A.A. Fomkin*** ON THE 120th ANNIVERSARY OF THE BIRTH OF ACADEMICIAN M.M. DUBININ	**5**
2	***K. Kaneko*** CONCERTED STRUCTURE AND DYNAMICS OF MOLECULES ON CARBON NANOSTRUCTURES	**8**
3	***A.V. Neimark*** THERMODYNAMICS OF ADSORPTION DEFORMATION OF MICROPOROUS CARBONS	**10**
4	***S. Lucena*** RECENT DEVELOPMENTS IN CARBONACEOUS MATERIAL CHARACTERIZATION	**11**
5	***Yu.K. Tovbin, E.S. Zaitseva*** THREE TYPES OF TWO-PHASE SURFACE TENSIONS OF ADSORBATE IN MESOPOROUS SYSTEMS AND METHODS FOR CALCULATING IT	**12**
6	***E.S. Zaitseva, Yu.K. Tovbin*** SURFACE TENSION OF STRATIFYING ADSORBATE INSIDE CYLINDRICAL PORES	**17**
7	***I. Popov, A. Tchougréeff*** DEVELOPMENT OF QUANTUM CHEMICAL METHODS FOR THEORETICAL STUDY OF COMPLEX CARBON-BASED ADSORBENTS	**20**
8	***C. Cleeton, A. Farmahini, L. Sarkisov*** ERROR PROPAGATION IN MULTISCALE SIMULATIONS OF PRESSURE-SWING ADSORPTION PROCESSES FOR CARBON CAPTURE	**22**
9	***G.Y. Gor*** COMPRESSIBILITY OF ADSORBED WATER FROM MOLECULAR SIMULATIONS	**24**
10	***A.V. Shkolin, V.V. Gaidamavichyute, A.A. Fomkin, I.E. Men'shchikov*** MOLECULAR DYNAMICS SIMULATION OF ADSORPTION OF A METHANE-ETHANE MIXTURE IN SLIT-LIKE MICROPORES	**25**
11	***V.V. Gaidamavichyute, A.V. Shkolin, A.A. Fomkin, I.E. Men'shchikov*** MOLECULAR DYNAMICS STUDY OF SPATIAL ORIENTATION OF THE N-PENTANE MOLECULE ADSORBED IN MODEL SLIT-LIKE PORES OF CARBON ADSORBENT	**28**
12	***S.Yu. Kudryashov, V.A. Gladarenko*** THE CALCULATION OF THE THERMODYNAMIC CHARACTERISTICS OF ISOMERS ADSORPTION ON THE GRAPHITE BY THE MONTE CARLO METHOD	**31**

13	***M.S. Mel'gunov*** MACHINE LEARNING EXERCISE FOR THE ADSORPTION-DESORPTION HYSTERESIS LOOP RECOGNITION	**34**
14	***A.B. Ayupov, S. Ehrling*** HIGH-RESOLUTION ADSORPTION ISOTHERMS WITH PRECISE TEMPERATURE CONTROL AS A TOOL FOR INSIGHT TO THE ADSORPTION THERMODYNAMICS AND MODELS	**36**
15	***J. Villarroel-Rocha, J.J. Arroyo-Gómez, D. Barrera, K. Sapag*** A METHODOLOGY TO OBTAIN MICROPORE VOLUME IN NANOPOROUS SOLIDS BASED ON THE DUBININ METHODS	**38**
16	***D.A. Bograchev, Yu.M. Volfkovich*** MATHEMATICAL MODELING AND EXPERIMENTAL VERIFICATION OF CV CURVES FOR SUPERCAPACITORS BASED ON ACTIVATED CARBON ELECTRODES	**42**
17	***A.V. Larin*** DISCRETE MODELS IN LINEAR ELUTION DYNAMICS OF ADSORPTION	**45**
18	***A.G. Dmitrienkova, A.V. Larin*** MINIMIZATION OF INTERVALS OF INTEGRATION IN THE METHOD OF MOMENTS USING NORMALIZED CONCENTRATIONS	**48**
19	***A.V. Shkolin, A.A. Fomkin, I.E. Men'shchikov*** ADSORPTION-STIMULATED DEFORMATION OF A PRECISION MICROPOROUS ADSORBENT UPON ADSORPTION OF GASES AND VAPORS	**50**
20	***A.V. Afineevskii, T.Yu. Osadchaya, D.A. Prozorov*** ADSORPTION DEFORMATION OF HETEROGENEOUS CATALYSTS FOR HYDROGENATION REACTIONS DURING CYCLIC TREATMENT BY A HYDRATED COMPOUND	**53**
21	***N.V. Avramenko, A.M. Parfenova, A.T. Rebrikova, L.O. Usoltseva, I.V. Mikheev, D.S. Volkov, V.M. Senyavin, M.V. Korobov*** SORPTION AND INTERPLANE TRANSFORMATION – TWO STAGES OF GRAPHITE OXIDE SWELLING IN POLAR SOLVENTS	**55**
22	***V.N. Simonov, A.A. Fomkin, A.V. Shkolin*** METHOD FOR STUDYING OF SORPTION-STIMULATED STRESSES IN ADSORBENT	**57**
23	***V.I. Dudarev, E.G. Filatova, D.I.Dudarev*** SPECIFICS OF OBTAINING CARBON ADSORBENTS FROM FOSSIL COALS	**60**
24	***V.V. Samonin, E.A. Spiridonova, E.D. Khrylova, M.L. Podvyaznikov*** CARBON ADSORBENTS FROM MAN-MADE ORGANIC WASTE	**63**
25	***L.G. P'yanova, A.V.Lavrenov, N.N. Leontieva, A.V. Sedanova*** PHYSICOCHEMICAL BASES OF THE SYNTHESIS OF MODIFIED CARBON SORBENTS FOR MEDICAL PURPOSES	**65**

26	***O. Petuhov, T. Lupascu, R. Nastas, I. Ginsari, I. Scutaru*** NEW TECHNOLOGIES FOR OBTAINING OF ACTIVATED CARBONS AND THEIR USE FOR THE POTABILIZATION OF NATURAL WATERS	**67**
27	***V.M. Mukhin, N.V. Korolev*** PREPARATION AND STUDY OF ACTIVE COALS WITH HIGH VOLUME MICROPOROSITY	**70**
28	***I.E. Menshchikov, A.A. Fomkin, A.V. Shkolin, A.A. Shiryaev, S.S. Chugaev*** SYNTHESIS OF BIPOROUS CARBON ADSORBENT FOR LONG-TERM LNG STORAGE SYSTEMS	**72**
29	***E.A. Farberova, E.A. Pershin, N.V. Limonov, E.A. Tingaev*** STUDY OF THE POSSIBILITY OF USING PLANT RAW MATERIALS FOR PRODUCING SPHERICALLY SHAPED ACTIVATED CARBONS	**75**
30	***A.V. Shkolin, A.A. Fomkin, I.E. Men'shchikov*** CARBON XEROGEL FOR CONCENTRATION OF METHANE VAPORS IN THE LNG STORAGE SYSTEMS	**77**
31	*O.V. Gorbunova, O.N. Baklanova, T.I. Gulyaeva, A.V. Lavrenov* EFFECT OF ALKALINE ACTIVATION CONDITIONS ON POROUS STRUCTURE OF PETROLEUM ASPHALT-BASED CARBON	**80**
32	***O.V. Solovtsova, I.E. Men'shchikov, A.V. Shkolin, A.A. Fomkin, E.V. Khozina*** PREPARATION OF HIGH-DENSITY CARBON ADSORBENTS BASED ON PLANT RAW MATERIALS	**82**
33	***A.N. Tsukanova, E.A. Farberova, E.A. Pershin, N.V. Limonov, N.B. Khodyashev*** PROPERTIES OF THE CUPRAMITE ABSORBER	**85**
34	***V.M. Mukhin, M.A. Gutnikova, S.I. Gutnikov*** SORBENT FOR THE ABSORPTION OF IODINE RADIONUCLIDES	**88**
35	***V.M. Mukhin, Yu.Ya. Spiridonov*** COMPARATIVE EVALUATION OF ANTIDOTE EFFECTIVENESS OF ACTIVE COALS	**89**
36	***Yu.M. Volfkovich, A.A. Mikhalin, A.Yu. Rychagov, V.E. Sosenkin, D.A. Bograchev*** ACTIVATED CARBONS AS NANOPOROUS ELECTRON-ION-EXCHANGERS	**91**
37	***A.E. Memetova, E.A. Neskoromnaya, A.D. Zelenin, N.R. Memetov, A.V. Babkin, R.A. Stolyarov, N.A.Chapaksov, A.A. Gusev, A.G.Tkachev*** COMPOSITE AEROGELS BASED ON REDUCED GRAPHENE OXIDE FOR ADSORPTION STORAGE AND TRANSPORTATION OF METHANE	**94**

38	***E.M. Rubin, A.V. Nistratov, A.V. Shkolin*** INFLUENCE OF TEMPERATURE ON THE COMPOSITION OF PYROLYSIS GASES OF WASTEWATER SEDIMENTS OF THE LUBERETSKIE TREATMENT FACILITIES	**97**
39	***M.Yu. Piskunova, A.V. Nistratov, D.V. Fedoseev, I.E. Menshchikov*** ESTIMATION OF ADSORPTION PROPERTIES OF THE PRODUCT OF PYROLYTIC PROCESSING OF WASTES OF PRODUCTION OF COMPOSITE SANITARY WARES	**100**
40	***G.A. Petukhova, L.A. Dubinina*** FEATURES OF FREON 114B2 SORPTION ONTO ACTIVATED CARBONS WITH DIFFERENT POROUS STRUCTURE	**103**
41	***K.O. Murdmaa, A.A. Pribylov*** ADSORPTION OF ALKANES ONTO CARBON ADSORBENTS AT SUB- AND SUPERCRITICAL TEMPERATURES	**106**
42	***A.A. Pribylov, K.O. Murdmaa*** METHANE ADSORPTION IN CARBON ADSORBENT S-1	**109**
43	***S.S. Chugaev, E.M. Strizhenov, A.V. Shkolin, I.E. Men'shchikov*** EXPERIMENTAL STUDY OF THE THERMAL MANAGEMENT PROCESS AT CIRCULATING CHARGING OF THE NATURAL GAS ADSORPTION ACCUMULATOR	**113**
44	***A.E. Memetova, I.V. Burakova, A.E. Burakov, N.R. Memetov, A.G. Tkachev*** EFFECTIVE TOLUENE AND BENZENE ADSORPTION ON COCONUT ACTIVATED CARBON MODIFIED WITH CARBON NANOTUBES: KINETICS, ISOTHERMS, THERMODYNAMICS	**116**
45	***D.S. Zaytsev, A.V. Tvardovsky, A.A. Fomkin, A.V. Shkolin*** ADSORPTION DEFORMATION OF FAS-3 CARBON ADSORBENT DURING ADSORPTION OF HYDROCARBONS	**117**
46	***E.B. Kalika, K.P. Katin, S. Kaya, Maslov M.M.*** EFFECT OF FLUORINATION ON INTERACTION OF METAL-DECORATED FULLERENES WITH ANTI-COVID DRUGS	**121**
47	***A.P. Karmanov, A. P. Voznyakovsky, L. S. Kocheva, N. G. Rachkova, N.I. Bogdanovich*** AN EXPERIMENTAL STUDY OF SORPTION-DESORPTION OF RADIUM 226 ON CARBON NANOMATERIALS	**123**
48	***A.L. Pulin, S.D. Artamonova, A.A. Fomkin, A.A. Berezanin, A.V. Shkolin, I.E. Men'shchikov*** ON SELECTIVITY OF XENON ADSORPTION FROM LEAN AIR MIXTURES	**125**
49	***M.B. Alekhina, M.M. Fidchenko, A.D. Varnavskaya*** ADSORPTION PROPERTIES OF CARBON-MINERAL MATERIALS BASED ON NATURAL MONTMORILLONITE CLAY AND TIRE CRUMB	**128**
50	***S.P. Khokhlachev, E.A. Spiridonova*** COMPOSITE SORPTION-ACTIVE MATERIAL BASED ON FULLERENE SOOT AND BENTONITE CLAY	**131**

51	***A.V. Bondarenko, M.L. Ruello, V.V.Bondarenko, Petukhova G.A., L.A. Dubinina*** FORMATION OF A MESO-POROUS STRUCTURE IN AN ALUMOSILICATE MATRIX OF NATURAL KAOLINITE AFTER THERMOCHEMICAL TREATMENT	**133**
52	***J.A. Ubaskina, M.B. Alekhina*** INFLUENCE OF A METHOD OF DIATOMITE TREATMENT DURING THE OBTAINING OF SORBENTS FOR WATER PURIFICATION ON THEIR PHYSICAL AND CHEMICAL PROPERTIES	**135**
53	***V.G. Tsitsishvili***, ***M.I. Panayotova,*** N.M. Dolaberidze**,** N.A. Mirdzveli**,**M.O. Nijaradze**,** Z.S. Amiridze BACTERICIDAL ZEOLITE ADSORBENTS: SYNERGISTIC EFFECTS	**138**
54	***H.V. Doan, K.M. Leung, A. Sartbaeva, V.P. Ting*** EFFECT OF MONO- AND DIVALENT EXTRA-FRAMEWORK CATIONS ON THE STRUCTURE AND ACCESSIBILITY OF POROSITY OF CHABAZITE ZEOLITES	**141**
55	***O.I. Pomazkina*** PURIFICATION OF WASTEWATER OF GALVANIC PRODUCTION BY MODIFIED ZEOLITES	**142**
56	***A.D. Chugunov, E.G. Filatova , Yu.N. Pozhidaev*** АДСОРБЦИЯ ИОНОВ ТЯЖЕЛЫХ МЕТАЛЛОВ ЦЕОЛИТОМ, МОДИФИЦИРОВАННЫМ КРЕМНИЙОРГАНИЧЕСКИМ СОЕДИНЕНИЕМ	**145**
57	***A.E. Smirnov, V.K. Dubovy, G.A. Suslov, N.A. Krinitsin, N.I. Bogdanovich*** HIGH EFFICIENT CATALYTIC PLANTS FOR PURIFICATION OF INDUSTRIAL EMISSIONS OF PULP AND PAPER MILLS USING PAPER-LIKE COMPOSITE MATERIALS BASED ON MINERAL FIBERS	**148**
58	***L.I. Belchinskaya, K.V. Zhuzhukin, N.A. Khodosova, L.A. Novikova, A.V. Zhabin*** SORPTION RESPONSIVITY OF NATURAL NANOPOROUS LAYERED CLAYS TO THE TREATMENT IN ELECTROMAGNETIC FIELD OF ULTRA-HIGH FREQUENCY, WEAK PULSED MAGNETIC FIELD AND THEIR SUBSEQUENT ALTERNATION	**150**
59	***A.I. Vezentsev, N.A. Volovicheva*** ASSESSMENT OF ANTIBACTERIAL PROPERTIES OF BENTONIT-LIKE CLAY OF BELGOROD REGION	**153**
60	***A.E. Panasenko, S.B. Yarusova, S.N. Somova, P.S. Gordienko, Yu.A. Parot'kina*** SILICATE SORBENT FROM RICE STRAW	**155**

61	***A.E. Panasenko, S.B. Yarusova, P.S. Gordienko, S.N. Somova, Yu.A. Parot'kina*** NANOSTRUCTURED BARIUM-CONTAINING SILICATE SORBENT FROM PLANT RAW MATERIALS	**159**
62	***O.O. Shichalin, S.B. Yarusova, E.K. Papynov, P.S. Gordienko, I.Yu. Buravlev, S.B. Bulanova, A.A. Belov*** CERAMIC MATRICES BASED ON WOLLASTONITE OBTAINED BY SPARK PLASMA SINTERING FOR IMMOBILIZATION OF COBALT-60	**163**
63	***L.S. Kocheva, A.V. Kanarsky, A.P. Karmanov, N.I. Bogdanovich*** STUDY OF THE SORPTION-DESORPTION PHENOMENA OF MYCOTOXINS ON THE NATURAL LIGNINS SURFACE	**166**
64	***V.A. Gorbunov, A.I. Fadeeva*** PREDICTIVE LATTICE MODELS OF SURFACE-CONFINED METAL-ORGANIC NETWORKS	
65	***A.E. Grinchenko, M.K. Knyazeva, A.A. Fomkin, A.V. Shkolin, A.L. Pulin*** SYNTHESIS AND INVESTIGATION OF THE ADSORPTION PROPERTIES OF THE Ce-BTC METAL-ORGANIC FRAMEWORK STRUCTURE	**168**
66	***M.K. Knyazeva, A.A. Fomkin, A.V. Shkolin*** CARBON DIOXIDE ADSORPTION ONTO THE Al-BTC METAL-ORGANIC FRAMEWORK	**171**
67	***I.V. Grenev, A.A. Shubin, M.V. Solovyeva, L.G. Gordeeva*** THE EFFECT OF STRUCTURAL DEFECTS AND FRAMEWORK FLEXIBILITY ON THE WATER ADSORPTION IN CAU-10-H	**176**
68	***I.A. Kirovskaya*** PREPARATION AND BULK PHYSICOCHEMICAL PROPERTIES OF NEW ADSORBENTS BASED ON THE InSb-ZnS SYSTEM	**179**
69	***I.A. Kirovskaya*** SURFACE PROPERTIES OF THE NEW ADSORBENTS $(InSb)_x(ZnS)_{1-x}$	**183**
70	***M. Ignat, P. Samoila, E. Mahu, T.F. Kouznetsova, A. Ivanets, V. Harabagiu*** DEVELOPMENT OF SUBSTITUTED ZINC FERRITE NANOPARTICLES: SYNTHESIS AND CHARACTERIZATION	**186**
71	Yu.E. Romanenko***, M.M. Klimushina, R.N. Rumyantsev*** SYNTHESIS OF A HYDROGENATION CATALYST SUPPORT BASED ON ALUMINUM OXIDE	**189**
72	***A.V. Ryabina, V. G. Shevchenko, V. N. Krasilnikov*** EXPERIMENTAL STUDY OF NITROGEN ADSORPTION ON ALUMINUM POWDER MODIFIED WITH COPPER FORMATE	**191**
73	***D.A. Prozorov, A.V. Afineevskii, D.V. Smirnov*** ADSORPTION IN CATALYTIC PROCESSES WITH THE PARTICIPATION OF HYDROGEN-CONTAINING GASES	**193**

74	***O.V. Nestroinaia, I.Yu. Goncharov, O.E. Lebedeva*** STUDY OF THE INFLUENCE OF MgCo/AlFe-LDH SYNTHESIS METHODS ON THE CHANGE OF SORPTION PROPERTIES	**195**
75	***I.V. Grenev, V.Yu. Gavrilov*** THE STUDY OF Si DISTRIBUTION IN THE SAPO-11 STRUCTURE: COMBINING SIMULATION AND EXPERIMENTAL ADSORPTION METHODS	**198**
76	***A.I. Ivanets, N.V. Kitikova, I.L. Shashkova, V.V. Milyutin, N.A. Nekrasova*** ADSORPTION OF 137Cs AND 90Sr RADIONUCLIDES FROM ELECTROLYTES SOLUTIONS BY COMPOSITE Zr-Ca-Mg PHOSPHATES	**201**
77	***I.I. Mikhalenko, D.A. Zaev*** UV DECOLORIZATION OF NITROPHENOL AND METHYL ORANGE SOLUTIONS WITH TITANIUM DIOXIDE DOPED BY Co, Rh, Ir IONS	**204**
78	***N.E. Vakhrushev, I.I. Mikhalenko, A.A. Ilyicheva, L.I. Podzorova*** INFLUENCE OF MICROWAVE TREATMENT ON THE ADSORPTION CAPACITY OF ALZR(YB) OXIDE POWDERS WITH POLYMER	**206**
79	***I.S. Garkushina*** HIGHLY SELECTIVE SORPTION OF BIOLOGICALLY ACTIVE SUBSTANCES BY MOLECULAR IMPRINTED POLYMER SORBENTS	**209**
80	***A.A. Osipenko, I.S. Garkushina*** SURFACE-IMPRINTED ORGANIC-INORGANIC AND POLYMERIC SORBENTS FOR SELECTIVE EXTRACTION OF CHOLESTEROL	**211**
81	***L.N. Borovikova, I.S. Garkushina*** SYNTHESIS OF A HYDROGENATION CATALYST SUPPORT BASED ON SPECTRAL CHARACTERISTICS OF THE ANTITUMOR ANTHRACYCLINE ANTIBIOTICS BY SELENIUM NANOPARTICLES	**215**
82	***S.E. Plotnikova, Yu.S. Peregudov, N.V. Voikina, S.I. Niftaliev*** THE STUDY OF AMMONIA ADSORPTION FROM GAS-AIR MIXTURES ON FIBROUS SORBENTS MODIFIED WITH COPPER (II) AND NICKEL (II) IONS	**218**
83	***E.S. Zapevalova, O.B. Belskaya, I.V.Anikeeva, Yu.G. Kryazhev*** ADSORBED PALLADIUM (II) CHLORIDE COMPLEXES ON POLYVINYLENES AS CATALYST SUPPORTS	**221**
84	***A.A. Yakovleva, Trung Thuy Nguyen*** ABOUT THE DIVERSITY OF SURFACE EFFECTS ON THE COASTAL SANDS OF NORTHERN AND CENTRAL VIETNAM IN THE CONDITIONS OF AGGRESSIVE IMPACT	**224**

85	***V.V. Milyutin*** MODERN PHYSICOCHEMICAL METHODS FOR REMOVING TOXIC IMPURITIES FROM AQUEOUS SOLUTIONS	**227**
86	***Yu.S. Peregudov, L.P. Bondareva, S.I. Niftaliev*** COMPLETE PURIFICATION OF WATER FROM METAL CATION WITH A FIBROUS ION EXCHANGER	**229**
87	***A.N. Filippov, N.A. Kononenko, N.V. Loza, V.I. Ivanov, D.A. Petrova*** NOVEL MF-4SC/PTMSP BILAYER MEMBRANES, ASYMMETRY OF THEIR TRANSPORT PROPERTIES, AND MODELING	**231**
88	***V.V. Kalistratova, V.V. Milyutin, E.V.Belova*** KINETIC MODEL OF THERMAL DECOMPOSITION OF ANIONITES ON THE EXAMPLE OF AV-17×8 IN NITRATE FORM	**233**
89	***M.V. Talipova, A.V. Liang*** ADSORBENTS APPLICATION PRACTICE FOR FORMING A RANGE OF MODERN FILTERS FOR GAS MASKS AND RESPIRATORS. REPORT 3	**236**
90	***S. Ehrling, R. Eschrich, A. Möller, C. Blum*** RECORDING OF SINGLE AND MULTI-COMPONENT ISOTHERMS USING DYNAMIC METHODS	**239**
91	***E.S. Kuznetsova, I.S. Pytskii, A.K. Buryak*** SURFACE MASS SPECTROMETRY AND ITS APPLICATION IN MODERN RESEARCH	**241**
	CONTENT	

Physicochemical problems of adsorption, structure, and surface chemistry of nanoporous materials: All-Russian conference with international participation (on 120th anniversary of M.M. Dubinin's birth), October 18–22, 2021, Moscow Russia. Book of Abstracts. – M.: IPCE RAS, 2021. – p.252

ISBN 978-5-4465-3448-7

Book of Abstracts

Signed to print 12.11.2021